

# **DEVELOPMENT OF THE TIMING SYSTEM FOR THE BUNCH-TO-BUCKET TRANSFER BETWEEN THE FAIR ACCELERATORS**

Vom Fachbereich  
Institut für Angewandte Physik  
der Goethe-Universität, Frankfurt am Main  
zur Erlangung des akademischen Grades  
eines Doktor der Naturwissenschaften  
genehmigte Dissertation

Von  
**Jiaoni Bai**  
geboren am 9. November 1986 in Taiyuan, Shanxi Province, China

Referent: Prof. Dr. U. Ratzinger  
Korreferent: Prof. Dr. O. Kester  
Tag der Einreichung: Date. Month Year  
Tag der mündlichen Prüfung: Date. Month Year

Darmstadt 2016

---

I would like to dedicate this dissertation to my dear parents,  
loving husband and good friends ...

# Acknowledgement

First and foremost, I would like to thank my professor Prof. Dr. Oliver Kester. It is a great honour for me to be his Ph.D. student. He gave me the chance to study at Goethe Universität, Frankfurt am Main and work in GSI for this interesting Ph.D. topic. I appreciate all his contributions of time and ideas to make my Ph.D. successful. I was deeply influenced by his enthusiasm for his research and his selfless support for his students. I was thankful for his support, that I participated many international conferences, schools and workshops. This experience enriched my life and broadened my horizons.

I wish to express my sincere gratitude to Dr. David Ondreka and Dr. Dietrich Beck for their supervision, valuable guidance and helpful suggestions throughout my Ph.D. study. I have been greatly lucky to have so good supervisors, who cared much about my work and who answered my doubts patiently. They were like a lighthouse in the ocean, which guides me in the right direction. They are not only my scientific supervisors, but also my mentors. They encouraged and motivated me during tough time of my Ph.D. Hence, I will keep a positive attitude and keep moving forward when I face with challenges, difficulties and temporary setbacks in the future.

I would like to acknowledge all colleagues in the timing group, CSCO department, GSI, Mathias Kreider, Stefan Rauch, Marcus Zweig, Alexander Hahn and former employee Dr. Wesley Terpstra, who provided me much technical support. I would like to extend my appreciation to department leader Dr. Ralph Bär, who gave much support for my Ph.D. topic. Thanks for their friendship and collaboration. I am especially grateful for the group member Cesar Prados, by whom I learned not only technical knowledge, but also how to work efficiently and how to become a good engineer. I would also like to thank Matthias Thieme, who provided me the devices for the test setup and Marko Stanislav Mandakovic for the discussion about the MPS. I would like to extend gratitude to Dr. Udo Krause and Peter Kainberger for the information about the GSI control system.

I am also thankful for the good cooperation with Thibault Ferrand, who studies at Technische Universität Darmstadt and works in PBRF department, GSI. Thanks for his valuable contribution of the development of the LLRF system for the B2B transfer system for FAIR. I would like to extend my sincerest thanks and appreciation to PBRF department leader Prof. Dr. Ing. Harald Klingbeil for his support. In addition, a special thanks is also extended to Dr. Dieter Lens and Stefan Schäfer for their technical support. Thanks for Dr. Bernhard Zipfel to give me support about BuTiS.

I wish to express my sincere gratitude to SBES department leader Dr. Markus Steck for his technical support of ESR and CRYRING, Dr. Udo Blell in PBHV department for the technical support of kicker and Dr. Michael Block in SHE-P department for the supply of two SRS function generators.

---

I must express my gratitude to GSI and also HGS-HiRe, who provided the scholarship which allowed me to undertake this research.

Lastly, I would like to thank my family for all their love and encouragement. My parents always support me to pursuing my dreams. Most of all, my loving husband Zigao Li is so appreciated, who always encourages me to realize my dreams. Thank you.

Jiaoni Bai  
Darmstadt, September 2016

# Abstract

This dissertation contributes to the conceptual development, systematic investigation and timing system realization of the Bunch-to-Bucket (B2B) transfer system for FAIR, Facility for Antiproton and Ion Research at GSI Helmholtzzentrum für Schwerionenforschung GmbH.

The B2B transfer system for FAIR plays an important role for the FAIR project, which will achieve various complex bunch to bucket transfer for FAIR accelerators in the future. It focuses first of all on the transfer from SIS18 to SIS100, but it will be firstly tested for the transfer from SIS18 to ESR and from ESR to CRYRING. The system is developed based on the FAIR existing infrastructures, Low Level Radio Frequency system (LLRF) and FAIR control systems. It coordinates with the Machine Protection System (MPS), which protects SIS100/SIS300 from fatal errors and considerable damage and indicates beam status for Beam Instrumentation (BI).

The B2B transfer system obtains the radio frequency (rf)-phase difference between two synchrotrons by means of a campus wide distributed reference signal with picosecond precision, which is provided by the Bunchphase Timing System (BuTiS). The part of the B2B electronic locates in the source synchrotron supply room and serves as a kind of “B2B transfer master“. The most important tasks of B2B transfer master are:

- The data collection (e.g. the rf phase collection).
- The data processing (e.g. the calculation of the synchronization window, the phase shift for the phase match between two rf systems, the phase correction for the bucket label, the B2B transfer status check and etc.).
- The data redistribution (e.g. the synchronization window).

The synchronization window is a coarse time frame for the transfer (coarse synchronization) and the bucket label signal is used to indicate a certain bucket to be injected within the window, which is called the “fine synchronization“. This system is applied to all FAIR B2B transfer cases and all transfers have to achieve the bunch-to-bucket injection center mismatch within the tolerance limits.

Because the system focuses first of all on the transfer from SIS18 to SIS100, the beam dynamic of the B2B transfer from SIS18 to SIS100 is simulated for two synchronization methods, the phase shift and the frequency beating method. In addition, the SIS18 extraction and SIS100 injection kickers are analyzed for different triggering strategies. This dissertation also explains the timing constraints of the system, the calculation of the synchronization window and presents the usage of the WR network for the B2B transfer system.

A test setup of the timing system of the B2B transfer system for FAIR is also presented in this dissertation.

# Kurzfassung

# Contents

<b>Abstract</b>	<b>v</b>
<b>Glossary</b>	<b>xiv</b>
<b>List of Abbreviations</b>	<b>xviii</b>
<b>List of Symbols</b>	<b>xxii</b>
<b>1 Introduction</b>	<b>2</b>
1.1 Usage of the bunch-to-bucket transfer worldwide . . . . .	5
1.2 Objectives, Contribution and Structure of the Dissertation . . . . .	6
<b>2 Theoretical background</b>	<b>9</b>
2.1 Bunch and bucket . . . . .	9
2.2 Phase match . . . . .	15
2.2.1 Circumference ratio is an integer . . . . .	16
2.2.2 Circumference ratio is close to an integer . . . . .	17
2.2.3 Circumference ratio is far away from an integer . . . . .	19
2.3 Phase alignment of two rf systems . . . . .	20
2.3.1 Phase shift method . . . . .	20
2.3.2 Frequency beating method . . . . .	24
2.4 Synchronization of extraction and injection kicker magnets . . . . .	25
<b>3 Technical basis for the B2B transfer system</b>	<b>29</b>
3.1 FAIR control system . . . . .	29
3.1.1 BuTiS . . . . .	29
3.1.2 GMT . . . . .	30
3.1.3 Settings Management . . . . .	30
3.1.4 FESA . . . . .	31
3.2 LLRF system . . . . .	31
3.3 MPS system . . . . .	33
3.4 Comparison between the FAIR B2B transfer system and the B2B transfer with the GSI control system . . . . .	34
<b>4 Concept of the FAIR B2B transfer system</b>	<b>37</b>
4.1 Basic idea of the FAIR B2B transfer system . . . . .	37
4.1.1 Phase alignment . . . . .	37
4.1.2 Calculation of the trigger time for the extraction and injection kickers . . . . .	38

## CONTENTS

---

4.2	Basic procedure of the FAIR B2B transfer system . . . . .	40
4.3	Realization of the FAIR B2B transfer system . . . . .	41
4.3.1	Phase measurement and corresponding timestamp of one rf system . . . . .	41
4.3.1.1	Measurement of actual phase values in one rf system	42
4.3.1.2	Phase extrapolation in one rf system . . . . .	42
4.3.1.3	Timestamp the extrapolated phase . . . . .	43
4.3.2	Exchange of the measured data . . . . .	44
4.3.3	Rf synchronization . . . . .	45
4.3.4	Coarse synchronization . . . . .	47
4.3.5	Bucket label . . . . .	48
4.3.6	Fine synchronization of the extraction and injection kicker . .	50
4.3.7	B2B transfer status check . . . . .	51
4.4	Data flow of the FAIR B2B transfer system . . . . .	52
<b>5</b>	<b>Application of the FAIR B2B transfer system for FAIR accelerators</b>	<b>55</b>
5.1	Circumference ratio is an integer . . . . .	56
5.1.1	use case of the $U^{28+}$ B2B transfer from SIS18 to SIS100 . . . . .	59
5.1.2	Use case of the $H^+$ B2B transfer from SIS18 to SIS100 . . . . .	60
5.1.3	Use case of the B2B transfer from ESR to CRYRING . . . . .	61
5.2	Circumference ratio is close to an integer . . . . .	62
5.2.1	Use case of h=4 B2B transfer from SIS18 to ESR . . . . .	64
5.2.2	Use case of h=1 B2B transfer from SIS18 to ESR . . . . .	66
5.3	Circumference ratio is far away from an integer . . . . .	66
5.3.1	Use case of $H^+$ B2B transfer from SIS100 to CR . . . . .	68
5.3.2	Use case of RIB B2B transfer from SIS100 to CR . . . . .	69
5.3.3	Use case of B2B transfer from CR to HESR . . . . .	70
5.3.4	Use case of B2B transfer from SIS18 to ESR via FRS . . . . .	71
5.4	Summary of the synchronization for different scenarios . . . . .	72
<b>6</b>	<b>Realization and systematic investigation of the FAIR B2B transfer system</b>	<b>75</b>
6.1	Investigation of two synchronization methods for $U^{28+}$ B2B transfer from SIS18 to SIS100 from the beam dynamics viewpoint . . . . .	75
6.1.1	Phase shift method . . . . .	75
6.1.1.1	Longitudinal dynamic analysis for the simulation . .	78
6.1.1.2	Transverse dynamics analysis for the simulation . . .	82
6.1.2	Frequency beating method . . . . .	82
6.1.2.1	Longitudinal dynamics analysis of the frequency beating for SIS18 . . . . .	83
6.2	GMT systematic investigation for the B2B transfer system . . . . .	83
6.2.1	Calculation of the synchronization window . . . . .	84
6.2.1.1	The best estimate of alignment and the probable range of alignment for the phase shift method . . . .	86
6.2.1.2	The best estimate of alignment and the probable range of alignment for the frequency beating method	88
6.2.1.3	Calculation the synchronization window and its accuracy . . . . .	90
6.2.2	Characterization of the WR network for the B2B transfer . .	91

## CONTENTS

---

6.2.2.1	WR network test setup . . . . .	93
6.2.2.2	Frame loss rate test result for B2B frames . . . . .	94
6.2.2.3	Latency and jitter test result for B2B frames . . . . .	95
6.2.2.4	Result and conclusion . . . . .	97
6.3	Kicker systematic investigation for the B2B transfer system . . . . .	98
6.3.1	SIS18 extraction kicker units . . . . .	99
6.3.2	SIS100 injection kicker units . . . . .	100
6.4	Test setup for the data collection, merging and redistribution of the B2B transfer system . . . . .	101
6.4.1	Test functional requirement . . . . .	101
6.4.2	Test setup . . . . .	102
6.4.3	The firmware of the B2B transfer system . . . . .	104
6.4.4	The time constraints of the B2B transfer system . . . . .	107
6.4.5	Test result . . . . .	109
<b>7</b>	<b>Conclusion and outlook</b>	<b>111</b>
<b>A</b>	<b>B2B timing frames</b>	<b>113</b>
<b>B</b>	<b>Timing frames transfer for the B2B transfer</b>	<b>115</b>
<b>C</b>	<b>Parameters of B2B transfer for FAIR accelerator pairs</b>	<b>117</b>
C.1	Parameters for the B2B transfer from SIS18 to SIS100 . . . . .	117
C.2	Parameters for the B2B transfer from SIS18 to ESR . . . . .	119
C.3	Parameters for the B2B transfer from SIS18 to ESR via FRS . . . . .	121
C.4	Parameters for the B2B transfer from ESR to CRYRING . . . . .	123
C.5	Parameters for the B2B transfer from CR to HESR . . . . .	124
C.6	Parameters for the B2B transfer from SIS100 to CR . . . . .	125
<b>Bibliography</b>		<b>125</b>
<b>Publications</b>		<b>130</b>

# List of Figures

1.1	Illustration of bunch-to-bucket transfer. . . . .	3
1.2	Structure of the dissertation. . . . .	7
2.1	The longitudinal focusing of particles by rf voltage ( $\eta > 0$ ). . . . .	11
2.2	The longitudinal motion of asynchronous particles in longitudinal phase space plane ( $\eta > 0$ ). . . . .	11
2.3	A stationary rf bucket. . . . .	13
2.4	A running rf bucket. . . . .	14
2.5	The bunch-to-bucket injection with errors. . . . .	14
2.6	Constant phase difference between two rf systems when circumference ratio is an integer. . . . .	17
2.7	Periodical phase difference between two rf systems when circumference ratio is close to an integer. . . . .	19
2.8	The illustration of the phase shift method. . . . .	21
2.9	The illustration of the frequency beating method. . . . .	24
2.10	Schematic diagram of kicker magnet. . . . .	26
2.11	The rise time, flat-top and fall time of an extraction kicker. . . . .	27
2.12	The rise time, flat-top and fall time of an injection kicker for multi batches injection. . . . .	28
3.1	Reference RF Signal distribution system . . . . .	32
3.2	Local Cavity Synchronization . . . . .	33
3.3	Bunch-to-bucket transfer between SIS18 and ESR with GSI control system. . . . .	34
4.1	The illustration of B2B transfer from SIS18 to SIS100. . . . .	38
4.2	The procedure for the B2B transfer within one acceleration cycle. . . . .	40
4.3	The realization of the phase advance measurement at one synchrotron	42
4.4	The realization of the phase advance extrapolation at one synchrotron	43
4.5	Implementation of the Phase Advance Prediction Module in the B2B source SCU . . . . .	44
4.6	The synchronization of the extrapolated phase to the timestamp in one synchrotron . . . . .	44
4.7	One example of the transfer path of the B2B timing frame in the WR network . . . . .	45
4.8	The normalized frequency and phase modulation profile and the actual profiles . . . . .	46
4.9	Implementation of the Phase Shift Module in the B2B source SCU . . . . .	47
4.10	Implementation of the Phase Correction Module in the Trigger SCU . . . . .	49

## LIST OF FIGURES

---

4.11	The realization of the bucket label for the normal extraction and injection. . . . .	49
4.12	The realization of the bunch gap for the emergency extraction. . . . .	50
4.13	Implementation of the Trigger Decision module in the Trigger SCU . . . . .	51
4.14	The data flow of the B2B transfer system . . . . .	54
5.1	The frequency of the bucket label signal for the phase shift method. . . . .	57
5.2	The frequency of the bucket label signal for the frequency beating method. . . . .	58
6.1	Examples of RF frequency modulation. . . . .	77
6.2	Time derivation of four modulations . . . . .	77
6.3	The phase shift modulation of four cases . . . . .	78
6.4	Average radial excursions of four cases. . . . .	78
6.5	Relative momentum shift of four cases. . . . .	79
6.6	Changes in synchronous phase of four cases . . . . .	80
6.7	Ratio of bucket areas of a running bucket to the stationary bucket of four cases . . . . .	81
6.8	Adiabaticity parameter estimation of case (3) and (4) . . . . .	82
6.9	RF frequency derivation of the $U^{28+}$ rf ramp . . . . .	83
6.10	The illustration of the best estimate of alignment, the probable range of alignment and the synchronization window . . . . .	84
6.11	The illustration of symbols for the calculation . . . . .	85
6.12	Scenarios for the phase shift method . . . . .	87
6.13	Two scenarios for the frequency beating method . . . . .	89
6.14	The illustration of the synchronization window and its accuracy . . . . .	90
6.15	The WR network test setup . . . . .	93
6.16	The frame loss rate for B2B Broadcast and B2B Unicast frames . . . . .	95
6.17	The average latency and jitter for B2B Broadcast frames . . . . .	95
6.18	The maximum latency and jitter for B2B Broadcast frames . . . . .	96
6.19	The average latency and jitter for B2B Unicast frames . . . . .	97
6.20	The maximum latency and jitter for B2B Unicast frames . . . . .	97
6.21	Three scenarios for the delay of SIS18 extraction kicker . . . . .	99
6.22	SIS100 injection kicker . . . . .	101
6.23	Schematic of the test setup . . . . .	102
6.24	The front and back view of the test setup . . . . .	103
6.25	Flow chart of the firmware for B2B source SCU. . . . .	104
6.26	Flow chart of the firmware for B2B target SCU. . . . .	106
6.27	The time constraints of the B2B transfer system. . . . .	108
B.1	Timing frames transfer for the B2B transfer . . . . .	116

# List of Tables

5.1	FAIR B2B transfer use cases . . . . .	56
5.2	Synchronization when the circumference ratio is an integer and the large synchrotron is the target . . . . .	59
5.3	Synchronization when the circumference ratio is an integer and the small synchrotron is the target . . . . .	59
5.4	Synchronization of $U^{28+}$ B2B transfer from SIS18 to SIS100 with the frequency beating method . . . . .	60
5.5	Synchronization of $H^+$ B2B transfer from SIS18 to SIS100 with the frequency beating method . . . . .	61
5.6	Synchronization of B2B transfer from ESR to CRYRING with the frequency beating method . . . . .	62
5.7	Synchronization when the circumference ratio is close to an integer and the large synchrotron is the target . . . . .	63
5.8	Synchronization when circumference ratio is close to an integer and the small synchrotron is the target . . . . .	64
5.9	Synchronization of $h=4$ B2B transfer from SIS18 to ESR with the frequency beating method . . . . .	65
5.10	Synchronization of $h=1$ B2B transfer from SIS18 to ESR with the frequency beating method . . . . .	66
5.11	Synchronization when circumference ratio is far away from an integer and the large synchrotron is the target . . . . .	67
5.12	Synchronization when circumference ratio is far away from an integer and the small synchrotron is the target . . . . .	68
5.13	Synchronization of $H^+$ B2B transfer from SIS100 to CR with the frequency beating method . . . . .	69
5.14	Synchronization of RIB B2B transfer from SIS100 to CR with the frequency beating method . . . . .	70
5.15	Synchronization of B2B transfer from CR to HESR with the frequency beating method . . . . .	71
5.16	Synchronization of B2B transfer from SIS18 to ESR via FRS with the frequency beating method . . . . .	72
5.17	Summary of the synchronization when the revolution period is shorter than the period for the phase alignment between two rf systems . . .	73
5.18	Summary of the synchronization when the revolution period is longer than the period for the phase alignment between two rf systems . . .	74
6.1	The maximum average radial excursion of four cases . . . . .	79
6.2	The maximum relative momentum shift of four cases . . . . .	79

## **LIST OF TABLES**

---

6.3	The minimum bucket area factor of four cases . . . . .	81
6.4	The B2B transfer requirements for the WR network . . . . .	93
6.5	The connection between the traffic generator and WR switches . . . . .	94
6.6	The average latency and jitter of the B2B Broadcast frames . . . . .	96
6.7	The maximum latency and jitter of the B2B Broadcast frames . . . . .	96
6.8	The result of the WR network test for the B2B transfer . . . . .	98
6.9	The delay for firing two crates of SIS18 extraction kicker . . . . .	100
6.10	The delay for firing SIS00 injection kicker . . . . .	101
A.1	B2B timing frames . . . . .	114
C.1	Parameters for the B2B transfer from SIS18 to SIS100 . . . . .	118
C.2	Parameters for the B2B transfer from SIS18 to ESR . . . . .	120
C.3	Parameters for the B2B transfer from SIS18 to ESR via FRS . . . . .	122
C.4	Parameters for the B2B transfer from ESR to CRYRING . . . . .	123
C.5	Parameters for the B2B transfer from CR to HESR . . . . .	124
C.6	Parameters for the B2B transfer from from SIS100 to CR . . . . .	125

# Glossary

accuracy	Closeness of agreement between the observed start and the best estimate of the start of the synchronization window, which is the sum of the precision and trueness
B2B target SCU	Collects the predicted phase of the target synchrotron and transfers it to the source synchrotron
B2B source SCU	Works as B2B transfer master
batch	A train of bunches circulating along a synchrotron to be transferred to buckets
best estimate of alignment	Fine time for the alignment of two RF Reference Signals
bucket pattern	Rules for the buckets to be filled
bucket area factor	Ratio of bucket size of a running bucket to a stationary bucket
bucket size	Area in longitudinal phase space plane enclosed by the bucket
bucket height	Maximum momentum deviation of the rf bucket
bunch	Collection of particles captured within one rf bucket
bunch gap	Area without any bunches in a batch
Cavity DDS	Cavity DDS provides rf signal for cavities

## Glossary

---

circumference ratio	Ratio of the circumference for synchrotrons of different size
coarse synchronization	Bunches are transferred into buckets with the bunch-to-bucket center mismatch smaller than the upper bound
error propagation	Uncertainties in the original measurements “propagate“ through calculations to cause uncertainties in the calculated final answers
extraction kicker	Diverts a circulating beam to leave a synchrotron
fall time	A period of time of kicker magnet to reduce to zero magnetic field
fine synchronization	Bunches are transferred into correct buckets
flat-top	A period of time of kicker magnet with a stable magnetic field
frame loss rate	The ratio of the number of the lost Ethernet frames to the number of the theoretic received frames of a tested port
Group DDS	DDS module that generates an Reference RF Signal for a group of cavities
harmonic number	Integer ratio between the rf frequency and the revolution frequency
injection kicker	Merges one beam into a circulating beam in a synchrotron
jitter	The absolute value of the difference between the latency of two consecutive received frames belonging to the same stream from one Xena port to another Xena port
latency	The time interval between the time of Xena port receiving frame and the time of another Xena port sending frame

## Glossary

---

longitudinal emittance	Area occupied by a bunch in the longitudinal phase space plane
machine cycle	One complete operation cycle of a machine, i.e. injection, ramp up, flattop, ejection and ramp down
precision	Closeness of agreement between the actual start of the synchronization window of different SCUs
probable range of alignment	Range within which the fine alignment lies because of the propagation of the uncertainty
Reference RF Signal	DDS module that generates an Reference RF Signal for a group of cavities
revolution frequency ratio	Ratio of the revolution frequencies for synchrotrons of different size
rise time	A period of time for kicker magnet to reach a stable magnetic field
running rf bucket	Rf system provides a region in the longitudinal phase space, within which all particles oscillate around the synchronous particle and stay together with energy gain/loss per turn
stationary rf bucket	Or rf bucket. Rf system provides a region in the longitudinal phase space, within which all particles oscillate around the synchronous particle and stay together without energy gain/loss per turn
Synchronization Reference Signal	Shared synchronous reference signal at each supply room (same frequency and in phase)
synchronous particle	A particle who always sees a constant rf phase at the rf cavity
synchrotron motion	Oscillation of asynchronous particles around the synchronous particle

## Glossary

---

timing frame	A specific Ethernet frame with 110 byte frame length, which contains one timing message
Trigger SCU	Production of the trigger signal for kicker electronics
trueness	Closeness of agreement between the average actual start of the synchronization window of different SCUs and the best estimation start of the synchronization window
tune	Number of particle trajectory oscillations during one revolution in the ring (transverse and longitudinal)
uncertainty	A non-negative parameter characterizing the dispersion of the values attributed to a measured quantity
virtual rf cavity	A virtual position around the ring, to which the Reference RF Signal corresponds

# List of Abbreviations

AGS	Alternating Gradient Synchrotron at BNL
API	Application Programming Interface
B2B	Bunch-to-bucket
BNL	Brookhaven National Laboratory
BuTiS	Bunchphase Timing System
CCS	Central Control System
CERN	Conseil Européen pour la Recherche Nucléaire
CM	Clock Master
CPU	Central Processing Unit
CR	Collector Ring at GSI
CSCO	Common Systems Control Systems
CSRe	Cooler Storage Ring experimental ring at IMP
CSRm	Cooler Storage Ring main ring at IMP
DDS	Direct Digital Synthesizer
DM	Data Master
DSP	Digital Signal Processor
ESR	Experimental Storage Ring at GSI
FAIR	Facility for Antiproton and Ion Research at GSI
FEC	Front End Controller

## List of Abbreviations

---

Fermilab	Fermi National Accelerator Laboratory
FESA	Front-End software Architecture
FPGA	Field Programmable Gate Array
FRS	Fragment Seperator
GCD	Greatest Common Divisor
GMT	General Machine Timing
GSI	GSI Helmholtzzentrum für Schwerionenforschung
GUI	Graphical User Interface
HESR	High Energy Storage Ring at GSI
HIRFL	Heavy Ion Research Facility at IMP
IMP	Institute of Modern Physics
J-PARC	Japan Proton Accelerator Complex
LEIR	Low Energy Ion Ring at CERN
LHC	Large Hadron Collider at CERN
LLRF	Low-level RF
LSA	LHC Software Architecture
MM	Management Master
MPS	Machine Protection System
MR	Main Ring at J-PARC
NESR	New Experimental Storage Ring at GSI
PAM	Phase Advance Measurement
PAP	Phase Advance Prediction
Pbar	Proton bar
PBVH	Primary Beam High Voltage

## List of Abbreviations

---

PBRF	Primary Beam Radio Frequency
PC	Personal Computer
PCM	Phase Correction Module
PS	Proton Synchrotron at CERN
PSB	Proton Synchrotron Booster at CERN
PSM	Phase Shift Module
RCS	Rapid Cycle Synchrotron at J-PARC
RESR	Recycled Experimental Storage Ring at GSI
rf	Radio Frequency
RHIC	Relativistic Heavy Ion Collide at BNL
RIB	Rare Isotope Beams
SBES	Experimentierspeicherring ESR
SCU	Scalable Control Unit
SFC	Sector Focusing Cyclotron at IMP
SHE-P	SHE-Physik
SIS100	SchwerIonen Synchrotron (100 Tm magnetic rigidity) at GSI
SIS18	SchwerIonen Synchrotron (18 Tm magnetic rigidity) at GSI
SIS300	SchwerIonen Synchrotron (300 Tm magnetic rigidity) at GSI
SM	Settings Management
SPS	Super Proton Synchrotron at CERN
SR	Signal Reproduction
SSC	Separated Sector Cyclotron at IMP

## **List of Abbreviations**

---

TD	Trigger Decision
TM	Timing Master
TOF	Time-Of-Flight
TTL	Transistor–Transistor Logic
UNILAC	Universal Linear Accelerator at GSI
VLAN	Virtual LAN
WR	White Rabbit

# List of Symbols

$p$	Particle momentum
$R$	Orbit radius
$\beta$	Relative speed to the speed of light
$c$	Speed of the light
$\gamma$	Relativistic factor, which measures the total particle energy, $E$ , in units of the particle rest energy, $E_0$
$E$	Total particle energy
$E_0$	Particle rest energy
$\alpha_p$	Momentum compaction factor
$\eta$	Phase-slip factor
$q$	Charge of a particle
$\alpha_b$	Bucket area factor
$\omega_{syn}$	Angular synchrotron frequency
$B$	Magnetic field
$\rho$	Bending radius of a particle immersed in a magnetic field $B$
$h^X$	Harmonic number of a specific synchrotron. $X = l$ , harmonic number of large synchrotron; $X = s$ , harmonic number of small synchrotron; $X = src$ , harmonic number of source synchrotron; $X = trg$ , harmonic number of target synchrotron

## List of Symbols

---

$\varepsilon$	Adiabaticity parameter
$\omega_{syn\_0}$	Angular synchrotron frequency with no frequency modulation
$Q_{x/y}$	Horizontal/vertical tune
$Q'_{x/y}$	Horizontal/vertical chromaticity
$\Delta Q_{x/y}$	Horizontal/vertical tune shift
$\Delta\varphi$	Maximum initial phase difference between two slightly different frequencies
$f_1$ and $f_2$	Two slightly different frequencies
$T_{sync\_win}$	Length of the synchronization window
$t_{bucket}$	Time delay for a specific bucket pattern
$t_{TOF}$	Time-of-Flight between two synchrotrons
$t_{v\_ext}$	Time corresponds to the distance between the virtual rf cavity driving signals and the extraction position of the source synchrotron
$t_{v\_inj}$	Time corresponds to the distance between the virtual rf cavity driving signals and the injection position of the target synchrotron
$t_{ext}$	Extraction kicker delay
$t_{inj}$	Injection kicker delay
$t_{diff\_sync}$	Time difference between rf systems of two synchrotrons after the synchronization
$\Delta\varphi 1$	Phase difference between the Reference RF Signal and the Synchronization Reference Signal of the source synchrotron, measured by PAM module
$\Delta\varphi 2$	Phase difference between the Reference RF Signal and the Synchronization Reference Signal of the target synchrotron, measured by PAM module

## List of Symbols

---

$\psi_1$	Predicted phase difference between the Reference RF Signal and the Synchronization Reference Signal of the source synchrotron
$\psi_2$	Predicted phase difference between the Reference RF Signal and the Synchronization Reference Signal of the target synchrotron
$t_{\psi_1}$	Time corresponding to the extrapolated phase $\psi_1$
$t_{\psi_2}$	Time corresponding to the extrapolated phase $\psi_2$
$f_{normalized}$	Normalized rf frequency modulation profile, preloaded from SM
$f_{actual}$	Actual rf frequency modulation profile, calculated by PSM
$t_{v\_emg}$	Time corresponds to the distance between the virtual rf cavity and the emergency extraction position of SIS100
$t_{emg}$	Extraction kicker delay of SIS100
$Q_x^{'}$	Horizontal chromaticity
$Q_y^{'}$	Vertical chromaticity
$\Delta Q_x$	Horizontal tune shift
$\Delta Q_y$	Vertical tune shift
$t_{best}$	Best estimate of alignment of zero crossing points of Reference RF Signals of source and target synchrotrons
$\delta t_{best}$	Uncertainty of the best estimate of alignment of zero crossing points of Reference RF Signals of source and target synchrotrons
$\psi_{h=1}^{SIS100}$	Predicted SIS100 h=1 rf phase at $t_\psi$
$\psi_{h=1/5}^{SIS18}$	Predicted SIS18 h=1/5 rf phase at $t_\psi$
$t_\psi$	Time of the predicted phase

## List of Symbols

---

$\phi_{h=2}^{SIS18}$	Rf phase at the cavity frequency h=2 of SIS18 at $t_\psi$
$\phi_{h=10}^{SIS100}$	Rf phase at the cavity frequency h=10 of SIS100 at $t_\psi$
$\delta t_\psi$	Uncertainty of the predicted phase advance at time domain
$\delta\psi_{h=1}^{SIS100}$	Uncertainty of the predicted SIS100 rf phase at h=1
$\delta\psi_{h=1/5}^{SIS18}$	Uncertainty of the predicted SIS18 rf phase at h=1/5
$\delta\phi_{h=10}^{SIS100}$	Uncertainty of rf phase at the cavity frequency h=10 of SIS100
$\delta\phi_{h=2}^{SIS18}$	Uncertainty of rf phase at the cavity frequency h=2 of SIS18
$T_{phase\_shift}^{upper\_bound}$	Upper bound time of the phase shift process
$\delta T_{phase\_shift}^{upper\_bound}$	Uncertainty of the upper bound time of the phase shift process
$\Delta\phi_{adjustment}$	Phase adjustment of the frequency beating method, calculated by B2B source SCU
$\Delta f$	Beating frequency
$\psi_{s.alignment}$	Rf phase of the cavity driving frequency at the start of the probable range of alignment
$\Delta t_{win.correct}$	Time correction for the start of the probable range of alignment $[t_{best}-\delta t_{best}, t_{best}+\delta t_{best}]$ to the best estimate of the start of the synchronization window
G	Bunch gap
L	Distance from the leftmost to the rightmost SIS18 extraction/SIS100 injection kicker unit
D	Sum distance of d and the 2nd crate
d	Distance between two extraction kicker crates of SIS18

## List of Symbols

---

$t_{B2B}$	Start time of the B2B transfer
$\Delta t$	Beating time for the synchronization
$\phi_s$	Synchronous phase
$f_{rf}$	Rf frequency
$h$	Harmonic number
$f_{rev}$	Revolution frequency
$V$	Longitudinal accelerating voltage at rf cavity
$V_0$	Amplitude of the rf voltage
$m_0$	Rest mass
$C^X$	Circumference of the extraction/injection orbit of a specific synchrotron
$f_{rev}^X$	oder $f_{h=1}^X$ . Revolution frequency of a specific synchrotron
$f_{rf}^X$	oder $f_{h=cavity\_harmonic}^X$ . Cavity frequency of a specific synchrotron
$\kappa$	Integer, $m$ and $n$ are also integer
$\lambda$	Decimal
$Y$	Greatest common divisor
$\Delta\phi$	Required phase shift for the phase shift method, bunch-to-bucket center mismatch for the frequency beating method
$\Delta f_{rf}$	Rf frequency modulation for the phase shift method
$T$	Period of rf frequency modulation for the phase shift method
$t_0$	Start time of the rf frequency modulation for the phase shift method
$T_{rev}^X$	Period of the revolution period of machine X

## List of Symbols

---

$T_{rf}^X$       Period of the cavity frequency of machine X

$k$       Slope of the phase advance

# Chapter 1

## Introduction

Beam of high energy particles is useful for both fundamental and applied research in the sciences, and also in many technical and industrial fields unrelated to fundamental research. It has been estimated that there are approximately 30000 accelerators worldwide. Only about 1% of them are research machines with energies above 1 GeV [1]. As we all known, particles are accelerated by the electric field. The radio frequency (rf) system is devoted to generate the electric field at rf cavities around the ring. Particles are accelerated when they pass through rf cavities. Every rf cavity has a limited frequency range, so particles at rest could not be accelerated to several tens of GeV energy in one ring accelerator. Hence, the acceleration must be divided into several energy stages: the first energy stage is achieved usually by a small ring, which is called "booster" and the second stage by a large ring, which is usually called "main ring". The energy of a beam is determined by the 'magnetic rigidity' of the dipole magnet, which is the multiplication of the magnetic field and the bending radius of a particle immersed in the magnetic field. At the time of the beam transfer, the magnetic rigidity of the booster must be equal to that of the main ring. Since the bending radius of the main ring is generally larger than that of the booster, the magnetic field in the main ring starts the further acceleration at a lower level. This allows a continuous increasing of the particle energy until the limits of the dipole magnets of the main ring. The usage of the booster and the main ring works faster to reach the required beam energy, because the booster can be filled and accelerated, when the main ring accelerates particles. The faster acceleration has the advantage to reduce the interaction time between the accelerated particles and the residual-gas atoms in the vacuum chamber, achieving a better beam quality [2]. Furthermore, the particle beam transfer among different rings is also used for the production of high intensity beam, e.g. the beam is transferred to a storage ring for the beam accumulation and the beam compression. Hence, the transfer of beam between rings is of great importance for high energy, high intensity and high quality beam.

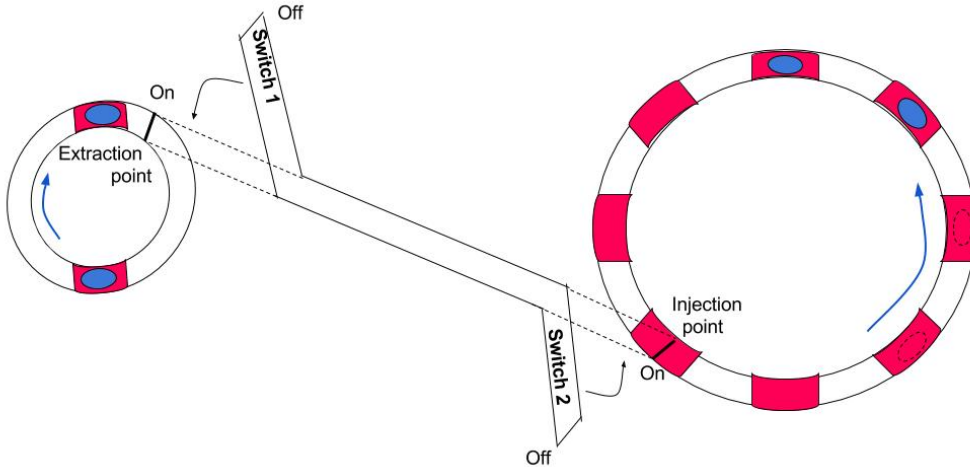


Figure 1.1: Illustration of bunch-to-bucket transfer.  
The red rectangles represent buckets and the blue dots bunches.

The beam transfer is not arbitrary. A bunch of particles running in a ring should be transferred into the correct position of another ring. Fig. 1.1 illustrates the transfer of a bunch of particles between two rings. The example in Fig. 1.1 is with the circumference ratio between the right and left rings of four. Bunches of particles are transferred from the left ring to the right one. The blue ellipse represents a bunch of particles and the red rectangle represents the allowable area for particles to be injected. The red rectangles are equally spaced around the ring and determined by the rf frequency. The white space between two red rectangles is forbidden for particles. The allowable area (red rectangle) for particles is termed as “bucket” and a bunch of particles (blue ellipse) as “bunch”. Definition of bunch and bucket from the accelerator physics perspective, please see Chap. 2. There are two buckets at the left ring and every bucket keeps a bunch. There are eight buckets in the right ring and two of them are filled with bunches. The left ring is connected to a track by a switch, which is called “switch 1”. When the switch 1 is off, bunches circulate around the ring. When it is on, bunches will be guided from the ring to the track at a specific position around the ring, which is called “extraction point” (represented as a black short bar on the left ring). The track is connected to the right ring by another switch, called “switch 2”. When the switch 2 is on, bunches will be guided from the track to the right ring at a specific position around the ring, which is called “injection point” (represented as a black short bar on the right ring). Generally both switches are off. The bunch-to-bucket (B2B) transfer is defined as that bunches of the left ring are transferred to the correct buckets at the right ring. For the B2B transfer, bunches at the left ring and buckets at the right ring must have not only a constant but same velocity. Because the circumference of the right ring is four times longer than that of the left ring, bunches run four cycles of the left ring when buckets run one cycle of the right ring. The distance between two bunches of the left ring is equal to the distance between two continuous buckets of the right ring. Besides, the relative position between bunches and buckets must match. Bunches of the left ring are guided to the track and transferred to the right ring. They are guided exactly to two empty buckets of the right ring. Everytime when a bunch of the left ring passes by the extraction point, a bucket of the right ring will pass by the injection point after a specific time delay, which equals to the time-of-flight of

## CHAPTER 1. INTRODUCTION

---

a bunch on the track. What's more, the switch of the track is of great importance, which decides buckets to be filled. In Fig. 1.1, two empty buckets closely following the filled buckets of the right ring need to be filled (represented as the dotted ellipse). The switch 2 must be switched on when the first empty bucket following two filled buckets passes the injection point and the switch 1 must be switched on a specific time earlier, when a bunch passes by the extraction point.

The ring is called “source ring”, from which the beam is extracted. The ring is called “target ring”, into which the beam is injected. From the above illustration, several preconditions are compulsory for the B2B transfer. The first precondition is that bunches of the source ring and buckets of the target ring have a constant speed, namely the revolution frequency of two rf systems of the source and target rings must be constant. Beam feedback loops on the rf system are usually implemented in order to keep the stability of the beam. The constant revolution frequency requires that the beam feedback loop must be switched off before the B2B transfer. The second one is that bunches and buckets are with same speed, which requires that the revolution frequency ratio between two rings is equal to the reciprocal of the circumference ratio. When the circumference ratio between two rings is an integer, the phase difference between two revolution frequencies is constant. It means that bunches always pass the extraction position a constant time earlier/later before/after buckets pass the injection position. But the constant phase difference is not correct for the transfer. In order to get the correct phase difference, an azimuthal positioning of bunches in the source ring or buckets in the target ring must be adjusted. This is called “phase shift method”. After the phase shift, the phase difference of two revolution frequencies is correct and the correct phase difference keeps infinite theoretically. Because the beam feedback loop is switched off, the beam is stable only for a period of time. So the beam must be transferred as soon as possible. When the circumference ratio is not an integer, the phase difference between two revolution frequencies varies periodically. Within one period, there must be one time point when the phase difference between two rf systems is correct. Before and after this time point, there exists the mismatch between bunches and buckets. The earlier and later than this time point, the larger the mismatch. This is called ”frequency beating method”. For both the phase shift and frequency beating methods, the transfer can only happen when the mismatch is smaller than the tolerance limit. The time frame is called “synchronization window”, which achieves the “coarse synchronization”.

Bunches are switched from one path to another path by kicker magnets (short: kicker). The extraction kicker magnet kicks bunches out of the source ring to the track and the injection kicker magnet kicks them from the track into buckets of the target ring. They are located at the extraction postion and injection position in Fig. 1.1. When the phase difference between two rf systems is correct, the extraction kicker could kick bunches of the source ring at the exact time-of-flight of the track before empty buckets pass the injection kicker. With the synchronization window, the extraction and injection kickers must be fired at the correct time in order to transfer bunches into correct empty buckets. The process of the kicker firing at the correct time is termed as “fine synchronization”.

### **1.1 Usage of the bunch-to-bucket transfer worldwide**

Nowadays, there are several accelerator institutes in the world, who operate the B2B transfer among rings for specific purposes. CERN, the European Organization for Nuclear Research, is one of the world's largest and most respected centres for scientific research. The Large Hadron Collider (LHC) beam injection chain achieves the proton beam with the energy of 7 TeV. After accelerated by a linear accelerator, bunches are injected into buckets of the Proton Synchrotron Booster (PSB) and further into the Proton Synchrotron (PS), the Super Proton Synchrotron (SPS) and LHC [3]. For the LHC heavy ion beam injection chain with the achievement of the energy of 2.76 TeV/u, bunches are first of all injected into the Low Energy Ion Ring (LEIR) and the following transfer from PSB to LHC is same as proton beam [3]. For Japan Proton Accelerator Complex (J-PARC), bunches are transferred from the Rapid Cycle Synchrotron (RCS) to buckets of the Main Ring (MR) [4]. The Booster of Brookhaven National Laboratory (BNL) transfers bunches to buckets of the Alternating Gradient Synchrotron (AGS) and bunches of AGS are transferred further into the Relativistic Heavy Ion Collider (RHIC) [5]. Fermi National Accelerator Laboratory's accelerator complex provides high energy proton beams for a broad range of experiments. Proton beams are injected into the Recycler from the Fermi National Accelerator Laboratory (Fermilab) Booster. Then the proton beam enters the Main Injector from the Recycler. The beam is accelerated to the energy of 120 GeV. Some of the proton beam from the Booster will be used to produce a beam of special particles for Muon Delivery Ring. The Muon Delivery Ring delivers the beam into a muon storage ring for further study [6]. Institute of Modern Physics of the Chinese Academy of Sciences (IMP) operates the Heavy Ion Research Facility (HIRFL) in Lanzhou. The two existing cyclotrons Sector Focusing Cyclotron (SFC) and the Separated Sector Cyclotron (SSC) are used as an injector system for the Cooler Storage Ring main ring (CSRm) for the accumulation, cooling and acceleration. Then the beam is extracted from CSRm to produce radioactive ion beams or highly-charged heavy ions, which can be transferred to the Cooler Storage Ring experimental ring (CSRe) for many experiments [7, 8].

FAIR, Facility for Antiproton and Ion Research, is a new international accelerator facility under construction at GSI Helmholtz center for Heavy Ion Research GmbH (short: GSI)<sup>1</sup> [9, 10]. It is aiming at providing high-energy beams of ions from antiprotons to uranium with high intensities. The new FAIR accelerator complex with storage rings consists of SIS100<sup>2</sup>, SIS300<sup>3</sup>, Collector Ring (CR), Recycled Experimental Storage Ring (RESR), New Experimental Storage Ring (NESR) and High Energy Storage Ring (HESR) [11, 12]. FAIR has so many rings, so the B2B transfer among FAIR ring accelerators is of great importance to accelerate beam to higher energy and achieve beam for various experiments. Based on the existing GSI UNILAC and SIS18 serving as injectors, high intensity ion beams over the whole range of stable isotopes will be accelerated in the new heavy ion machine SIS100/SIS300 to higher energies. The beam from SIS100 will be transferred to CR

---

<sup>1</sup>Planckstrasse 1, 64291 Darmstadt, www.gsi.de

<sup>2</sup>SIS18 stands for SchwerIonen Synchrotron (100 Tm magnetic rigidity).

<sup>3</sup>SIS300 stands for SchwerIonen Synchrotron (300 Tm magnetic rigidity).

## **1.2. Objectives, Contribution and Structure of the Dissertation**

---

via proton bar (Pbar)<sup>4</sup> or Superconducting Fragment Separator (Super-FRS)<sup>5</sup>. CR has the purpose of stochastic precooling of both secondary rare isotope and antiproton beams and of measuring nuclear masses in an isochronous mode [13, 14]. The CR transfers the beam to HESR and further to RESR for the accumulation. HESR serves experiments with high energy antiprotons and rare isotope beams [15]. The proton and heavy ion beam could also be transported from SIS18 to the existing GSI Experimental Storage Ring (ESR) and further to the first FAIR-storage ring CRYRING@ESR (short: CRYRING) for the atomic and nuclear physics experiment [16, 17]. The proton and heavy ion could also be transferred from SIS18 to ESR via the Fragment Separator (FRS)<sup>6</sup>.

For many FAIR accelerator pairs, the circumference ratio between the large and small rings is an integer, e.g. SIS100 and SIS18, so the phase difference between two revolution frequencies of rings is constant. The frequency is in the MHz range. In this scenario, the phase shift method must be used for the match of the phase difference. When the circumference ratio between FAIR accelerators is not an integer, e.g. SIS18 and ESR<sup>7</sup>, the phase difference between two revolution frequencies shifts automatically. The frequency of the phase difference variability is in the kHz range. The synchronization window for FAIR is in the us range. The beams of ion species, from hydrogen to uranium as well as antiprotons, should be transferred among all rings. And every transfer must be achieved within the upper bound 10 ms and the B2B injection mismatch of less than  $\pm 1^\circ$ . Both the phase shift and the frequency beating method should be applicable in the upcoming FAIR facilities. The B2B transfer system is designed to work in parallel operation, e.g. the transfer from SIS18 to SIS100 and transfer from ESR to CRYRING can be performed at the same time. It is cable to transfer the beam between two rings via FRS or Super FRS. The B2B transfer system must coordinate with the SIS100 emergency dump for unacceptable failure or situation.

## **1.2 Objectives, Contribution and Structure of the Dissertation**

This dissertation contributes to the development of the FAIR B2B transfer system from the timing perspective. It concentrates on the introduction of the concept of the FAIR B2B transfer system and its application for FAIR accelerators. In addition, it explains the systematic investigation for the FAIR B2B transfer system in details.

The dissertation is structured as follows and as depicted in Fig. 1.2.

In Chap.2, the theoretical background for the B2B transfer are reviewed. First of all, the energy, phase and voltage match between the source and target synchrotrons are introduced. Secondly, two rf synchronization methods are discussed from the perspective of beam dynamics in order for the phase alignment. At the end of

---

<sup>4</sup>Pbar is used to produce antiprotons in inelastic collisions of high energy protons with nucleons of a target nucleus.

<sup>5</sup>Super-FRS is used to produce rare isotopes of all elements up to uranium at relativistic energies and spatially separate them within a few hundred nanoseconds.

<sup>6</sup>An ion-optical device used to focus and separate products from the collision of relativistic ion beams with thin targets.

<sup>7</sup>ESR has an injection/extraction orbit, which is 15 cm longer than the design orbit. The orbit of ESR in this dissertation means the injection/extraction orbit.

## 1.2. Objectives, Contribution and Structure of the Dissertation

---

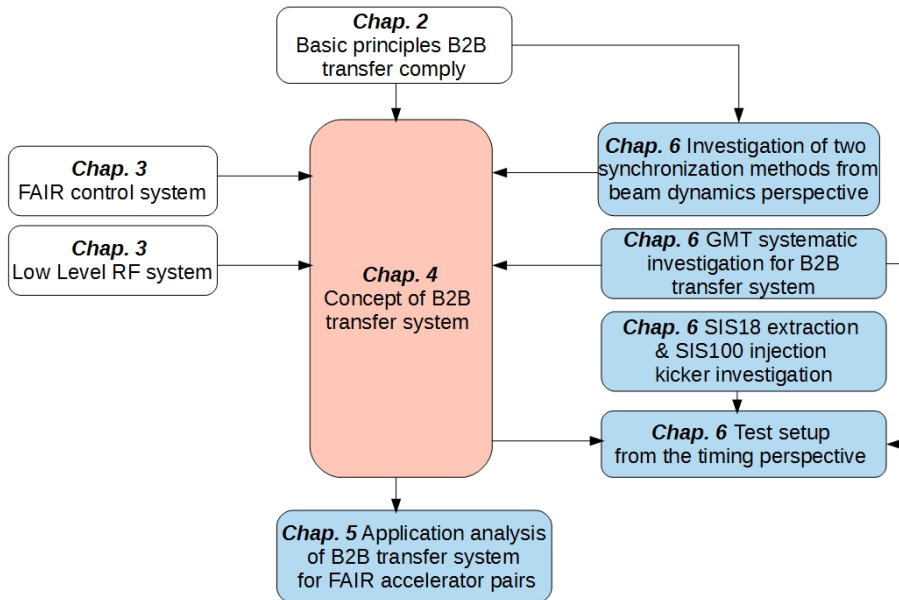


Figure 1.2: Structure of the dissertation.

Contributions are marked blue and red is team work; existing system or theory are not colored.

this chapter, the synchronization of the extraction and injection kicker magnets are discussed.

Chap.3 is concerned with the existing FAIR technical basis for the development of the B2B transfer system and the uniqueness of the system. The B2B transfer system is realized based on the FAIR control system and low-level rf system, so these two systems are introduced. In addition, the uniqueness of the B2B transfer system for FAIR is discussed before the chapter ends.

In Chap.4, a brief overview on the basic idea of the B2B transfer system is presented. After that the basic procedure of the B2B transfer is introduced and the realization of each step of the procedure. In addition, the B2B transfer system is explained from the data flow perspective.

The application of the B2B transfer system for FAIR accelerators are outlined in Chap.5. The applications are classified into two categories according to the feature of the circumference ratio. The ratio of the circumference between many pair of machines in FAIR is not an integer, e.g. SIS18 and ESR, SIS100 and CR, CR and HESR. the phase match is achieved by the frequency beating. For pairs with an integer ratio of the circumference, e.g. SIS18 and SIS100, ESR and CRYRING, there is a constant phase difference between two rf system. Although the phase shift can be used for the phase match, the frequency beating method is preferred via the detune of one rf system<sup>8</sup>. For each category, the corresponding FAIR applications are presented.

Chap.6 presents the systematic investigation for the B2B transfer system, mainly focusing on the timing aspect. The calculation of the synchronization window is explained and the transfer of the B2B messages via the WR network is tested. In addition, for the B2B transfer from SIS18 to SIS100, two synchronization methods

<sup>8</sup>The phase shift must be executed slowly enough to guarantee the beam quality, which needs much longer time than the frequency beating method.

## **1.2. Objectives, Contribution and Structure of the Dissertation**

---

are analyzed from the perspective of beam dynamics. The SIS18 extraction and SIS100 injection kicker are systematically investigated. Finally, the test setup is presented and the result is analyzed.

# Chapter 2

## Theoretical background

In Chap. 1, the bunch and bucket are with understandable definition. In this chapter, the bunch and bucket are first of all defined from the accelerator physics perspective in Sec. 2.1. Transferring bunches from a synchrotron into specific buckets of another synchrotron has several underlying basic principles. The energy of the beam is same before and after the B2B transfer, so the energy of the source synchrotron must match that of the target synchrotron. Principally speaking, every synchrotron has its independent rf system. The phase difference between bunches and the buckets must be precisely controlled before the transfer. Besides, the voltage match of two rf systems is needed to ensure that buckets capture bunches efficiently. In Sec. 2.2, the energy match, phase match and voltage match are explained. Two methods for the phase alignment between two rf systems are discussed in Sec. 2.3. For the correct bucket injection, the bunch extraction must happen exactly one time-of-flight before the required bucket of the target synchrotron passes the injection kicker. The synchronization of extraction and injection kicker magnets are presented in Sec. 2.4.

### 2.1 Bunch and bucket

For a ring accelerator, particles gain energy from electric field in longitudinal direction and are deflected by magnetic field to a particle orbit. A rf cavity operating at a resonance condition is used to provide longitudinal accelerating voltage  $V^1$  in the vacuum chamber.

$$V = V_0 \sin(\phi_s + 2\pi f_{rf} t) \quad (2.1)$$

where  $V_0$  is the amplitude of the rf voltage,  $\phi_s$  is a phase factor, and  $f_{rf}$  is the rf frequency. In order to accelerate particles with an accelerating voltage at rf cavity, the rf frequency must always be an integer multiple of the revolution frequency of particles.

$$f_{rf} = h f_{rev} \quad (2.2)$$

where the integer multiple  $h$  is called “harmonic number“.

A particle who always sees rf phase  $\phi_s$  at the rf cavity with the revolution frequency  $f_{rev}$  and the momentum  $p$  is called a “synchronous particle“. For circular accelerators, the revolution frequency is decided by the machine circumference and

---

<sup>1</sup>Rf voltage with a single harmonic operation is considered in this dissertation.

## 2.1. Bunch and bucket

---

the particle velocity.

$$f_{rev} = \frac{\beta c}{2\pi R} \quad (2.3)$$

where  $R$  is the radius of the machine,  $\beta$  the relative velocity to the speed of light and  $c$  the speed of light. The differential of eq. 2.3 is

$$\frac{\Delta f_{rev}}{f_{rev}} = \frac{\Delta\beta}{\beta} - \frac{\Delta R}{R} \quad (2.4)$$

Because of the relation  $\Delta f_{rf}/f_{rf} = \Delta f_{rev}/f_{rev}$ , so eq. 2.4 can be written as

$$\frac{\Delta f_{rf}}{f_{rf}} = \frac{\Delta\beta}{\beta} - \frac{\Delta R}{R} \quad (2.5)$$

The momentum of the synchronous particle  $p$  is related to the particle energy and its velocity.

$$p = \gamma\beta m_0 c \quad (2.6)$$

where  $m_0$  is the rest mass and  $\gamma = (1 - \beta^2)^{-\frac{1}{2}}$ .  $\gamma$  is the relativistic factor, which measures the total particle energy,  $E = pc/\beta$ , in units of the particle rest energy,  $E_0 = m_0 c^2$ .

The fractional change in  $\beta$  is related to the fractional change in  $p$ .

$$\frac{\Delta p}{p} = \gamma^2 \frac{\Delta\beta}{\beta} \quad (2.7)$$

Substituting  $\Delta\beta/\beta$  into eq. 2.5, we get

$$\frac{\Delta f_{rf}}{f_{rf}} = \frac{1}{\gamma^2} \frac{\Delta p}{p} - \frac{\Delta R}{R} \quad (2.8)$$

For the constant magnetic field, a particle will have a different orbit, if it is slightly shifted in momentum. The “momentum compaction factor”  $\alpha_p$ <sup>2</sup> is defined as:

$$\frac{\Delta R}{R} = \alpha_p \frac{\Delta p}{p} \quad (2.9)$$

Substituting eq. 2.9 into eq. 2.8, we finally obtain the required relation between frequency offset and momentum error.

$$\frac{\Delta f_{rf}}{f_{rf}} = \left( \frac{1}{\gamma^2} - \alpha_p \right) \frac{\Delta p}{p} \quad (2.10)$$

The phase-slip factor  $\eta$  is defined as

$$\eta = \frac{1}{\gamma^2} - \alpha_p \quad (2.11)$$

which gives the relationship between revolution frequency and momentum for a given accelerator. When particles are at low energy ( $\eta > 0$ ), they run faster and arrive earlier at the rf cavity. When they are at high energy close to the speed of light ( $\eta < 0$ ), they can not run faster, but rather obtain more mass and are pushed to a dispersive orbit, resulting a late arrival at rf cavity [18].

## 2.1. Bunch and bucket

---

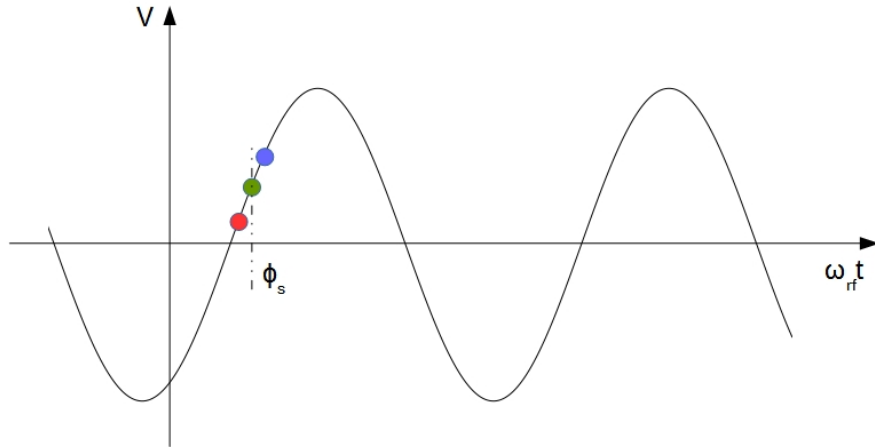


Figure 2.1: The longitudinal focusing of particles by rf voltage ( $\eta > 0$ ).  
The red spot represents a particle with higher energy, the blue spot a particle with lower energy and the green dot the synchronous particle.

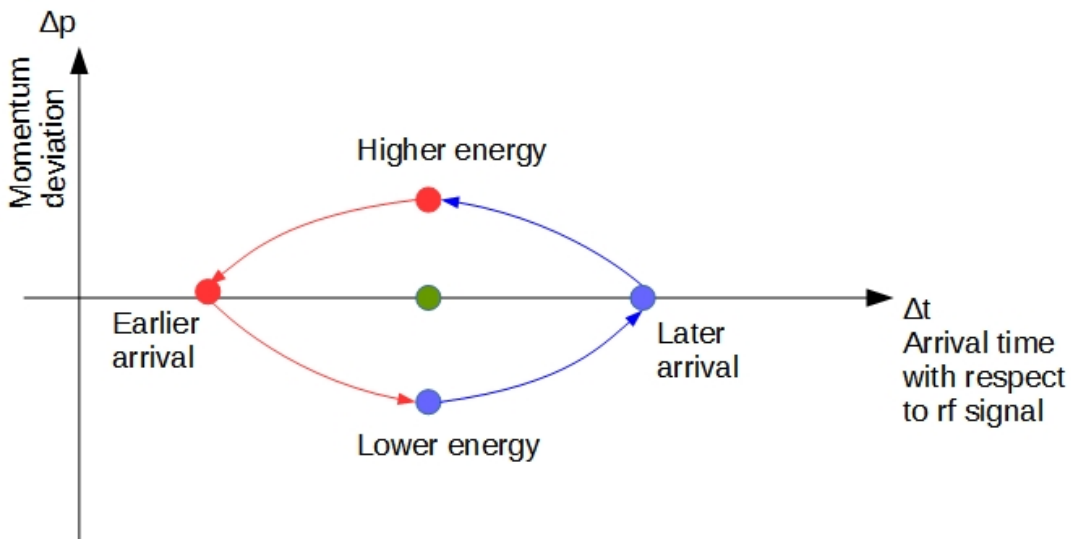


Figure 2.2: The longitudinal motion of asynchronous particles in longitudinal phase space ( $\eta > 0$ ).

The red spot represents a particle with higher energy, the blue spot a particle with lower energy and the green dot the synchronous particle. The red arrow shows the trend of a particle with higher energy and the blue arrow the trend of a particle with lower energy.

A bunch of particles consists of particles with slightly different momentum as the synchronous particle, which are called “asynchronous particle”. When  $\eta > 0$ , the longitudinal focusing of particles is explained in Fig. 2.1.

The synchronous particle is indicated by the green spot in Fig. 2.1. It will gain energy of  $qV_0 \sin \phi_s$  per passage through a rf cavity, where  $q$  is the charge of a par-

---

<sup>2</sup>FAIR complex is with  $\alpha_p > 0$ .

## 2.1. Bunch and bucket

---

ticle. When  $\eta > 0$ , a particle with smaller energy (blue spot) than the synchronous particle will run slower and have longer revolution period, arriving the same rf cavity later and seeing a higher accelerating voltage. This particle has a decreasing revolution period to the revolution period of the synchronous particle. During the decreasing process, the lack of energy is compensated step-by-step, closing to the synchronous particle. Oppositely for a particle with higher energy. As it is faster than the synchronous particle and has shorter revolution period, it will arrive at the rf cavity earlier, seeing a smaller accelerating voltage. This particle has an increasing revolution period to the revolution period of the synchronous particle. During the increasing process, the excess energy will be reduced step-by-step approaching to the synchronous particle. Particles will oscillate longitudinally around the synchronous particle. The oscillations are called “synchrotron oscillations”. This longitudinal motion is plotted in longitudinal phase space plane, See Fig. 2.2.

All particles oscillate around the synchronous particle and stay together, forming a “bunch”. The “bunch gap” is the area without any bunches. The area occupied by a bunch in the longitudinal phase space plane is called “longitudinal emittance”. First of all, we consider the synchronous phase is  $0^\circ$ . In this scenario, particles with small energy deviation follow an elliptical path inside the bunch. For a given rf system with specific rf voltage and harmonic number, there exists a maximum energy deviation. For particles with the energy deviations larger than the maximum energy deviation, they can not be trapped around the synchronous particle. The trajectory of a particle with the maximum energy deviation in longitudinal phase space plane defines a region with a specific size and form. This region is called “rf bucket” or “stationary rf bucket”, see Fig. 2.3. The maximum momentum deviation of the rf bucket is called “bucket height”. These buckets will exist as soon as the rf system is on and the number of circulating buckets is determined by the harmonic number and the bucket area and height are proportional to the rf voltage [18]. The order of buckets to be filled is called “bucket pattern”.

So far we give the definition of the bucket, when the synchronous particle sees no accelerating rf voltage. When the synchronous particle is accelerated, seeing the synchronous phase  $\phi_s$ , per passage through an rf cavity, it will gain energy of  $eV_0 \sin \phi_s$ . Particles oscillate around the synchronous particle at  $\phi_s$  with an elliptical orbit. The particle at  $\pi - \phi_s$  traces a closed fish-shaped orbit, which defines a “running rf bucket”, see Fig. 2.4. Particles at bigger phase than  $\pi - \phi_s$  can not be captured by the bucket.

The “bucket size” is defined as the area of longitudinal phase space plane enclosed by the bucket [18]. For the same rf voltage, the running bucket is always smaller than the stationary bucket. The ratio of bucket size of a running bucket to a stationary bucket is called “bucket area factor”,  $\alpha_b$ . The bucket area factor could be calculated by [18].

$$\alpha_b(\phi_s) \approx (1 - \sin(\phi_s))(1 + \sin(\phi_s)) \quad (2.12)$$

The oscillation of the asynchronous particles is called “synchrotron motion”. The angular synchrotron frequency <sup>3</sup>  $\omega_{syn}$  is [18]

$$\omega_{syn} = 2\pi f_{rev} \sqrt{\frac{hqV_0|\eta \cos \phi_s|}{2\pi\beta^2 E_0}} \quad (2.13)$$

---

<sup>3</sup>For the small-amplitude synchrotron motion.

## 2.1. Bunch and bucket

---

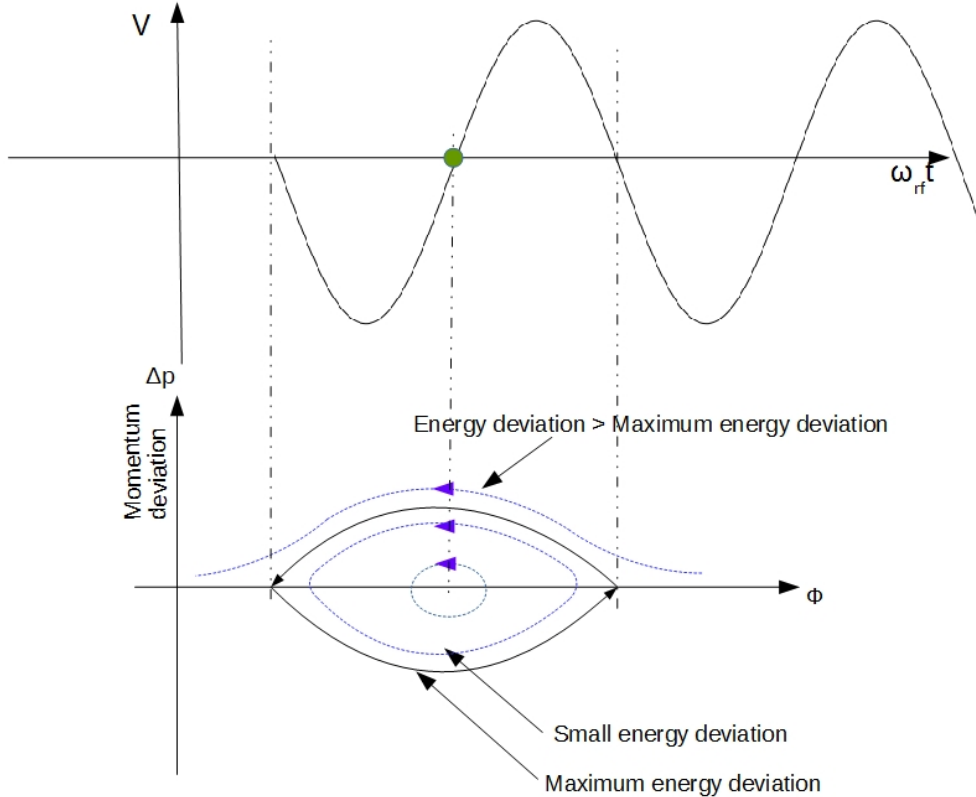


Figure 2.3: A stationary rf bucket.

The green dot represents the synchronous particle (top), the blue path the orbit of asynchronous particles and the black path the boundary of a stationary rf bucket (bottom).

Bunches are always captured in buckets. A synchrotron can have same amount of bunches as buckets. It is also possible for a synchrotron to have less amount of bunches than buckets, e.g. only a part of buckets are filled by bunches. A train of bunches circulating along a synchrotron to be transferred to buckets is defined as a “batch”.

The energy of a beam is related to the ‘magnetic rigidity’, which is defined as the following:

$$B\rho = \frac{p}{q} \quad (2.14)$$

where  $B$  is magnetic field, and  $\rho$  is the bending radius of a particle immersed in a magnetic field  $B$ . The ratio of  $p$  to  $q$  describes the “stiffness” of a beam, it can be considered as a measure of how much angular deflection results when a particle travels through a given magnetic field [19]. A rf cavity requirement for beam acceleration rate is

$$V_0 \sin \phi_s = 2\pi R \rho \dot{B} \quad (2.15)$$

Bunches must be injected exactly in the center of buckets for the preservation of the longitudinal emittance, which requires the energy and phase match between bunches and buckets. Besides, the shape of bunches to be transferred must match the shape of buckets to be injected in the longitudinal phase space plane. If the source and target synchrotrons have same rf frequencies, buckets of the source synchrotron must have same size and height as that of the target synchrotron for the match

## 2.1. Bunch and bucket

---

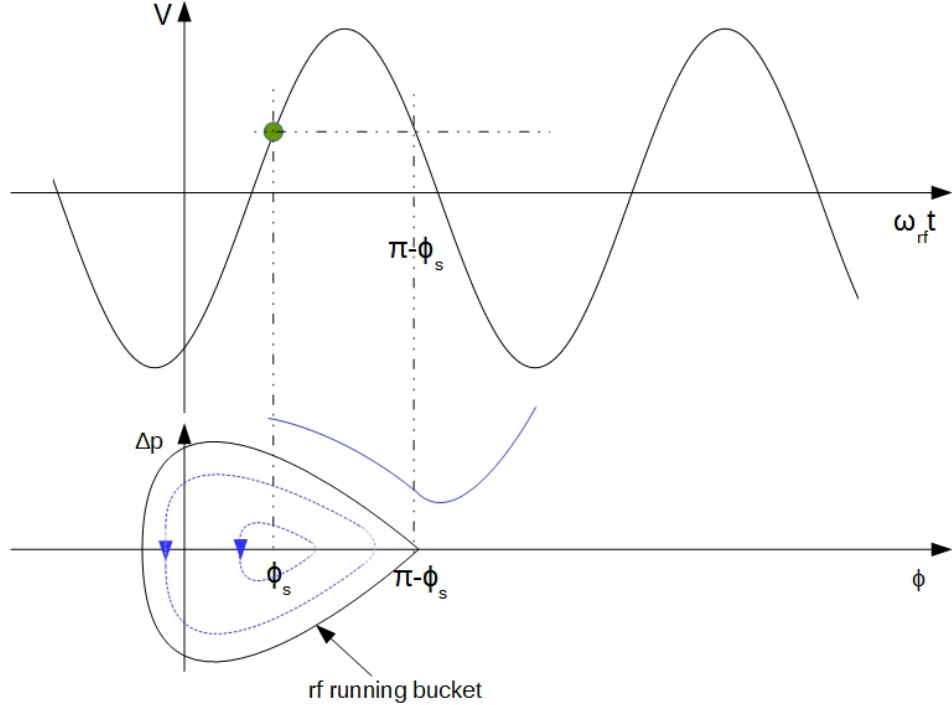


Figure 2.4: A running rf bucket.

The green dot represents the synchronous particle (top), the blue path the orbit of asynchronous particles and the black path the boundary of a running rf bucket (bottom).

between bunches and buckets. The voltage mismatch between bunches and buckets will cause an emittance blow-up. Fig. 2.5 illustrates a bunch-to-bucket injection with an energy, phase or voltage error.

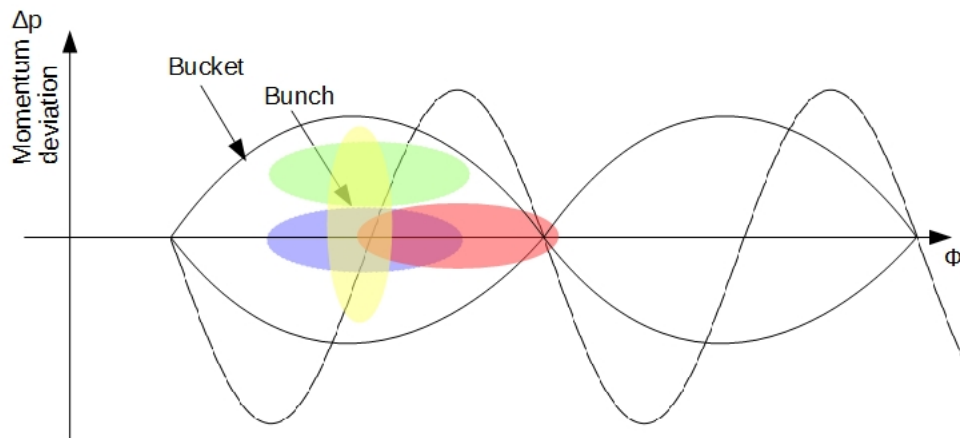


Figure 2.5: The bunch-to-bucket injection with errors.

The blue dot represents a injection without any error, the red dot a injection with a phase error, the green a injection with a energy error and the yellow a injection with a voltage error.

The bunch coordinates in the longitudinal phase space plane of the source synchrotron, just before transfer, must be accurately controlled, according to the bucket to be filled [20]. The bunch is transferred from the source to the target synchrotron

## 2.2. Phase match

---

with the same energy. So the beam has the same momentum for both synchrotrons. According to eq. 2.14, the magnetic rigidity of two synchrotrons must be same.

$$(B\rho)^{src} = \frac{p}{q} = (B\rho)^{trg} \quad (2.16)$$

Where the superscript of the symbol denotes the synchrotron, *src* represents the source synchrotron and *trg* the target synchrotron. The energy and voltage match will be done by machine physicists, which are out of the scope of this dissertation.

Before the B2B transfer, the revolution frequency of two synchrotrons must meet the following relation based on eq. 2.3.

$$C^{src} f_{rev}^{src} = \beta c = C^{trg} f_{rev}^{trg} \quad (2.17)$$

where  $C^X$  represents the circumference of a specific synchrotron. A group of new symbols are necessary to be defined. The revolution frequency and rf cavity frequency by  $f_{rev}^X$  and  $f_{rf}^X$ , the harmonic number by  $h^X$ . The superscript  $X$  could be either *src* or *trg* denoting the source or target synchrotron.

Due to the relation between the revolution frequency and rf frequency, eq. 2.2, the ratio between rf frequencies of two rf systems is

$$\frac{f_{rf}^{src}}{f_{rf}^{trg}} = \frac{h^{src}}{h^{trg}} \cdot \frac{f_{rev}^{src}}{f_{rev}^{trg}} = \frac{h^{src}}{h^{trg}} \cdot \frac{C^{trg}}{C^{src}} \quad (2.18)$$

## 2.2 Phase match

Rf voltage of two rf systems of the large and small synchrotrons,  $V^l$  and  $V^s$ , are

$$V^l = V_0 \sin(2\pi f_{rf}^l t + \theta_1) \quad (2.19)$$

$$V^s = V_0 \sin(2\pi f_{rf}^s t + \theta_2) \quad (2.20)$$

where  $\theta_1$  and  $\theta_2$  are initial phases of two rf system. The phase difference between the synchrotron *a* and *b*,  $\Delta\phi_{a,b}$ , is defined as the corresponding phase of the rf system of the synchrotron *a* when the rf system of the synchrotron *b* has its positive zero-crossing points.

In order to get the phase difference between the large and small synchrotrons  $\Delta\phi_{l-s}$ , positive zero-crossing points of the small synchrotron happen at

$$t = \frac{2\pi x - \theta_2}{2\pi f_{rf}^s} \quad (2.21)$$

where  $x$  is a positive integer. Positive zero-crossing points correspond to phases of  $2\pi x$ . The phase difference  $\Delta\phi_{l-s}$  is

$$\Delta\phi_{l-s} = \frac{f_{rf}^l}{f_{rf}^s} (2\pi x - \theta_2) + \theta_1 \mod 2\pi \quad (2.22)$$

The phase difference must be with a required value when bunches are transferred to buckets. For the phase shift method, two rf frequencies of two rf systems with

## 2.2. Phase match

---

same frequency are needed. For the frequency beating method, two slightly different frequencies are required for the beating. These two rf frequencies are called “synchronization rf frequency”, denoted as  $f_{syn}^X$ .

Due to the circumference ratio between the source and target synchrotrons, there are several scenarios of the phase difference. For simplicity’s sake, the following analysis is from the perspective of the large/small synchrotrons instead of the source/-target synchrotrons. The superscript  $X$  of  $C^X$ ,  $f_{rev}^X$ ,  $f_{rf}^X$  and  $h^X$  will be either  $l$  or  $s$  denoting the large or small synchrotron.  $\Delta f$  represents the beating frequency,  $\kappa$ ,  $m$ ,  $n$ ,  $x$  and  $g$  are used to represent positive integers and  $\lambda$  the decimal number.

### 2.2.1 Circumference ratio is an integer

If the ratio of the circumference of the injection/extraction orbit of the large synchrotron to that of the small synchrotron is an integer, we have the following relation.

$$\frac{C^l}{C^s} = \kappa \quad (2.23)$$

From the circumference ratio, the revolution frequency ratio of two synchrotrons can be calculated.

$$\frac{f_{rev}^l}{f_{rev}^s} = \frac{1}{\kappa} \quad (2.24)$$

Based on eq. 2.24 and harmonic number, the  $f_{rf}^X$  is calculated by eq. 2.25 and eq. 2.26

$$f_{rf}^s = h^s \cdot f_{rev}^s = h^s \cdot \kappa \cdot f_{rev}^l \quad (2.25)$$

$$f_{rf}^l = h^l \cdot f_{rev}^l \quad (2.26)$$

Dividing eq. 2.26 by eq. 2.25, we get

$$\frac{f_{rf}^l}{f_{rf}^s} = \frac{h^l}{h^s \cdot \kappa} \quad (2.27)$$

Substituting  $\frac{f_{rf}^l}{f_{rf}^s}$  in eq. 2.27 into eq. 2.22, we get the phase difference between the large and small synchrotrons  $\Delta\phi_{l-s}$ .

$$\Delta\phi_{l-s} = \frac{h^l}{h^s \cdot \kappa} (2\pi x - \theta_2) + \theta_1 \mod 2\pi = \textcolor{red}{x} \cdot \frac{h^l}{h^s \kappa} \cdot 2\pi - \frac{h^l}{h^s \kappa} \theta_2 + \theta_1 \mod 2\pi \quad (2.28)$$

Only  $x$  is a variable in eq. 2.28, which is marked in red color. From the 1<sup>st</sup> item in eq. 2.36, we know that the phase difference  $\Delta\phi_{l-s}$  is constant when  $x$  is the integer multiple of the  $h^s \kappa$ . Namely, the rf signal of the large synchrotron has a constant phase every  $(h^s \kappa)^{th}$  positive zero-crossing of the rf signal of the small synchrotron. The constant phase of the rf system of the large synchrotron happens at the frequency of  $f_{rf}^l/h^l$  and the corresponding positive zero-crossing of the rf system of the small synchrotron at the frequency of  $f_{rf}^s/(h^s \kappa)$ . Similarly, we can get these two rf frequencies for the phase difference between the small and large synchrotrons  $\Delta\phi_{s-l}$ . Hence,  $f_{rf}^l/h^l$  and  $f_{rf}^s/(h^s \kappa)$  are the synchronization rf frequencies for the phase shift method, namely,  $f_{syn}^l = f_{rf}^l/h^l$  and  $f_{syn}^s = f_{rf}^s/(h^s \kappa)$ . In this scenario, the phase match must be achieved by a phase shift of one of rf systems.

## 2.2. Phase match

---

So far we get only one possible pair of the synchroniation rf frequencies for the phase shift method, but this pair is not the best one. It is easier for the LLRF system to produce rf frequencyies closer to  $f_{rf}^l$  or  $f_{rf}^s$ . What is more, the possible pair with large frequencies reduces the period of the occurance of the required phase difference. Hence, the pair of the synchroniation rf frequencies with largest frequencies are preferred. They are

$$f_{syn}^l = \frac{f_{rf}^l}{h^l/Y} \quad (2.29)$$

$$f_{syn}^s = \frac{f_{rf}^s}{h^s\kappa/Y} \quad (2.30)$$

where  $Y$  is defined as the Greatest Common Divisor (GCD) of  $h^l$  and  $h^s \cdot \kappa$ .

Fig. 2.6 illustrates an example with  $\kappa = 5$ ,  $h^s = 1$  and  $h^l = 10$ . So  $f_{rf}^l = 2f_{rf}^s$ . GCD of  $h^l$  and  $h^s \cdot \kappa$  is 5. Hence, according to eq. 2.29 and eq. 2.30, two synchronization rf frequencies are  $f_{syn}^l = f_{rf}^l/2$  and  $f_{syn}^s = f_{rf}^s$ . The constant phase difference  $\Delta\phi_{l,s}$  happens every  $h^l/Y = 2$  rf period of the large synchrotron or every  $(h^s \cdot \kappa)/Y = 1$  rf period of the small synchrotron (red rectangle in Fig. 2.6).

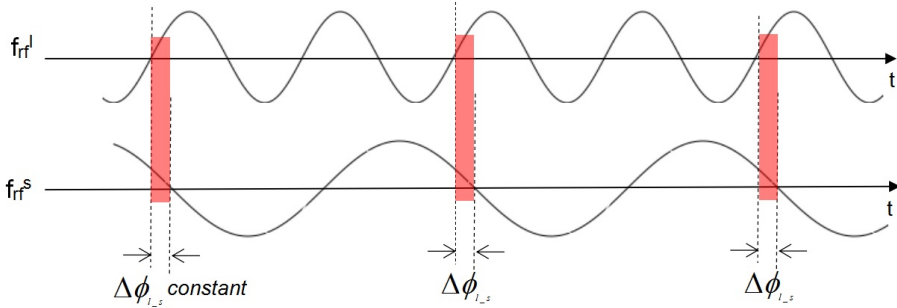


Figure 2.6: Constant phase difference between two rf systems when circumference ratio is an integer.

The red rectangles represent the constant phase difference periodically.

### 2.2.2 Circumference ratio is close to an integer

If the ratio of the circumference of the injection/extraction orbit of the large synchrotron to that of the small synchrotron is close to an integer. Eq. 2.23 changes to

$$\frac{C^l}{C^s} = \kappa + \lambda \quad (2.31)$$

where  $\lambda$  is the decimal and in the range of  $10^{-3}$ . From the circumference ratio, the revolution frequency ratio of two synchrotrons can be calculated.

$$\frac{f_{rev}^l}{f_{rev}^s} = \frac{1}{\kappa + \lambda} \quad (2.32)$$

Based on eq. 2.32 and harmonic number, the  $f_{rf}^X$  are calculated by eq. 2.33 and eq. 2.34

$$f_{rf}^s = h^s \cdot f_{rev}^s = h^s \cdot (\kappa + \lambda) \cdot f_{rev}^l \quad (2.33)$$

## 2.2. Phase match

---

$$f_{rf}^l = h^l \cdot f_{rev}^l \quad (2.34)$$

We could get the relation between  $f_{rf}^s$  and  $f_{rf}^l$  by dividing eq. 2.34 by eq. 2.33.

$$\frac{f_{rf}^l}{f_{rf}^s} = \frac{h^l}{h^s \cdot (\kappa + \lambda)} = \frac{h^l}{h^s \cdot \kappa + h^s \cdot \lambda} \quad (2.35)$$

Substituting  $\frac{f_{rf}^l}{f_{rf}^s}$  in eq. 2.35 into eq. 2.22, we get the phase difference between the large and small synchrotrons  $\Delta\phi_{l-s}$ .

$$\begin{aligned} \Delta\phi_{l-s} &= \frac{h^l}{h^s \kappa + h^s \lambda} (2\pi x - \theta_2) + \theta_1 \mod 2\pi \\ &= \frac{h^l}{h^s \kappa + h^s \lambda} \cdot 2\pi x - \frac{h^l}{h^s \kappa + h^s \lambda} \cdot \theta_2 + \theta_1 \mod 2\pi \end{aligned} \quad (2.36)$$

In eq. 2.36,  $h^s \lambda$  is much smaller than  $h^s \kappa$ . When  $x$  is the integer multiple of  $h^s \kappa$ , namely  $x = gh^s \kappa$  ( $g$  represents a positive integer), we have the following relation from eq. 2.36.

$$\Delta\phi_{l-s} = \cancel{g} \cdot h^l \cdot 2\pi - \cancel{g} \cdot \frac{h^l h^s \lambda}{h^s \kappa + h^s \lambda} 2\pi - \frac{h^l}{h^s \kappa - h^s \lambda} \theta_2 + \theta_1 \mod 2\pi \quad (2.37)$$

Only  $g$  is a variable in eq. 2.37, which is marked in red color. From the 2<sup>nd</sup> item in eq. 2.37, we know that the phase difference  $\Delta\phi_{l-s}$  increases at the speed of  $\frac{h^l h^s \lambda}{h^s \kappa + h^s \lambda} \cdot 2\pi$  ( $h^l h^s \lambda$  is much smaller than  $h^s \kappa + h^s \lambda$ ) every the  $(h^s \kappa)^{th}$  positive zero-crossing of the rf system of the small synchrotron. From the 1<sup>st</sup> item in eq. 2.37, the phase step growth of the rf system of the large synchrotron happens at the frequency of  $f_{rf}^l/h^l$  and the corresponding positive zero-crossing of the rf system of the small synchrotron at the frequency of  $f_{rf}^s/(h^s \kappa)$ . Similarly, we can get these two rf frequencies for the phase difference between the small and large synchrotrons  $\Delta\phi_{s-l}$ . Hence,  $f_{rf}^l/h^l$  and  $f_{rf}^s/(h^s \kappa)$  are the synchronization rf frequencies for the frequency beating method, namely,  $f_{syn}^l = f_{rf}^l/h^l$  and  $f_{syn}^s = f_{rf}^s/(h^s \kappa)$ . In this scenario, the rf frequency can be detuned on one of rf systems.

Similarly as the scenario of the integer circumference ratio, the pair of the synchronization rf frequencies with largest frequencies are

$$f_{syn}^l = \frac{f_{rf}^l}{h^l/Y} \quad (2.38)$$

$$f_{syn}^s = \frac{f_{rf}^s}{h^s \kappa/Y} \quad (2.39)$$

$Y$  is the GCD of  $h^l$  and  $h^s \cdot \kappa$ . In this scenario, the phase difference between two rf systems varies periodically. The frequency of the phase variation is defined as the beating frequency  $\Delta f$ . There is one time of point within the beating period, when two rf systems match phase. The beating frequency is

$$\Delta f = |f_{syn}^l - f_{syn}^s| \quad (2.40)$$

Fig. 2.7 illustrates an example. The beating frequency must not be too large in order to guarantee the precise of the phase match due to the step grown phase, but also not too small to satisfy the time constraint for the phase match.

## 2.2. Phase match

---

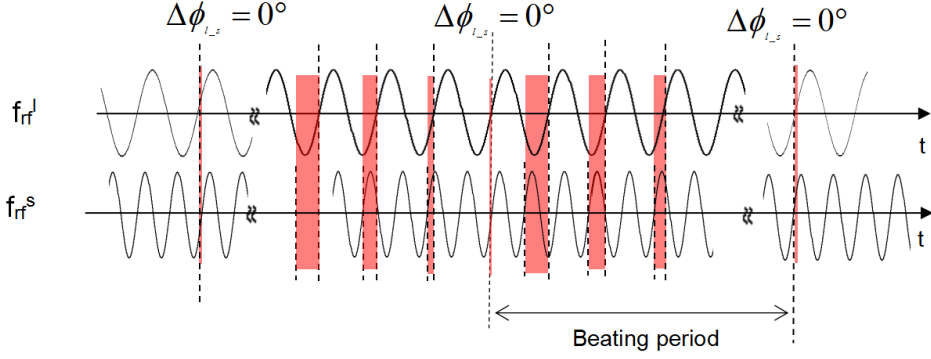


Figure 2.7: Periodical phase difference between two rf systems when circumference ratio is close to an integer.

The red rectangles represent the step grown phase difference.

### 2.2.3 Circumference ratio is far away from an integer

When the circumference ratio of the large synchrotron to that of the small synchrotron is far away from an integer, the circumference ratio of eq. 2.41 can be expressed as

$$\frac{C^l}{C^s} = \frac{m}{n} + \lambda \quad (2.41)$$

Substituting  $\kappa$  by  $m/n$  into eq. 2.35, we could get the relation between  $f_{rf}^s$  and  $f_{rf}^l$ .

$$\frac{f_{rf}^l}{f_{rf}^s} = \frac{h^l \cdot n}{h^s \cdot m + h^s \cdot \lambda \cdot n} \quad (2.42)$$

Substituting  $\frac{f_{rf}^l}{f_{rf}^s}$  in eq. 2.42 into eq. 2.22, we get the phase difference between the large and small synchrotrons  $\Delta\phi_{l,s}$ .

$$\begin{aligned} \Delta\phi_{l,s} &= \frac{h^l \cdot n}{h^s \cdot m + h^s \cdot \lambda \cdot n} (2\pi x - \theta_2) + \theta_1 \mod 2\pi \\ &= \frac{h^l \cdot n}{h^s \cdot m + h^s \cdot \lambda \cdot n} 2\pi x - \frac{h^l \cdot n}{h^s \cdot m + h^s \cdot \lambda \cdot n} \theta_2 + \theta_1 \mod 2\pi \end{aligned} \quad (2.43)$$

In eq. 2.43,  $h^s \lambda n$  is much smaller than  $h^s m$ . When  $x$  is the integer multiple of  $h^s m$ , namely  $x = gh^s m$ , we have the following relation from eq. 2.43.

$$\Delta\phi_{l,s} = g \cdot h^l n \cdot 2\pi - g \cdot \frac{h^l h^s \lambda n^2}{h^s m + h^s \lambda n} 2\pi - \frac{h^l \cdot n}{h^s \cdot m + h^s \cdot \lambda \cdot n} \theta_2 + \theta_1 \mod 2\pi \quad (2.44)$$

Only  $g$  is a variable in eq. 2.44, which is marked in red color. From the 2<sup>nd</sup> item in eq. 2.44, we know that the phase difference  $\Delta\phi_{l,s}$  increase at the speed of  $\frac{h^l h^s \lambda n^2}{h^s m + h^s \lambda n} \cdot 2\pi$  ( $h^l h^s \lambda n^2$  is much smaller than  $h^s m + h^s \lambda n$ ) every the  $(h^s m)^{th}$  positive zero-crossing of the rf system of the small synchrotron. From the 1<sup>st</sup> item in eq. 2.44, we know that the phase step growth of the rf system of the large synchrotron happens at the frequency of  $f_{rf}^l / (h^l n)$  and the corresponding positive zero-crossing of the rf system of the small synchrotron at the frequency of  $f_{rf}^s / (h^s m)$ . Similarly, we

### 2.3. Phase alignment of two rf systems

---

can get these two rf frequencies for the phase difference between the small and large synchrotrons  $\Delta\phi_{s,l}$ . Hence,  $f_{rf}^l/(h^l n)$  and  $f_{rf}^s/(h^s m)$  are the synchronization rf frequencies for the frequency beating method, namely,  $f_{rf}^l/(h^l n)$  and  $f_{syn}^s = f_{rf}^s/(h^s m)$ . In this scenario, the rf frequency can be detuned on one of rf systems.

Similarly as the scenario of the integer circumference ratio, the pair of the synchronization rf frequencies with largest frequencies are

$$f_{syn}^l = \frac{f_{rf}^l}{h^l n / Y} \quad (2.45)$$

$$f_{syn}^s = \frac{f_{rf}^s}{h^s m / Y} \quad (2.46)$$

$Y$  is the GCD of  $h^l n$  and  $h^s m$ . In this scenario, the phase difference between two rf systems varies periodically. The beating frequency is

$$\Delta f = |f_{syn}^l - f_{syn}^s| \quad (2.47)$$

In this scenario, the phase difference between two rf systems also varies periodically. There is one time of point within the beating period, when two rf systems match phase.

There are various combination of  $m/n$  and  $\lambda$ .  $\lambda$  determines the beating speed. The smaller, the more precise the phase match.  $(h^l \cdot n)/Y$  and  $(h^s \cdot m)/Y$  determines the two slightly different frequencies. The bigger  $(h^l \cdot n)/Y$  and  $(h^s \cdot m)/Y$ , the smaller two synchronization rf frequencies, which has higher requirement for rf system. So we have to find a proper combination of  $m/n$  and  $\lambda$ .

## 2.3 Phase alignment of two rf systems

Before the B2B transfer process, feedback loops for the deviations correction of the particles from reference states (e.g. position and velocity) must switch off or freeze. e.g. beam phase feedback loop [21] and bunch-by-bunch longitudinal rf feedback loop [22].

For different scenarios mentioned in Sec. 2.2, two methods available for the phase alignment of two rf systems. The synchronization is achieved by an azimuthal positioning of the bunch in the source synchrotron or the bucket in the target synchrotron. This is so-called "phase shift method". When two rf frequencies are slightly different, they are beating, perceived as periodic variations in phase difference, whose rate is the difference between the two frequencies. The synchronization is automatically achieved. This is so-called "frequency beating method". Both methods provide a time frame for the B2B transfer, within which a bunch could be transferred into a bucket with the bunch-to-bucket center mismatch smaller than the upper bound. The time frame is called "synchronization window".

### 2.3.1 Phase shift method

The rf system of the source or target or both synchrotrons are modulated away from their nominal value for a period of time and then modulated back so that the phase shift created by the frequency modulation could compensate for the required phase difference. During the phase shift process, particles are accelerated or decelerated.

### 2.3. Phase alignment of two rf systems

---

Eq. 2.48 gives the relation between the required phase shift  $\Delta\phi$  and the frequency modulation.

$$\Delta\phi = 2\pi \int_{t_0}^{t_0+T} \Delta f_{rf}(t) dt \quad (2.48)$$

The required phase shift is determined by the frequency offset  $\Delta f_{rf}$  and the duration of the frequency modulation  $T$ . It starts at  $t_0$ . For the phase alignment, the phase of either synchrotron can be shifted backward or forward.

After the phase shift, the bunches of the source synchrotron are phase aligned with buckets of the target synchrotron. Theoretically the synchronization window is infinitely long by the phase shift method. In fact, the beam feedback loop on the rf system is frozen or switched off before the B2B transfer, so the beam is stable for short time, e.g. 10 ms. Hence, bunches must be transferred as soon as possible. The phase shift process must be performed slowly enough for the beam to follow.

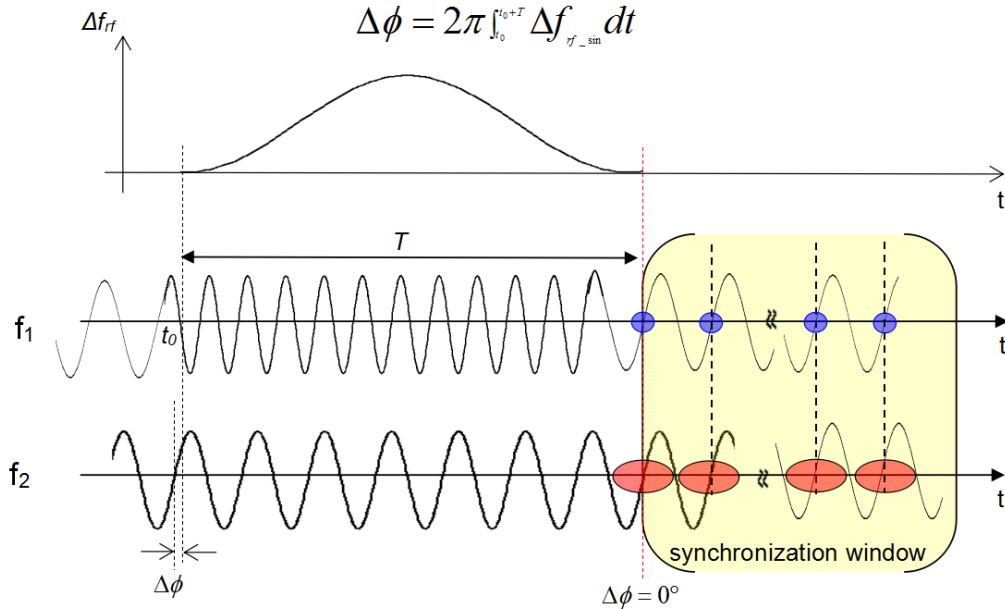


Figure 2.8: The illustration of the phase shift method.  
The blue dots represent bunches of the source synchrotron and the red dots  
buckets of the target synchrotron.

Fig. 6.12 illustrates the phase shift method. The first and second sinusoidal signals are rf signals with specific harmonic numbers respectively from the source and target synchrotrons. For the phase shift method, two signals are of the same frequency. The time-of-flight between bunches and buckets is compensated here. The red dashed line shows the end of the phase shift process ( $\Delta\phi = 0^\circ$ ) and the beginning of the synchronization window, drawn in yellow. After the phase shift, bunches match with buckets. A sinusoidal frequency modulation  $\Delta f_{rf\_sin}$  with a fixed duration time  $T$  is used as an example for the phase shift.

$$\Delta f_{rf\_sin} = A[1 - \cos \frac{2\pi}{T}(t - t_0)] \quad (2.49)$$

where  $A$  is the amplitude of the sinusoidal wave. Based on eq. 2.48, the area of the

### 2.3. Phase alignment of two rf systems

---

sinusoidal wave equals to  $\Delta\phi/2\pi$ . We can calculate the amplitude  $A$

$$A = \frac{\Delta\phi}{2\pi} \cdot \frac{1}{T} \quad (2.50)$$

A particular case of the B2B synchronization occurs, when the target synchrotron is empty, i.e. it did not capture any bunch yet, the phase jump can be done for the target synchrotron.

Now we analyze the rf frequency modulation of the phase shift from the beam dynamics perspective.

- Momentum shift and radial excursion

A rf frequency modulation introduces the momentum shift.

$$\frac{\Delta p}{p} = \frac{1}{\frac{1}{\gamma^2} - \alpha_p} \cdot \frac{\Delta f_{rf}}{f_{rf}} \quad (2.51)$$

Substituting  $\Delta R/R$  in eq. 2.9 into eq. 2.51, we get the radial excursion according to a rf frequency modulation.

$$\frac{\Delta R}{R} = \frac{1}{\frac{1}{\alpha_p \gamma^2} - 1} \cdot \frac{\Delta f_{rf}}{f_{rf}} \quad (2.52)$$

The rf frequency modulation causes a radial excursion. There is a limit on the maximum radial excursion of every synchrotron, so there is a maximum frequency offset for the rf frequency modulation.

- Shift of synchronous phase

The beam acceleration or deceleration accompanies with the rf frequency modulation, so the synchronous phase deviates from  $0^\circ$  and the momentum is shifted from  $p$  to  $p + \dot{\Delta}p$ . Based on eq. 2.14, we can get the first derivative of the magnetic rigidity

$$\dot{B}\rho = \frac{\dot{\Delta}p}{q} = B\rho \frac{\dot{\Delta}p}{p} \quad (2.53)$$

Substituting  $\dot{B}\rho$  in eq. 2.53 into eq. 2.15, we get

$$V_0 \sin \phi_s = 2\pi(R + R_0)B\rho \frac{\dot{\Delta}p}{p} \quad (2.54)$$

Substituting  $\dot{\Delta}p$  in the first derivative of eq. 2.9 into eq. 2.54, we get the simplified relation, eq. 2.55, between the change in the synchronous phase  $\phi_s$  and the radius change rate based on the prerequisite that  $\Delta R/R$  is very small and negligible. The maximum radial excursion of FAIR synchrotons  $\Delta R/R$  is in the  $10^{-4}$  range. The full formula is listed in [23].

$$V_0 \sin \phi_s = \frac{2\pi B\rho}{\alpha_p} \frac{\dot{\Delta}p}{p} \quad (2.55)$$

Eq. 2.55 shows that the synchronous phase is proportional to the momentum change rate. According to eq. 2.51, the momentum change rate is proportional to the rf frequency modulation rate. Hence, the synchronous phase is proportional to  $\dot{\Delta}f_{rf}$ .

## 2.3. Phase alignment of two rf systems

---

- Bucket size

At the flattop, the bucket is a stationary bucket. During the frequency modulation process, the bucket becomes a running bucket with  $\phi_s \neq 0^\circ$ . The bucket area factor is calculated by eq. 2.12. Buckets must be big enough to capture bunches. Eq. 2.12 shows that the bucket area factor is in inverse proportion to the synchronous phase. The synchronous phase must be small enough to guarantee the bucket size, so  $\Delta\dot{f}_{rf}$  must be small enough, namely the change of the rf frequency modulation must be slow enough.

- Adiabaticity

A process is called “adiabatic” when the rf frequency is changed slowly enough for the beam to follow. The condition that the rf frequency varies slowly can be expressed by

$$\varepsilon = \frac{1}{\omega_{syn}^2} \left| \frac{d\omega_{syn}}{dt} \right| \ll 1 \quad (2.56)$$

where  $\varepsilon$  is the adiabaticity parameter. For the synchrotron frequency, eq. 2.13, all of the other variables change very slowly compared with  $\phi_s$ . From eq. (2.56) and eq. (2.13), the adiabaticity can be written as follows [23]:

$$\varepsilon \approx \frac{1}{2\omega_{syn,0}} \left| \tan \phi_s \dot{\phi}_s \right| \quad (2.57)$$

where  $\omega_{syn,0}$  is the synchrotron frequency with no frequency modulation. Form the adiabaticity eq. 2.57,  $\phi_s$  and  $\dot{\phi}_s$  must be small enough to guarantee the adiabaticity. So not only  $\Delta\dot{f}_{rf}$  but also  $\ddot{f}_{rf}$  must be existing and small enough. Namely,  $\Delta\dot{f}_{rf}$  must be continuous.

- Tune shift

So far the rf frequency modulation is analyzed from the longitudinal beam dynamics perspective. Because of the momentum shift, the rf frequency modulation has an influence on the transverse beam dynamics as well. The beam particle’s tune  $Q_{x/y}$ , defined as the frequency of the horizontal/vertical oscillations, and chromaticity  $Q'_{x/y}$  as their horizontal/vertical dependence on particle momentum ???. The momentum spread  $\Delta p/p \neq 0$  during the phase shift process causes horizontal/vertical tune shifts  $\Delta Q_{x/y}$  [24].

$$\Delta Q_{x/y} = Q_{x/y} \frac{\Delta p}{p} \quad (2.58)$$

The momentum shift of FAIR synchrotrons  $\Delta p/p_0$  is in the  $10^{-4}$  range and the chromaticity is about 10 Hz. So the tune shift is relative small and has almost no influence on the transverse motion.

According to the beam dynamics analysis, there are several requirements for the rf frequency modulation. There exists a maximum rf frequency offset.  $\Delta\dot{f}_{rf}$  must be not only continuous but also small enough. What is more,  $\ddot{f}_{rf}$  must be small enough.

### 2.3.2 Frequency beating method

The frequency beating method uses the effect of two rf signals of slightly different frequencies, perceived as periodic variations in phase difference whose rate is the difference between the two frequencies. When the circumference ratio of two synchrotrons are not integer, they are beating automatically. Or the rf frequency of the source or the target or both synchrotrons is detuned for the achievement of beating. During the frequency dutune process, particles are not accelerated or decelerated for the energy match. The synchronization is realized when the phase difference of the two rf frequencies corresponds to the required phase difference. The  $\Delta\phi$  is the mismatch between the bunch center and the corresponding bucket center. Because of the slightly different rf frequencies, a mismatch between the bunch and bucket centers exists. In principle, the B2B transfer requirement for FAIR allows a bunch-to-bucket center mismatch of  $\pm 1^\circ$ , which brings a symmetric time frame with respect to the time of the required phase difference. This is called the maximum synchronization window, drawn in yellow, see Fig. 2.9. The red dashed line shows the time for the required phase difference.

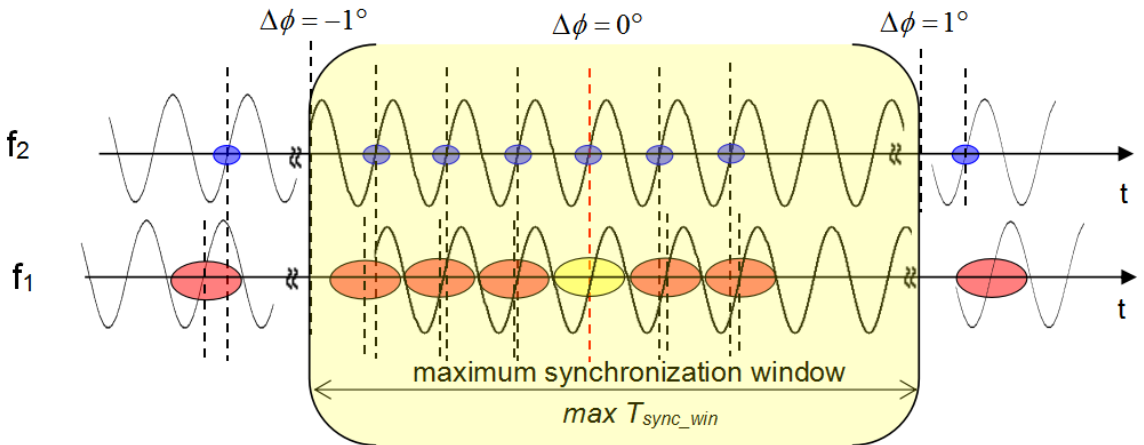


Figure 2.9: The illustration of the frequency beating method.

The blue dots represent bunches of the source synchrotron and the red dots buckets of the target synchrotron.

- For one bunch to one bucket injection per B2B transfer, the bunch is “perfectly“ injected into the center of the bucket. The “perfect“ injection does not mean that the bunch-to-bucket center mismatch  $\Delta\phi$  is  $0^\circ$ . It means the smallest mismatch with regard to other injection. The “perfect“ injection is determined by the beating frequency and the initial phase difference between these two signals. The maximum initial phase difference  $\Delta\varphi$  is calculated by eq. 2.59.

$$\frac{|1/(f_1 - f_2)|}{360^\circ} = \frac{1/f_1}{\Delta\varphi} \quad (2.59)$$

where  $f_1$  and  $f_2$  are two slightly different rf frequencies, the beating frequency is expressed as  $f_1 - f_2$ .

When the initial phase difference is  $0^\circ$ , the “perfect“ injection is with the mismatch  $\Delta\phi = 0^\circ$ .

## 2.4. Synchronization of extraction and injection kicker magnets

---

When the initial phase difference is slightly less than  $\Delta\varphi$ , the “perfect” injection is with the mismatch  $\Delta\theta$  slightly less than  $\Delta\varphi$ .

- For many bunches to many buckets injection per B2B transfer, only one bunch is “perfectly” injected into the corresponding bucket, which is represented by the yellow dot in Fig. 2.9. Other bunches on both sides of this bunch are injected into their corresponding buckets (red dots) with the mismatch due to two slightly different frequencies. The maximum synchronization window  $T_{sync\_win}$  is determined by the maximum tolerable bunch-to-bucket center mismatch  $\pm 1^\circ$ , see eq. 2.60.

$$\frac{|1/(f_1 - f_2)|}{360^\circ} = \frac{T_{sync\_win}}{1^\circ - (-1^\circ)} \quad (2.60)$$

The rf frequency is detuned at the end of the ramp. During the rf frequency detune process, the magnetic field and radius excursion react to the frequency detune in order to guarantee the energy match.

- Radius excursion and magnetic field modification

Because the momentum should not be affected by the frequency detune for the energy match, namely  $\Delta p=0$ , we can get the general relation between the radial excursion and rf frequency change by substituting  $\Delta p=0$  into eq. 2.9.

$$\frac{\Delta f_{rf}}{f_{rf}} = -\frac{\Delta R}{R} \quad (2.61)$$

When  $\Delta p = 0$ , we have the following relation between  $\Delta B/B$  and  $\Delta R/R$  [25].

$$\frac{1}{\alpha_p} \frac{\Delta R}{R} = -\frac{\Delta B}{B} \quad (2.62)$$

Substituting eq. 2.62 into eq. 2.61, we get the general relation between the magnetic field change and rf frequency change.

$$\frac{\Delta f_{rf}}{f_{rf}} = \alpha_p \cdot \frac{\Delta B}{B} \quad (2.63)$$

## 2.4 Synchronization of extraction and injection kicker magnets

A kicker magnet (or kicker) is a dipole magnet, which is used to rapidly switch particles between two paths. An injection kicker merges one beam into a circulating beam in a synchrotron and an extraction kicker diverts a circulating beam to leave a synchrotron. The B2B transfer needs a fast beam extraction and injection, which extracts and injects beam in a single-turn. Hence, a pulsed kicker magnet must be used with rapid rise time and fall time and the variable pulse flat-top [26]. Fig. 2.10 shows the schematic diagram of a kicker magnet. The energy storage module is charged with a high voltage power supply. It will be discharged via the transmission cable and the kicker magnet by switching on the pulse start switch. Before the

## 2.4. Synchronization of extraction and injection kicker magnets

---

increase of the magnetic field, there exist a preparation time for the kicker magnet. The magnet needs a certain period of time to increase from zero to a stable magnetic field, which is so-called a “rise time”. The pulse “flat-top” length can be modified by switching on the stop switch in correlation with the pulse start switch. When the pulse stop switch is switched off, the magnet needs a certain period of time to reduce to zero magnetic field. This period is so-called a “fall time” [27]. For the proper B2B transfer, the extraction and injection kickers must be synchronized with the beam. As soon as the tail of the circulating bunch passes the kicker, the start switch can be switched on. The pulse stop switch must be switched off in time in order not to affect the head of the next coming bunch in the synchrotron. The kicker control electronic produces the ignition signal to switch on/off two switches. Generally a preparation time of FAIR kickers is within the 5–10  $\mu\text{s}$  range. Compared with the FAIR rf frequency in the MHz range, a preparation time is not negligible, which could cause an increase of the bunch-to-bucket injection center mismatch especially for the frequency beating method. The kicker control electronic must take the preparation time into consideration, igniting kickers in advance of the preparation time.

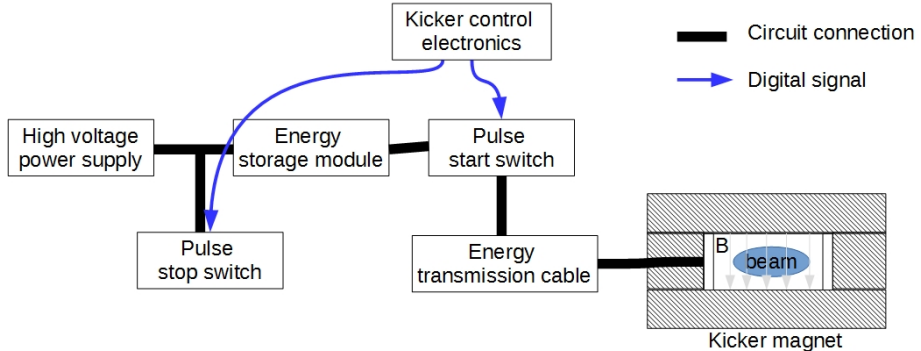


Figure 2.10: Schematic diagram of kicker magnet.

Most commonly, an extraction kicker is used to eject all bunches. Fig. 2.11 illustrates the rise time, flat-top and fall time of an extraction kicker. The tail of the circulating bunch passes the kicker at  $t_0$ . The start switch is switched on the preparation time earlier than  $t_0$ . The rise time starts at  $t_0$ . The flat-top of the magnetic field must be achieved before the head of the next circulating bunch passes the kicker at  $t_1$ . So the rise time of the extraction kicker must be shorter than the bunch gap. The flat-top has at least the length of bunches to be extracted. The stop switch is switched on earliest at  $t_2$ , when all bunches are extracted. Then there is no more bunch left in the synchrotron, so there is no constraint for the fall time.

For multi batches injection, see Fig. 2.12, the tail of the circulating bunch passes the kicker at  $t_0$ . The start switch is switched on the preparation time earlier than  $t_0$ . The rise time starts at  $t_0$ . The flat-top of the magnetic field must be achieved before bunches are injected at  $t_1$ . So the rise time of the injection kicker must be shorter than the bunch gap. For a single batch injection, the rise time is not constrained. The length of the flat-top is determined by the length of bunches to be injected. The stop switch is switched on as soon as the tail of the last injected bunch passes the kicker at  $t_2$ . The magnetic field must be reduced to zero before the head of the circulating bunch passes the kicker at  $t_3$ . So the fall time must be shorter than  $t_3 - t_2$ .

## 2.4. Synchronization of extraction and injection kicker magnets

---

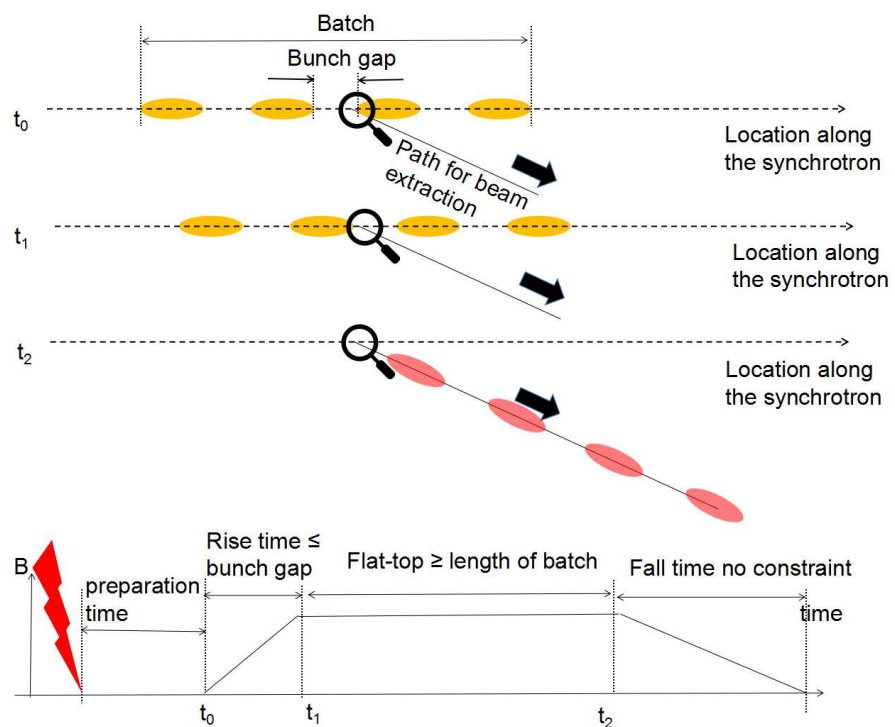


Figure 2.11: The rise time, flat-top and fall time of an extraction kicker. The yellow ellipses represent circulating bunches in the synchrotron, the red ones extracted bunches and the red lighting bolts kicker firing.

## 2.4. Synchronization of extraction and injection kicker magnets

---

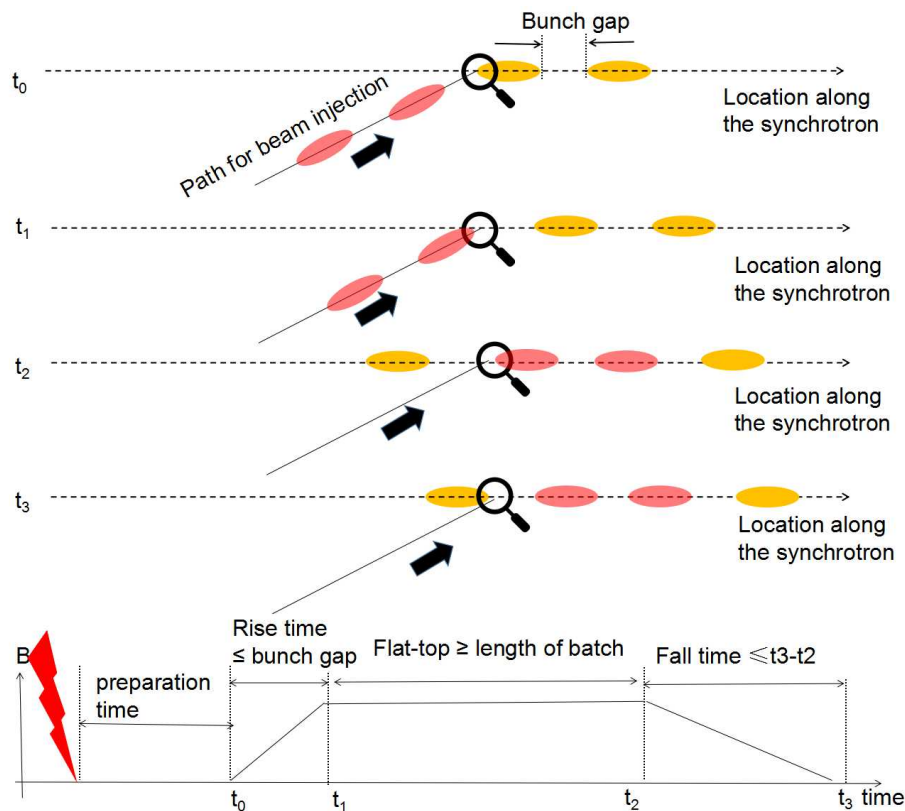


Figure 2.12: The rise time, flat-top and fall time of an injection kicker for multi batches injection.

The yellow ellipses represent circulating bunches in the synchrotron, the red ones bunches to be injected and the red lightning bolts kicker firing.

# Chapter 3

## Technical basis for the B2B transfer system

For the FAIR accelerator complex, synchronization of the B2B transfer will be realized by the FAIR control system and the Low-Level RF (LLRF) system. For the synchronization of LLRF system, the General Machine Timing (GMT) system is complemented and linked to the Bunchphase Timing System (BuTiS). Machine Protection System (MPS) protects SIS100 and subsequent accelerators or experiments from damage. Hence, the B2B transfer system for FAIR coordinates with the MPS system.

### 3.1 FAIR control system

The FAIR control system takes advantage of collaborations with CERN in using framework solutions like Front-End System Architecture (FESA) [28], LHC Software Architecture (LSA), White Rabbit (WR) [29]. It consists of the equipment layer, middle layer and application layer. The equipment layer consists of equipment interfaces, GMT and software representations of the equipment FESA. The middle layer provides service functionality both to the equipment layer and the application layer through the IP control system network. LSA is used for the Settings Management (SM). The application layer combines the applications for operators as GUI applications or command line tools. The application layer and the middle layer only request what the FAIR accelerator complex should do and transmit set values to the equipment layer. The SM supplies the schedule for the GMT by LSA [29, 30].

#### 3.1.1 BuTiS

Bunch Phase Timing System (BuTiS) serves as a campus-wide clocks distribution system with sub nanosecond resolution and stability over distances of several hundred meters while maintaining 100 ps per km timing stability [31]. Two BuTiS reference clocks 100 kHz P0 pulse and 10 MHz S1 phase reference signal are generated centrally in the BuTiS center. A star-shaped optical fiber BuTiS distribution system transfers these two reference clocks to the BuTiS local reference synthesizer all over the FAIR campus. The optical signal transmission delay between the BuTiS center and the different BuTiS local reference synthesizer is measured by a measurement setup in the BuTiS center. This measurement information is used to correct

### 3.1. FAIR control system

---

the phases of the signals generated in each BuTiS local reference synthesizer for the delay compensation. So at each BuTiS reference synthesizer, two delay compensated clock signals, 200 MHz C2 sine and 100 kHz T0 ident clocks, are generated from 100 kHz P0 and 10 MHz S1 reference clocks [31, 32]. The main task of BuTiS is the supply of the reference clock signals for Reference RF Signal RF systems, see Sec. 3.2 .

#### 3.1.2 GMT

The GMT system is contained in the equipment layer. It does not only synchronize all timing nodes with nanosecond accuracy over the whole FAIR campus, but also distributes timing messages to all timing nodes and controls all timing nodes to execute real-time actions at a designated time [30]. The GMT system is a time based system. The GMT consists of the Timing Master (TM), the White Rabbit (WR) timing network and timing nodes. The timing master is a logical device, containing the data master (DM), the clock master (CM) and the management master (MM). The data master receives a schedule for the operation of the FAIR accelerator complex from the Settings Management and provides the real-time schedule by broadcasting timing messages to the WR timing network, which will be received and executed by the corresponding timing node at the designated time. The clock master is a dedicated WR switch. It is the topmost switch layer of the WR timing network and provides the grandmaster clock and timestamps which are distributed to all other timing nodes in the timing network. The clock master derives its clock from BuTiS 200 MHz C2 and 100 kHz T0 clocks and timestamps distributed are phase locked to BuTiS clocks. The GMT system could generate BuTiS T0 and C2 with any timing nodes and timing nodes are capable to timestamp clock edges. All active components including timing nodes and WR switches are registered to the MM. The MM monitors and manages the active components of the GMT system [33, 34].

A timing message is sent across the WR network, so it must be contained in the Ethernet frame. An Ethernet frame including one timing message has a length of 110 byte, which is called “timing frame” in this dissertation. A Virtual LAN (VLAN)<sup>1</sup> is a group of FECs in the WR network that is logically segmented by function or application, without regard to the physical locations of the FECs. All FECs in the WR network are assigned to the DM VLAN, within which the DM forwards broadcast timing telegrams downwards to all FECs.

#### 3.1.3 Settings Management

The Settings Management (SM) is based on a physics model for accelerator optics, parameter space and overall relations between parameters and between accelerators. It supports off-line generation of accelerator settings, sending these settings to all involved devices, and programming the schedule for the GMT system [29]. The core component of SM is the LSA framework. A standardized LSA-API allows accessing data in a common way as basis for generic client applications for all accelerators. Using the LSA-API, applications can coherently modify settings [29]. E.g. the LSA generates timing constraints (e.g. ramp curve) as well as the equipment’s data

---

<sup>1</sup>[https://en.wikipedia.org/wiki/Virtual\\_LAN](https://en.wikipedia.org/wiki/Virtual_LAN)

### 3.2. LLRF system

---

settings (e.g. current) for all devices derived from physics parameters (e.g. beam energy). For FAIR, LSA is extended to model the overall schedule of all accelerators. Beams are described as “Beam Production Chains“ to allow a description from beam source to beam target for settings organization and data correlation.

#### 3.1.4 FESA

The FESA<sup>2</sup> is a framework used to fully integrate the large amount of front-end equipments into the accelerator control system. FESA was developed by CERN and has already been implemented into the CERN control system. Now it is developed further in collaboration with GSI for the FAIR project. For the FAIR project the necessary interaction with the timing nodes is realized by FESA. For a specific type of equipments, a FESA implementation accesses to the control interface of the equipments. The FESA class models the equipment as device, so the FESA output is called device class. The FEC use FESA to implement generic and equipment specific functions in form of the device classes. FESA provides JAVA based graphical user interfaces (GUI) to design, deploy, instantiate and test the device classes. Interaction with the equipment is also synchronized with the GMT system [28].

For time multiplexed operation of the accelerators, the FESA supports defining multiplexed properties. Before an accelerator schedule is started, the setting properties of FESA classes are pre-supplied by LSA from SM for all scheduled beams with specific settings accordingly. At runtime, FESA real time software actions are triggered by timing message, the actual beam specific data is then selected based on information carried by the timing message and send to the equipment.

## 3.2 LLRF system

The FAIR low-level rf (LLRF) system will be used in the existing synchrotrons SIS18 and ESR, as well as in the FAIR synchrotrons SIS100 and SIS300 and in CR, NESR, and RESR. It supports fast ramp rates and large frequency span for the acceleration of a variety of ion species, It supports different RF manipulations, including operation at different harmonic numbers, barrier bucket generation, bunch compression and longitudinal feedback. [35].

Each RF supply room has a Reference RF Signal distribution system shown in Fig. 3.1. The Reference RF Signals in different supply rooms are synchronized by BuTiS. BuTiS 200MHz C2 and 100kHz T0 clock signals are generated by BuTiS receivers in different supply rooms in phase. In Fig. 3.1, a number of Group DDS units are located in each supply room, which are synchronized by BuTiS local reference. The Group DDS signals can be routed to the different cavity systems by a Switch Matrix. All cavities in a synchrotron could be providing with the same Group DDS signal. The cavities at different harmonic numbers could be realized by using Group DDS signals with different harmonic numbers and by adjusting the harmonic number at the Cavity DDS accordingly. The Group DDS concept allows to synchronize a variety of cavities in a very flexible way [35].

All the cavities of SIS18 are driven from one supply room. The SIS100 cavities will be gathered in five acceleration sections, each of them is driven by a dedicated

---

<sup>2</sup><https://www-acc.gsi.de/wiki/FESA/WhatIsFESA>

### 3.2. LLRF system

---

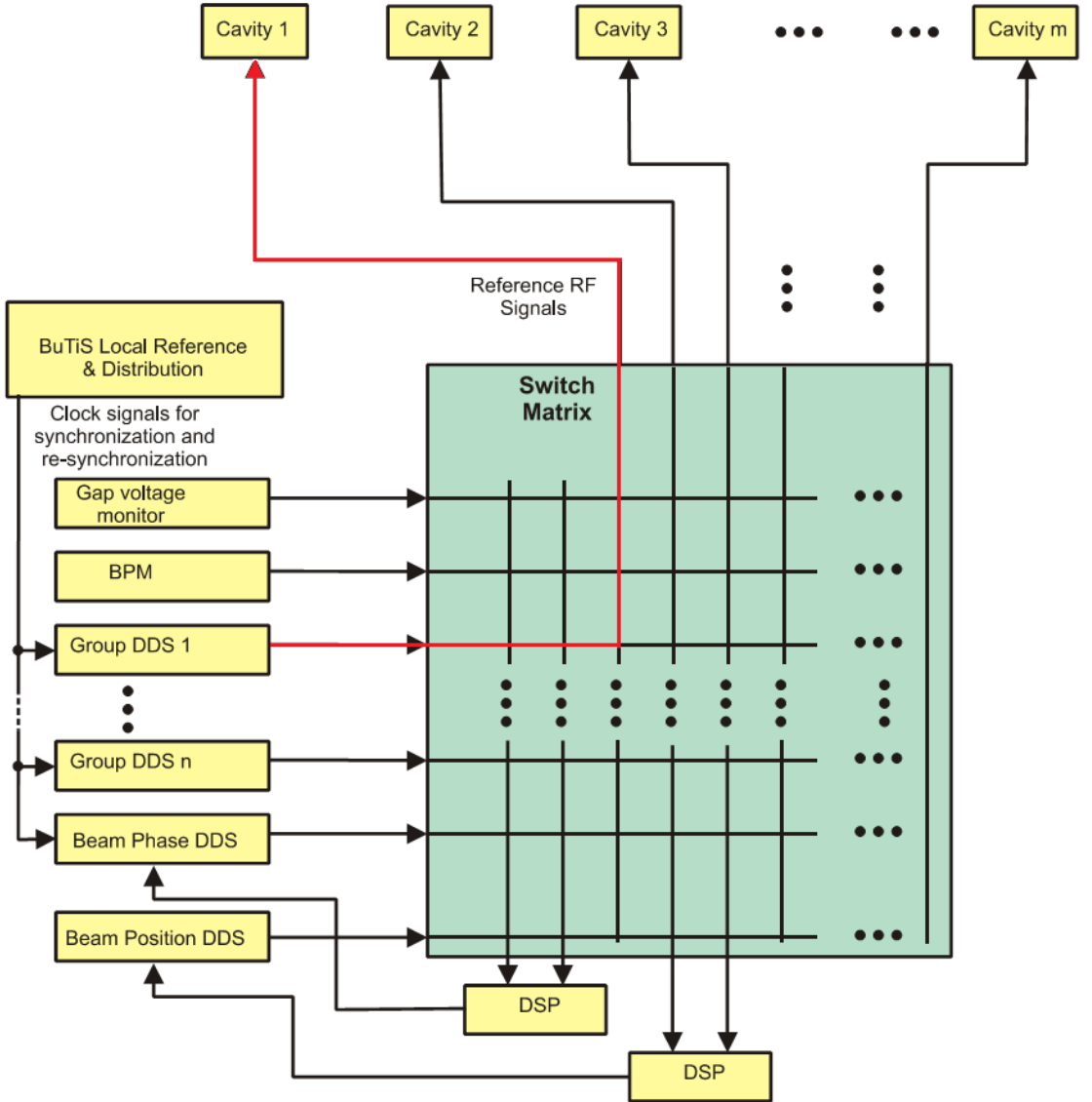


Figure 3.1: Reference RF Signal distribution system  
[35]

supply room.

RF cavities are driven by one of Reference RF Signals, which are supplied in every supply room . Fig. 3.2 shows the local cavity synchronization system, which synchronizes the local Cavity Direct Digital Synthesizer (DDS) unit to the Reference RF Signal. The cavity gets the RF signal from a local Cavity DDS unit, which receives RF Frequency Ramps from the Central Control System (CCS). A Digital Signal Processor (DSP)-System measures the phase difference between the Reference RF Signal and the gap voltage of the cavity. In the DSP system, a closed-loop control algorithm is implemented, which generates frequency corrections for the local Cavity DDS unit. This process is called local synchronization loop, which ensures that the phase of the gap voltage follows the phase of the Reference RF signal [35]. The path from the Group DDS 1 to Cavity 1 marked with the red line in Fig. 3.1 is realized by the local cavity synchronization in Fig. 3.2. The virtual rf cavity is a virtual position around the ring, to which the Reference RF Signal corresponds.

### 3.3. MPS system

---

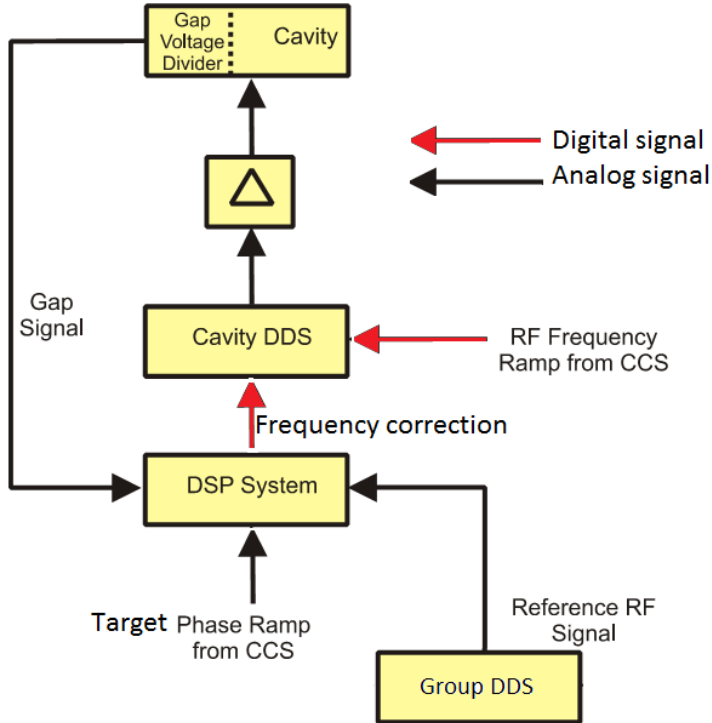


Figure 3.2: Local Cavity Synchronization  
[35]

In order to damp coherent longitudinal rigid dipole oscillations, the beam phase control loop is used. The phase difference between the beam signal and the Reference RF Signal is fed back via an FIR filter. The beam signal is obtained by a fast current transformer or a beam position monitor. The filter output is converted in a phase-correction and forwarded to the Group DDS. The corrections are added to the phase of the frequency ramp in the Cavity DDS, which results in a change of the phase of the gap voltage and thus a feedback to the beam [36]. Unfortunately, the actual beam phase control loop in SIS18 is not able to damp incoherent longitudinal rigid dipole oscillations. For SIS100, a bunch-by-bunch longitudinal rf feedback loop will be developed. The bunch-by-bunch longitudinal rf feedback loop generates a correction voltage in dedicated feedback cavities for a specified bunch [22].

## 3.3 MPS system

A MPS protects current accelerator and subsequent accelerators or experiments from damage or unacceptable failure, e.g. beam position is out of tolerance, rf cavity failure and so on. Thereby, the individual equipment is assumed self-protecting, which could trigger accelerator safety critical actions, such as an emergency beam dump<sup>3</sup>, a shutdown of magnets or a beam injection inhibit. In case of relevant equipment failures or other inappropriate equipment states, a MPS signal is generated from

---

<sup>3</sup>A beam dump is a device designed to absorb the beam.

### 3.4. Comparison between the FAIR B2B transfer system and the B2B transfer with the GSI control system

this equipment [37]. The FAIR B2B transfer must coordinate with the SIS100 emergency dump signal and the beam injection inhibit signal from the MPS.

The SIS100 emergency dump signal indicates that the beam should be transferred to the emergency dump as soon as possible. If the beam injection inhibit signal is off, the B2B transfer extraction and injection kickers are allowed to be fired. If the beam injection inhibit signal is on, the injection and extraction kickers will be blocked for firing.

## 3.4 Comparison between the FAIR B2B transfer system and the B2B transfer with the GSI control system

The existing GSI control system realizes the B2B transfer from SIS18 to ESR and ESR back to SIS18. It is an event based system, that event execution will start at the corresponding immediately upon event receipt. Events are directly sent from a “Pulszentrale”, who makes the schedule. Each accelerator has its own Pulszentrale, e.g. ESR is equipped with ESR-Pulszentrale and SIS18 with SIS-Pulszentrale. All devices are connected to distributed Equipment Controllers (EC) via field bus. ES is responsible for the receipt of the event and produces the pulse for the devices [38, 39].

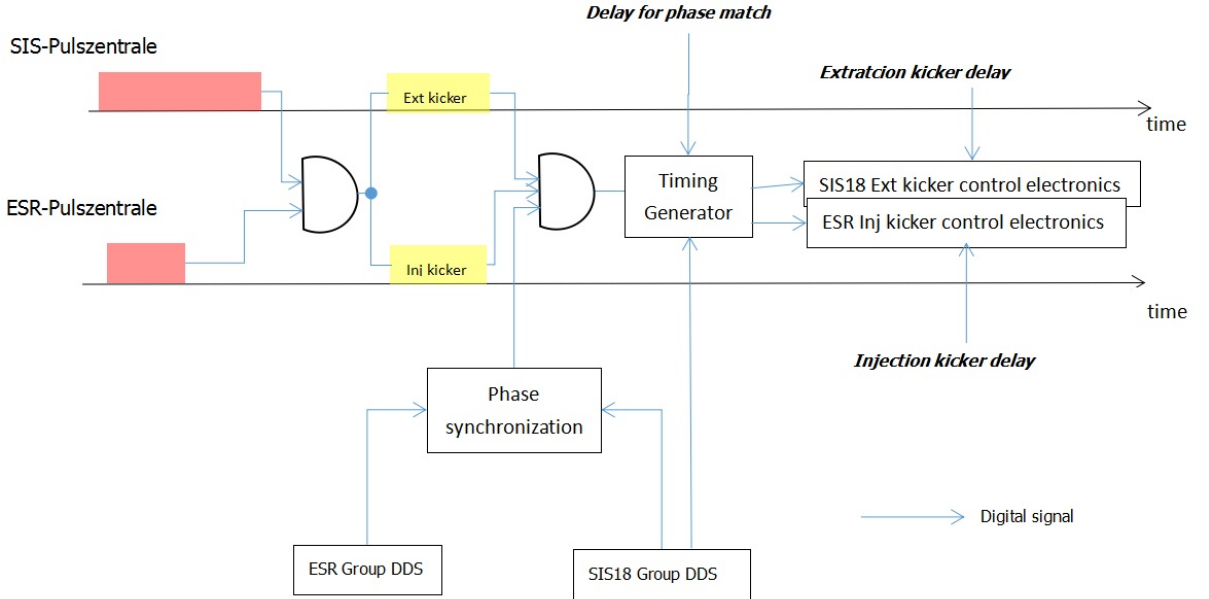


Figure 3.3: Bunch-to-bucket transfer between SIS18 and ESR with GSI control system.

Fig. 3.3 illustrates the realization of the B2B transfer from SIS18 to ESR with GSI control system. SIS18 needs longer time for the preparation, e.g. beam injection, beam acceleration, before the extraction than that of ESR before injection, so ESR is earlier fully prepared for the transfer. The preparation process is represented as red rectangle in Fig. 3.3. When SIS18 is fully prepared with

### 3.4. Comparison between the FAIR B2B transfer system and the B2B transfer with the GSI control system

---

the bunches to be transferred, the ready signal from ESR-Pulszentrale and SIS-Pulszentrale are inputed into a logic *AND* gate. When both SIS18 and ESR are prepared, namely the output of the logic *AND* gate is high, the extraction kicker charge event is sent from SIS-Pulszentrale and injection kicker charge event from ESR-Pulszentrale. The charge process of kicker is represented as yellow rectangle in Fig. 3.3. When two kickers are fully charged, the ready signal of extraction and injection kicker from ESR-Pulszentrale and SIS-Pulszentrale are inputed into the second logic *AND* gate, as well as the “phase synchronization signal” from the RF system. The phase synchronization signal indicates the alignment of the zero-crossing of Reference RF Signals from Group DDS of SIS18 and ESR. The output of the second *AND* gate is an indication signal, starting the delay on the SIS18 rf signal for the correct phase match between SIS18 and ESR rf systems, denoted as “delay for phase match” in Fig. 3.3. ESR uses the injection orbit instead of the desin orbit, so the circumference ratio between SIS18 and ESR is close to an interger,  $C^{SIS18}/C^{ESR} = 2 - 0.003$ , SIS18 has four bunches,  $h^{SIS18} = 4$  and ESR has two buckets,  $h^{ESR} = 2$ , so  $f_{rf}^{SIS18}/f_{rf}^{ESR} = 4/(4 - 0.006)$ , see Sec. 2.2.1. The phase difference between rf systems of SIS18 and ESR varies at the speed of the beating frequency  $\Delta f = -0.003f_{rf}^{ESR}/(2 - 0.003) = -1898$  Hz., see eq. ???. More detailed parameters about SIS18 and ESR, please see Appendix C.2. The required phase difference  $\Delta\phi$  happens the delay for phase match  $\Delta t$  after the indication signal, see eq. 3.1.

$$\frac{1/\Delta f}{360^\circ} = \frac{\Delta t}{\Delta\phi} \quad (3.1)$$

When the delay for phase match is expired, trigger pulses are produced by the timing generator for both SIS18 extraction and ESR injection kicker control electronics. Every kicker control electronics adds a separate delay to trigger pulses, denoted as “extraction kicker delay” and “injection kicker delay” in Fig. 3.3. The delay for phase match, extraction kicker delay and injection kicker delay are configurable by operators. The precision of the ignition signal from the kicker control electronics is 1 ns.

The existing B2B transfer with the GSI control system only supports the B2B transfer with the frequency beating method. It dose not support B2B transfer with the phase shift method. Parameters (e.g. the delay for phase match, extraction kicker delay and injection kicker delay) must be properly configured and adjusted by operators. The phase synchronization signal is delay compensated, but the transfer of the signal to the second *AND* gate is not delay compensated and with the jitter of 1 us, resulting a default bunch-to-bucket injection center mismatch of  $\pm 0.68^\circ$ . It does not support buckets filling by multi batches, e.g. eight out of ten SIS100 buckets are filled by four SIS18 batches, each of them has two bunches.

Compared with the existing B2B transfer with the GSI control system, the FAIR B2B transfer system has many advantages. It supports both the phase shift and frequency beating methods. The FAIR B2B transfer system is based on the GMT system, which is a time based system. All timing nodes of the GMT system are time synchronized with nano second accuracy, which achieves the smaller bunch-to-bucket injection center mismatch. Besides, the FAIR B2B transfer system is more flexible. It supports several B2B transfers running at the same time, e.g. B2B transfer from SIS18 to SIS100 and B2B transfer from ESR to CRYRING. It is capable to transfer different species beam from one machine cycle to another without the operator’s

### **3.4. Comparison between the FAIR B2B transfer system and the B2B transfer with the GSI control system**

---

configuration. It is capable to transfer the beam between two synchrotrons via FRS, Pbar or Super FRS. It can achieve various complicated bucket pattern. What is more, the FAIR B2B transfer system coordinates with the MPS system, which protects SIS100/SIS300 from unacceptable failure or situation.

# Chapter 4

## Concept of the FAIR B2B transfer system

In this Chapter, the basic idea of the FAIR B2B transfer system is presented in Sec. 4.1. The standard procedure of the system is defined and described in Sec. 4.2. Sec. 4.3 illustrates how the basic functionalities of the system are realized. In Sec. 4.4, the data flow of the system is described.

### 4.1 Basic idea of the FAIR B2B transfer system

The basic idea of the B2B transfer is simple. First of all, two rf systems of the source and target synchrotrons must be phase aligned. Secondly, the trigger for the extraction and injection kickers must be calculated. In the end, the actual beam injection must be indicated for the beam instrumentation and diagnostics, which shows the properties and the behavior of the beam.

#### 4.1.1 Phase alignment

The phase alignment is one of the most important prerequisites for the B2B transfer. It makes sure that there must be buckets to be filled by the extracted bunch at the correct time. If the rf frequency of one rf system is integer times of the rf frequency of the other rf system, the phase difference between two rf systems is a constant. The phase difference must be adjusted by the phase shift method. Or the phase difference is adjusted automatically because of the beating frequency.

For the phase alignment, the following idea must be followed.

1. Measurement of the phase of the rf system and the corresponding timestamp in each synchrotron.
2. Exchange of the measured data.
3. Phase comparison between two rf systems.
4. Adjustment of the phase of one rf system.
5. Calculation of the time for the phase alignment of two rf systems.

## 4.1. Basic idea of the FAIR B2B transfer system

### 4.1.2 Calculation of the trigger time for the extraction and injection kickers

For the proper B2B transfer, not only the relative position of the bunch and bucket, but also the firing of the extraction and injection kicker must be precisely controlled. The extraction kicker must kick the bunch exactly the time-of-flight between two rings before a specific bucket passes the injection kicker. For the calculation of the trigger time for the extraction and injection kickers, the following idea must be followed.

1. Kicker firing requires the B2B injection center phase mismatch less than  $\pm 1^\circ$ , which defines “coarse synchronization”.
2. Bucket counting requires the kicker firing based on  $h=1$  rf signal. With the help of the bucket counting, bunches are injected into correct buckets. This process is called “fine synchronization”.

Before the detailed idea of the calculation are explained, some basic concepts and their symbols are introduced, see Fig. 4.1.

- The bucket pattern  $t_{bucket}$ .
- The Time-Of-Flight (TOF) between two synchrotrons  $t_{TOF}$ .
- The Time-Of-Flight between the virtual RF cavity and the extraction/injection kicker,  $t_{v\_ext}$  and  $t_{v\_inj}$ .
- The sum of the preparation time and rise time of an extraction/injection kicker,  $t_{ext}$  and  $t_{inj}$ .

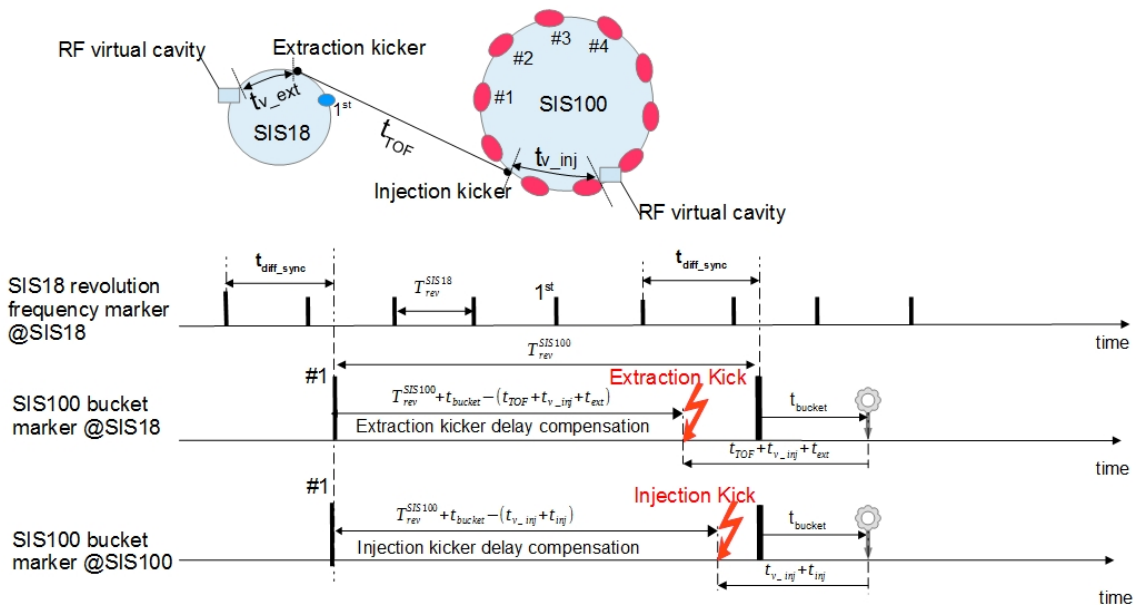


Figure 4.1: The illustration of B2B transfer from SIS18 to SIS100. The blue dot represents bunch, the red one bucket, the red lightning bolt the kicker firing and the gray gear the bucket pattern.

## 4.1. Basic idea of the FAIR B2B transfer system

---

Fig. 4.1 illustrates the B2B transfer from SIS18 to SIS100. The SIS18  $U^{28+}$  super cycle consists of four SIS18 cycles. Each cycle produces two  $U^{28+}$  bunches. From SIS18, four cycles, each of two bunches, are injected into eight out of ten buckets of SIS100. The SIS18  $H^+$  super cycle consists of four SIS18 cycles. Each cycle produces one  $H^+$  bunch. From SIS18, four cycles, each of one bunch, are injected into four out of ten buckets of SIS100 [40, 41]. The SIS18 and SIS100 revolution frequency markers (black bars on the first time axis and bars on the second/third time axis in Fig. 4.1) indicate the time when the first bunch or the first bucket pass by the RF virtual cavity (black bars correspond to 1<sup>st</sup> and #1). The extraction and injection kicker firing (red lighting bolts) have a delay with respect to the first bars of the SIS100 revolution frequency marker at SIS18 and SIS100. This delay is called extraction/injection kicker delay compensation. The mentioned four instances of time are related to the second bars of the SIS100 revolution frequency marker.  $T_{rev}^X$  represents the revolution period of the synchrotron X, e.g. SIS18 revolution period  $T_{rev}^{SIS18}$ .  $T_{rf}^X$  represents the period of the cavity frequency of synchrotron X, e.g. SIS18 rf period of the cavity frequency  $T_{rf}^{SIS18}$ . After the rf phase alignment, the time difference between the SIS18 and SIS100 revolution frequency markers is represented by  $t_{diff\_sync}$ , e.g.  $t_{diff\_sync}=t_{v\_ext}+t_{TOF}+t_{v\_inj}$  for  $U^{28+}$  and  $H^+$  odd bucket injection,  $t_{diff\_sync}=t_{v\_ext}+t_{TOF}+t_{v\_inj}-T_{rf}^{SIS100}$  for  $H^+$  even bucket injection, more details about the use case from SIS18 to SIS100, please see Sec. ?? and Sec. ??.

The kicker magnet must have zero magnetic field when the bunch passes by it and the kicker magnet only can be switched on during the bunch gap. The bunch gap depends on the cavity frequency, the filling pattern and the bunch length.

- Extraction kick

In order to inject into specific buckets, the extraction kicker delay compensation for the first bar of the SIS100 revolution frequency marker is  $T_{rev}^{SIS100} + t_{bucket}$ , see gray gear at the SIS100 revolution frequency marker at SIS18. For example, when two  $U^{28+}$  bunches of SIS18 are to be injected into the bucket #3 and #4 of SIS100,  $t_{bucket} = 1 \cdot T_{rev}^{SIS18}$ . The extraction kicker must be fired  $t_{v\_inj} + t_{TOF} + t_{ext}$  earlier as the bucket passes the virtual rf cavity, so the extraction kicker delay compensation is  $T_{rev}^{SIS100} + t_{bucket} - (t_{TOF} + t_{v\_inj} + t_{ext})$ , see red lighting bolt at the SIS100 revolution frequency marker at SIS18.

- Injection kick

With the consideration of the bucket pattern, the injection kicker delay compensation for the first bar of the SIS100 revolution frequency marker is  $T_{rev}^{SIS100} + t_{bucket}$ , see gray gear at the SIS100 revolution frequency marker at SIS100. The injection kicker must be fired  $t_{v\_inj} + t_{inj}$  time earlier as the bucket passes the virtual rf cavity, so the injection kicker delay compensation is  $T_{rev}^{SIS100} + t_{bucket} - (t_{v\_inj} + t_{inj})$ , see red lighting bolt at the SIS100 revolution frequency marker at SIS100.

## 4.2 Basic procedure of the FAIR B2B transfer system

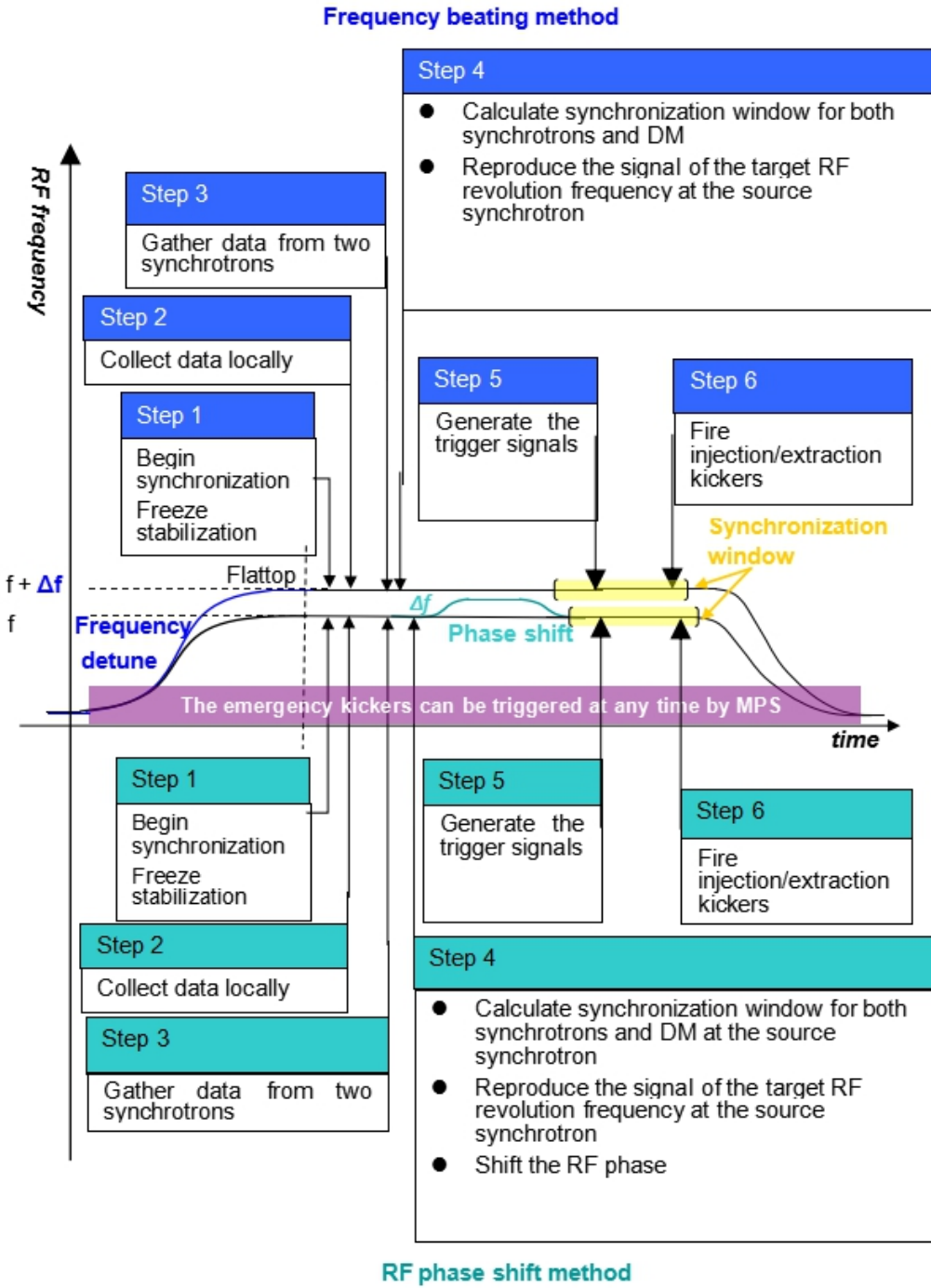


Figure 4.2: The procedure for the B2B transfer within one acceleration cycle. Shown are the frequency beating method (blue, top) and the phase shift method (green, bottom).

Fig. 4.2 illustrates the basic procedure of the B2B transfer with two different synchronization scenarios. The top part shows the chronological steps with the frequency

### **4.3. Realization of the FAIR B2B transfer system**

---

beating method, while the bottom part shows the steps with the phase shift method. The emergency kickers can be triggered at any time during the acceleration cycle by the MPS. The purple region shows the valid time for the emergency kicker. The yellow region shows the synchronization window.

The B2B transfer process basically needs to follow six steps [42]:

1. The DM announces the B2B transfer and requests the freez of the feedback loop (e.g. beam phase feedback loop), when required.
2. The two synchrotrons measure the rf phase locally.
3. The source synchrotron receives the measured rf phase from the target synchrotron.
4. The source synchrotron calculates the synchronization window with the kicker delay and sends it to both synchrotrons and to the DM. Besides, it reproduces the revolution frequency marker of the target synchrotron at the source synchrotron.

For the phase shift method, the source synchrotron generally achieves the phase shift. But when the target synchrotron is empty, the phase shift is achieved by the method of the phase jump at the target synchrotron for simplicity's sake. Although the synchronization window is infinite theoretically, the B2B should be transferred as soon as the phase shift is done, in order to guarantee the stability of the beam. The duration of the synchronization window is defined as two revolution periods of the large synchrotron.

5. The trigger signal is generated for the kickers with the delay compensation.
6. The kicker electronics fire the kickers. The actual beam injection time and the B2B transfer status are send from the source synchrotron to the DM and the DM sends them further to the beam instrumentation.

## **4.3 Realization of the FAIR B2B transfer system**

In this section, how the FAIR B2B transfer system is realized based on the FAIR control system and LLRF system is introduced.

### **4.3.1 Phase measurement and corresponding timestamp of one rf system**

Two rf systems are assumed to be stable during the B2B transfer process. The phase measurement of one rf system follows the following principles.

1. Measurement of the actual phase values.
2. Extrapolation of the phase value in the future based on the measured phase values.
3. Timestamp the extrapolated phase values.

## 4.3. Realization of the FAIR B2B transfer system

---

### 4.3.1.1 Measurement of actual phase values in one rf system

The phase measurement of one rf system is achieved by measuring the phase advance between the rf system and a reference sine signal. The phase advance is a linear relationship, with the range from  $-180^\circ$  to  $+180^\circ$ .

In order to get the phase difference between two rf systems of the source and target synchrotrons, a shared reference signal at both source and target synchrotrons is used, which is called “Synchronization Reference Signal”. It is with the fixed frequency and always in the same phase at two synchrotrons. It is a sine wave, whose frequency is a multiple of 100 kHz and whose zero-crossing is aligned with the first zero-crossing of C2 clocks after T0 edges in order to ensure the synchronization of the Synchronization Reference Signal in different synchrotrons [43, 44].

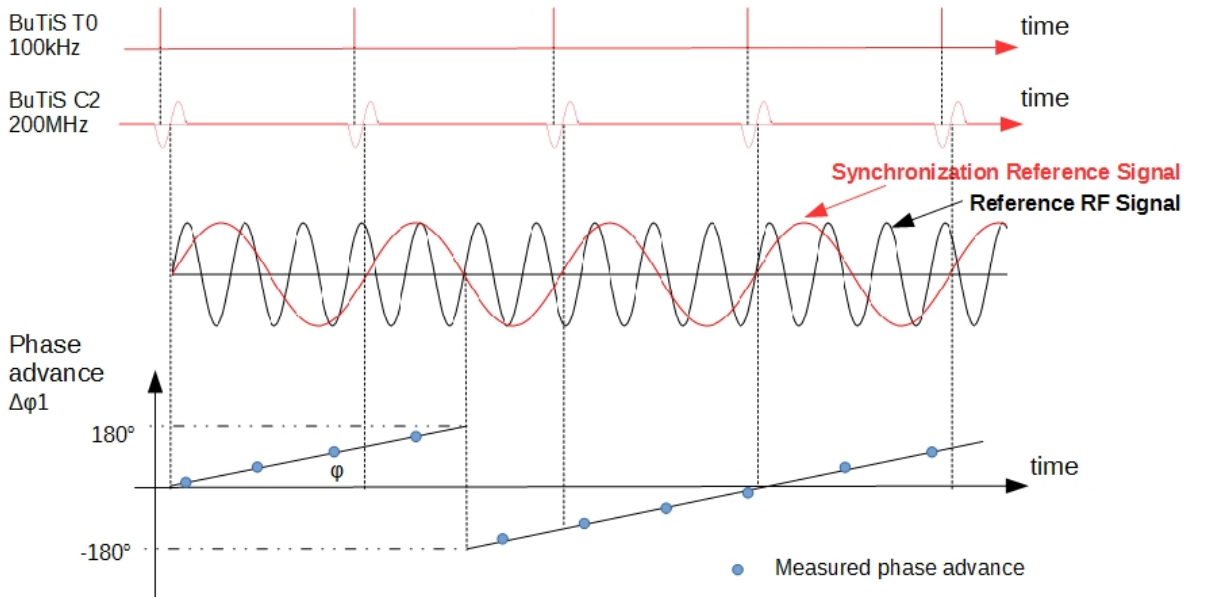


Figure 4.3: The realization of the phase advance measurement at one synchrotron

Fig. 4.3 shows the phase measurement of a rf system at a synchrotron. The red sine wave represents the Synchronization Reference Signals (e.g 100 kHz) in two synchrotrons and the black wave the Reference RF Signals (e.g. 1000/3 kHz) from the Group DDS. The phase advance  $\Delta\varphi_1$  between the Reference RF Signal and the Synchronization Reference Signal is measured by the Phase Advance Measurement (PAM) Module at the source synchrotrons and  $\Delta\varphi_2$  at the target synchrotron. The phase advance measurement is performed synchronously to an internal clock, which is represented by the blue dots. For more details about the implementation and realization of the PAM module, please see “Development of the LLRF system for a deterministic Bunch-to-Bucket transfer for FAIR” [45].

### 4.3.1.2 Phase extrapolation in one rf system

The phase advance can be extrapolated due to the linear relationship between time and the phase advance. Based on a series of the phase advance measurements, the phase advance at first zero-crossing of C2 clocks after T0 edges  $\psi_1$  and  $\psi_2$

## 4.3. Realization of the FAIR B2B transfer system

---

could be extrapolated at the source and target synchrotrons by the Phase Advance Prediction (PAP) Module. The extrapolated phase advance,  $\psi_1$  and  $\psi_2$  at the source and target synchrotron, is represented by the red diamonds in Fig. 4.4. Because the phase advance extrapolation is synchronized with the first zero-crossing of C2 clocks after T0 edges and the Synchronization Reference Signal is zero phase aligned with the first zero-crossing of C2 clocks after T0 edges,  $\psi_1$  and  $\psi_2$  are the phase of the Reference RF Signals (represented as the black dot in Fig. 4.4). For more details about the implementation and realization of the PAP module, please see “Development of the LLRF system for a deterministic Bunch-to-Bucket transfer for FAIR“ [45].

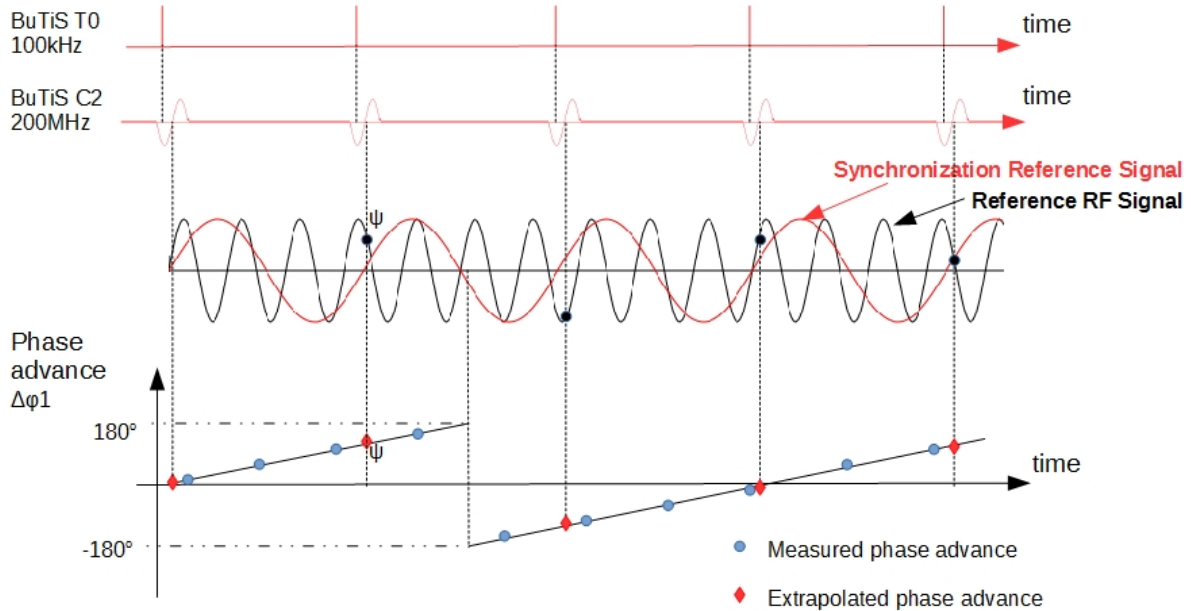


Figure 4.4: The realization of the phase advance extrapolation at one synchrotron

### 4.3.1.3 Timestamp the extrapolated phase

The timestamp of the first zero-crossing of C2 clocks after T0 edges corresponds to the extrapolated phase.

The timing nodes, the B2B source and target SCUs [30, 46], are equipped in the source and target synchrotrons. The PAP module is as a slave<sup>1</sup> in the B2B source and target SCU, see Fig. 4.5. Both B2B source and target SCUs could get the timestamp of zero-crossing of BuTiS C2 clocks.

Fig. 4.6 illustrates the synchronization of the extrapolated phase to the timestamp. DM broadcasts the timing frame of CMD\_START\_B2B to the WR network. This timing frame will be received by the B2B source SCU and B2B target SCU. The B2B source and target SCUs start the B2B process at the designated time, the first zero-crossing of C2 clock after a specified T0 edge (represented as the pink dot in Fig. 4.6). They need maximum 1  $\mu$ s to inform the PAP modules to start the phase advance extrapolation respectively. The PAP modules use e.g. 500  $\mu$ s for the phase extrapolation and updates the extrapolated phase value every first

<sup>1</sup>[https://en.wikipedia.org/wiki/Master/slave\\_\(technology\)](https://en.wikipedia.org/wiki/Master/slave_(technology))

### 4.3. Realization of the FAIR B2B transfer system

---

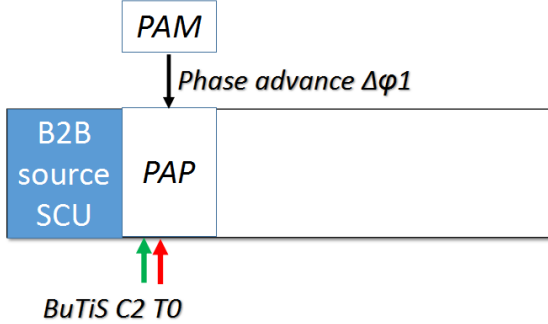


Figure 4.5: Implementation of the Phase Advance Prediction Module in the B2B source SCU

zero-crossing of C2 clocks after T0 edges. After 500  $\mu$ s, the B2B source and target SCUs need another maximum 1  $\mu$ s to get the extrapolated phase  $\psi$  (represented as the red diamond in Fig. 4.6) from the PAP modules and they also get the timestamp of the first zero-crossing of C2 clock after T0 edge  $t_\psi$  which corresponds to the extrapolated phase, as well as the slope of the phase advance  $k$ . The B2B source SCU gets  $\psi_1$ ,  $t_{\psi 1}$  and  $k$  at the source synchrotron and the B2B target SCU  $\psi_2$ ,  $t_{\psi 2}$  and  $k$  at the target synchrotron.

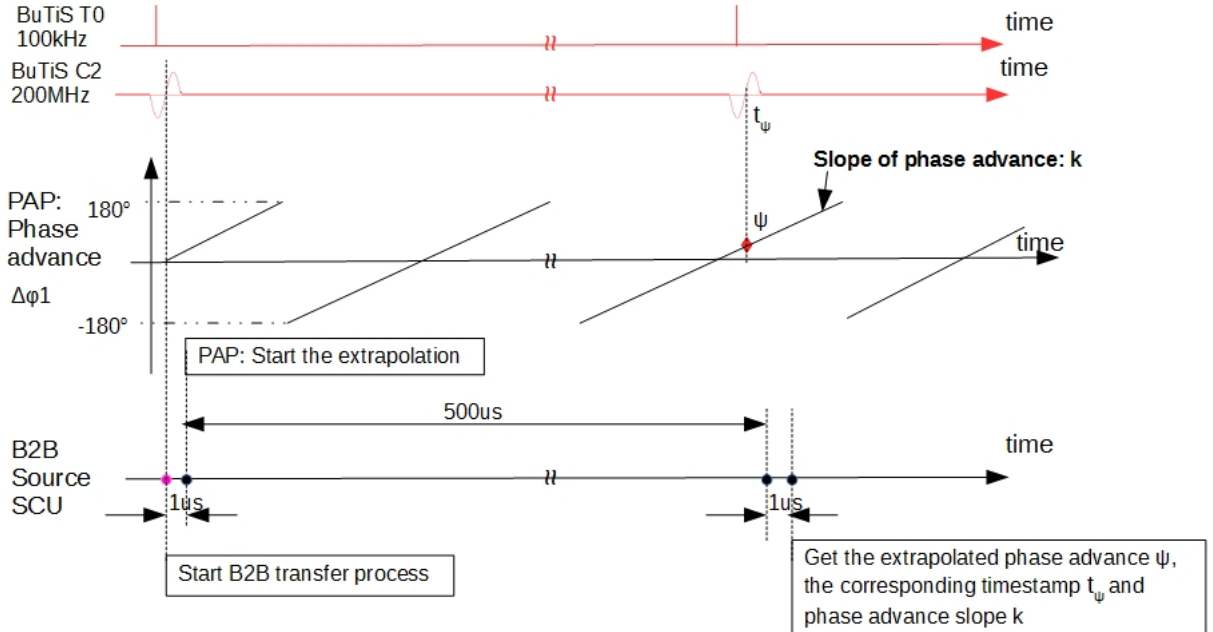


Figure 4.6: The synchronization of the extrapolated phase to the timestamp in one synchrotron

#### 4.3.2 Exchange of the measured data

For the B2B transfer, there is a “B2B transfer master“, which is responsible for the data collection of two synchrotrons, data calculation, data redistribution and B2B transfer status check. The data of the source and target synchrotron must be

## 4.3. Realization of the FAIR B2B transfer system

---

transferred to the “B2B transfer master“ via the deterministic WR network in the format of the timing frame.

For the simplicity, the B2B source SCU works as “B2B transfer master“, so the extrapolated phase  $\psi_2$ , the corresponding timestamp  $t_{\psi_2}$  and the phase advance slope  $k$  are transferred by the B2B target SCU to the B2B source SCU via the WR network. The transfer of the data is achieved by the timing frame TGM \_PHASE \_TIME. The B2B transfer involves a certain amount of timing frames. More details about the B2B timing frames, please see Appendix A. The timing frames are not sent via DM in order to reduce the traffic of the WR network and reduce the timing frame transfer delay on the WR network [47], so a specified VLAN, B2B VLAN, is defined for the B2B timing frames. All SCUs for the B2B transfer are assigned to the B2B VLAN. Fig. 4.7 illustrates an example of the transfer path of the B2B timing frame in the WR network. The frame is transferred along the path with orange color instead of the path with blue color.

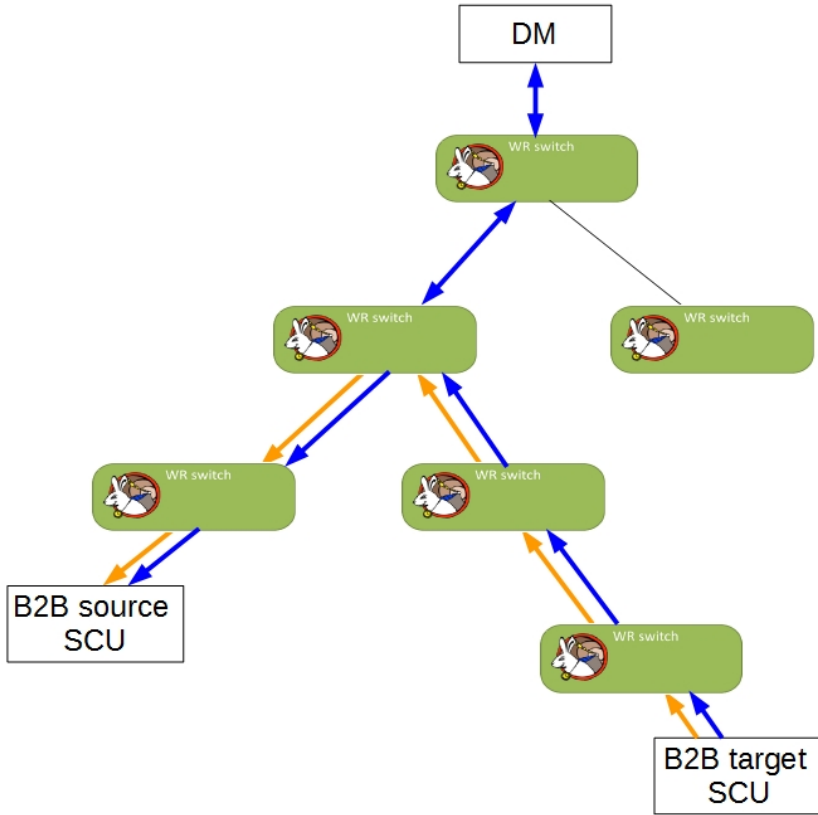


Figure 4.7: One example of the transfer path of the B2B timing frame in the WR network

### 4.3.3 Rf synchronization

The FAIR B2B transfer system is available for both the phase shift and frequency beating methods, see Sec. 2.3. The phase difference between two rf systems allows for the realization of the rf synchronization. With the phase shift method, a frequency modulation with a fixed duration is applied to one rf system. With the

### 4.3. Realization of the FAIR B2B transfer system

---

frequency beating method, the phase difference varies at the rate of the frequency difference between two rf systems.

- Rf synchronization with the phase shift method

Eq. 2.48 gives the relation between the required phase shift and the frequency modulation. The phase shift must be executed adiabatically, see Sec. 2.3. For the RF synchronization, the maximum phase shift required of one synchrotron is one bucket length of the other synchrotron, namely  $360^\circ$ . Because the phase can be shifted backward or forward, a phase shift of up to  $\pm 180^\circ$  can be implemented for the simplicity of the rf frequency modulation. A normalized frequency modulation profile  $f_{normalized}$  for  $180^\circ$  can be precalculated, which guarantees the adiabaticity. The actual frequency modulation profile  $f_{actual}$  is decided by the normalized frequency modulation profile and the required phase shift, see eq. 4.1. The required phase shift,  $\Delta\phi$ , is calculated by the B2B source SCU.

$$\frac{\Delta\phi}{180^\circ} = \frac{f_{actual}}{f_{normalized}} \quad (4.1)$$

Fig. 4.8 shows an example of a normalized and several actual frequency modulation profiles and the corresponding phase shift profiles. The magenta profile is the normalized profile  $f_{normalized}$  with the phase shift of  $180^\circ$ . The blue one is  $1/2 f_{normalized}$  with the phase shift of  $90^\circ$  and the green one is  $1/3 f_{normalized}$  with  $60^\circ$ .

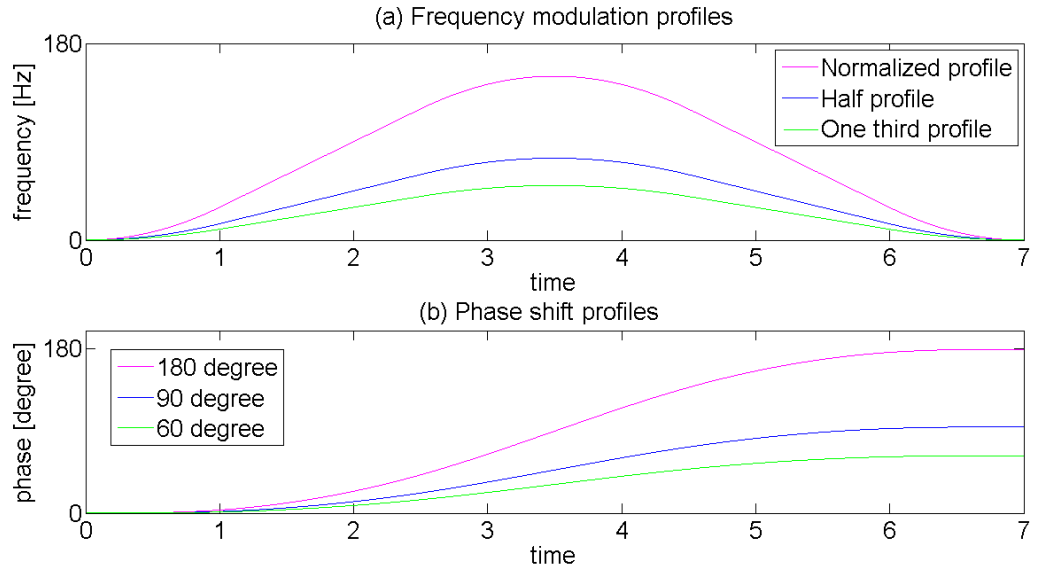


Figure 4.8: The normalized frequency and phase modulation profile and the actual profiles

Fig. 4.9 shows the implementation of the Phase Shift Module (PSM) in the B2B source SCU. The B2B source SCU sends the required phase shift to the PSM, which controls the phase shift of the Reference RF Signal of Group DDS by means of either frequency (Fig. 4.8 (a)) or phase (Fig. 4.8 (b)) modulation. The Reference RF Signal is routed to the different cavity systems by a Switch Matrix to realize the phase shift of all cavities on the synchrotron. For more

### 4.3. Realization of the FAIR B2B transfer system

---

details about the implementation and realization of the PSM module, please see “Development of the LLRF system for a deterministic Bunch-to-Bucket transfer for FAIR“ [45].

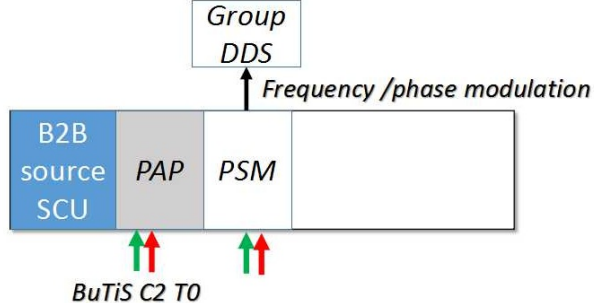


Figure 4.9: Implementation of the Phase Shift Module in the B2B source SCU

A particular case of the B2B synchronization occurs, when the target synchrotron is empty, i.e. it does not capture any bunch yet, the phase shift can be done for the target synchrotron without adiabatical consideration (e.g. phase jump is possible). In this case, the B2B source SCU sends the timing frame TGM\_PHASE\_JUMP to the B2B target SCU, which contains the required phase jump. After the B2B target SCU receives the timing frame, it sends the value to the PSM for the phase jump of the Group DDS of the target synchrotron.

- Rf synchronization with the frequency beating method

The frequency is detuned at one rf system at the acceleration ramp. The ratio of the circumference between many pair of machines in FAIR is not a perfect integer, the frequencies of two synchrotrons begin beating automatically. For the pairs with the perfect integer ratio of the circumference, the rf frequency of the source synchrotron is detuned by modifying the magnetic field and radial excursion during the acceleration ramp. The Group DDS produces the detuned Reference RF Signal.

#### 4.3.4 Coarse synchronization

The coarse synchronization is achieved by the synchronization window with a certain length. Within this window, bunches are transferred into buckets with the center mismatch smaller than the upper bound<sup>2</sup>. The length of the synchronization window  $T_{sync\_win}$  is two times the period of the reproduced signal for the bucket label, see Sec. 4.3.5. For the phase shift method, the bunch-to-bucket injection center mismatch within the synchronization window is almost  $0^\circ$ . For the frequency beating method, the maximum bunch-to-bucket center mismatch  $\Delta\phi$  with the synchronization window is calculated by

$$\frac{T_{sync\_win}}{1/\Delta f} = \frac{\Delta\phi}{360^\circ} \quad (4.2)$$

<sup>2</sup>B2B transfer from SIS18 to SIS100: upper bound of the bunch-to-bucket center mismatch is  $\pm 1^\circ$

### 4.3. Realization of the FAIR B2B transfer system

---

The B2B source SCU is capable of receiving the values (extraction/injection kicker delay compensation, rf frequencies of the source and target synchrotrons and the upper bound time for the phase shift of the source synchrotron) from the SM by FESA classes via the accelerator network. The B2B source SCU calculates the synchronization window, taking kicker delays into consideration and transfers the timestamp of the start of the synchronization window, TGM \_SYNCH \_WIN, to the DM and the source and target Trigger SCUs via the WR network. The Trigger SCUs are used to produce the kicker trigger signal. The TGM \_SYNCH \_WIN could also be used for the triggering of the bunch rotation of both machines (e.g. SIS100 and CR) with a specified advance.

#### 4.3.5 Bucket label

The bucket label is realized by a delay based on an indication signal. The indication signal is used to indicate the first bucket and the delay is used to indicate a specific bucket. The indication signal is with the revolution frequency of the target synchrotron. Because the evolution of the phase advance of the rf system of the target synchrotron  $\psi$  can be calculated according to the slope of the phase advance  $k$ , see eq. 4.3.

$$\psi = kt + d \quad (4.3)$$

Where  $\psi_2$  and  $t_{\psi_2}$  coincide with the linear relationship, so  $d$  can be calculated as  $\psi_2 - kt_{\psi_2}$ .

The indication signal can be corrected exactly in phase with the revolution frequency of the target synchrotron. The indication signal is exactly a copy of the revolution frequency of the target synchrotron<sup>3</sup>, so it is called "reproduced signal", or "bucket label signal" from the functional perspective. The reproduced signal could be reproduced campus-wide. A specific bucket is just a certain number of the rf periods delay based on the reproduced signal.

The FAIR B2B transfer system needs the bucket label not only at the rf flattop, but also during the whole acceleration cycle. The former is used for the normal extraction and injection and the latter could be used for the emergency dump. For the emergency kick, the reproduced signal has always the same frequency and is always in phase with the revolution signal, so it is called the "real-time reproduced signal". The delay based on the real-time reproduced signal always indicates the bunch gap.

The bucket label is realized by the Trigger SCU, the Signal Reproduction (SR) module and the Phase Correction Module (PCM), see Fig. 4.10. The reproduced signal is produced by SR module. The Trigger SCU is responsible for the receipt of the phase correction value from the B2B source SCU and the transfer of this value to PCM. The PCM module is used to correct phase of the reproduced signal. The PCM module is as a slave in the Trigger SCU. For more details about the implementation and realization of the PCM and SR modules, please see "Development of the LLRF system for a deterministic Bunch-to-Bucket transfer for FAIR" [45].

- Bucket label for the normal extraction and injection

---

<sup>3</sup>This is the simplest scenario. More details about the frequency of the indication signal, please see Chap. 5.

### 4.3. Realization of the FAIR B2B transfer system

---

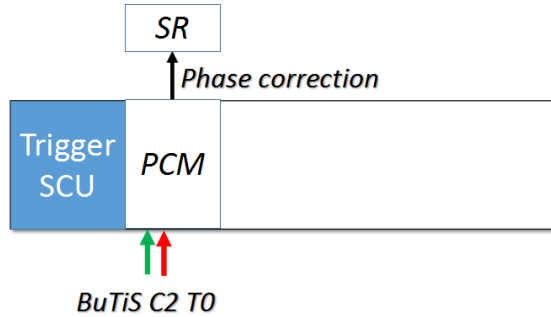


Figure 4.10: Implementation of the Phase Correction Module in the Trigger SCU

For the bucket label for the normal extraction and injection, three steps are necessary. Fig. 4.11 shows these three steps for the reproduction of the bucket label. Here the B2B transfer from SIS18 to SIS100 is taken as an example.

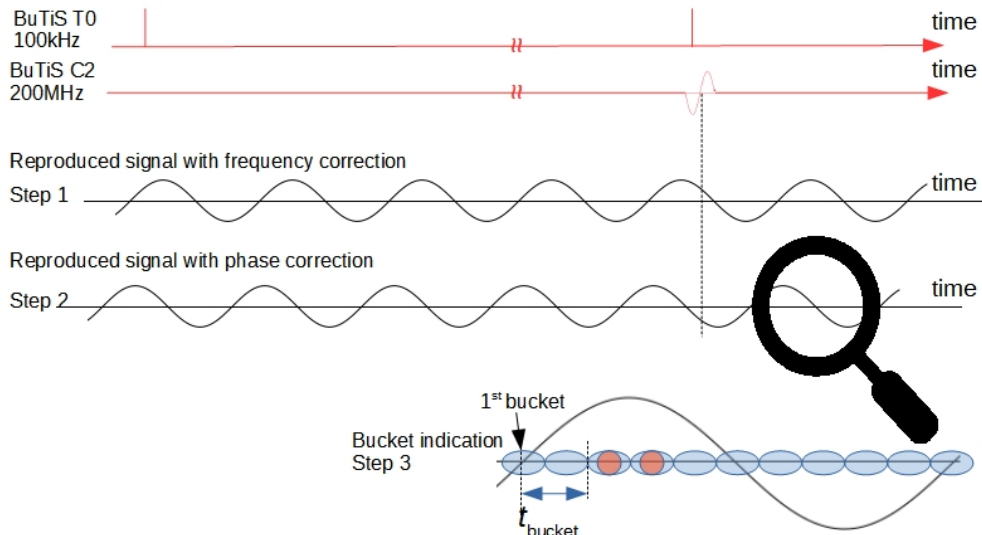


Figure 4.11: The realization of the bucket label for the normal extraction and injection.

- Step 1. Frequency correction

The SR module produces the "reproduced signal" with the same frequency as the Reference RF Signal at the flattop of the target synchrotron (e.g. rf revolution frequency of SIS100). The zero-crossing of the reproduced signal always indicates the start of the 1st bucket.

- Step 2. Phase correction

The reproduced signal must do phase correction at a specified first zero-crossing of C2 clock after T0 edge. The phase correction value is calculated by the B2B source SCU and transferred by the timing frame TGM \_PHASE \_CORRECTION to the Trigger SCU. Then the Trigger SCU gives the phase correction value to the SR module.

- Step 3. Bucket indication

### 4.3. Realization of the FAIR B2B transfer system

---

The SM considers the bucket pattern  $t_{bucket}$  within the kicker delay compensation, see Sec. 4.1.2. In Fig. 4.11, the 3rd and 4th buckets will be filled with  $t_{bucket} = 1 \cdot T_{rev}^{SIS18}$ .

- Bunch gap label for the emergency extraction

Only for SIS100 emergency procedure, the bunch gap label is important during the whole acceleration cycle. There are two steps for the realization of the bunch gap label, see Fig. 4.12.

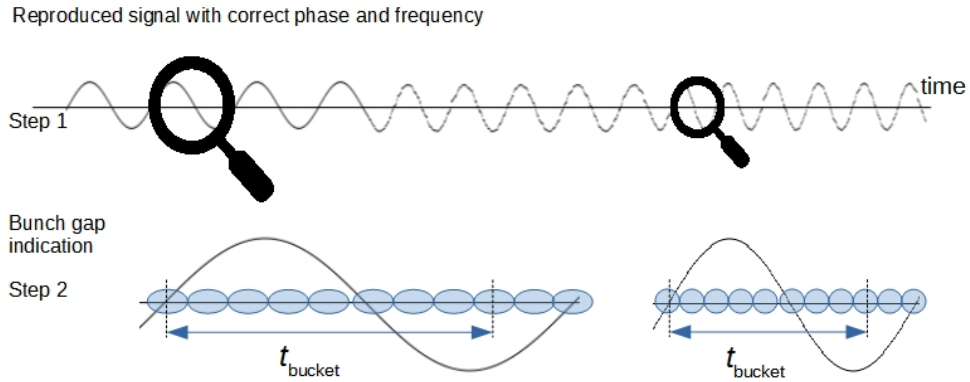


Figure 4.12: The realization of the bunch gap for the emergency extraction.

- Step 1. The real-time reproduced signal is directly distributed from the switch matrix, which synchronizes with the Reference RF Signal in frequency and phase.

- Step 2. Bunch gap indication

The SM considers the bunch gap  $t_{bucket}$  within the kicker delay compensation. In Fig. 4.12, the 9th and 10th buckets are taken as an example as the bunch gap. The  $t_{bucket} = 4 \cdot T_{rev}^{SIS18}$ .

#### 4.3.6 Fine synchronization of the extraction and injection kicker

After the synchronization between two rf systems, the exact TOF between two synchrotrons before a specific bucket passes the injection kicker, the extraction kicker must kick the bunch in the source synchrotron. When there are some emergency, the emergency kicker must kick the beam into the emergency dump as soon as possible. This achieves the “fine synchronization”.

The first pulse of the reproduced signal within the synchronization window is selected. The triggers for the extraction and injection kicker are produced after the selected reproduced signal with the delay of the extraction and injection kicker delay compensation. When some emergency happens, the coming bunch gap label outputs to trigger the emergency kicker. Fig. 4.13 shows the implementation of the Trigger Decision (TD) module in the Trigger SCU. The TD module is responsible for the production of trigger for the kicker.

## 4.3. Realization of the FAIR B2B transfer system

---

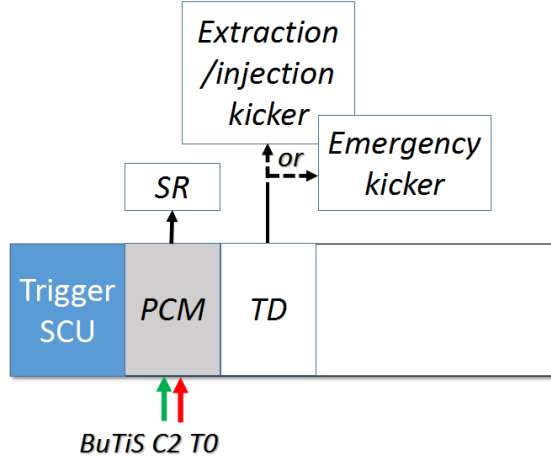


Figure 4.13: Implementation of the Trigger Decision module in the Trigger SCU

For the normal B2B extraction/injection, the synchronization window is a gating signal, which is received by the source and target Trigger SCUs from the WR network by TGM \_SYNCH \_WIN. Within this window, the first reproduced signal from the SR module will be selected by the TD module. The extraction and injection kicker are synchronized with the bunch and bucket by the extraction and injection kicker delay compensation. The extraction kicker will be triggered by the extraction kick delay compensation,  $T_{rev}^{SIS100} + T_{rev}^{SIS18} - (t_{TOF} + t_{v,inj} + t_{ext})$  and the injection kicker will be triggered by the injection kick delay compensation,  $T_{rev}^{SIS100} + T_{rev}^{SIS18} - (t_{v,inj} + t_{inj})$ , see Fig. 4.1. Both extraction and injection kick delay compensation values are preloaded from the SM to the Trigger SCU and the Trigger SCU gives these values to the TD module. The kicker delay compensation is applied to the first selected reproduced signal by TD module. When the beam injection inhibit signal from the MPS is on, the TD module will block the extraction/injection trigger.

For the SIS100 emergency kick, the extraction delay compensation is calculated by  $T_{rev}^{SIS100} + t_{bucket} - (t_{v,emg} + t_{emg})$ , where  $t_{v,emg}$  is the time delay between the virtual rf cavity and the emergency extraction position and  $t_{emg}$  the emergency kicker delay. The emergency extraction delay compensation values are preloaded from the SM to the Trigger SCU and the Trigger SCU gives these values to the TD module. The kicker delay compensation is applied to the real-time reproduced signal by TD module. Only when the emergency dump signal from MPS is valid, the emergency kicker will be triggered by the TD module.

### 4.3.7 B2B transfer status check

The B2B transfer status must be known by the DM. The B2B source SCU, the B2B transfer master, is responsible for the status check. The B2B source SCU receives the trigger time of the extraction kicker and actual beam extraction time, TGM \_KICKER \_TRIGGER \_TIME \_S, from the source Trigger SCU via the WR network and also the trigger time of the injection kicker and actual beam injection time, TGM \_KICKER \_TRIGGER \_TIME \_T, from the target Trigger SCU via the WR network. The Trigger SCU collects the kicker trigger time and the beam extraction/injection time. The B2B source SCU examines the status of the B2B transfer system and transfers the status and the actual beam injection time, TGM

#### 4.4. Data flow of the FAIR B2B transfer system

---

\_B2B\_STATUS, to the DM. If all components of the B2B transfer system work correctly and the B2B transfer process is successful. Otherwise it is defeat.

## 4.4 Data flow of the FAIR B2B transfer system

In this section, the procedure for the B2B transfer is explained from the perspective of the data flow, which follows the basic six steps in Fig. 4.2. Fig. 4.14 shows the data flow in the source and target synchrotrons and between two synchrotrons. The rectangle with the different color represents the basic six steps. The left part in each rectangle presents the data flow in the source synchrotron and the right part the data flow in the target synchrotron.

1. The DM sends the timing frame CMD\_START\_B2B to the B2B source and target SCUs for the start of the B2B transfer via the WR network. Besides, it requests the freez of the feedback loop.
2. After receiving CMD\_START\_B2B, the B2B source and target SCUs start the PAM module to measure the phase advance  $\Delta\varphi$  with the help of the PAP module locally and the PAP module extrapolates the phase advance in the furture. After a period of time, the B2B source and target SCU reads the extrapolated phase advance  $\psi$  and the slope of the phase advance  $k$  from the PAP module locally, timestamping the  $\psi$ .
3. The B2B target SCU sends the extrapolated phase  $\psi_2$ , the corresponding timestamp  $t_{\psi_2}$  and the slope  $k$  in the format of the timing frame TGM\_PHASE\_TIME to the B2B source SCU via the WR network.
4. When the B2B source SCU receives the timing frame TGM\_PHASE\_TIME, it calculates the synchronization window and transfers the timestamp of the start of the window to the DM in the format of the timing frame TGM\_SYNCH\_WIN, as well as to the Trigger SCUs at the source and target synchrotrons. The B2B source SCU calculates the phase correction value and transfers it to all Trigger SCUs via the WR network in the format of the timing frame TGM\_PHASE\_CORRECTION. Then the Trigger SCUs transfer the phase correction value to its PCM. The PCM starts the phase correction of the SR module.

Only for the phase shift method, the B2B source SCU calculates the required shifted phase  $\Delta\phi$  and transfers it to the PSM. Then the PSM transfers the phase or frequency modulation profile to the Group DDS.

5. When the source and target Trigger SCUs receive the timing frame TGM\_SYNCH\_WIN, they produces the synchronization window pulse for the TD module. With the help of the reproduced signal from the SR module, the kicker delay compensation from the Trigger SCU and the indication signals (the emergency dump signal and the beam injection inhibit signal) from the MPS, the TD module produces the normal extraction/injection trigger signals or the emergency kick trigger for the kicker.

#### **4.4. Data flow of the FAIR B2B transfer system**

---

6. The extraction and injection kickers or emergency kicker are fired. After that, the source Trigger SCU gets the actual beam extraction time and the timestamp of the extraction trigger signal from the TD module and transfers them to the source B2B SCU in the format of the timing frame TGM \_KICKER \_TRIGGER \_TIME \_S. The target Trigger SCU gets the timestamp of actual beam injection time and the timestamp of the injection trigger signal from the TD module and transfers them to the source B2B SCU in the format of the timing frame TGM \_KICKER \_TRIGGER \_TIME \_T. Then the B2B source SCU checks the B2B transfer status and transfers the status together with the beam injection time to the DM in the format of the timing frame TGM \_B2B \_STAUS (represented as the red line in the rectangle of step 6 in Fig. 4.14).

#### 4.4. Data flow of the FAIR B2B transfer system

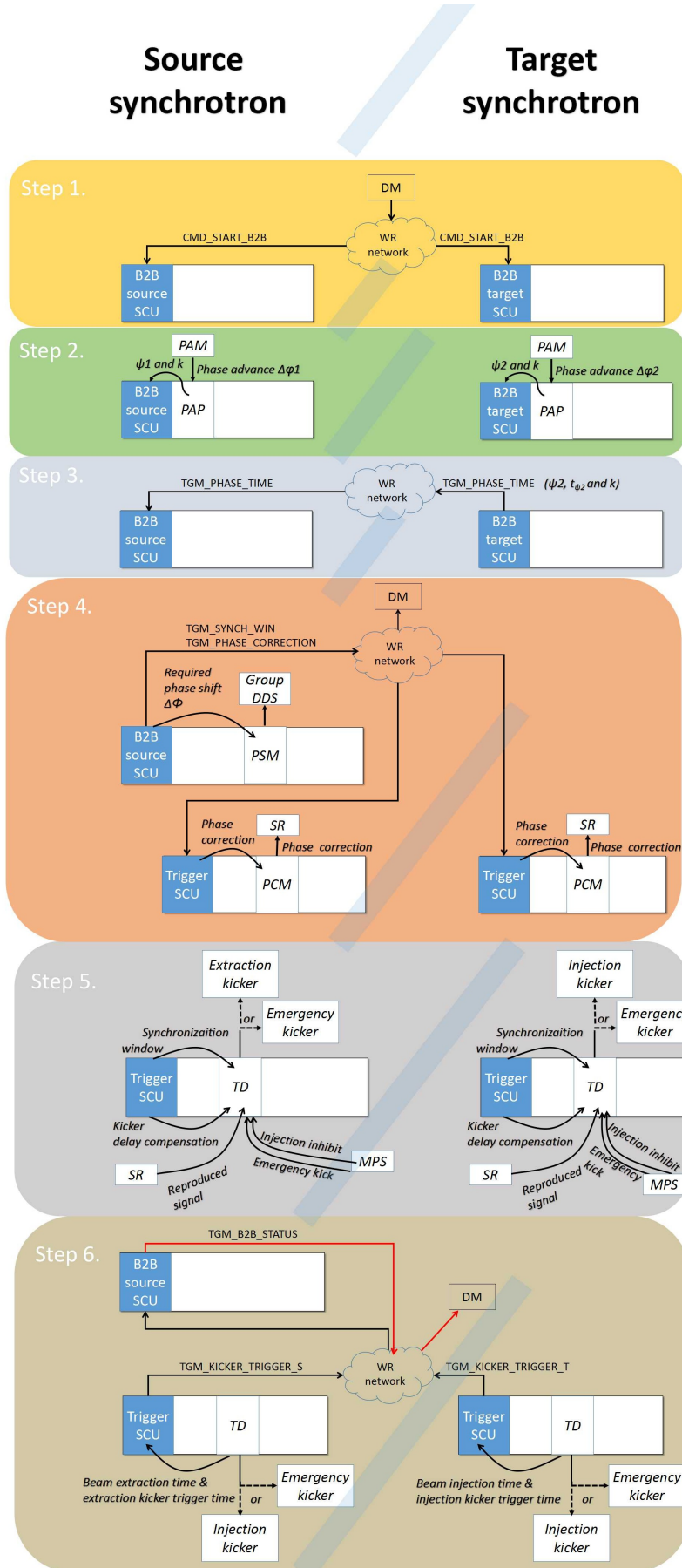


Figure 4.14: The data flow of the B2B transfer system

# Chapter 5

## Application of the FAIR B2B transfer system for FAIR accelerators

The phase shift must be executed slowly enough to preserve the beam emittance, which needs much longer time than the frequency beating method. Besides, many FAIR accelerator pairs are beating automatically due to the non integer ratio of the circumference between two synchrotrons. So all FAIR use cases with the frequency beating method will be discussed in details in this chapter. Based on the circumference ratio, there are three scenarios of the B2B transfer for FAIR with the frequency beating method.

- The circumference ratio between the large and small synchrotron is an integer.
  - Four  $U^{28+}$  batches, B2B transfer from SIS18 to SIS100
  - $H^+$  B2B transfer from SIS18 to SIS100
  - B2B transfer from ESR to CRYRING
- The circumference ratio between the large and small synchrotron is close to an integer.
  - $h=4$  B2B transfer from SIS18 to ESR
  - $h=1$  B2B transfer from SIS18 to ESR
- The circumference ratio between the large and small synchrotron is far away from an integer.
  - B2B transfer from CR to HESR

Besides, FAIR has many use cases of B2B transfers that the extraction and injection beam have different energy because of the targets installed between two synchrotrons (e.g. Pbar, FRS or Super FRS). In this situation, the beam revolution frequency ratio between the small and large synchrotrons is equivalent to the circumference ratio between the large and small synchrotrons.

- The revolution frequency ratio between the small and large synchrotron is far away from an integer.

## 5.1. Circumference ratio is an integer

---

- $H^+$  B2B transfer from SIS100 to CR via Pbar
- Rare Isotope Beams (RIB) B2B transfer from SIS100 to CR via Super FRS
- B2B transfer from SIS18 to ESR via FRS

Tab. 5.1 lists all FAIR use cases of the B2B transfer.

Table 5.1: FAIR B2B transfer use cases

Circumference ratio <sup>1</sup>	$C^l/C^s$	$\frac{f_{rev}^s}{f_{rev}^l}$	Use case of FAIR accelerators
$C^l/C^s = \kappa$ an integer	5		$U^{28+}$ B2B transfer from SIS18 to SIS100
	5		$H^+$ B2B transfer from SIS18 to SIS100
	5		B2B transfer from ESR to CRYRING
$C^l/C^s = \kappa + \lambda$ or $frev^s/frev^l = \kappa + \lambda$ close to an integer	2-0.003		$h=4$ B2B transfer from SIS18 to ESR
	2-0.003		$h=1$ B2B transfer from SIS18 to ESR
$C^l/C^s = m/n + \lambda$ or $frev^s/frev^l = m/n + \lambda$ far away from an integer)		4.9-0.0004	$H^+$ B2B transfer from SIS100 to CR
		4.4-0.0046	RIB B2B transfer from SIS100 to CR
	2.6-0.003		B2B transfer from CR to HESR
		1.8+0.048	B2B transfer from SIS18 to ESR via FRS

## 5.1 Circumference ratio is an integer

When the circumference ratio of the large synchrotron to that of the small synchrotron is an integer, there exists the following relation between two rf frequencies. More details, please see see Sec. 2.2.1.

$$\frac{f_{rf}^l}{f_{rf}^s} = \frac{h^l}{h^s \cdot \kappa} \quad (5.1)$$

$Y$  is the GCD of  $h^l$  and  $h^s \cdot \kappa$ .

For the phase shift method, two rf frequencies of two rf systems with same frequency are needed. For the frequency beating method, two slightly different

### 5.1. Circumference ratio is an integer

---

frequencies are required. From eq. 2.27, we get

$$\frac{f_{rf}^l}{h^l/Y} = \frac{f_{rf}^s}{(h^s \cdot \kappa)/Y} \quad (5.2)$$

Two rf frequencies,  $f_{syn}^l = \frac{f_{rf}^l}{h^l/Y}$  and  $f_{syn}^s = \frac{f_{rf}^s}{(h^s \cdot \kappa)/Y}$ , are chosen for the phase shift method. There is a constant phase difference between these two rf frequencies. There is no difference of the implementation of the phase shift on the large or small synchrotron, because they implement their species dependent rf frequency modulation profiles for a same required phase shift. Only when the target synchrotron is empty, the phase will be shifted for the target synchrotron by the phase jump. For the frequency beating method, two slightly different frequencies is based on  $f_{syn}^l$  and  $f_{syn}^s$  by detuning one of them.

For the phase shift method, the bucket label signal indicates the passing time of the first bucket of the target synchrotron, when it is phase aligned with the rf system of the source synchrotron, see Fig. 5.1.

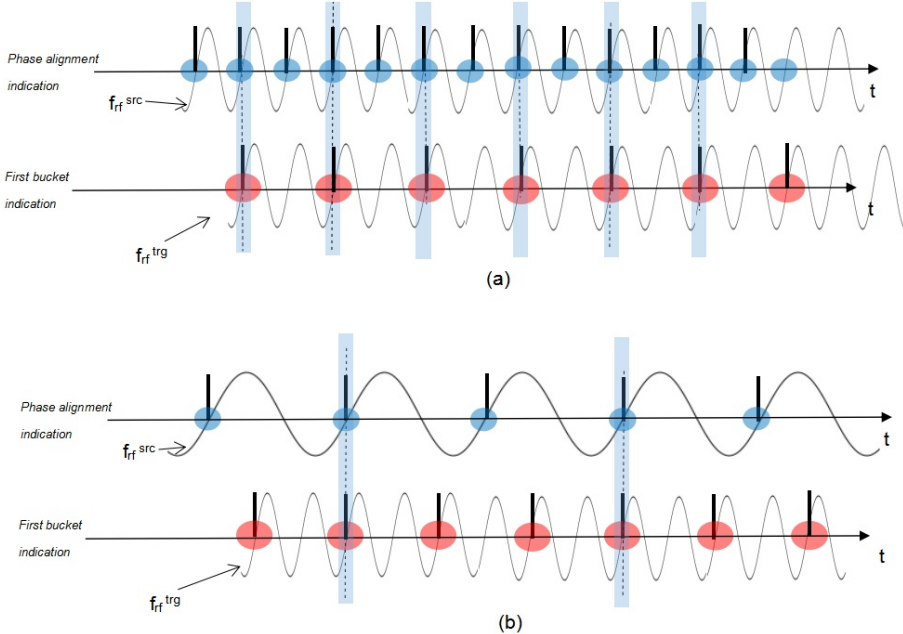


Figure 5.1: The frequency of the bucket label signal for the phase shift method. The red dots represent buckets and the blue ones bunches, the black bars chosen by blue rectangle are used by the bucket label signal. The phase of two rf systems in this example is aligned at  $0^\circ$ . (a) The frequency of the bucket label signal when  $f_{syn}^s \geq f_{rev}^s$  and the large synchrotron is the target. (b) The frequency of the bucket label signal when  $f_{syn}^s < f_{rev}^s$ .

When the large synchrotron is the target, there exists  $f_{syn}^l \geq f_{rev}^l = \frac{f_{rf}^l}{h^l}$ . The revolution period is  $Y$  times long as the period of  $f_{syn}^l$ . The period of  $f_{syn}^l$  is not long enough to contain all buckets. So the bucket label signal is with the frequency of  $f_{rev}^l$  for this case, see Fig. 5.1 (a).

When the small synchrotron is the target, the relation between  $f_{syn}^s = f_{rev}^s \frac{Y}{\kappa}$  and  $f_{rev}^s = \frac{f_{rf}^s}{h^s}$  is not fixed. If  $f_{rev}^s \frac{Y}{\kappa} \geq f_{rev}^s$ , namely  $\frac{Y}{\kappa} \geq 1$ , the revolution period is

## 5.1. Circumference ratio is an integer

---

$\frac{Y}{\kappa}$  times long as the period of  $\frac{f_{rf}^s}{(h^s \cdot \kappa)/Y}$ . Hence, the bucket label signal is with the frequency of  $f_{rev}^s$ , see Fig. 5.1 (a). Oppositely, if  $f_{rev}^s \frac{Y}{\kappa} < f_{rev}^s$ , namely  $\frac{Y}{\kappa} < 1$ , the period of  $f_{syn}^s$  is  $\frac{\kappa}{Y}$  times long as the revolution period. Hence, the rf frequency with  $\frac{f_{rf}^s}{(h^s \cdot \kappa)/Y}$  is used as a bucket label signal, see Fig. 5.1 (b).

For the frequency beating method, the rf frequency of the source synchrotron is preferred to be detuned, because there exists circulating bunches in the target synchrotron. The bucket label signal indicates the passing time of the first bucket of the target synchrotron, when it is correct phase aligned with the rf system of the source synchrotron, see Fig. 5.2. When the large synchrotron is the target, the bucket label signal is with the frequency of  $f_{rev}^l$ , see Fig. 5.2 (a). When the small synchrotron is the target, the frequency of the bucket label signal is depend on the relation between  $f_{syn}^s = f_{rev}^s \frac{Y}{\kappa}$  and  $f_{rev}^s = \frac{f_{rf}^s}{h^s}$ . The rule is same as that for the phase shift method. When the large synchrotron is the target, the bucket label signal is with the frequency of  $f_{rev}^l$ , see Fig. 5.2 (a) and (b) are for cases  $f_{rev}^s \frac{Y}{\kappa} \geq f_{rev}^s$  and  $f_{rev}^s \frac{Y}{\kappa} < f_{rev}^s$ .

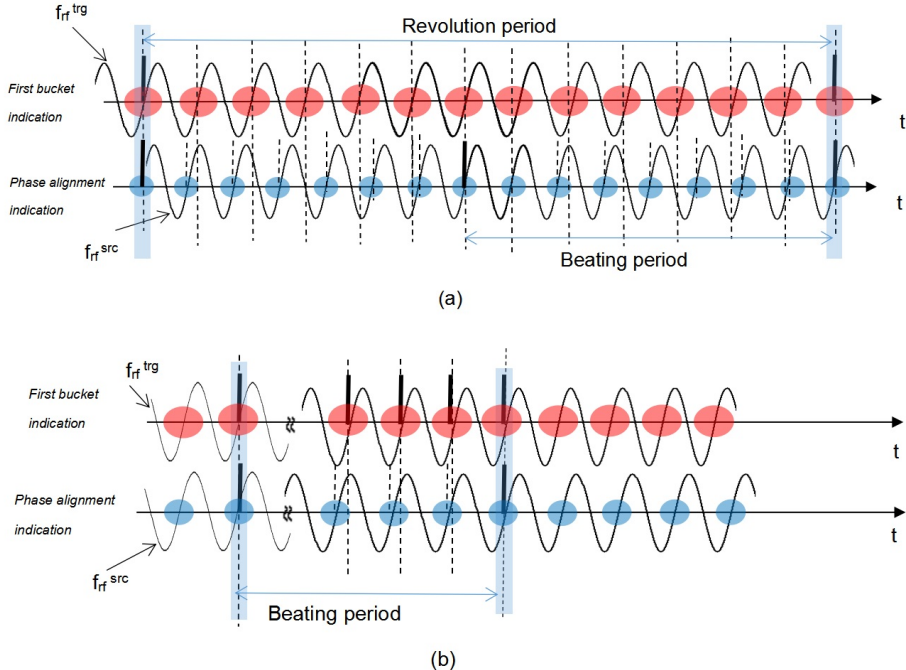


Figure 5.2: The frequency of the bucket label signal for the frequency beating method.

The red dots represent buckets and the blue ones bunches, the black bars chosen by blue rectangle are used by the bucket label signal. The phase of two rf systems in this example is aligned at  $0^\circ$ . (a) The frequency of the bucket label signal when  $f_{rev}^s \frac{Y}{\kappa} \geq f_{rev}^s$  and the large synchrotron is the target. (b) The frequency of the bucket label signal when  $f_{rev}^s \frac{Y}{\kappa} < f_{rev}^s$ .

Tab. 5.2 shows the formulas for the frequency of the bucket label signal, two slightly different frequencies for beating, the length of the synchronization window and the bunch and bucket center mismatch when the large synchrotron is the target. Tab. 5.3 shows the formulas when the small synchrotron is the target.

### 5.1. Circumference ratio is an integer

---

Table 5.2: Synchronization when the circumference ratio is an integer and the large synchrotron is the target

	Large synchrotron is target synchrotron
Frequency of bucket label	$f_{rev}^l$
Two slightly different frequencies	$f_{syn}^s = \frac{f_{rf}^s}{(h^s \cdot \kappa)/Y} + \Delta f$ and $f_{syn}^l = \frac{f_{rf}^l}{h^l/Y}$
Length of synchronization window	$2 \cdot T_{rev}^l$
Bunch-to-bucket injection center mismatch	$\pm \frac{1}{2} \cdot \frac{2 \cdot T_{rev}^l}{1/\Delta f} \cdot 360^\circ$

Table 5.3: Synchronization when the circumference ratio is an integer and the small synchrotron is the target

	Small synchrotron is target synchrotron	
Cases	$\frac{f_{rf}^s}{(h^s \cdot \kappa)/Y} \geq f_{rev}^s$ $(\frac{Y}{\kappa} \geq 1)$	$\frac{f_{rf}^s}{(h^s \cdot \kappa)/Y} < f_{rev}^s$ $(\frac{Y}{\kappa} < 1)$
Frequency of bucket label	$f_{rev}^s$	$\frac{f_{rf}^s}{(h^s \cdot \kappa)/Y}$
Two slightly different frequencies	$f_{syn}^l = \frac{f_{rf}^l}{h^l/Y} + \Delta f$ and $f_{syn}^s = \frac{f_{rf}^s}{(h^s \cdot \kappa)/Y}$	
Length of synchronization window	$2 \cdot T_{rev}^s$	$2 \cdot [(h^s \cdot \kappa)/Y] \cdot T_{rf}^s$
Bunch-to-bucket injection center mismatch	$\pm \frac{1}{2} \cdot \frac{2 \cdot T_{rev}^s}{1/\Delta f} \cdot 360^\circ$	$\pm \frac{1}{2} \cdot \frac{2 \cdot [(h^s \cdot \kappa)/Y] \cdot T_{rf}^s}{1/\Delta f} \cdot 360^\circ$

#### 5.1.1 use case of the $U^{28+}$ B2B transfer from SIS18 to SIS100

The use case of the  $U^{28+}$  B2B transfer from SIS18 to SIS100 belongs to this scenario. Four batches of  $U^{28+}$  at 200 MeV/u are injected into continuous eight out of ten buckets of SIS100. Each batch consists of two bunches [40, 41]. The large synchrotron is SIS100 and the small one SIS18.  $\kappa = 5$ ,  $h^{SIS100} = 10$  and  $h^{SIS18} = 2$ . The GCD of  $h^{SIS100} = 10$  and  $h^{SIS18} \cdot \kappa = 2 \cdot 5 = 10$  is 10, namely  $Y = 10$ . Substituting these

### 5.1. Circumference ratio is an integer

---

values into eq. 2.27, we get

$$\frac{f_{rf}^{SIS100}}{f_{rf}^{SIS18}} = \frac{h^{SIS100}}{h^{SIS18} \cdot \kappa} = \frac{10}{2 \cdot 5} = \frac{10}{10} \quad (5.3)$$

For the frequency beating method, the frequency is detuned either for SIS18 or SIS100, because of  $h^{SIS100} = h^{SIS18} \cdot \kappa$ . Because SIS100 is the target, substituting  $h^X$ ,  $\kappa$ ,  $f_{rf}^X$ ,  $f_{rev}^X$  and  $Y$  into formulas in Tab. 5.2, the synchronization of  $U^{28+}$  B2B transfer from SIS18 to SIS100 is obtained, see Tab. 5.4. Here we assume that SIS18 is detuned with 200 Hz.

Table 5.4: Synchronization of  $U^{28+}$  B2B transfer from SIS18 to SIS100 with the frequency beating method

	Large synchrotron (SIS100) is target synchrotron
Frequency of bucket label	$f_{rev}^{SIS100}$
Two slightly different frequencies	$f_{syn}^s = f_{rf}^{SIS18} + 200\text{Hz}$ and $f_{syn}^l = f_{rf}^{SIS100}$
Length of synchronization window	$2 \cdot T_{rev}^{SIS100} = 12.718\text{ us}$
Bunch-to-bucket injection center mismatch	$\pm \frac{1}{2} \cdot \frac{2 \cdot T_{rev}^{SIS100}}{1/200} \cdot 360^\circ = \pm 0.50^\circ$

After the synchronization, the phase difference between the SIS18 and SIS100 revolution frequency markers equals to the sum of  $t_{v\_inj}$ ,  $t_{v\_ext}$  and  $t_{TOF}$ . The SIS100 revolution frequency marker works for the bucket label. When the 1st and 2nd buckets are to be filled,  $t_{pattern}=0$ . When the 3rd and 4th buckets,  $t_{pattern}=T_{rev}^{SIS18}$ . When the 5th and 6th buckets,  $t_{pattern}=2 \cdot T_{rev}^{SIS18}$ . When the 7th and 8th buckets,  $t_{pattern}=3 \cdot T_{rev}^{SIS18}$ . Detailed parameters of  $U^{28+}$  B2B transfer from SIS18 to SIS100, please see Appendix C.1.

#### 5.1.2 Use case of the $H^+$ B2B transfer from SIS18 to SIS100

Four batches of  $H^+$  at 4 GeV/u are injected into continuous four out of ten buckets of SIS100. Each batch consists of one bunch [40, 41]. The large synchrotron is SIS100 and the small one SIS18.  $\kappa = 5$ ,  $h^{SIS100} = 10$  and  $h^{SIS18} = 1$ . The GCD of  $h^{SIS100} = 10$  and  $h^{SIS18} \cdot \kappa = 1 \cdot 5$  is 5, namely  $Y = 5$ . Substituting these values into eq. 2.27, we get

$$\frac{f_{rf}^{SIS100}}{f_{rf}^{SIS18}} = \frac{h^{SIS100}}{h^{SIS18} \cdot \kappa} = \frac{10}{1 \cdot 5} = \frac{2}{1} \quad (5.4)$$

For the frequency beating method, the frequency detune is preferred for SIS18. Because SIS100 is the target, substituting  $h^X$ ,  $\kappa$ ,  $f_{rf}^X$ ,  $f_{rev}^X$  and  $Y$  into formulas in

### 5.1. Circumference ratio is an integer

---

Tab. 5.2, the synchronization of  $H^+$  B2B transfer from SIS18 to SIS100 is obtained, see Tab. 5.5. Here we assume that SIS18 is detuned with 200 Hz for the frequency beating method.

Table 5.5: Synchronization of  $H^+$  B2B transfer from SIS18 to SIS100 with the frequency beating method

	Large synchrotron (SIS100) is target synchrotron
Frequency of bucket label	$f_{rev}^{SIS100}$
Two slightly different frequencies	$f_{syn}^l = \frac{f_{rf}^{SIS100}}{2}$ and $f_{syn}^s = f_{rf}^{SIS18} + \Delta f$
Length of synchronization window	$2 \cdot T_{rev}^{SIS100} = 7.356 \text{ us}$
Bunch-to-bucket injection center mismatch	$\pm \frac{1}{2} \cdot \frac{2 \cdot T_{rev}^{SIS100}}{1/200} \cdot 360^\circ = \pm 0.31^\circ$

In order to inject into the odd and even number buckets, there are two scenarios of the phase difference between the SIS18 and SIS100 revolution frequency markers after the synchronization.

- Injection into the odd number buckets

The phase difference between the SIS18 and SIS100 revolution frequency markers equals to  $t_{v\_ext} + t_{v\_inj} + t_{TOF}$ . When the 1st bucket is to be filled,  $t_{pattern}=0$ . When the 3rd bucket is to be filled,  $t_{pattern}=2 \cdot T_{rev}^{SIS18}$ .

- Injection into the even number buckets

The phase difference between the SIS18 and SIS100 revolution frequency markers equals to  $t_{v\_ext} + t_{v\_inj} + t_{TOF} - T_{rf}^{SIS100}$ . When the 2nd bucket is to be filled,  $t_{pattern}=1 \cdot T_{rev}^{SIS18}$ . When the 4th bucket is to be filled,  $t_{pattern}=3 \cdot T_{rev}^{SIS18}$ .

The SIS100 revolution frequency marker works for the bucket label. Detailed parameters of the  $H^+$  B2B transfer from SIS18 to SIS100, please see Appendix C.1.

#### 5.1.3 Use case of the B2B transfer from ESR to CRYRING

Only one bunch is injected into one bucket of CRYRING [16, 48]. The large synchrotron is SIS18 and the small one is CRYRING.  $\kappa = 2$ ,  $h^{ESR} = 1$  and  $h^{CRYRING} = 1$ . The GCD of  $h^{ESR} = 1$  and  $h^{CRYRING} \cdot \kappa = 1 \cdot 2$  is 1, namely  $Y = 1$ . substituting into eq. 2.27.

$$\frac{f_{rf}^{ESR}}{f_{rf}^{CRYRING}} = \frac{h^{ESR}}{h^{CRYRING} \cdot \kappa} = \frac{1}{1 \cdot 2} = \frac{1}{2} \quad (5.5)$$

## 5.2. Circumference ratio is close to an integer

---

For the rf synchronization, the phase jump for CRYRING is preferred, because CRYRING is empty before the injection. For the frequency beating method, the frequency detune is preferred for ESR. Here we assume 200 Hz frequency detune for 30 MeV/u proton of ESR. The small synchrotron is the target one and there exists  $\frac{f_{rf}^s}{(h^s \cdot \kappa) / Y} = \frac{f_{rf}^{CRYRING}}{(1.2)/1} < f_{rev}^s = \frac{f_{rf}^{CRYRING}}{1}$ , so substituting  $h^X$ ,  $\kappa$ ,  $f_{rf}^X$ ,  $f_{rev}^X$  and  $Y$  into formulas in the right column in Tab. 5.3, the synchronization of the B2B transfer from ESR to CRYRING is obtained, see Tab. C.4.

Table 5.6: Synchronization of B2B transfer from ESR to CRYRING with the frequency beating method

	Small synchrotron (CRYRING) is target synchrotron
Frequency of bucket label	$1/2 f_{rf}^{CRYRING}$
Two slightly different frequencies	$f_{syn}^l = f_{rf}^{ESR} + 200\text{Hz}$ and $f_{syn}^s = \frac{f_{rf}^{CRYRING}}{2}$
Length of synchronization window	$2 \cdot (2 \cdot T_{rf}^{CRYRING}) = 5.488\text{ us}$
Bunch-to-bucket injection center mismatch	$\pm \frac{1}{2} \cdot \frac{2 \cdot 2 \cdot T_{rf}^{CRYRING}}{1/200} \cdot 360^\circ = \pm 0.20^\circ$

The  $1/2$  CRYRING revolution frequency marker works for the bucket label. The phase difference between the ESR and  $1/2$  CRYRING revolution frequency markers equals to  $t_{v\_ext} + t_{v\_inj} + t_{TOF}$  after the synchronization. Detailed parameters of the B2B transfer from ESR to CRYRING, please see Appendix C.4.

## 5.2 Circumference ratio is close to an integer

When the circumference ratio of the large synchrotron to that of the small synchrotron is very close to an integer, there exists the relation between two rf frequencies.

$$\frac{f_{rf}^l}{f_{rf}^s} = \frac{h^l}{h^s \cdot (\kappa + \lambda)} = \frac{h^l}{h^s \cdot \kappa + h^s \cdot \lambda} \quad (5.6)$$

$Y$  is the GCD of  $h^l$  and  $h^s \cdot \kappa$ .

Besides, it is also grouped to this scenario, that the revolution frequency ratio between the small and large synchrotrons is close to an integer when the beam passes some target (e.g. FRS, Pbar) between two synchrotrons. The ratio between the revolution frequencies can be expressed as

$$\frac{f_{rev}^s}{f_{rev}^l} = \kappa + \lambda \quad (5.7)$$

The realtion between two cavity rf frequencies is same as eq. 5.6.

## 5.2. Circumference ratio is close to an integer

---

Two synchrotrons are beating automatically. Two slightly different frequencies are  $f_{syn}^l = \frac{f_{rf}^l}{h^l/Y}$  and  $f_{syn}^s = \frac{f_{rf}^s}{(h^{s,\kappa})/Y}$ . When the large synchrotron is the target, the bucket label signal is with the frequency of  $f_{rev}^l$ , because  $f_{syn}^l >= f_{rev}^l$ . Tab. 5.7 shows the formulas for the frequency of the bucket label signal, two slightly different frequencies for beating, the length of the synchronization window and the bunch and bucket center mismatch when the large synchrotron is the target.

Table 5.7: Synchronization when the circumference ratio is close to an integer and the large synchrotron is the target

	Large synchrotron is target synchrotron
Frequency of bucket label	$f_{rev}^l$
Two slightly different frequencies	$f_{syn}^s = \frac{f_{rf}^s}{(h^{s,\kappa})/Y}$ and $f_{syn}^l = \frac{f_{rf}^l}{h^l/Y}$
Beating frequencies	$\Delta f = \left  \frac{f_{rf}^s}{(h^{s,\kappa})/Y} - \frac{f_{rf}^l}{h^l/Y} \right $
Length of synchronization window	$2 \cdot T_{rev}^l$
Bunch-to-bucket injection center mismatch	$\pm \frac{1}{2} \cdot \frac{2 \cdot T_{rev}^l}{1/\Delta f} \cdot 360^\circ$

When the small synchrotron is the target, the frequency of the bucket label signal is dependent on the relation between  $\frac{f_{rf}^s}{(h^{s,\kappa})/Y}$  and  $f_{rev}^s$ . When  $\frac{f_{rf}^s}{(h^{s,\kappa})/Y} >= f_{rev}^s$ , the revolution period is longer than the period for the phase alignment. Hence, the frequency of the bucket label signal is  $f_{rev}^s$ . Or the bucket label signal with the frequency of  $\frac{f_{rf}^s}{(h^{s,\kappa})/Y}$ . Tab. 5.8 shows the formulas when the small synchrotron is the target.

In fact, two slightly different frequencies could be a fraction (between 1/Y and 1) times of  $\frac{f_{rf}^l}{h^l/Y}$  and  $\frac{f_{rf}^s}{(h^{s,\kappa})/Y}$ . When we use one of two slightly different frequencies as the bucket label signal, the bucket label frequency is proportional to  $\frac{f_{rf}^l}{h^l/Y}$  or  $\frac{f_{rf}^s}{(h^{s,\kappa})/Y}$  and the beating frequency to  $\frac{f_{rf}^l}{h^l/Y} - \frac{f_{rf}^s}{(h^{s,\kappa})/Y}$  by the coefficient of the fraction and the length of the synchronization window is inversely proportional to  $\frac{f_{rf}^l}{h^l/Y}$  or  $\frac{f_{rf}^s}{(h^{s,\kappa})/Y}$  by the coefficient of the reciprocal for the fraction. The bunch to bucket center mismatch is proportional to the synchronization window and the beating frequency, whose coefficient product is 1, so the fraction does not affect the mismatch. In other words, when two rf frequency are beating slower/faster, there will be a longer/shorter synchronization window. The ratio between the length of the synchronization window and the beating period is a constant for a specified mismatch. When we use one of two revolution frequencies as the bucket label signal, the length

## 5.2. Circumference ratio is close to an integer

---

Table 5.8: Synchronization when circumference ratio is close to an integer and the small synchrotron is the target

	Small synchrotron is target synchrotron	
Cases	$\frac{f_{rf}^s}{(h^s \cdot \kappa)/Y} \geq f_{rev}^s$ $(\frac{Y}{\kappa} \geq 1)$	$\frac{f_{rf}^s}{(h^s \cdot \kappa)/Y} < f_{rev}^s$ $(\frac{Y}{\kappa} < 1)$
Frequency of bucket label	$f_{rev}^s$	$\frac{f_{rf}^s}{(h^s \cdot \kappa)/Y}$
Two slightly different frequencies	$f_{syn}^l = \frac{f_{rf}^l}{h^l/Y}$ and $f_{syn}^s = \frac{f_{rf}^s}{(h^s \cdot \kappa)/Y}$	
Beating frequencies		$\Delta f = \left  \frac{f_{rf}^l}{h^l/Y} - \frac{f_{rf}^s}{(h^s \cdot \kappa)/Y} \right $
Length of synchronization window	$2 \cdot T_{rev}^s$	$2 \cdot [(h^s \cdot \kappa)/Y] \cdot T_{rf}^s$
Bunch-to-bucket injection center mismatch	$\pm \frac{1}{2} \cdot \frac{2 \cdot T_{rev}^s}{1/\Delta f} \cdot 360^\circ$	$\pm \frac{1}{2} \cdot \frac{2 \cdot [(h^s \cdot \kappa)/Y] \cdot T_{rf}^s}{1/\Delta f} \cdot 360^\circ$

of the synchronization window is constant and the beating frequency is proportional to  $\frac{f_{rf}^l}{h^l/Y} - \frac{f_{rf}^s}{(h^s \cdot \kappa)/Y}$  by the coefficient of the fraction. The bunch to bucket center mismatch is only affected by the beating frequency with the proportion of the fraction. In other words, the slower the beating between two rf frequencies, namely the smaller the fraction, the smaller the mismatch within the synchronization window.

### 5.2.1 Use case of h=4 B2B transfer from SIS18 to ESR

Continuous two of four bunches are injected into two buckets of the injection orbit of ESR [49]. The beam is accumulated in ESR. The large synchrotron is SIS18 and the small one is ESR.  $h^{SIS18} = 4$  and  $h^{ESR} = 2$ . The GCD of  $h^{SIS18} = 4$  and  $h^{ESR} \cdot \kappa = 2 \cdot 2 = 2$  is 4, namely  $Y = 4$ . Substituting the circumference of SIS18 and ESR into eq. 2.31, we get

$$\frac{C^l}{C^s} = \kappa + \lambda = 2 - 0.003 \quad (5.8)$$

Substituting  $h^{SIS18}$ ,  $h^{ESR}$ ,  $\kappa$  and  $\lambda$  into eq. 2.35, we get

$$\frac{f_{rf}^{SIS18}}{f_{rf}^{ESR}} = \frac{h^{SIS18}}{h^{ESR} \cdot (\kappa + \lambda)} = \frac{4}{2 \cdot (2 - 0.003)} \quad (5.9)$$

ESR is the target and there exists  $\frac{f_{rf}^s}{(h^s \cdot \kappa)/Y} = \frac{f_{rf}^s}{(2 \cdot 2)/4} = f_{rev}^s$ , so substituting  $h^X$ ,  $\kappa$ ,  $\lambda$ ,  $f_{rf}^X$  and  $Y$  into formulas in the second column in Tab. 5.8, the synchronization

## 5.2. Circumference ratio is close to an integer

---

Table 5.9: Synchronization of h=4 B2B transfer from SIS18 to ESR with the frequency beating method

	Small synchrotron (ESR) is target synchrotron
Frequency of bucket label	$f_{rev}^{ESR}$
Two slightly different frequencies	$f_{syn}^l = f_{rf}^{SIS18} = 1.373\,200 \text{ MHz}$ and $f_{syn}^s = f_{rf}^{ESR} = 1.371\,302 \text{ MHz}$
Beating frequencies	1898 Hz
Length of synchronization window	$2 \cdot T_{rf}^{ESR} = 0.729 \text{ us}$
Bunch-to-bucket injection center mismatch	$\pm \frac{1}{2} \cdot \frac{2 \cdot T_{rf}^{ESR}}{1/1898} \cdot 360^\circ = \pm 0.27^\circ$

of h=4 B2B transfer from SIS18 to ESR is obtained, see Tab. 5.9. Here we use 30 MeV/u heavy ion as an example.

Detailed parameters of the  $h = 4$  B2B transfer from SIS18 to ESR, please see Appendix C.2.

In the real operation, ESR uses different methods, e.g. barrier bucket or unstable fixed point, to accumulate beam instead of normal bucket [49]. Presently two general schemes of the particle accumulation are possible: moving or fixed barrier rf bucket [50]. In the scheme with moving barrier rf bucket, the bunch is injected in the longitudinal gap prepared by two barrier pulses. The injected beam becomes coasting after switching off the barrier voltages and merges with the previously stacked beam. The barrier voltages are switched on and moved away from each other to prepare the empty space for the next beam injection. In the fixed barrier bucket scheme, one prepares a stationary voltage distribution consisting of two barrier pulses of opposite sign. The resulting stretched rf potential separates the longitudinal phase space into a stable and an unstable region. After injection onto the unstable region (potential maximum), the particles circulate along all phases and cooling application leads to their capture in the stable region of the phase space (potential well). After some time of the beam cooling the unstable region is free for a next injection without losing of the stored beam. With the barrier bucket, the bunch should be injected into the longitudinal gap or the unstable region of the barrier bucket.

After the synchronization, the phase difference between the SIS18 and ESR cavity rf frequency markers depends on the accumulation method.

### 5.2.2 Use case of h=1 B2B transfer from SIS18 to ESR

One bunch is injected into one bucket of the injection orbit of ESR. The beam is accumulated in ESR. The large synchrotron is SIS18 and the small one is ESR.  $h^{SIS18} = 1$  and  $h^{ESR} = 1$ . The GCD of  $h^{SIS18} = 1$  and  $h^{ESR} \cdot \kappa = 1 \cdot 2 = 2$  is 1, namely  $Y = 1$ . Substituting the circumference of SIS18 and ESR into eq. 2.31, we get

$$\frac{C^l}{C^s} = \kappa + \lambda = 2 - 0.003 \quad (5.10)$$

Substituting  $h^{SIS18}$ ,  $h^{ESR}$ ,  $\kappa$  and  $\lambda$  into eq. 2.35, we get

$$\frac{f_{rf}^{SIS18}}{f_{rf}^{ESR}} = \frac{h^l}{h^s \cdot (\kappa + \lambda)} = \frac{1}{1 \cdot (2 - 0.003)} \quad (5.11)$$

ESR is the target and there exists  $\frac{f_{rf}^s}{(h^s \cdot \kappa)/Y} = \frac{f_{rf}^s}{(2 \cdot 1)/1} < f_{revs}$ , so substituting  $h^X$ ,  $\kappa$ ,  $\lambda$ ,  $f_{rf}^X$  and  $Y$  into formulas in the last column in Tab. 5.8, the synchronization of h=1 B2B transfer from SIS18 to ESR is obtained, see Tab. 5.10. Here we use 400 MeV/u proton as an example.

Table 5.10: Synchronization of h=1 B2B transfer from SIS18 to ESR with the frequency beating method

	Small synchrotron (ESR) is target synchrotron
Frequency of bucket label	$\frac{f_{rf}^{ESR}}{2}$
Two slightly different frequencies	$f_{syn}^l = \frac{f_{rf}^{SIS18}}{1} = 989.756 \text{ kHz}$ and $f_{syn}^s = \frac{f_{rf}^{ESR}}{2} = 988.388 \text{ kHz}$
Beating frequencies	1368 Hz
Length of synchronization window	$2 \cdot 2 \cdot T_{rf}^{ESR} = 2.034 \text{ us}$
Bunch-to-bucket injection center mismatch	$\pm \frac{1}{2} \cdot \frac{2 \cdot 2 \cdot T_{rf}^{ESR}}{1/1368} \cdot 360^\circ = \pm 0.50^\circ$

Detailed parameters of the  $h = 1$  B2B transfer from SIS18 to ESR, please see Appendix C.2. After the synchronization, the phase difference between the SIS18 and 1/2 ESR cavity rf frequency markers depends on the accumulation method.

### 5.3 Circumference ratio is far away from an integer

When the circumference ratio of the large synchrotron to that of the small synchrotron is far away from an integer, there exists the relation between two rf fre-

### 5.3. Circumference ratio is far away from an integer

---

quencies.

$$\frac{f_{rf}^l}{f_{rf}^s} = \frac{h^l \cdot n}{h^s \cdot m + h^s \cdot \lambda \cdot n} \quad (5.12)$$

$Y$  is the GCD of  $h^l \cdot n$  and  $h^s \cdot m$ .

Besides, it is also grouped to this scenario, that the revolution frequency ratio between the small and large synchrotrons is far away from an interger when the beam passes some target between two synchrotrons. The revolution frequency ratio can be expressed as

$$\frac{f_{rev}^s}{f_{rev}^l} = \frac{m}{n} + \lambda \quad (5.13)$$

The relation between two rf cavity frequencies is same as eq. 5.12.

$f_{syn}^l = \frac{f_{rf}^l}{(h^l \cdot n)/Y}$  and  $f_{syn}^s = \frac{f_{rf}^s}{(h^s \cdot m)/Y}$  are two slightly frequencies. When the large synchrotron is the target, the bucket label signal is the frequency of  $f_{rev}^l$ , if  $f_{syn}^l >= f_{rev}^l$ , or the bucket label signal is the frequency of  $f_{syn}^s$ . When the small synchrotron is target, the bucket label signal is the frequency of  $f_{rev}^s$ , if  $f_{syn}^s >= f_{rev}^s$ , or the bucket label signal is the frequency of  $f_{syn}^l$ .

Tab. 5.11 shows the formulas for the frequency of the bucket label signal, two slightly different frequencies for beating, the length of the synchronization window and the bunch and bucket center mismatch when the large synchrotron is the target. Tab. 5.12 shows them when the small synchrotron is the target.

Table 5.11: Synchronization when circumference ratio is far away from an integer and the large synchrotron is the target

	Large synchrotron is target synchrotron	
Cases	$\frac{f_{rf}^l}{(h^l \cdot n)/Y} >= f_{rev}^l$ $(\frac{Y}{n} >= 1)$	$\frac{f_{rf}^l}{(h^l \cdot n)/Y} < f_{rev}^l$ $(\frac{Y}{n} < 1)$
Frequency of bucket label	$f_{rev}^l$	$\frac{f_{rf}^l}{(h^l \cdot n)/Y}$
Two slightly different frequencies	$f_{syn}^s = f_{syn}^l = \frac{f_{rf}^s}{(h^s \cdot m)/Y}$ and $f_{syn}^s = f_{syn}^l = \frac{f_{rf}^l}{(h^l \cdot n)/Y}$	
Beating frequencies		$\Delta f = \left  \frac{f_{rf}^s}{(h^s \cdot m)/Y} - \frac{f_{rf}^l}{(h^l \cdot n)/Y} \right $
Length of synchronization window	$2 \cdot T_{rev}^l$	$2 \cdot [(h^l \cdot n)/Y] \cdot T_{rf}^l$
Bunch-to-bucket injection center mismatch	$\pm \frac{1}{2} \cdot \frac{2 \cdot T_{rev}^l}{1/\Delta f} \cdot 360^\circ$	$\pm \frac{1}{2} \cdot \frac{2 \cdot [(h^l \cdot n)/Y] \cdot T_{rf}^l}{1/\Delta f} \cdot 360^\circ$

There are various combination of  $\frac{m}{n}$  and  $\lambda$ ,  $\lambda$  determines the beating speed. The smaller, the more precise bunch-to-bucket injection.  $(h^l \cdot n)/Y$  and  $(h^s \cdot m)/Y$

### 5.3. Circumference ratio is far away from an integer

---

Table 5.12: Synchronization when circumference ratio is far away from an integer and the small synchrotron is the target

Small synchrotron is target synchrotron		
Cases	$\frac{f_{rf}^s}{(h^s \cdot m)/Y} \geq f_{rev}^s$ $(\frac{Y}{m} \geq 1)$	$\frac{f_{rf}^s}{(h^s \cdot m)/Y} < f_{rev}^s$ $(\frac{Y}{m} < 1)$
Frequency of bucket label	$f_{rev}^s$	$\frac{f_{rf}^s}{(h^s \cdot m)/Y}$
Two slightly different frequencies	$f_{syn}^s = \frac{f_{rf}^s}{(h^s \cdot m)/Y}$ and $f_{syn}^l = \frac{f_{rf}^l}{(h^l \cdot n)/Y}$	
Beating frequencies		$\Delta f = \left  \frac{f_{rf}^s}{(h^s \cdot m)/Y} - \frac{f_{rf}^l}{(h^l \cdot n)/Y} \right $
Length of synchronization window	$2 \cdot T_{rev}^s$	$2 \cdot [(h^s \cdot m)/Y] \cdot T_{rf}^s$
Bunch-to-bucket injection center mismatch	$\pm \frac{1}{2} \cdot \frac{2 \cdot T_{rev}^s}{1/\Delta f} \cdot 360^\circ$	$\pm \frac{1}{2} \cdot \frac{2 \cdot [(h^s \cdot m)/Y] \cdot T_{rf}^s}{1/\Delta f} \cdot 360^\circ$

determines the two slightly different frequencies. The bigger  $(h^l \cdot n)/Y$  and  $(h^s \cdot m)/Y$ , the smaller two slightly different frequencies, which has higher requirement for LLRF system. So we have to find a balance between the precision of the bunch-to-bucket injection and the low frequencies for beating.

Two slightly different frequencies could also be a fraction (between 1/Y and 1) times of the  $\frac{f_{rf}^l}{(h^l \cdot n)/Y}$  and  $\frac{f_{rf}^s}{(h^s \cdot m)/Y}$ , see Sec. 5.2.

#### 5.3.1 Use case of $H^+$ B2B transfer from SIS100 to CR

Only one out of five bunches of proton is extracted from SIS100 and goes to Pbar, then antiproton is produced and injected into one bucket of CR [49]. The large synchrotron is SIS100 and the small one is CR,  $h^{SIS100} = 5$  and  $h^{CR} = 1$ . Here we take an example, that the proton energy before the Pbar is 28.8 GeV/u and the antiproton energy after the Pbar is 3 GeV/u. The GCD of  $h^{SIS100} \cdot n = 5 \cdot 10 = 50$  and  $h^{CR} \cdot m = 1 \cdot 49 = 49$  is 1, namely  $Y = 1$ . Substituting the extraction and injection revolution frequencies into eq. 5.13, we get

$$\frac{f_{rev}^{CR}}{f_{rev}^{SIS100}} = 4.9 - 0.0004 = \frac{m}{n} + \lambda = \frac{49}{10} - 0.0004 \quad (5.14)$$

Substituting  $h^{SIS100}$ ,  $h^{CR}$ , m, n and  $\lambda$  into eq. 2.42, we get

$$\frac{f_{rf}^{SIS100}}{f_{rf}^{CR}} = \frac{h^{SIS100} \cdot n}{h^{CR} \cdot m + h^{CR} \cdot \lambda \cdot n} = \frac{5 \cdot 10}{1 \cdot 49 - 1 \cdot 0.0004 \cdot 10} \quad (5.15)$$

### 5.3. Circumference ratio is far away from an integer

---

CR is the small synchrotron and the target and there exists  $\frac{f_{rf}^s}{(h^s \cdot m)/Y} = \frac{f_{rf}^s}{(1 \cdot 49)/1} < f_{rev}^s = f_{rf}^s$ , so substituting  $h^X$ ,  $m$ ,  $n$ ,  $\lambda$ ,  $f_{rf}^X$  and  $Y$  into formulas in the last column in Tab. 5.12, the synchronization of proton B2B transfer from SIS100 to CR is obtained, see Tab. 5.13.

Table 5.13: Synchronization of  $H^+$  B2B transfer from SIS100 to CR with the frequency beating method

	Small synchrotron (CR) is target synchrotron
Frequency of bucket label	$\frac{f_{rf}^{CR}}{49}$
Two slightly different frequencies	$f_{syn}^l = \frac{f_{rf}^{SIS100}}{50} = 26.658 \text{ kHz}$ and $f_{syn}^s = \frac{f_{rf}^{CR}}{49} = 26.873 \text{ kHz}$
Beating frequencies	215 Hz
Length of synchronization window	$2 \cdot 49 \cdot T_{rf}^{CR} = 74.382 \text{ us}$
Bunch-to-bucket injection center mismatch	$\pm \frac{1}{2} \cdot \frac{2 \cdot 49 \cdot T_{rev}^{CR}}{1/215} \cdot 360^\circ = \pm 2.88^\circ$

The CR is empty before the injection, so the phase jump is preferred for CR. Detailed parameters of the  $H^+$  B2B transfer from SIS100 to CR , please see Appendix C.6.

#### 5.3.2 Use case of RIB B2B transfer from SIS100 to CR

Only one out of two bunches is extracted from SIS100 and goes to Super FRS, then RIB is produced and injected into one bucket of CR. The large synchrotron is SIS100 and the small one is CR.  $h^{SIS100} = 2$  and  $h^{CR} = 1$ . Here we take an example, that the energy of the heavy ion beam before the Super FRS is 1.5 GeV/u and the RIB energy after the Super FRS is 740 MeV/u. Substituting the extraction and injection revolution frequencies into eq. 5.13, we get

$$\frac{f_{rev}^{CR}}{f_{rev}^{SIS100}} = 4.4 - 0.0046 = \frac{m}{n} + \lambda = \frac{22}{5} - 0.0046 \quad (5.16)$$

Substituting  $h^{SIS100}$ ,  $h^{CR}$ ,  $m$ ,  $n$  and  $\lambda$  into eq. 2.42, we get

$$\frac{f_{rf}^{SIS100}}{f_{rf}^{CR}} = \frac{h^{SIS100} \cdot n}{h^{CR} \cdot m + h^{CR} \cdot \lambda \cdot n} = \frac{2 \cdot 5}{1 \cdot 22 - 1 \cdot 0.0046 \cdot 5} \quad (5.17)$$

The GCD of  $h^{SIS100} \cdot n = 2 \cdot 5 = 10$  and  $h^{CR} \cdot m = 1 \cdot 22 = 22$  is 2, namely  $Y = 2$ . CR is the small synchrotron and the target and there exists  $\frac{f_{rf}^s}{(h^s \cdot m)/Y} = \frac{f_{rf}^s}{(1 \cdot 22)/1} <$

### 5.3. Circumference ratio is far away from an integer

---

$f_{rev}^s = f_{rf}^s$ , so substituting  $h^X$ ,  $m$ ,  $n$ ,  $\lambda$ ,  $f_{rf}^X$  and  $Y$  into formulas in the last column in Tab. 5.12, the synchronization of RIB B2B transfer from SIS100 to CR is obtained, see Tab. 5.14.

Table 5.14: Synchronization of RIB B2B transfer from SIS100 to CR with the frequency beating method

	Small synchrotron (CR) is target synchrotron
Frequency of bucket label	$\frac{f_{rf}^{CR}}{11}$
Two slightly different frequencies	$f_{syn}^l = \frac{f_{rf}^{SIS100}}{5} = 102.326 \text{ kHz}$ and $f_{syn}^s = \frac{f_{rf}^{CR}}{11} = 102.218 \text{ kHz}$
Beating frequencies	108 Hz
Length of synchronization window	$2 \cdot (22/2) \cdot T_{rf}^{CR} = 19.558 \text{ us}$
Bunch-to-bucket injection center mismatch	$\pm \frac{1}{2} \cdot \frac{2 \cdot 22 \cdot T_{rev}^{CR}}{1/54} \cdot 360^\circ = \pm 0.39^\circ$

The CR is empty before the injection, so the phase jump is preferred for CR. Detailed parameters of RIB B2B transfer from SIS100 to CR, please see Appendix C.6.

#### 5.3.3 Use case of B2B transfer from CR to HESR

One bunch of CR is injected into one bucket of HESR. The beam is accumulated in HESR [15]. The large synchrotron is HESR and the small one is CR.  $h^{HESR} = 1$  and  $h^{CR} = 1$ . The GCD of  $h^{HESR} \cdot n = 1 \cdot 5 = 5$  and  $h^{CR} \cdot m = 1 \cdot 13 = 13$  is 1, namely  $Y = 1$ . Substituting the circumference of HESR and CR to eq. 2.41, we have

$$\frac{C^{HESR}}{C^{CR}} = 2.6 - 0.003 = \frac{m}{n} + \lambda = \frac{13}{5} - 0.003 \quad (5.18)$$

Substituting  $h^{HESR}$ ,  $h^{CR}$ ,  $m$ ,  $n$  and  $\lambda$  into eq. 2.42, we get

$$\frac{f_{rf}^{HESR}}{f_{rf}^{CR}} = \frac{h^{HESR} \cdot n}{h^{CR} \cdot m + h^{ESR} \cdot \lambda \cdot n} = \frac{1 \cdot 5}{1 \cdot 13 - 1 \cdot 0.003 \cdot 5} \quad (5.19)$$

HESR is the large synchrotron and the target and there exists  $\frac{f_{rf}^l}{(h^l \cdot n)/Y} = \frac{f_{rf}^l}{(1 \cdot 5)/1} < f_{rev}^l = f_{rf}^l$ , so substituting  $h^X$ ,  $m$ ,  $n$ ,  $\lambda$ ,  $f_{rf}^X$  and  $Y$  into formulas in the last column in Tab. 5.11, the synchronization of B2B transfer from CR to HESR is obtained. Tab. 5.15 shows two operations for antiproton and RIB.

### 5.3. Circumference ratio is far away from an integer

---

Table 5.15: Synchronization of B2B transfer from CR to HESR with the frequency beating method

	Larger synchrotron (HESR) is target synchrotron
Frequency of bucket label	$\frac{f_{rf}^{HESR}}{5}$
	3 GeV/u antiproton
Two slightly different frequencies	$f_{syn}^s = \frac{f_{rf}^{CR}}{13} = 101.290 \text{ kHz}$ and $f_{syn}^l = \frac{f_{rf}^{HESR}}{5} = 101.426 \text{ kHz}$
Beating frequencies	136 Hz
Length of synchronization window	$2 \cdot 5 \cdot T_{rf}^{HESR} = 19.719 \text{ us}$
Bunch-to-bucket injection center mismatch	$\pm \frac{1}{2} \cdot \frac{2 \cdot 5 \cdot T_{rev}^{CR}}{1/136} \cdot 360^\circ = \pm 0.48^\circ$
	740 MeV/u RIB
Two slightly different frequencies	$f_{rf}^{CR} = 86.493 \text{ kHz}$ and $f_{rf}^{HESR} = 86.608 \text{ kHz}$
Beating frequencies	113 Hz
Length of synchronization window	$2 \cdot 5 \cdot T_{rf}^{HESR} = 23.090 \text{ us}$
Bunch-to-bucket injection center mismatch	$\pm \frac{1}{2} \cdot \frac{2 \cdot 5 \cdot T_{rev}^{CR}}{1/113} \cdot 360^\circ = \pm 0.47^\circ$

After the synchronization, the phase difference between the 1/13 CR and 1/5 HESR rf frequency markers depends on the accumulation method. Detailed parameter about the B2B transfer from CR to HESR, please see Appendix C.5.

#### 5.3.4 Use case of B2B transfer from SIS18 to ESR via FRS

Only one bunch is extracted from SIS18 and goes to FRS, then RIB is produced and injected into one bucket of ESR. The large synchrotron is SIS18 and the small one is ESR.  $h^{SIS18} = 1$  and  $h^{ESR} = 1$ . Here we take an applied case as an example, that the energy of the heavy ion beam before the FRS is 550 MeV/u and the RIB energy after the FRS is 400 MeV/u. Substituting the extraction and injection revolution

## 5.4. Summary of the synchronization for different scenarios

---

frequencies into eq. 5.13, we get

$$\frac{f_{rev}^{ESR}}{f_{rev}^{SIS18}} = 1.8 + 0.048 = \frac{m}{n} + \lambda = \frac{9}{5} + 0.048 \quad (5.20)$$

Substituting  $h^{SIS18}$ ,  $h^{ESR}$ , m, n and  $\lambda$  into eq. 2.42, we get

$$\frac{f_{rf}^{SIS18}}{f_{rf}^{ESR}} = \frac{h^{SIS18} \cdot n}{h^s \cdot m + h^{ESR} \cdot \lambda \cdot n} = \frac{1 \cdot 5}{1 \cdot 9 + 1 \cdot 0.048 \cdot 5} \quad (5.21)$$

The GCD of  $h^{SIS18} \cdot n = 1 \cdot 5 = 5$  and  $h^s \cdot m = 1 \cdot 9 = 9$  is 1, namely  $Y = 1$ . ESR is the small synchrotron and the target and there exists  $\frac{f_{rf}^s}{(h^s \cdot m)/Y} = \frac{f_{rf}^s}{(1 \cdot 9)/1} < f_{rev}^s = f_{rf}^s$ , so substituting  $h^X$ , m, n,  $\lambda$ ,  $f_{rf}^X$  and Y into formulas in the last column in Tab. 5.12, the synchronization of B2B transfer from SIS18 to ESR via FRS is obtained, see Tab. 5.16.

Table 5.16: Synchronization of B2B transfer from SIS18 to ESR via FRS with the frequency beating method

	Small synchrotron (ESR) is target synchrotron
Frequency of bucket label	$\frac{f_{rf}^{ESR}}{9}$
Two slightly different frequencies	$f_{syn}^l = \frac{f_{rf}^{SIS18}}{5} = 215.393 \text{ kHz}$ and $f_{syn}^s = \frac{f_{rf}^{ESR}}{9} = 219.642 \text{ kHz}$
Beating frequencies	4.249 kHz
Length of synchronization window	$2 \cdot 9 \cdot T_{rf}^{ESR} = 9.106 \text{ us}$
Bunch-to-bucket injection center mismatch	$\pm \frac{1}{2} \cdot \frac{2 \cdot 9 \cdot T_{rev}^{ESR}}{1/4249} \cdot 360^\circ = \pm 6.92^\circ$

More parameters about the B2B transfer from SIS18 to ESR via FRS, please see Appendix C.3. For the detailed realization and implementation of two slightly different frequencies, please see “Development of the LLRF system for a deterministic Bunch-to-Bucket transfer for FAIR“.

## 5.4 Summary of the synchronization for different scenarios

In this section, all the synchronization methods are summarized. Tab. 5.17 summarizes the formulas when the revolution period is shorter than the period for the phase alignment between two rf systems. Tab. 5.18 summarizes the formulas when the revolution period is longer than the period for the phase alignment.

## 5.4. Summary of the synchronization for different scenarios

Table 5.17: Summary of the synchronization when the revolution period is shorter than the period for the phase alignment between two rf systems

The formulas with black text are based on the assumption that the large synchrotron is the target and the formulas with red text the assumption that the small one is the target.

Circumference ratio	rf cavity frequency ratio $f_{rf}^l/f_{rf}^s$	Frequency of bucket label	Frequency beating Two slightly different frequencies	Frequency beating bunch-to-bucket center mismatch
$C^l/C^s = \kappa$ Integer	$\frac{h^l}{h^s \cdot \kappa}$	$\frac{f_{rf}^l}{h^l/Y}$	$f_{syn} = \frac{f_{rf}^l}{h^l/Y}$ and $f_{syn}^s = \frac{f_{rf}^s}{(h^s \cdot \kappa)/Y} + \Delta f$ or $f_{syn} = \frac{f_{rf}^l}{h^l/Y} + \Delta f$ and $f_{syn}^s = \frac{f_{rf}^s}{(h^s \cdot \kappa)/Y}$	$\pm \frac{1}{2} \cdot \frac{2 \cdot (h^l/Y) \cdot T_{rf}^l}{1/\Delta f} \cdot 360^\circ$ $\pm \frac{1}{2} \cdot \frac{2 \cdot [(h^s \cdot \kappa)/Y] \cdot T_{rf}^s}{1/\Delta f} \cdot 360^\circ$
$C^l/C^s = \kappa + \lambda$ or $f_{rev}^s/f_{rev}^l = \kappa + \lambda$ close to integer	$\frac{h^l}{h^{s+\lambda}}$	$\frac{f_{rf}^l}{h^l/Y}$	$f_{syn}^l = \frac{f_{rf}^l}{h^l/Y}$ and $f_{syn}^s = \frac{f_{rf}^s}{(h^s \cdot \kappa)/Y}$ $\Delta f = \frac{f_{rf}^l}{h^l/Y} - \frac{f_{rf}^s}{(h^s \cdot \kappa)/Y}$	$\pm \frac{1}{2} \cdot \frac{2 \cdot (h^l/Y) \cdot T_{rf}^l}{1/\Delta f} \cdot 360^\circ$ $\pm \frac{1}{2} \cdot \frac{2 \cdot [(h^s \cdot \kappa)/Y] \cdot T_{rf}^s}{1/\Delta f} \cdot 360^\circ$
$C^l/C^s = m/n + \lambda$ or $f_{rev}^s/f_{rev}^l = m/n + \lambda$ far away from integer	$\frac{h^l}{h^{s+(m/n+\lambda)}}^2$	$\frac{f_{rf}^l}{(h^l \cdot n)/Y}$	$f_{syn}^l = \frac{f_{rf}^l}{(h^l \cdot n)/Y}$ and $f_{syn}^s = \frac{f_{rf}^s}{(h^s \cdot m)/Y}$ $\Delta f = \frac{f_{rf}^l}{(h^l \cdot n)/Y} - \frac{f_{rf}^s}{(h^s \cdot m)/Y}$	$\pm \frac{1}{2} \cdot \frac{2 \cdot (h^l \cdot n)/Y \cdot T_{rf}^l}{1/\Delta f} \cdot 360^\circ$ $\pm \frac{1}{2} \cdot \frac{2 \cdot [(h^s \cdot m)/Y] \cdot T_{rf}^s}{1/\Delta f} \cdot 360^\circ$
The phase shift could be implemented either for the large or small synchrotron. When the target synchrotron is empty, the phase jump is implemented for the target synchrotron.				

$$\frac{2 f_{rf}^l}{f_{rf}s} = \frac{h^l f_{rev}^l}{h^s f_{rev}^s} = \frac{h^l C_s}{h^s C_l} = \frac{h^l}{h^s (m/n+\lambda)} = \frac{h^l}{h^{s-m+n\lambda} n}$$

#### 5.4. Summary of the synchronization for different scenarios

Table 5.18: Summary of the synchronization when the revolution period is longer than the period for the phase alignment between two rf systems

The formulas with black text are based on the assumption that the large synchrotron is the target and the formulas with red text the assumption that the small one is the target.

Circumference ratio	rf cavity frequency ratio $f_{rf}^l/f_{rf}^s$	Frequency of bucket label	Frequency beating Two slightly different frequencies	Frequency beating bunch-to-bucket center mismatch
$C^l/C^s = \kappa$ Integer	$\frac{h^l}{h^s \cdot \kappa}$	$f_{rev}^l$	$f_{syn}^l = \frac{f_{rf}^l}{h^l/Y}$ and $f_{syn}^s = \frac{f_{rf}^s}{(h^s \cdot \kappa)/Y} + \Delta f$ or $f_{syn}^l = \frac{f_{rf}^l}{h^l/Y} + \Delta f$ and $f_{syn}^s = \frac{f_{rf}^s}{(h^s \cdot \kappa)/Y}$	$\pm \frac{1}{2} \cdot \frac{2 \cdot T_{rev}^l}{1/\Delta f} \cdot 360^\circ$ $\pm \frac{1}{2} \cdot \frac{2 \cdot T_s}{1/\Delta f} \cdot 360^\circ$
$C^l/C^s = \kappa + \lambda$ or $f_{rev}^s/f_{rev}^l = \kappa + \lambda$ close to integer	$\frac{h^l}{h^s \cdot (\kappa + \lambda)}$	$f_{rev}^l$ $f_{rev}^s$	$f_{syn}^l = \frac{f_{rf}^l}{h^l/Y}$ and $f_{syn}^s = \frac{f_{rf}^s}{(h^s \cdot \kappa)/Y}$ $\Delta f = \frac{f_{rf}^l}{h^l/Y} - \frac{f_{rf}^s}{(h^s \cdot \kappa)/Y}$	$\pm \frac{1}{2} \cdot \frac{2 \cdot T_{rev}^l}{1/\Delta f} \cdot 360^\circ$ $\pm \frac{1}{2} \cdot \frac{2 \cdot T_s}{1/\Delta f} \cdot 360^\circ$
$C^l/C^s = m/n + \lambda$ or $f_{rev}^s/f_{rev}^l = m/n + \lambda$ far away from integer	$\frac{h^l}{h^s \cdot (m/n + \lambda)}$	$f_{rev}^l$ $f_{rev}^s$	$f_{syn}^l = \frac{f_{rf}^l}{(h^l \cdot n)/Y}$ and $f_{syn}^s = \frac{f_{rf}^s}{(h^s \cdot m)/Y}$ $\Delta f = \frac{f_{rf}^l}{(h^l \cdot n)/Y} - \frac{f_{rf}^s}{(h^s \cdot m)/Y}$	$\pm \frac{1}{2} \cdot \frac{2 \cdot T_{rev}^l}{1/\Delta f} \cdot 360^\circ$ $\pm \frac{1}{2} \cdot \frac{2 \cdot T_s}{1/\Delta f} \cdot 360^\circ$

The phase shift could be implemented either for the large or small synchrotron.

When the target synchrotron is empty, the phase jump is implemented for the target synchrotron.

# Chapter 6

## Realization and systematic investigation of the FAIR B2B transfer system

!!!!!!!!!!!!!!please check List of symbol and abbreviation ... for chapter 5 and 6.

This chapter concentrates on the realization and systematic investigation of the B2B transfer system. In Sec. 6.1, both the phase shift and frequency beating synchronization methods are analyzed from the beam dynamic viewpoint. The WR network is investigated for the B2B transfer and the calculation of the synchronization window are presented in Sec. 6.2. The B2B transfer system for FAIR focuses first of all on SIS18 to SIS100 transfer, so the trigger possibility of the SIS18 extraction and SIS100 injection kicker is systematically investigated in Sec. 6.3. Besides, the test setup from the timing aspect is built in Sec. 6.4.

### 6.1 Investigation of two synchronization methods for $U^{28+}$ B2B transfer from SIS18 to SIS100 from the beam dynamics viewpoint

This section analyzes the phase shift and frequency beating methods from the beam-dynamics viewpoint for the synchronization of SIS18 with SIS100. In this chapter, the circumference of SIS18 and SIS100 are denoted by  $C^{SIS18}$  and  $C^{SIS100}$ , the revolution frequency by  $f_{h=1}^{SIS18}$  and  $f_{h=1}^{SIS100}$  and the rf frequency by  $f_{h=2}^{SIS18}$  and  $f_{h=10}^{SIS100}$ . Since SIS18 and SIS100 harmonic number are 2 and 10, the relationship between the revolution and rf frequencies are  $f_{h=2}^{SIS18} = 2f_{h=1}^{SIS18}$  and  $f_{h=10}^{SIS100} = 10f_{h=1}^{SIS100}$ . Since  $C^{SIS100}$  is five times as long as  $C^{SIS18}$ , we could get the relation  $f_{h=1}^{SIS18} = 5f_{h=1}^{SIS100}$  and  $f_{h=10}^{SIS100} = f_{h=2}^{SIS18}$ .

#### 6.1.1 Phase shift method

To achieve a required phase shift, the rf frequency is modulated away from the nominal value for a period of time and modulated back [23]. Let  $\Delta\phi_{shift}$  be the phase shift to be achieved and  $\Delta f_{rf}$  the RF frequency variation to accomplish it;

## 6.1. Investigation of two synchronization methods for $U^{28+}$ B2B transfer from SIS18 to SIS100 from the beam dynamics viewpoint

---

then,

$$\Delta\phi_{shift} = 2\pi \int_{t_0}^{t_0+T} \Delta f_{rf}(t) dt \quad (6.1)$$

where  $T$  is the period of frequency modulation and  $t_0$  is the time at which the modulation begins. To make the frequency modulation effective, the stabilization system, beam-phase feedback loop, must be frozen before the modulation begins.

The following four examples of frequency modulation are analyzed. Case (1) trapezoid modulation, Case (2) triangular modulation, Case (3) sinusoidal modulation and Case (4) parabolic modulation. Here I assume the phase shift must be achieved within 7ms. These frequency modulations are shown in Fig. 6.1. All the four modulations give the same phase shift,  $\Delta\phi_{shift} = \pi$ , which is proved by substituting each form of  $\Delta f_{rf}(t)$  into eq. 6.1 and performing integration.

Case (1)

$$\Delta f_{rf}(t) = \begin{cases} 50Hz/ms \cdot (t - t_0) & t_0 + 0 < t \leq t_0 + 2ms \\ 100Hz & t_0 + 2 < t \leq t_0 + 5ms \\ 100Hz - 50Hz/ms \cdot (t - t_0) & t_0 + 5ms < t \leq t_0 + 7ms \end{cases} \quad (6.2)$$

Case (2)

$$\Delta f_{rf}(t) = \begin{cases} \frac{10^3}{7-3.5}Hz/ms \cdot (t - t_0) & t_0 + 0 < t \leq t_0 + 3.5ms \\ \frac{10^3}{7}Hz - \frac{10^3}{7-3.5}Hz/ms \cdot (t - t_0 - 3.5ms) & t_0 + 3.5ms < t \leq t_0 + 7ms \end{cases} \quad (6.3)$$

Case (3)

$$\Delta f_{rf}(t) = \frac{10^3}{14}Hz \cdot (1 - \cos(\frac{2\pi}{7}rad/ms \cdot (t - t_0))) \quad t_0 + 0 < t \leq t_0 + 7ms \quad (6.4)$$

Case (4)

$$\Delta f_{rf}(t) = \frac{20}{21} \cdot \begin{cases} 30Hz/ms^2 \cdot (t - t_0)^2 & t_0 + 0 < t \leq t_0 + 1ms \\ 30Hz + 60Hz/ms \cdot (t - t_0 - 1ms) & t_0 + 1ms < t \leq t_0 + 2.5ms \\ 30Hz/ms^2 \cdot [5ms^2 - (t - t_0 - 3.5ms)^2] & t_0 + 2.5ms < t \leq t_0 + 4.5ms \\ 30Hz + 60Hz/ms \cdot [6ms - (t - t_0)] & t_0 + 4.5ms < t \leq t_0 + 6ms \\ 30Hz/ms^2 \cdot [7ms^2 - (t - t_0)]^2 & t_0 + 6ms < t \leq t_0 + 7ms \end{cases} \quad (6.5)$$

## 6.1. Investigation of two synchronization methods for $U^{28+}$ B2B transfer from SIS18 to SIS100 from the beam dynamics viewpoint

---

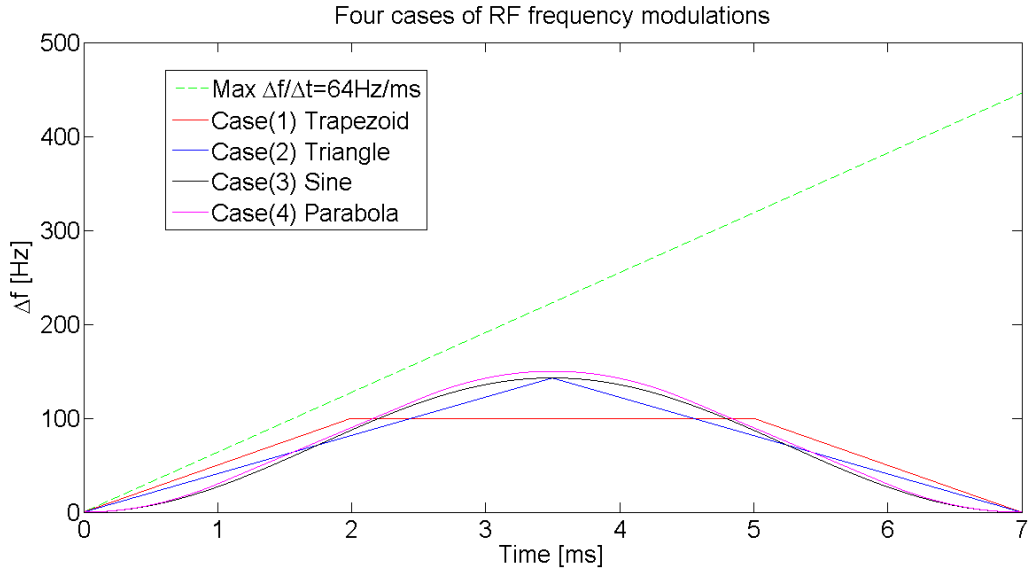


Figure 6.1: Examples of RF frequency modulation.

Fig. 6.2 shows the time derivation of four rf frequency modulations, which are smaller than the maximum time derivative of rf frequency during the acceleration ramp 64Hz/ms for the adiabaticity consideration. The acceleration ramp is an adiabatical process.

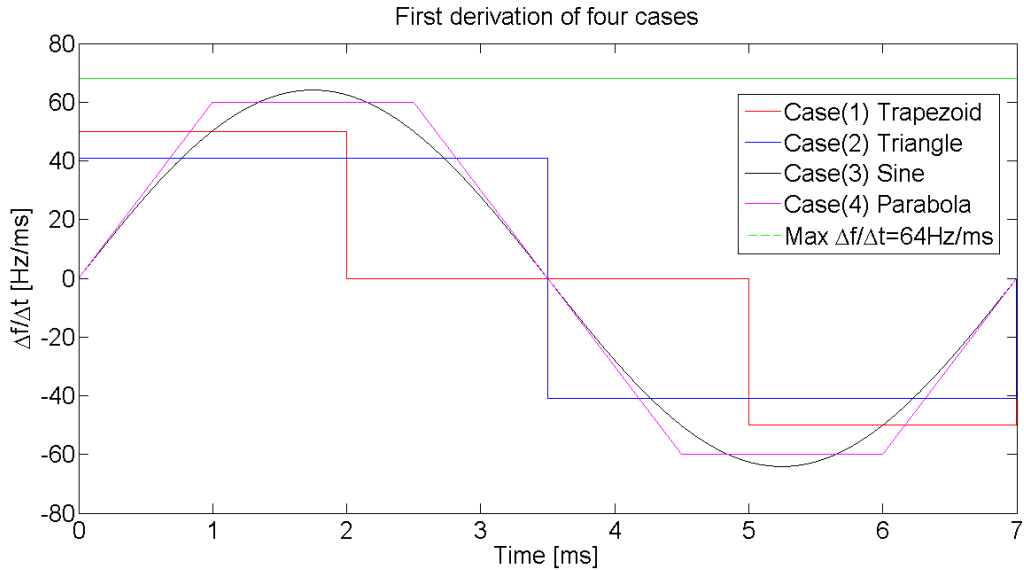


Figure 6.2: Time derivation of four modulations

Fig. 6.3 shows the corresponding phase shift modulation of four cases.

## 6.1. Investigation of two synchronization methods for $U^{28+}$ B2B transfer from SIS18 to SIS100 from the beam dynamics viewpoint

---

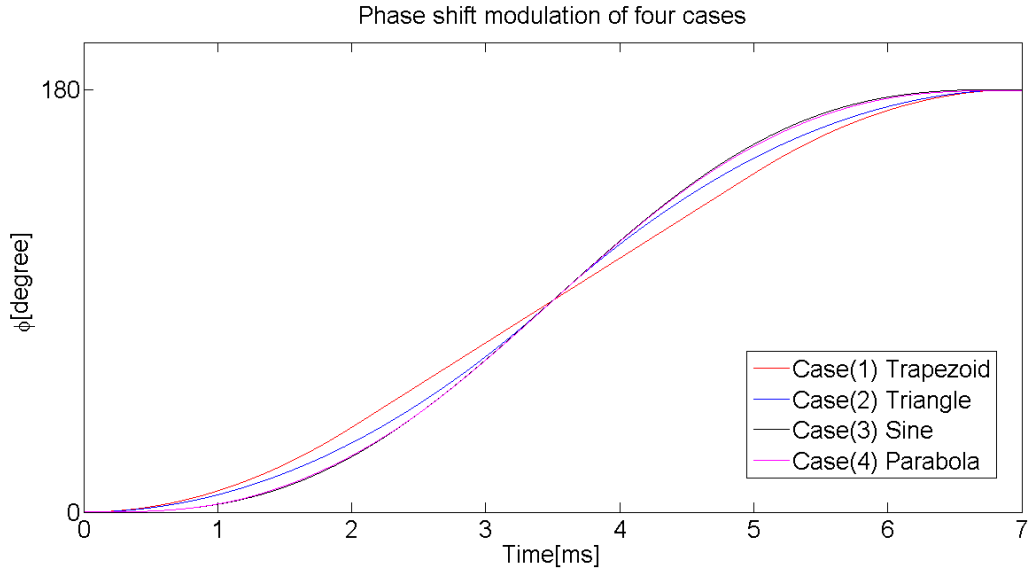


Figure 6.3: The phase shift modulation of four cases

### 6.1.1.1 Longitudinal dynamic analysis for the simulation

In this section, the average radial excursion, the relative momentum shift, synchronous phase, bucket size and adiabaticity of four rf frequency modulations are analyzed.

- Average radial excursion

The average radial excursion is calculated for the four cases of rf frequency modulations by eq. (2.52). Fig. 6.4 shows the calculation result [51].

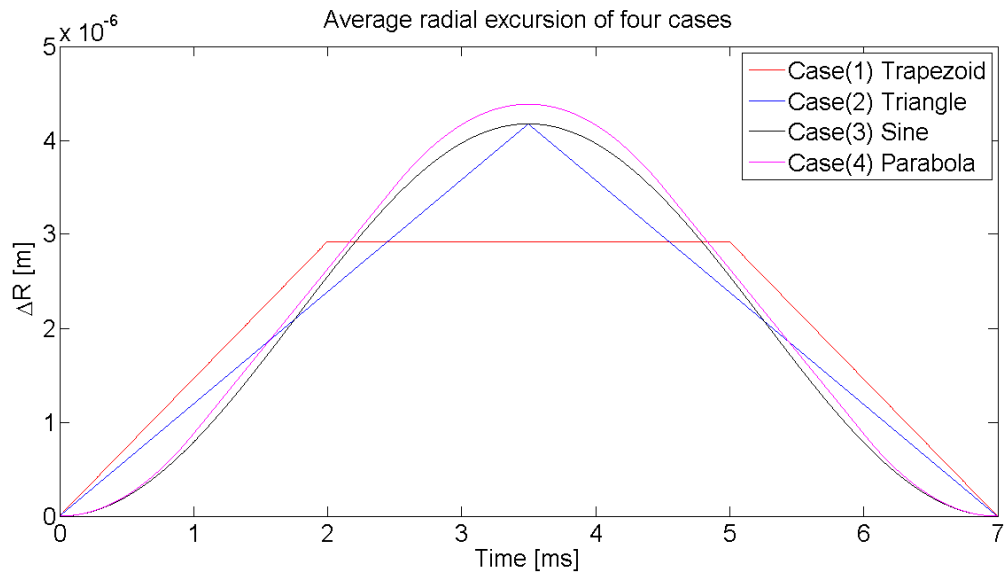


Figure 6.4: Average radial excursions of four cases.

## 6.1. Investigation of two synchronization methods for $U^{28+}$ B2B transfer from SIS18 to SIS100 from the beam dynamics viewpoint

---

Table 6.1: The maximum average radial excursion of four cases

	Case (1)	Case (2)	Case (3)	Case (4)
Max avg radial excursion	$2.93 \cdot 10^{-6}$	$4.17 \cdot 10^{-6}$	$4.18 \cdot 10^{-6}$	$4.38 \cdot 10^{-6}$
Time	flat	3.5 ms	3.5 ms	3.5 ms

Tab. 6.1 shows the maximum average radial excursion and the time for four cases. The maximum tolerable radial excursion of SIS18 is  $\pm 2.4 \cdot 10^{-4}$ . For all cases, the average radial excursion is within the acceptable range. Hence, all cases are applicable.

- Relative momentum shift

The relative momentum shift is calculated for the four cases of rf frequency modulations by eq. (??). Fig. 6.5 shows the calculation result.

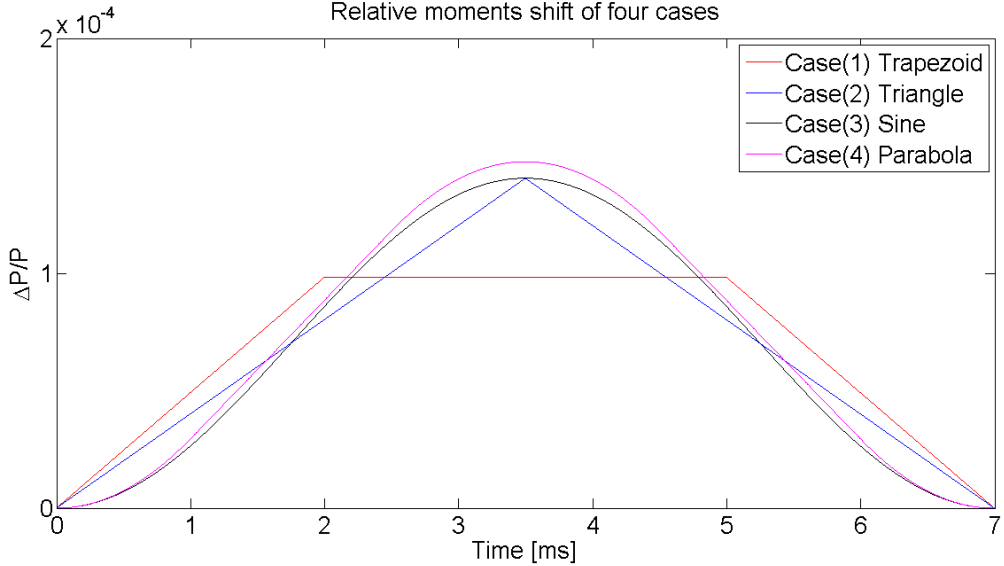


Figure 6.5: Relative momentum shift of four cases.

Table 6.2: The maximum relative momentum shift of four cases

	Case (1)	Case (2)	Case (3)	Case (4)
Max relative momentum shift	$9.83 \cdot 10^{-5}$	$1.38 \cdot 10^{-4}$	$1.40 \cdot 10^{-4}$	$1.48 \cdot 10^{-4}$
Time	flat	3.5 ms	3.5 ms	3.5 ms

Tab. 6.2 shows the maximum relative momentum shift and the time for four cases. The maximum tolerable relative momentum shift of SIS18 is  $\pm 0.008$ . For all cases, the maximum relative momentum shift is within the acceptable range. Hence, all cases are applicable.

## 6.1. Investigation of two synchronization methods for $U^{28+}$ B2B transfer from SIS18 to SIS100 from the beam dynamics viewpoint

---

- Synchronous phase

The rf frequency modulations make the synchronous phase deviate from the nominal value  $0^\circ$ . Fig. 6.6 shows the changes in the synchronous phase,  $\Delta\phi_s(t)$ . It is calculated by substituting values into eq. ???. For case (1), the phase jumps in  $\Delta\phi_s$  appear at the start and end of the frequency modulation, and at two points where the slope of modulation changes from upward to flat and from flat to downward. For case (2), the phase jumps in  $\Delta\phi_s(t)$  appear at the start and end of the frequency modulation, and at the midpoint where the slope of modulation changes from upward to downward. For case (3) and (4), the synchronous phase  $\Delta\phi_s(t)$  during the modulations are continuous. The phase jumps endanger the beam stability. Hence, only case (3) and (4) are applicable.

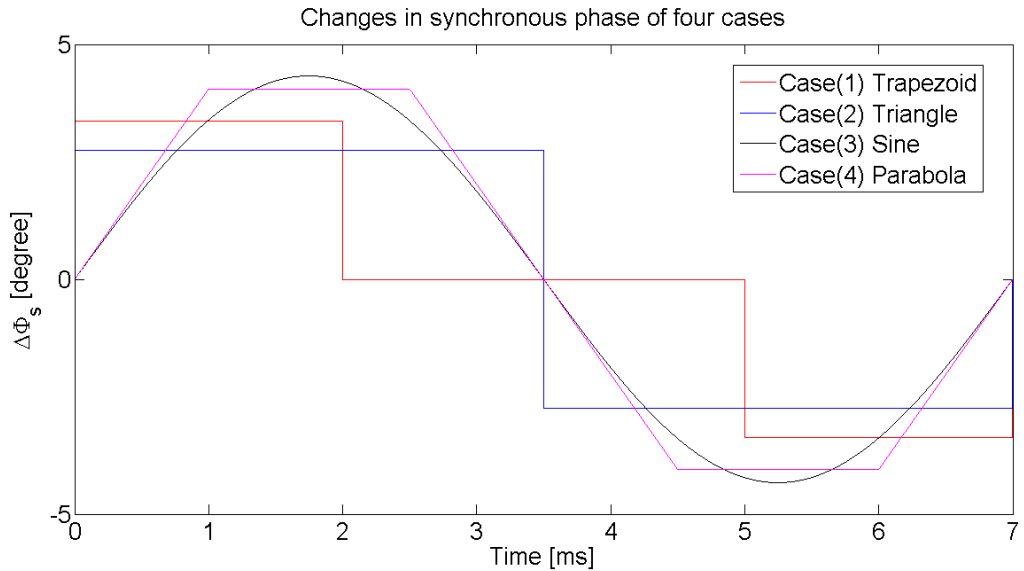


Figure 6.6: Changes in synchronous phase of four cases

- Bucket size

The bucket area factor  $\alpha_b$  varies during rf frequency modulations. Before the modulations, the synchronous phase  $\phi_s=0^\circ$  and  $\alpha_b(0^\circ) = 1$ . By substituting the changes in synchronous phase into eq. (6.6), we get the ratio of bucket areas of a running bucket to the stationary bucket for four cases, see Fig. (6.7).

$$\alpha_b(\phi_s) \approx \frac{1 - \sin\phi_s}{1 + \sin\phi_s} \quad (6.6)$$

## 6.1. Investigation of two synchronization methods for $U^{28+}$ B2B transfer from SIS18 to SIS100 from the beam dynamics viewpoint

---

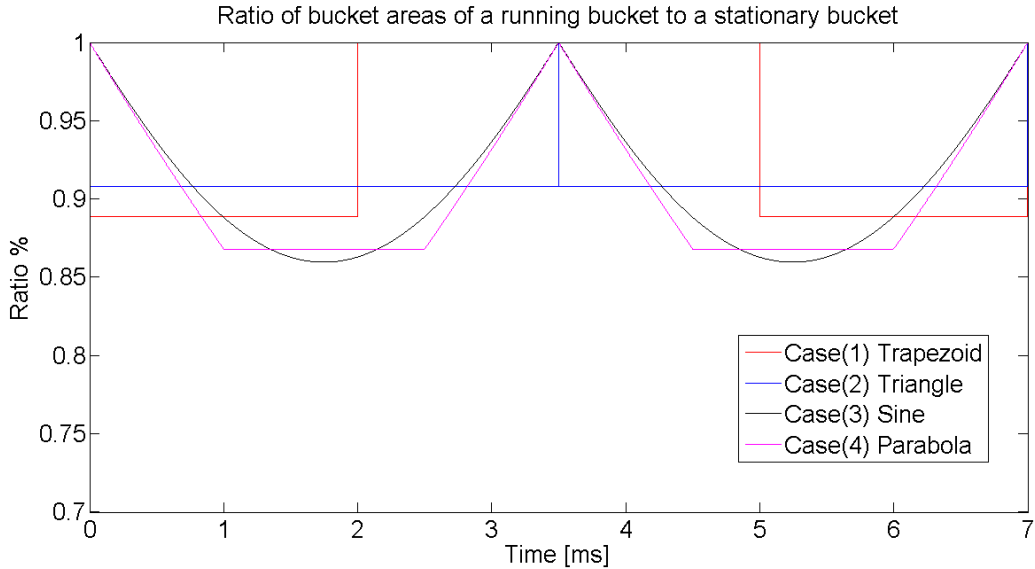


Figure 6.7: Ratio of bucket areas of a running bucket to the stationary bucket of four cases

Tab. 6.3 shows the bucket area factor for four cases. For all cases, the running bucket area factor is larger than 85%. Hence, all cases are applicable.

Table 6.3: The minimum bucket area factor of four cases

	Case (1)	Case (2)	Case (3)	Case (4)
Min bucket area factor	88%	90%	86%	86%

- Adiabaticity

By substituting the values of  $d\Delta\phi_s(t)/dt$  obtained from Fig. 6.6 and the other appropriate values into eq. 2.57, we can calculate the adiabaticity parameter,  $\varepsilon$ , for the case (3) and (4), see Fig. 6.8. Because  $d\Delta\phi_s(t)$  changes discontinuously for case (1) and (2), this abrupt change gives rise to a coherent bunch oscillation at a synchrotron frequency, resulting in emittance dilution. So the rf frequency modulations of case (1) and (2) are not applicable.

For case (4), the maximum of  $\varepsilon$ , 0.000059, occurs at 1ms, 2.5ms, 4.5ms and 6ms. From Fig. 6.6, we could see the change of the synchronous phase  $d\Delta\phi_s(t)/dt$  at these time points is big but smoothly. For case (3), the maximum of  $\varepsilon$  is 0.000030. So the frequency modulation is adiabatical for case (3) and (4).

## 6.1. Investigation of two synchronization methods for $U^{28+}$ B2B transfer from SIS18 to SIS100 from the beam dynamics viewpoint

---

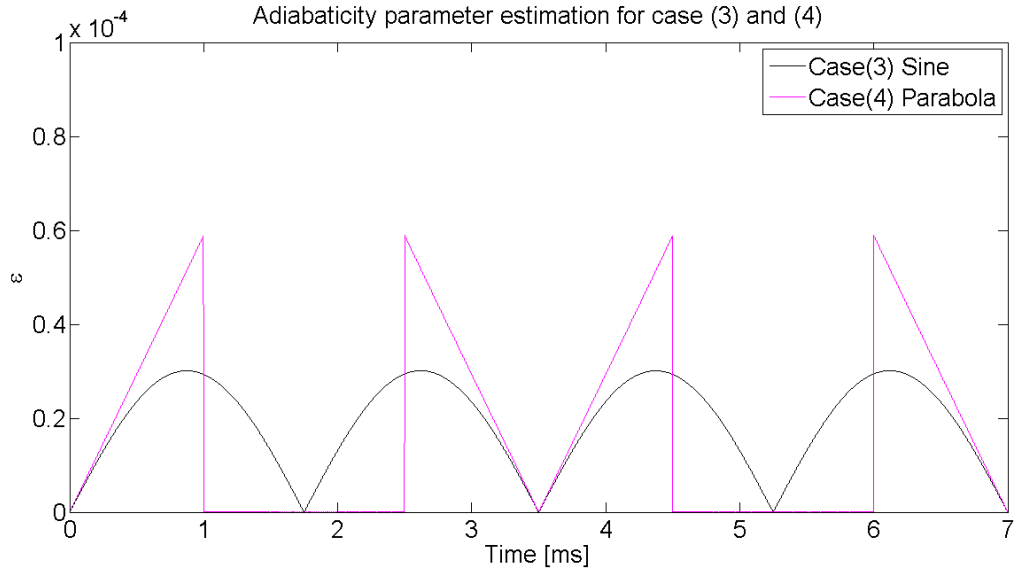


Figure 6.8: Adiabaticity parameter estimation of case (3) and (4)

### 6.1.1.2 Transverse dynamics analysis for the simulation

For SIS18, the chromaticity  $Q'_x$  and  $Q'_y$  is 4.17 and 3.4. Substituting chromaticity and maximum momentum shift (see. Tab. 6.2) into eq. ???. The chromatic tune shift  $\Delta Q_x$  and  $\Delta Q_y$  during rf modulations for four cases can be calculated.

Case (1)

$$\Delta Q_x = 4.17 \cdot 9.83 \cdot 10^{-5} = 4.10 \cdot 10^{-4} \quad (6.7)$$

$$\Delta Q_y = 3.4 \cdot 9.83 \cdot 10^{-5} = 3.34 \cdot 10^{-4} \quad (6.8)$$

Case (2)

$$\Delta Q_x = 4.17 \cdot 1.38 \cdot 10^{-4} = 5.75 \cdot 10^{-4} \quad (6.9)$$

$$\Delta Q_y = 3.4 \cdot 1.38 \cdot 10^{-4} = 4.69 \cdot 10^{-4} \quad (6.10)$$

Case (3)

$$\Delta Q_x = 4.17 \cdot 1.40 \cdot 10^{-4} = 5.84 \cdot 10^{-4} \quad (6.11)$$

$$\Delta Q_y = 3.4 \cdot 1.40 \cdot 10^{-4} = 4.76 \cdot 10^{-4} \quad (6.12)$$

Case (4)

$$\Delta Q_x = 4.17 \cdot 1.48 \cdot 10^{-4} = 6.17 \cdot 10^{-4} \quad (6.13)$$

$$\Delta Q_y = 3.4 \cdot 1.48 \cdot 10^{-4} = 5.03 \cdot 10^{-4} \quad (6.14)$$

The chromatic tune shift for four cases are significantly small, which could be negligible.

## 6.1.2 Frequency beating method

In the case of the frequency beating method, we guarantee the extraction and injection energy always match, which means that the momentum is not affected by the frequency detune, namely  $\Delta p = 0$ , So the frequency beating method has no influence on the transverse dynamics.

### 6.1.2.1 Longitudinal dynamics analysis of the frequency beating for SIS18

For the frequency beating method, the rf frequency de-tune is done accompanying with the RF ramp. Accepting to decentre the orbit by 8mm [40] for the SIS18

$$\frac{\Delta R}{R} = \pm 2.4 \cdot 10^{-4} \quad (6.15)$$

From eq. 2.61 and eq. 2.63, the RF frequency and the magnetic field change at the  $U^{28+}$  extraction energy 200MeV/u ( $\gamma_t = 5.8$ ) are

$$\frac{\Delta f}{f} = \pm 2.4 \cdot 10^{-4} \quad (6.16)$$

$$\frac{\Delta B}{B} = \frac{\Delta f}{f} \gamma_t^2 = \pm 8.1 \cdot 10^{-3} \quad (6.17)$$

where the maximum RF frequency de-tune is approximate to 370 Hz at 1.57 MHz for the  $U^{28+}$ . Fig. 6.9 shows the rf frequency derivation during the rf ramp. In the simulation, it is assumed that the rf frequency is detuned at 0.2756s with  $6.08 \cdot 10^6$ Hz/s, see blue rectangle in Fig. 6.9. For the sake of simplicity, 200 Hz is used as the rf frequency detune. SIS18 needs approximate 33us to reach 200 Hz with  $6.08 \cdot 10^6$ Hz/s.

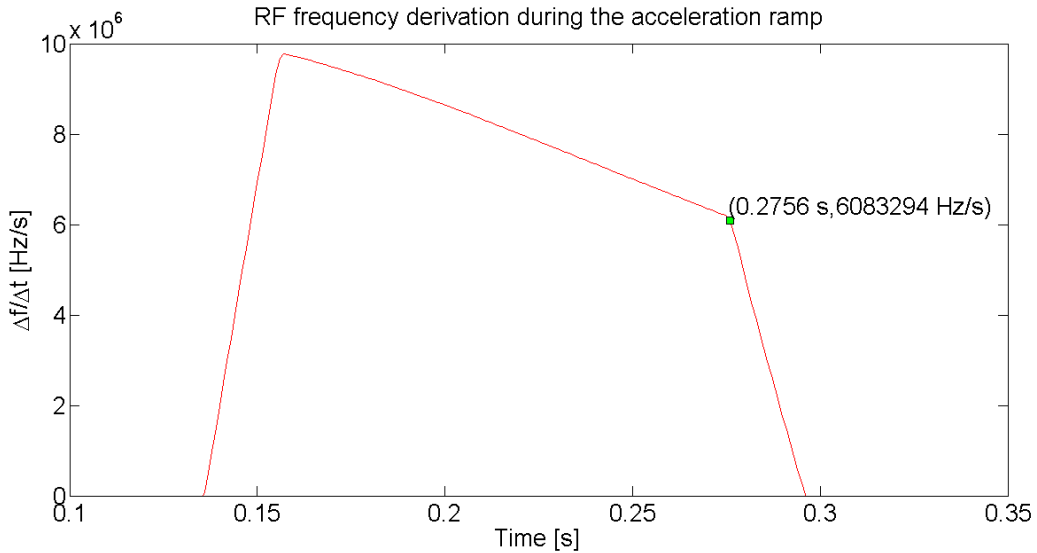


Figure 6.9: RF frequency derivation of the  $U^{28+}$  rf ramp

From eq. 2.61 and eq. 2.63, we could get the corresponding radial excursion and the magnetic field change during the detune process. The maximum radial excursion is  $-1.27 \cdot 10^{-4}$  at 33us of the rf detune process. The maximum magnetic field change is  $4.3 \cdot 10^{-3}$  at 33us of the rf detune process.

## 6.2 GMT systematic investigation for the B2B transfer system

The B2B transfer system makes use of certain aspects of the GMT system to realize the data collection, merging and redistribution. The main task of the data merging

## 6.2. GMT systematic investigation for the B2B transfer system

---

is the calculation of the synchronization window, within which the bunch could be injected into the correct bucket with the bunch to bucket center mismatch smaller than the upper bound. The data collection and redistribution make use of the WR network, so the measurement of the WR network latency is necessary.

### 6.2.1 Calculation of the synchronization window

According to the phase difference between two synchrotrons, the fine time for the alignment of two Reference RF Signals for both the phase shift and frequency beating methods can be calculated. This time is called “best estimate of alignment” and denoted by  $t_{best}$ , see Fig. 6.10. Because of the uncertainty [52] of the phase advance prediction and rf frequency modulation, the fine alignment lies between  $t_{best} - \delta t_{best}$  and  $t_{best} + \delta t_{best}$ , where  $\delta t_{best}$  is the uncertainty of the alignment.  $[t_{best} - \delta t_{best}, t_{best} + \delta t_{best}]$  is called “probable range of alignment”. In Sec. 6.2.1.1 and Sec. 6.2.1.2, the calculation of the best estimation of alignment and the probable range of alignment for the phase shift and frequency beating method will be explained. The probable range of alignment is within the synchronization window. For the correct selection of the same revolution frequency marker at different SCUs, the start of the synchronization window must be properly calculated. In Sec. 6.2.1.3, the calculation of the synchronization window will be explained.

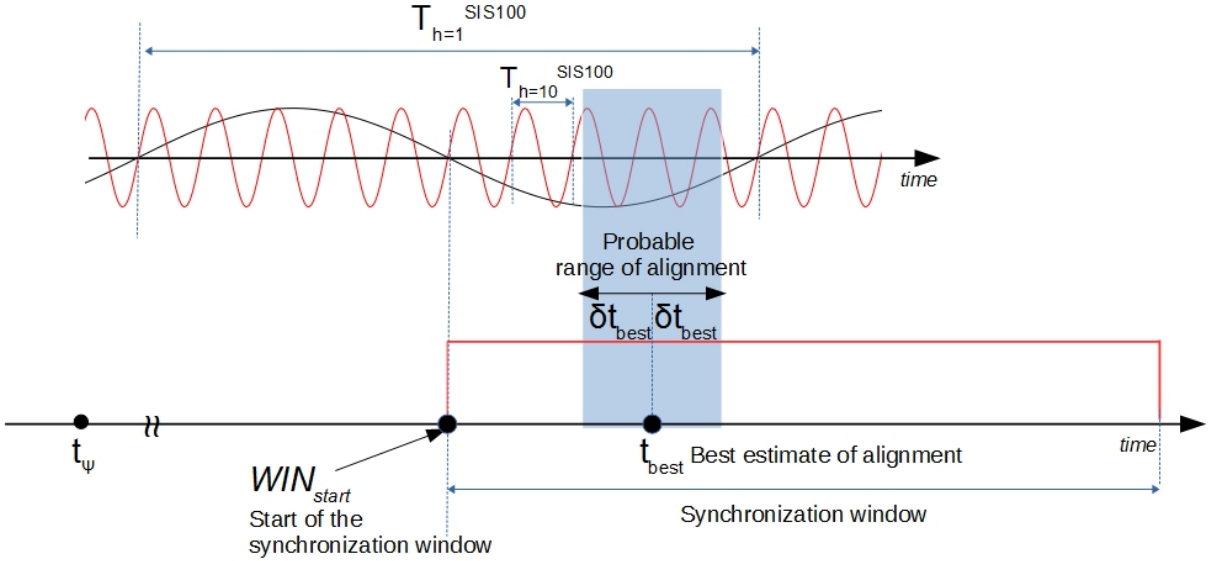


Figure 6.10: The illustration of the best estimate of alignment, the probable range of alignment and the synchronization window

For both the phase shift and frequency beating method, the calculation is based on the predicted phase of the rf signal locally. For example of the  $U^{28+}$  B2B transfer from SIS18 to SIS100, the PAP module extrapolates the rf phase  $\psi_{h=1}^{SIS100}$  for SIS100 rf  $h=1$  (157kHz) signal and  $\psi_{h=1/5}^{SIS18}$  for SIS18 rf  $h=1/5$  (157kHz) signal at  $t_\psi$  [44]. The more time is spent for the phase advance prediction, the better the predicted phase will be. Fig. 6.11 illustrates some basic definition of symbols for the calculation.  $\phi_{h=2}^{SIS18}$  and  $\phi_{h=10}^{SIS100}$  are individual rf phase of SIS18 and SIS100 Reference RF Signals

## 6.2. GMT systematic investigation for the B2B transfer system

---

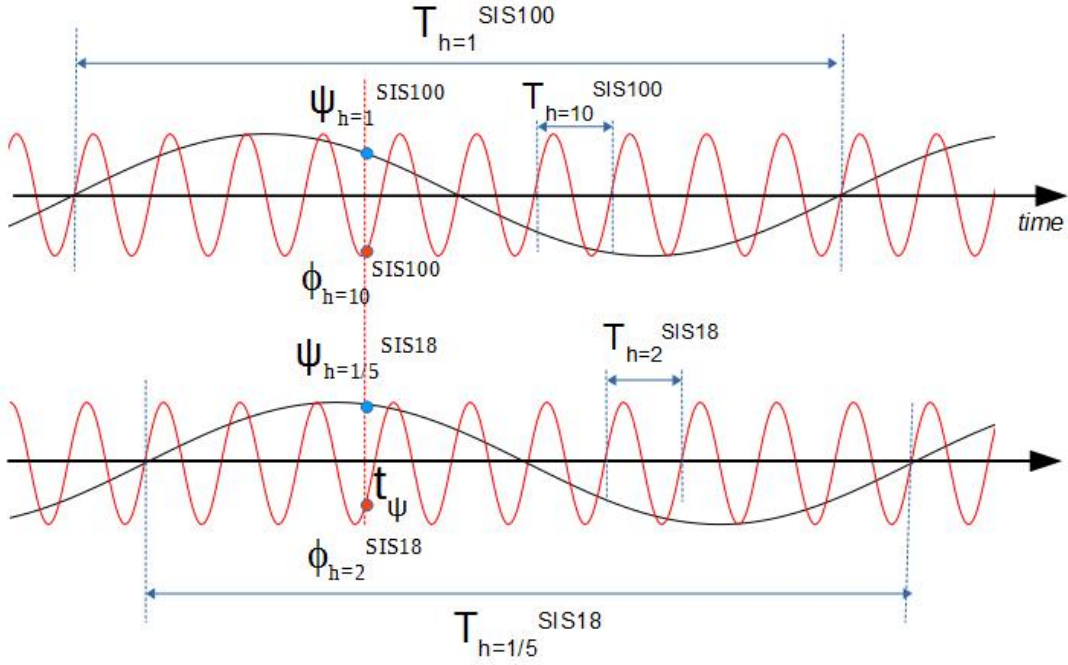


Figure 6.11: The illustration of symbols for the calculation

at  $t_\psi$ . The relationship between  $\phi_{h=2}^{SIS18}$ ,  $\phi_{h=10}^{SIS100}$  and  $\psi_{h=1/5}^{SIS18}$ ,  $\psi_{h=1}^{SIS100}$  are given by eq. 6.18 and eq. 6.19.

$$\phi_{h=2}^{SIS18} = \frac{\frac{\psi_{h=1/5}^{SIS18}}{360^\circ} \cdot T_{h=1/5}^{SIS18} \bmod T_{h=2}^{SIS18}}{T_{h=2}^{SIS18}} \cdot 360^\circ \quad (6.18)$$

$$\phi_{h=10}^{SIS100} = \frac{\frac{\psi_{h=1}^{SIS100}}{360^\circ} \cdot T_{h=1}^{SIS100} \bmod T_{h=10}^{SIS100}}{T_{h=10}^{SIS100}} \cdot 360^\circ \quad (6.19)$$

substituting  $T_{h=2}^{SIS18} \cdot 10 = T_{h=1/5}^{SIS18}$ ,  $T_{h=10}^{SIS100} \cdot 10 = T_{h=1}^{SIS100}$  into eq.6.18 and eq.6.19 yields

$$\phi_{h=2}^{SIS18} = \frac{\frac{\psi_{h=1/5}^{SIS18} \cdot 10}{360^\circ} \cdot T_{h=2}^{SIS18} \bmod T_{h=2}^{SIS18}}{T_{h=2}^{SIS18}} \cdot 360^\circ \quad (6.20)$$

$$\phi_{h=10}^{SIS100} = \frac{\frac{\psi_{h=1}^{SIS100} \cdot 10}{360^\circ} \cdot T_{h=10}^{SIS100} \bmod T_{h=10}^{SIS100}}{T_{h=10}^{SIS100}} \cdot 360^\circ \quad (6.21)$$

Here we explain the inevitable uncertainty of the phase advance prediction and rf frequency modulation.

- Uncertainty of the predicted phase advance

If the phase prediction time is 500us, the uncertainty of the predicted phase advance  $\delta t_\psi$  is 100ps [45]. We calculate the uncertainty of the predicted phase advance,  $\delta\psi_{h=1}^{SIS100}$  and  $\delta\psi_{h=1/5}^{SIS18}$ , from the time to phase domain.

$$\delta t_\psi = 100\text{ps} \quad (6.22)$$

## 6.2. GMT systematic investigation for the B2B transfer system

---

$$\delta\psi_{h=1/5}^{SIS18} = \delta\psi_{h=1}^{SIS100} = \frac{100ps}{1/157kHz} \cdot 360^\circ \approx 0.006^\circ \quad (6.23)$$

Based on the eq. 6.23, eq. 6.20 and eq. 6.21, the uncertainty of the phase at the Reference RF Signal of SIS18 and SIS100,  $\delta\phi_{h=10}^{SIS100}$  and  $\delta\phi_{h=2}^{SIS18}$ , is calculated.

$$\delta\phi_{h=2}^{SIS18} = \sqrt{\left(\frac{\partial\phi_{h=2}^{SIS18}}{\partial\psi_{h=2}^{SIS18}}\delta\psi_{h=2}^{SIS18}\right)^2} = \sqrt{(10 \cdot \delta\psi_{h=2}^{SIS18})^2} = 0.06^\circ \quad (6.24)$$

$$\delta\phi_{h=10}^{SIS100} = \sqrt{\left(\frac{\partial\phi_{h=10}^{SIS100}}{\partial\psi_{h=1}^{SIS100}}\delta\psi_{h=1}^{SIS100}\right)^2} = \sqrt{(10 \cdot \delta\psi_{h=1}^{SIS100})^2} = 0.06^\circ \quad (6.25)$$

- Uncertainty of the rf frequency modulation

For the rf frequency modulation, the uncertainty is  $0.2^\circ$  at 5.4MHz [53]. We calculate the uncertainty in time domain, see eq. 6.26.

$$\delta\Delta f_{(t)} = \frac{0.2^\circ}{360^\circ} \cdot \frac{1}{5.4MHz} = 100ps \quad (6.26)$$

### 6.2.1.1 The best estimate of alignment and the probable range of alignment for the phase shift method

Different relation between  $\phi_{h=2}^{SIS18}$  and  $\phi_{h=10}^{SIS100}$  requires different phase adjustment for SIS18. Fig. 6.12 illustrates all scenarios of their relation and the required phase adjustment for each scenario. We would like to introduce a phase shift of up to  $\pm 180^\circ$ . The blue and red line represents the phase of SIS100 and SIS18 Reference RF Signal. The clockwise arrow from the SIS18 to SIS100 rf phase represents the negative phase adjustment for SIS18 and the anticlockwise represents the positive phase adjustment. The required phase adjustment of SIS18 is denoted by  $\Delta\phi_{shift}$ .

- Scenario (a):  $\phi_{h=10}^{SIS100} \in [0, 90^\circ]$ , see Fig. 6.13 (a).
  - $\phi_{h=10}^{SIS100} < \phi_{h=2}^{SIS18} < \phi_{h=10}^{SIS100} + 180^\circ$ , which denotes by the yellow semicircle in Fig. 6.13 (a). The phase adjustment is
 
$$\Delta\phi_{shift} = -(\phi_{h=2}^{SIS18} - \phi_{h=10}^{SIS100}) \quad (6.27)$$
  - $\phi_{h=2}^{SIS18} < \phi_{h=10}^{SIS100}$  or  $\phi_{h=2}^{SIS18} > \phi_{h=10}^{SIS100} + 180^\circ$ , which denotes by the white semicircle in Fig. 6.13 (a). The phase adjustment is
 
$$\Delta\phi_{shift} = 360^\circ - \phi_{h=2}^{SIS18} + \phi_{h=10}^{SIS100} \quad (6.28)$$

## 6.2. GMT systematic investigation for the B2B transfer system

---

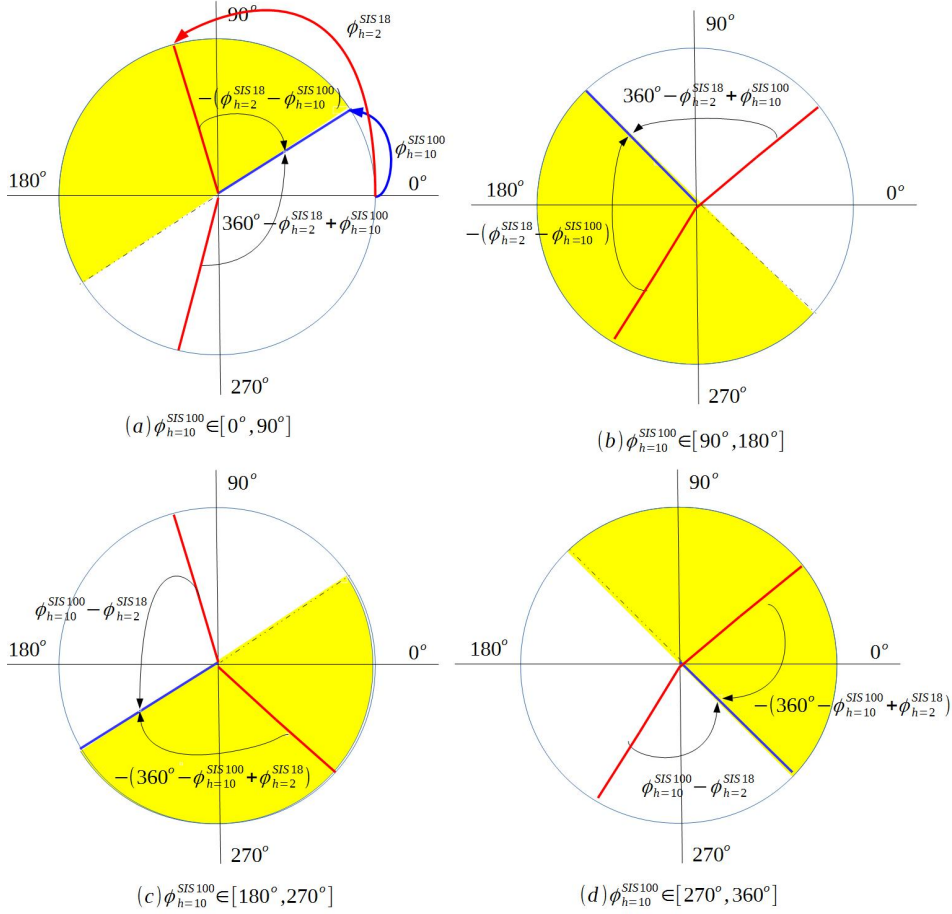


Figure 6.12: Scenarios for the phase shift method

- Scenario (b):  $\phi_{h=10}^{SIS100} \in [90^\circ, 180^\circ]$ , see Fig. 6.13 (b).
  - $\phi_{h=10}^{SIS100} < \phi_{h=2}^{SIS18} < \phi_{h=10}^{SIS100} + 180^\circ$ , which denotes by the yellow semicircle in Fig. 6.13 (b). The phase adjustment is
 
$$\Delta\phi_{shift} = -(\phi_{h=2}^{SIS18} - \phi_{h=10}^{SIS100}) \quad (6.29)$$
  - $\phi_{h=2}^{SIS18} < \phi_{h=10}^{SIS100}$  or  $\phi_{h=2}^{SIS18} > \phi_{h=10}^{SIS100} + 180^\circ$ , which denotes by the white semicircle in Fig. 6.13 (b). The phase adjustment is
 
$$\Delta\phi_{shift} = 360^\circ - \phi_{h=2}^{SIS18} + \phi_{h=10}^{SIS100} \quad (6.30)$$
- Scenario (c):  $\phi_{h=10}^{SIS100} \in [180^\circ, 270^\circ]$ , see Fig. 6.13 (c). The phase adjustment is
  - $\phi_{h=2}^{SIS18} > \phi_{h=10}^{SIS100}$  or  $\phi_{h=2}^{SIS18} < \phi_{h=10}^{SIS100} + 180^\circ - 360^\circ$ , which denotes by the yellow semicircle in Fig. 6.13 (c). The phase adjustment is
 
$$\Delta\phi_{shift} = -(360^\circ - \phi_{h=10}^{SIS100} + \phi_{h=2}^{SIS18}) \quad (6.31)$$
  - $\phi_{h=10}^{SIS100} - 180^\circ < \phi_{h=2}^{SIS18} < \phi_{h=10}^{SIS100}$ , which denotes by the white semicircle in Fig. 6.13 (c). The phase adjustment is
 
$$\Delta\phi_{shift} = \phi_{h=10}^{SIS100} - \phi_{h=2}^{SIS18} \quad (6.32)$$

## 6.2. GMT systematic investigation for the B2B transfer system

---

- Scenario (d):  $\phi_{h=10}^{SIS100} \in [270, 360^\circ]$ , see Fig. 6.13 (d).
- $\phi_{h=10}^{SIS100} - 180^\circ < \phi_{h=2}^{SIS18} < \phi_{h=10}^{SIS100}$ , which denotes by the yellow semicircle in Fig. 6.13 (d). The phase adjustment is
$$\Delta\phi_{shift} = \phi_{h=10}^{SIS100} - \phi_{h=2}^{SIS18} \quad (6.33)$$
- $\phi_{h=2}^{SIS18} > \phi_{h=10}^{SIS100}$  or  $\phi_{h=2}^{SIS18} < \phi_{h=10}^{SIS100} + 180^\circ - 360^\circ$ , which denotes by the white semicircle in Fig. 6.13 (d).
$$\Delta\phi_{shift} = -(360^\circ - \phi_{h=10}^{SIS100} + \phi_{h=2}^{SIS18}) \quad (6.34)$$

The phase adjustment is achieved by the phase shift method within the upper bound time,  $T_{phase\_shift}^{upper\_bound}$ . For the  $U^{28+}$  B2B transfer from SIS18 to SIS100, we assume that  $T_{phase\_shift}^{upper\_bound}$  equals to 7ms, which means that the phase shift  $\Delta\phi_{shift}$  is achieved within 7ms. So the best estimate of alignment is expressed by

$$t_{best} = t_\psi + T_{phase\_shift}^{upper\_bound} \quad (6.35)$$

The uncertainty in the phase prediction  $\delta t_\psi$  is 100ps, see eq. 6.22. The phase shift uncertainty  $\delta\Delta\phi_{phase}$  is caused by the rf frequency modulation, whose jitter is 100ps, see eq. 6.26. The phase shift uncertainty equals to the uncertainty in the phase shift upper bound time,  $\delta T_{phase\_shift}^{upper\_bound} = 100$ ps. Both cause an uncertainty in the best estimate of alignment  $t_{best}$ .

$$\begin{aligned} \delta t_{best} &= \sqrt{\left(\frac{\partial t_{best}}{\partial t_\psi} \delta t_\psi\right)^2 + \left(\frac{\partial t_{best}}{\partial T_{phase\_shift}^{upper\_bound}} \delta T_{phase\_shift}^{upper\_bound}\right)^2} \\ &= \sqrt{(\delta t_\psi)^2 + (T_{phase\_shift}^{upper\_bound})^2} = \sqrt{100ps^2 + 100ps^2} \approx 140ps \end{aligned} \quad (6.36)$$

The uncertainty of the alignment for the phase shift method is about 140ps. So the proper range of alignment is  $[t_{best}-140ps, t_{best}+140ps]$  for  $U^{28+}$  B2B transfer from SIS18 to SIS100.

### 6.2.1.2 The best estimate of alignment and the probable range of alignment for the frequency beating method

Fig. 6.13 illustrates two scenarios for the frequency beating method. With the frequency beating method, SIS18 can only achieve positive phase adjustment, which is denoted by  $\Delta\phi_{adjustment}$ . Eq. 6.37 shows the best estimate of alignment for the phase adjustment of  $\Delta\phi_{adjustment}$ .

$$t_{best} = t_\psi + \frac{\Delta\phi_{adjustment}}{360^\circ \cdot \Delta f} \quad (6.37)$$

where  $\Delta f$  is the beating frequency.

According to the relation between  $\phi_{h=2}^{SIS18}$  and  $\phi_{h=10}^{SIS100}$ , there are two scenarios, see Fig. 6.13.

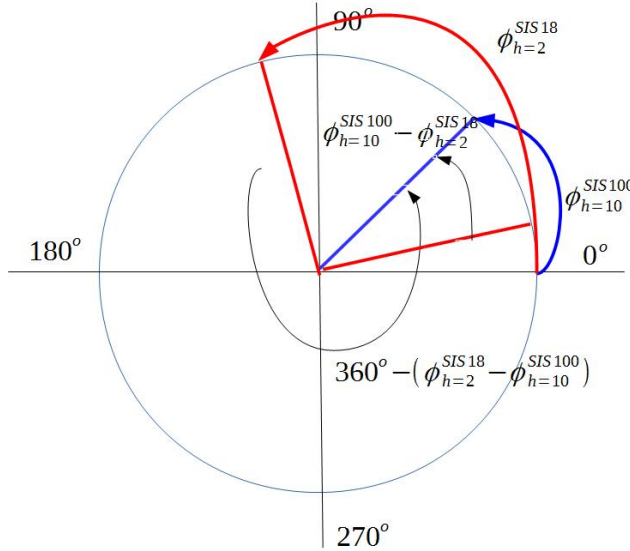


Figure 6.13: Two scenarios for the frequency beating method

- Scenario (a):  $\phi_{h=2}^{SIS18} < \phi_{h=10}^{SIS100}$

$$\Delta\phi_{adjustment} = \phi_{h=10}^{SIS100} - \phi_{h=2}^{SIS18} \quad (6.38)$$

Replacing  $\Delta\phi_{adjustment}$  in eq. 6.37 with eq. 6.38, we have

$$t_{best} = t_\psi + \frac{\phi_{h=10}^{SIS100} - \phi_{h=2}^{SIS18}}{360^\circ \cdot \Delta f} \quad (6.39)$$

- Scenario (b):  $\phi_{h=2}^{SIS18} \geq \phi_{h=10}^{SIS100}$

$$\Delta\phi_{adjustment} = 360^\circ - (\phi_{h=2}^{SIS18} - \phi_{h=10}^{SIS100}) \quad (6.40)$$

Replacing  $\Delta\phi_{adjustment}$  in eq. 6.37 with eq. 6.40, we have

$$t_{best} = t_\psi + \frac{360^\circ - (\phi_{h=2}^{SIS18} - \phi_{h=10}^{SIS100})}{360^\circ \cdot \Delta f} \quad (6.41)$$

Based on these two scenarios, we could deduce the formula for the best estimate of alignment.

$$t_{best} = t_\psi + \frac{\Delta n \cdot 360^\circ - (\phi_{h=2}^{SIS18} - \phi_{h=10}^{SIS100})}{360^\circ \cdot \Delta f} \quad (6.42)$$

where  $\Delta n$  equals 0 when  $\phi_{h=2}^{SIS18} < \phi_{h=10}^{SIS100}$  and equals 1 when  $\phi_{h=2}^{SIS18} \geq \phi_{h=10}^{SIS100}$ .

The uncertainty of the alignment is the result of the error propagation of uncertainties of the phase prediction and rf frequency detune, see eq. 6.43. Because the rf frequency detune has the long term stability,  $\int \delta \Delta f = 0$ , the uncertainty caused by rf frequency detune is 0. The uncertainty of the phase prediction  $\phi_{h=2}^{SIS18}$  and  $\phi_{h=10}^{SIS100}$  is  $0.06^\circ$ , see eq. 6.24 and eq. 6.25.  $\Delta f$  is 200Hz. The maximum

## 6.2. GMT systematic investigation for the B2B transfer system

$\Delta n \cdot 2\pi - (\phi_{h=2}^{SIS18} - \phi_{h=10}^{SIS100})$  is  $2\pi$ .

$$\begin{aligned}
 \delta t_{best} &= \sqrt{\left(\frac{\partial t_{best}}{\partial \phi_{h=2}^{SIS18}} \delta \phi_{h=2}^{SIS18}\right)^2 + \left(\frac{\partial t_{best}}{\partial \phi_{h=10}^{SIS100}} \delta \phi_{h=10}^{SIS100}\right)^2 + \left(\frac{\partial t_{best}}{\partial \Delta f} \delta \Delta f\right)^2} \\
 &= \sqrt{\left(\frac{-1}{2\pi \cdot \Delta f} \delta \phi_{h=2}^{SIS18}\right)^2 + \left(\frac{1}{2\pi \cdot \Delta f} \delta \phi_{h=10}^{SIS100}\right)^2 + \left(-\frac{\Delta n \cdot 2\pi - (\phi_{h=2}^{SIS18} - \phi_{h=10}^{SIS100})}{2\pi \cdot \Delta f^2} \delta \Delta f\right)^2} \\
 &\leq \sqrt{\left(\frac{-1}{2\pi \cdot 200} 0.06^\circ\right)^2 + \left(\frac{1}{2\pi \cdot 200} 0.06^\circ\right)^2 + 0} \\
 &\approx 1.178\text{us}
 \end{aligned} \tag{6.43}$$

From eq. 6.43 we could get the uncertainty of the alignment is 1.178us, so the probable range of alignment is  $[t_{best} - 1.178\text{us}, t_{best} + 1.178\text{us}]$ .

### 6.2.1.3 Calculation the synchronization window and its accuracy

In the last section, we get the probable range of alignment, within which the two Reference Rf Signals could be aligned with each other. The synchronization window is used to select the revolution frequency marker for the extraction and injection kicker firing, which is closest to the probable range of alignment, See Fig. 6.14. For the selection, the length of the synchronization window must be a least one SIS100 revolution period. The best estimate of the start of the synchronization window is exactly half revolution period before the selected revolution frequency marker. The blue and orange rectangles represent two scenarios of the probable range of alignment. In Fig. 6.14, the 2nd revolution frequency marker is the closest one to the probable range of alignment. The best estimate of the start of the synchronization window aligns with the negative zero crossing point of the revolution marker signal.

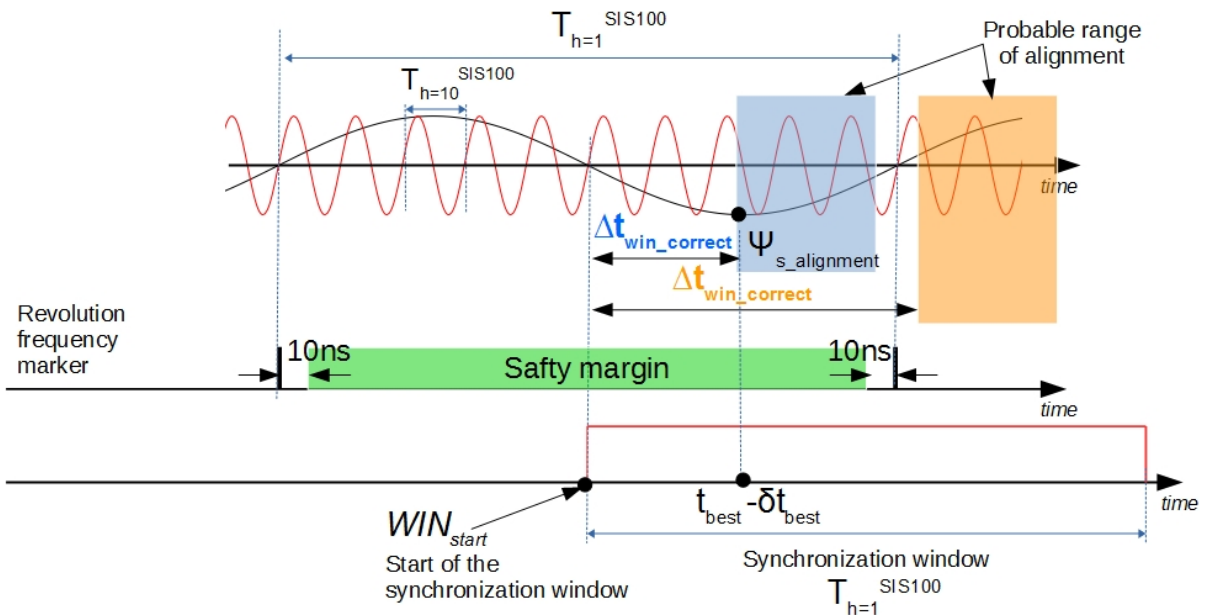


Figure 6.14: The illustration of the synchronization window and its accuracy

For SIS100, the rf phase of the revolution frequency is  $\psi_{h=1}^{SIS100}$  at  $t_\psi$ . We could calculate the rf phase  $\psi_{s.alignment}$  of the revolution frequency at the start of the

## 6.2. GMT systematic investigation for the B2B transfer system

---

probable rang of alignment,  $t_{best} - \delta t_{best}$ .

$$\psi_{s\_alignment} = \frac{(t_{best} - \delta t_{best} - t_\psi - \frac{360^\circ - \psi_{h=1}^{SIS100}}{360^\circ} \cdot T_{h=1}^{SIS100}) \bmod T_{h=1}^{SIS100}}{T_{h=1}^{SIS100}} \cdot 360^\circ \quad (6.44)$$

For the calculation of the best estimate of the start of the synchronization window, there are two scenarios.  $\Delta t_{win\_correct}$  is the time correction for the start of the probable range of alignment to the best estimate of the start of the synchronization window, see Fig. 6.14.

- $\psi_{s\_alignment} \in [0^\circ, 180^\circ]$ , the orange rectangle in Fig. 6.14

$$\Delta t_{win\_correct} = \frac{\psi_{s\_alignment}}{360^\circ} \cdot T_{h=1}^{SIS100} + \frac{T_{h=1}^{SIS100}}{2} \quad (6.45)$$

$$WIN_{start} = t_{best} - \delta t_{best} - \Delta t_{win\_correct} \quad (6.46)$$

- $\psi_{s\_alignment} \in [180^\circ, 360^\circ]$ , the blue rectangle in Fig. 6.14

$$\Delta t_{win\_correct} = \frac{\psi_{s\_alignment} - 180^\circ}{360^\circ} \cdot T_{h=1}^{SIS100} \quad (6.47)$$

$$WIN_{start} = t_{best} - \delta t_{best} - \Delta t_{win\_correct} \quad (6.48)$$

The actual start of the synchronization window is impossible to be exactly at the best estimate of the start of the synchronization window because of the precision and trueness [54]. The precision is defined as the closeness of agreement between the actual start of the synchronization window of different SCUs and the trueness as the closeness of agreement between the average actual start of the synchronization window of different SCUs and the best estimation start of the synchronization window. The precision comes from the random error, e.g. IO port TTL signal rising osillation. The trueness is the systematic error, e.g. FPGA process time. The accuracy is defined as the closeness of agreement between the observed start and the best estimate of the start of the synchronization window, which is the sum of the precision and trueness. The B2B transfer system will be used for many transfers for FAIR. Therefore, we have to find the most stringent accuracy requirement. The shortest revolution period of the target machine is 433 ns, which comes from RIB transfer from CR to HESR. We keep 10ns as a forbidden range, which means that the actual start is not allowed 10 ns before and after the revolution frequency marker. The green region in Fig. 6.14 represents the safty margin for the start of the synchronization window. So the accuracy of the start of the synchronization window must meet the requirement calculated by eq. 6.49.

$$Accuracy = \pm \frac{433 - 10 \cdot 2}{2} \approx \pm 200 \text{ ns} \quad (6.49)$$

### 6.2.2 Characterization of the WR network for the B2B transfer

Within this dissertation, a network analyzed by Xena is used to characterize the properties of the WR network, which are relevant to B2B transfer. The WR network measurement is achieved by the Xena traffic generator<sup>1</sup>, which offers a new

---

<sup>1</sup><http://xenanetworks.com/layer-2-3-platform/>

## 6.2. GMT systematic investigation for the B2B transfer system

---

class of professional Layer 2-3 Gigabit Ethernet test platform. It is used to measure the frame loss rate<sup>2</sup>, latency<sup>3</sup> and jitter<sup>4</sup> for the WR network. For the measurement, Xena traffic generator sends the traffic streams with a unique stream ID for identifying latency, jitter and packet loss. For the measurements, the following types of traffic are considered [55].

- DM Broadcast

DM forwards broadcast timing frames<sup>5</sup> with 110 bytes ethernet frame length downwards to all FECs. The average bandwidth for the DM broadcast is 100 Mbit/s. The burst<sup>6</sup> speed is 12 packets per 100 µs.

- DM Unicast

DM sends 10Mbit/s unicast timing frames with 110 bytes ethernet frame length to some specified FECs at the burst speed of 3 packets per 300 µs.

- B2B Unicast

The source B2B SCU sends the timing frame with 110 bytes ethernet frame length upwards to the DM. For the B2B transfer upper bound time 10 ms of each supercycle, 2 unicast timing frames are send to the DM. The maximum repetition frequency is of the  $U^{28+}$  supercycle, 2.82 Hz. For the estimation of the upper bound bandwidth, we use 3Hz/s as the maximum repetition frequency. So the bandwidth is  $3 \text{ Hz/s} \cdot 2 \text{ packets/supercycle} \cdot 110 \text{ byte} \cdot 8 \text{ bit} \approx 5.5 \text{ kbit/s}$ .

- B2B Broadcast

Maximum 10 B2B broadcast timing frames with 110 ethernet frame length are sent within 10 ms. So the bandwidth is  $3 \text{ Hz/s} \cdot 10 \text{ packets/supercycle} \cdot 110 \text{ byte} \cdot 8 \text{ bit} \approx 26.5 \text{ kbit/s}$ .

- Management Traffic

The average bandwidth for the management traffic is 10 Mbit/s. It broadcasts packets with random ethernet frame length from 64 bytes to 1518 bytes.

The requirements for the B2B Broadcast and Unicast traffic are summarized in Tab. A.1 [55].

For the WR network for FAIR, three VLANs with different priorities are applied according to the importance of the traffic.

---

<sup>2</sup>The ratio of the number of the lost frames to the number of the theoretic received frames of a tested port.

<sup>3</sup>The time interval between the time of Xena port receiving frame and the time of another Xena port sending frame.

<sup>4</sup>The absolute value of the difference between the latency of two consecutive received frames belonging to the same stream from one Xena port to another Xena port.

[http://www.xenatenetworks.com/wp-content/uploads/Measuring\\_Frame\\_latency\\_Variation.pdf](http://www.xenatenetworks.com/wp-content/uploads/Measuring_Frame_latency_Variation.pdf)

<sup>5</sup><https://www-acc.gsi.de/wiki/Timing/TimingSystemEvent>

<sup>6</sup>A group of consecutive frames with shorter interframe gaps than frames arriving before or after the burst of frames.

## 6.2. GMT systematic investigation for the B2B transfer system

---

Table 6.4: The B2B transfer requirements for the WR network

	Frame Loss Rate	Upper bound latency of WR network	Upper bound latency per WR switch layer
B2B Broadcast	$10^{-12}$	500 $\mu$ s	30 $\mu$ s
B2B Unicast	$10^{-12}$	500 $\mu$ s	30 $\mu$ s

### 6.2.2.1 WR network test setup

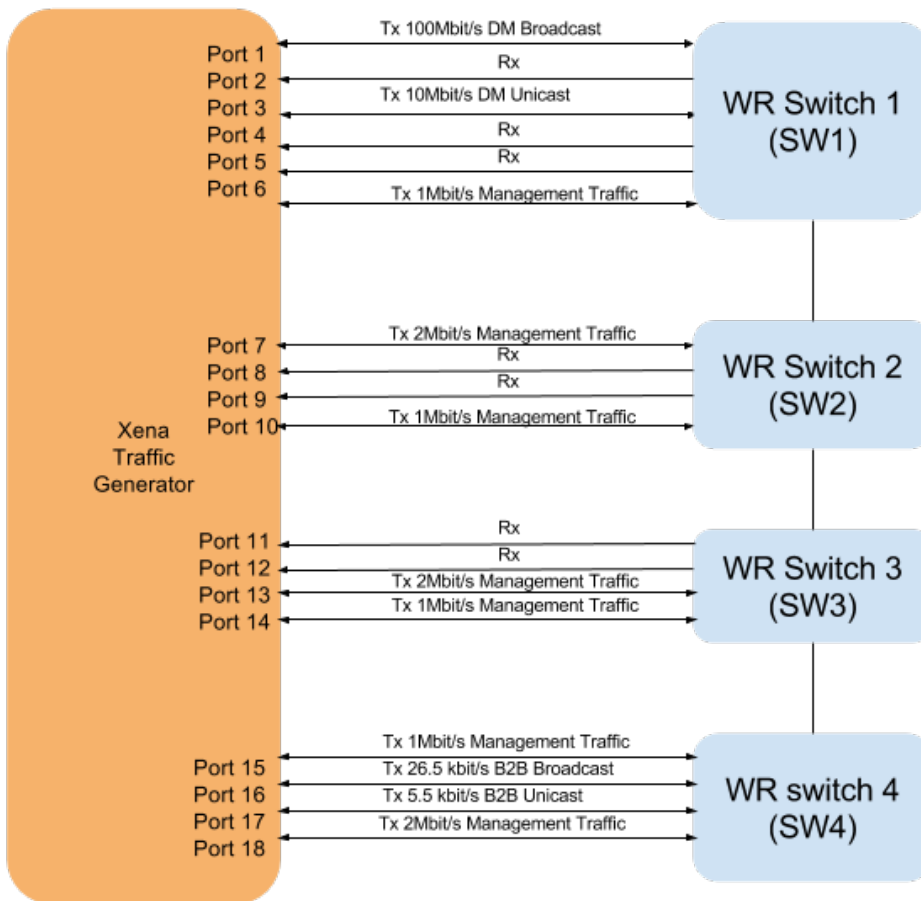


Figure 6.15: The WR network test setup

Based on the mentioned traffic, the measurement setup is built, see Fig. 6.15 [55]. Four WR switches are connected to the port 1 to 18 of the Xena traffic generator. All ports of four WR switches are assigned to three VLANs, VLAN 5, VLAN 6 and VLAN 7. Tab. 6.5 shows the bandwidth, VLAN, VLAN priority and usage of the traffic of each Xena port in details. The test is running for 14 hours.

## 6.2. GMT systematic investigation for the B2B transfer system

---

Table 6.5: The connection between the traffic generator and WR switches

Switch	Xena Port	Traffic	VLAN	Priority	Usage
WR switch 1	Port 1	100 Mbit/s 110bytes	7	7	DM Broadcast
	Port 2	Rx traffic			
	Port 3	10 Mbit/s 110bytes	7	7	DM Unicast
	Port 4	Rx traffic			
	Port 5	Rx traffic			
	Port 6	1 Mbit/s 64 - 1518 bytes	5	5	Management Broadcast
WR switch 2	Port 7	2 Mbit/s 64 - 1518 bytes	5	5	Management Broadcast
	Port 8	Rx traffic			
	Port 9	Rx traffic			
	Port 10	1 Mbit/s 64 - 1518 bytes	5	5	Management Broadcast
WR switch 3	Port 11	Rx traffic			
	Port 12	Rx traffic			
	Port 13	2 Mbit/s 64 - 1518 bytes	5	5	Management Broadcast
	Port 14	1 Mbit/s 64 - 1518 bytes	5	5	Management Broadcast
WR switch 4	Port 15	1 Mbit/s 64 - 1518 bytes	5	5	Management Broadcast
	Port 16	26.5 kbit/s 110bytes	6	6	B2B Broadcast
	Port 17	5.5 kbit/s 110bytes	7	7	B2B Unicast
	Port 18	2 Mbit/s 64 - 1518 bytes	5	5	Management Broadcast

### 6.2.2.2 Frame loss rate test result for B2B frames

The frame loss rate of the stream from port 17 to port 1 is measured for the B2B Unicast frames. The frame loss rate of the stream from port 16 to other ports is measured for the B2B Broadcast frame. Fig. 6.16 [55] shows the test result for both traffics. For the B2B Broadcast frames, the frame loss rate of each port is 0 %. For the B2B Unicast frames, the frame loss rate of port 1 is 0 %. So there is no B2B frame loss of the test WR network.

## 6.2. GMT systematic investigation for the B2B transfer system

---

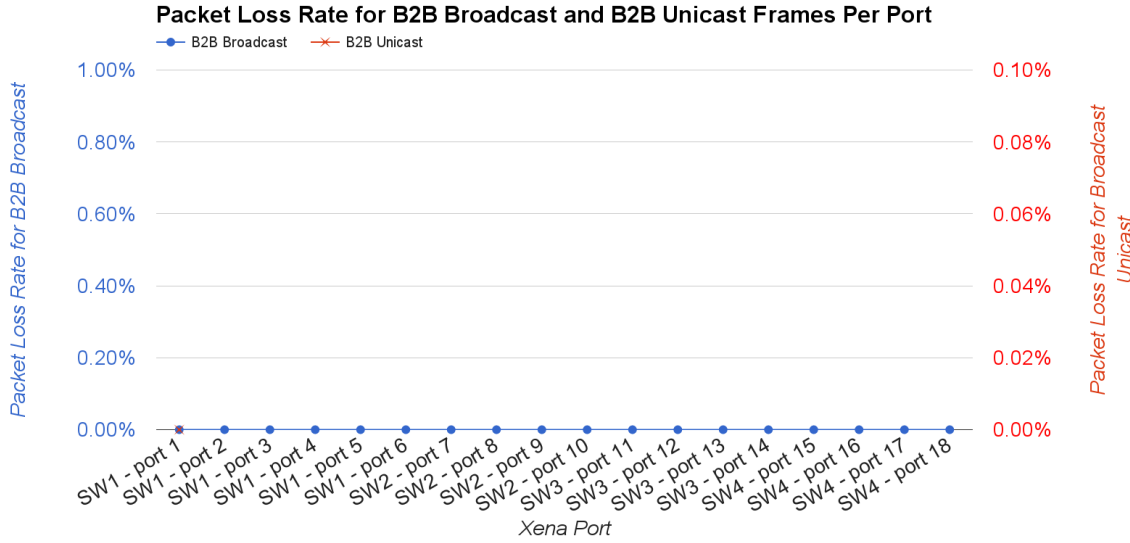


Figure 6.16: The frame loss rate for B2B Broadcast and B2B Unicast frames

### 6.2.2.3 Latency and jitter test result for B2B frames

The latency and jitter of the stream from port 16 to other ports are measured.

- Latency and jitter for B2B Broadcast frames
  - Average Latency and jitter

Fig. 6.17 [55] shows the test result for the average latency and jitter for the B2B Broadcast frames. Tab. 6.6 shows the average latency and jitter of different WR switch layers. They meet the requirements of the B2B transfer.

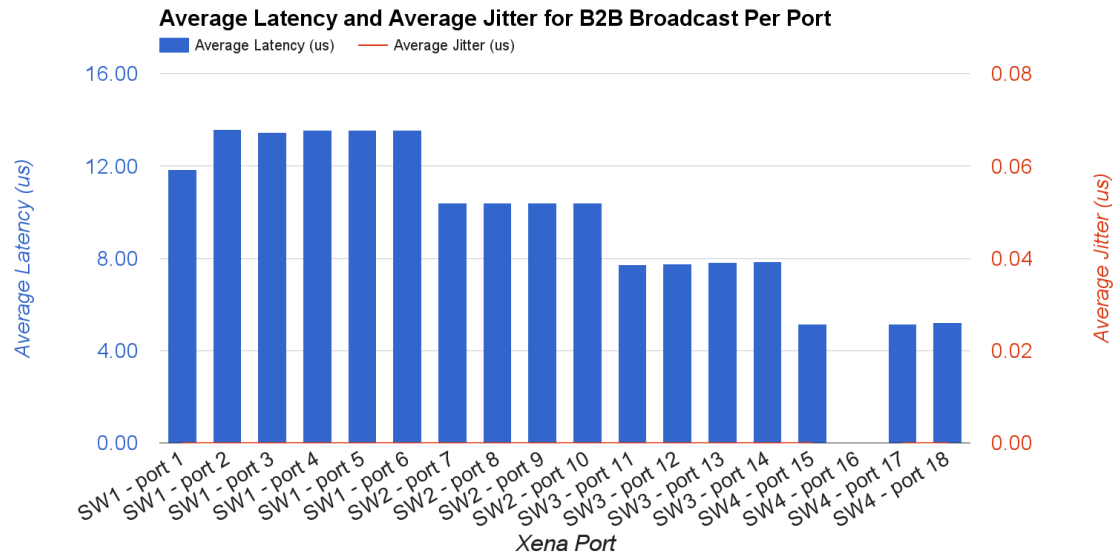


Figure 6.17: The average latency and jitter for B2B Broadcast frames

## 6.2. GMT systematic investigation for the B2B transfer system

---

Table 6.6: The average latency and jitter of the B2B Broadcast frames

	WR switch 4	WR switch 4, 3	WR switch 4, 3, 2	WR switch 4, 3, 2, 1
Avg latency	6 $\mu$ s	8 $\mu$ s	11 $\mu$ s	14 $\mu$ s
Avg jitter	0 ns	0 ns	0 ns	0 ns

- Maximum Latency and jitter

Fig. 6.18 [55] shows the test result for the maximum latency and jitter for the B2B Broadcast frames. Tab. 6.7 shows the maximum latency and jitter of different WR switch layers. They meet the requirements of the B2B transfer.

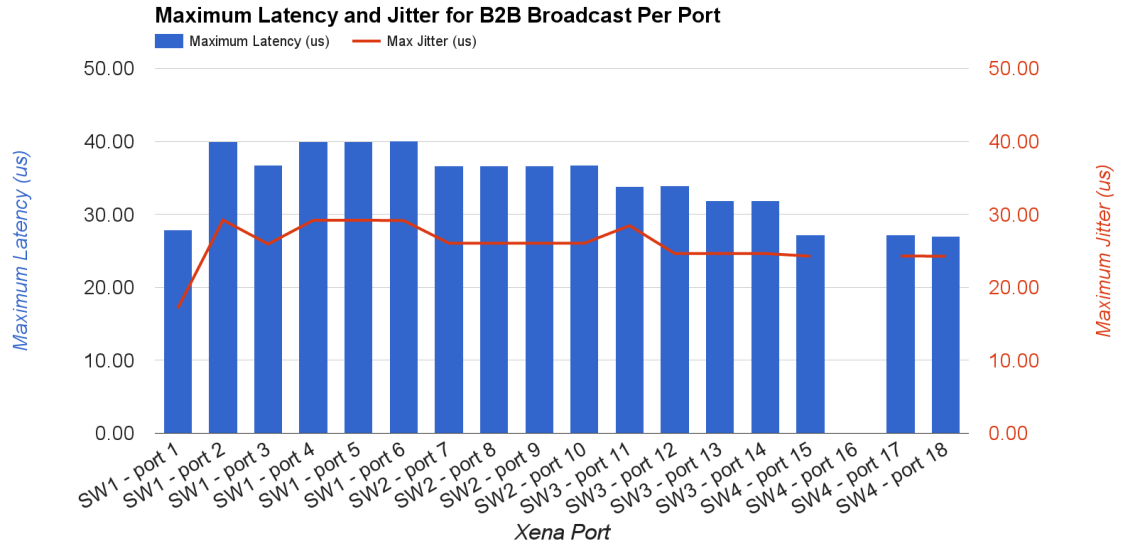


Figure 6.18: The maximum latency and jitter for B2B Broadcast frames

Table 6.7: The maximum latency and jitter of the B2B Broadcast frames

	WR switch 4	WR switch 4, 3	WR switch 4, 3, 2	WR switch 4, 3, 2, 1
Max latency	28 $\mu$ s	34 $\mu$ s	37 $\mu$ s	41 $\mu$ s
Max jitter	25 $\mu$ s	25 $\mu$ s	27 $\mu$ s	30 $\mu$ s

- Latency and jitter for B2B Unicast frames

For the B2B unicast frames, the latency and jitter of the stream from port 16 to port 1 are measured.

## 6.2. GMT systematic investigation for the B2B transfer system

- Average Latency and jitter

For the B2B Unicast frames, 4 WR switch network has approximate 11  $\mu$ s average latency and 0  $\mu$ s average jitter.

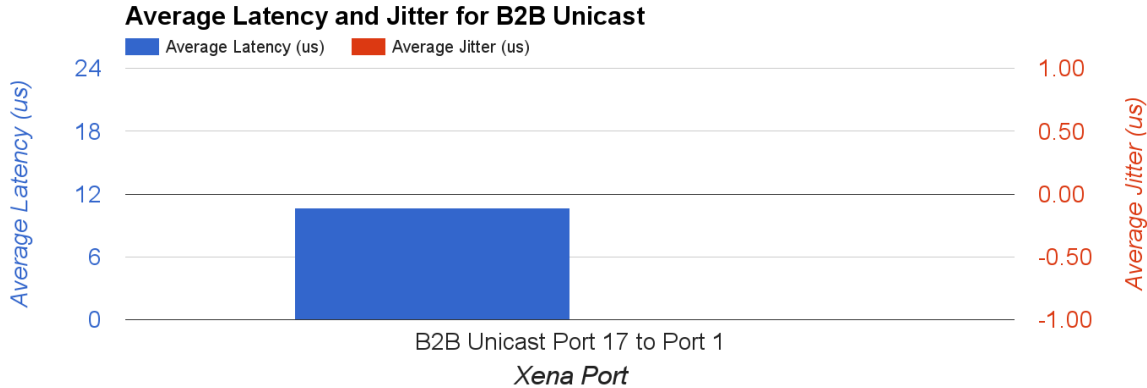


Figure 6.19: The average latency and jitter for B2B Unicast frames

- Maximum Latency and jitter

For the B2B unicast frames, 4 WR switch network has approximate 23  $\mu$ s maximum latency and 13  $\mu$ s maximum jitter.

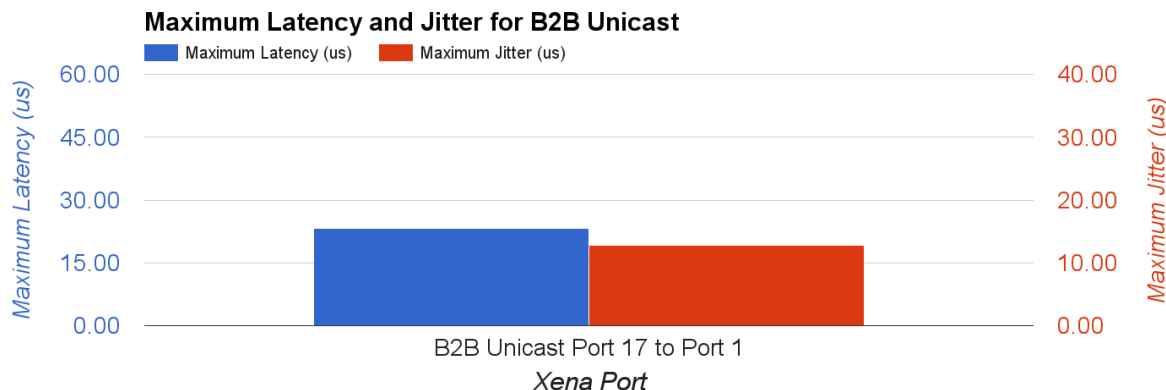


Figure 6.20: The maximum latency and jitter for B2B Unicast frames

More test configuration and results, please see “Testing the WR Network of the FAIR General Machine Timing System“.

### **6.2.2.4 Result and conclusion**

Tab. 6.8 shows the result of the test. The frame loss rate and latency meet the requirements of the B2B Broadcast and B2B Unicast traffic.

### 6.3. Kicker systematic investigation for the B2B transfer system

---

Table 6.8: The result of the WR network test for the B2B transfer

	Frame Loss Rate	Average Latency	Maximum Latency	Average Jitter	Maximum Jitter
B2B Broadcast	0 %	6 $\mu$ s/switch	28 $\mu$ s/switch	0 $\mu$ s/switch	25 $\mu$ s/switch
B2B Unicast	0 %	11 $\mu$ s/4switch 3 $\mu$ s/switch	23 $\mu$ s/4switch 6 $\mu$ s/switch	0 $\mu$ s/4switch 0 $\mu$ s/switch	13 $\mu$ s/4switch 4 $\mu$ s/switch

For the B2B transfer system, the upper bound latency of the frames in the B2B Broadcast and B2B Unicast traffic is 500  $\mu$ s, see Tab.6.4. The latency of the WR network is decided by the layers of WR switches and the length of the optical fiber. The latency of the optical fiber is about 204 m/ $\mu$ s [56] and the longest distance in the FAIR campus is around 2 km, so the latency of a 2 km optical fiber is about 10  $\mu$ s. The layers of WR switches play a more important role in the latency.

- B2B Broadcast

Here we calculate the layer of the WR switch between the B2B source SCU and B2B target SCU, between B2B source SCU and source trigger SCU and between B2B source SCU and target trigger SCU.

$$\frac{500 \mu\text{s} - 10 \mu\text{s}}{28 \mu\text{s}/\text{switch}} \approx 17 \quad (6.50)$$

- B2B Unicast

Here we calculate the layer of the WR switch between the B2B source SCU and DM.

$$\frac{500 \mu\text{s} - 10 \mu\text{s}}{6 \mu\text{s}/\text{switch}} \approx 81 \quad (6.51)$$

## 6.3 Kicker systematic investigation for the B2B transfer system

The SIS18 extraction kicker consists of 9 kicker units. In the existing topology, 5 kicker units are installed in the 1st crate and the other 4 units are in the 2nd crate. The width of each kicker unit is 0.25m and the distance between two kicker units is 0.09m. The distance between two crates is 19.167m. SIS100 injection kicker consists of 6 kicker units, which are equally located. The width of each kicker unit is 0.22m and the distance between two units is 0.23m. For the B2B transfer, the rise time of SIS18 extraction kicker and SIS100 injection kicker unit are 90ns and 1/20 of the revolution period. The rise time of these kickers must fit within the bunch gap, 25% of rf reference period [27, 41]. The bunch gap is denoted by G. All the analysis in this section dose not consider the jitter of the kicker trigger signal. Here we are discussing about the following possibilities.

### 6.3. Kicker systematic investigation for the B2B transfer system

- For SIS18, whether the kicker units in the 2nd crate could be fired a fixed delay after the firing of the kicker units in the 1st crate for ion beams over the whole range of stable isotopes.
- For SIS100, whether the kicker units could be fired instantaneously.

#### 6.3.1 SIS18 extraction kicker units

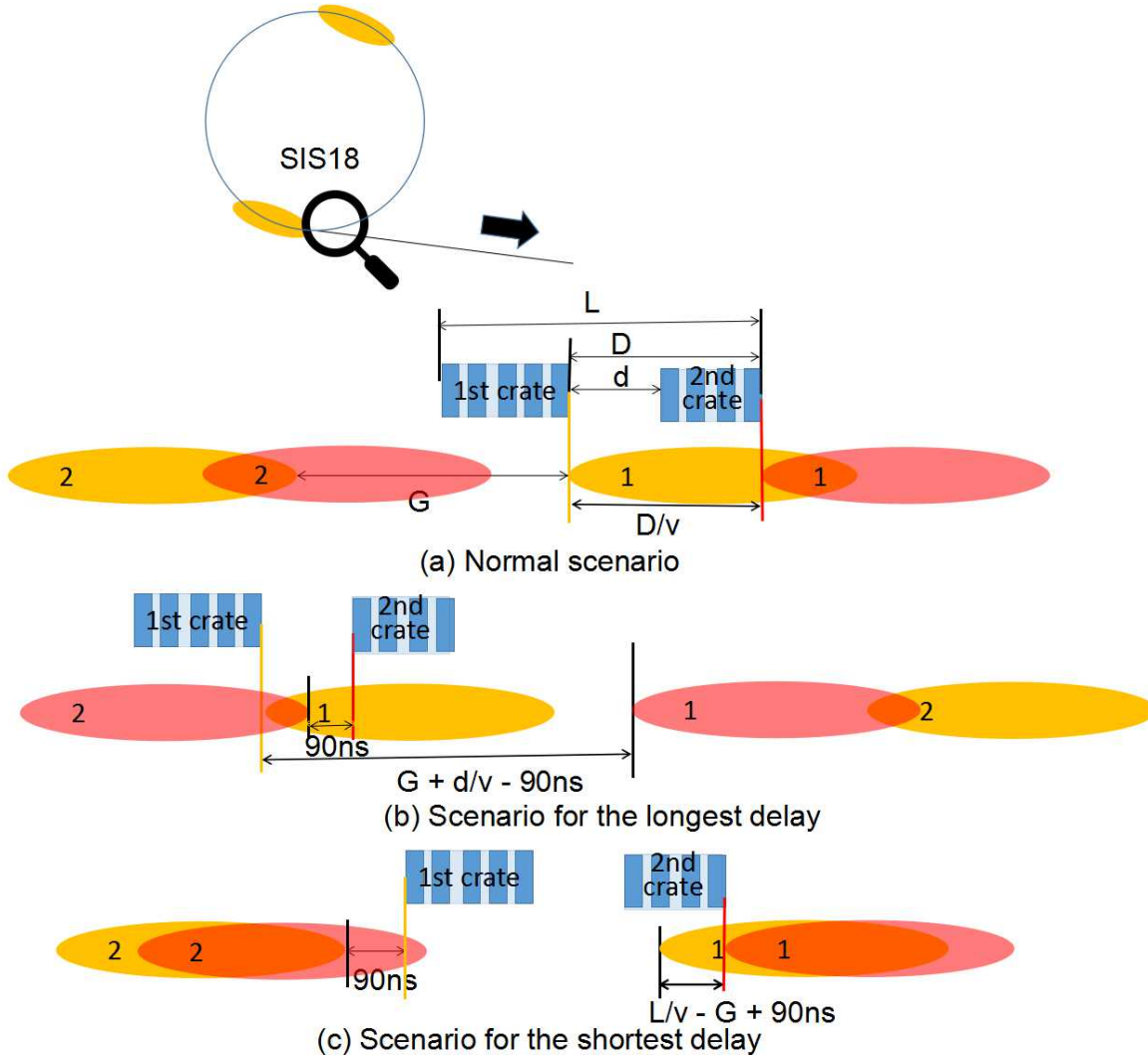


Figure 6.21: Three scenarios for the delay of SIS18 extraction kicker

Here we take three ion beams,  $H^+$ ,  $U^{28}$  and  $U^{73+}$ , to check the possibility, because the boundary ion species have the most stringent requirements. Fig. 6.21 shows three scenarios of the firing delay between two crates. Beam is firstly kicked by kicker units in the 1st crate and than kicked by the units in the 2nd crate to the transfer line. The yellow and red ellipse represents the position of the bunches, when the kicker units in the 1st and 2nd crate are fired. The number in the ellipse is used to tell different bunches. The head of the bunch is at the right side. The bunch 2 is firstly kicked. Here we assume that the kicker units in the same crate are triggered instantaneous.  $d$  denotes the distance between two crates.  $L$  denotes the distance

### 6.3. Kicker systematic investigation for the B2B transfer system

---

from the leftmost to the rightmost kicker unit. D denotes the sum distance of d and the 2nd crate. d equals to 19.167 meter. L equals to  $22.047m = d + 9 \cdot 0.25m + 7 \cdot 0.09m$ . D equals to  $20.437m = d + 4 \cdot 0.25m + 3 \cdot 0.09m$ .

Fig. 6.21 (a) is the easiest scenario. The kicker units in the 1st crate are fired when the tail of the bunch 1 passes by the 1st crate completely. The kicker units in the 2nd crate are fired when the tail of the bunch 1 passes by the 2nd crate completely. The delay for the firing two crates in this scenario is  $D/\beta c$ .

Fig. 6.21 (b) shows the scenario of the maximum delay between the firing of two crates. The kicker units in the 1st crate are fired when the tail of the bunch 1 passes by the 1st crate completely. The kicker units in the 2nd crate are fired 90ns before the head of the bunch 2 passes by it. The delay equals to  $G+d/\beta c-90ns$ .

Fig. 6.21 (c) shows the scenario of the minimum delay. The kicker units in the 1st crate are fired 90ns before the head of the bunch 2 passes by it. The kicker units in the 2nd crate are fired when the bunch 1 passes by the 2nd crate. The delay is  $L/\beta c-G+90ns$ .

Tab. 6.9 shows delay for three scenarios and related parameters. The fixed delay is determined primarily by the boundary delay range from  $H^+$ ,  $U^{28}$  and  $U^{73+}$  beams, the delay range for other heavy ion species beams must be contained in these boundary range. According to the result, a fixed delay is available for firing kicker units in two crate for different beams. e.g. 80ns.

Table 6.9: The delay for firing two crates of SIS18 extraction kicker

Beam	$\beta$	time $L/\beta c$	bunch gap G	minimum delay $L/\beta c-G+90ns$	delay $D/\beta c$	maximum delay $G+d/\beta c-90ns$
$H^+$	0.982	75ns	184ns	0ns	69ns	163ns
$U^{28+}$	0.568	130ns	159ns	61ns	120ns	189ns
$U^{73+}$	0.872	84ns	104ns	70ns	78ns	92ns

#### 6.3.2 SIS100 injection kicker units

Two bunches from SIS18 will be continuously injected into two RF buckets after the other in SIS100. See Fig. 6.10. The yellow ellipse represents the circulating bunch in SIS100 and the red one represents the bunch to be injected. The head of the bunch is at the left side. The preparation of the SIS100 injection kicker must be done during the bunch gap and it must be established for at least one SIS18 revolution period. For the instantaneous firing, all kicker units are fired only if the tail of the circulating bunch passes the leftmost kicker unit. The kicker pass time is the time needed for the tail of a bunch to pass from the rightmost unit to the leftmost kicker unit. The rise time of the kicker unit is 1/20 of the revolution period [27]. Therefor the preparation time is the sum of the kicker pass time and rise time. The distance from the rightmost to the leftmost kicker unit is 3.79m,  $6 \cdot 0.22m + 5 \cdot 0.23m$ . If the preparation time is shorter than bunch gap, all kicker units could be fired instantaneous. Tab. 6.10 shows the preparation time for  $H^+$ ,  $U^{28}$  and  $U^{73+}$  beams and their bunch gap. The preparation time is much shorter than the bunch gap. So the kicker units could be fired instantaneous.

## 6.4. Test setup for the data collection, merging and redistribution of the B2B transfer system

---

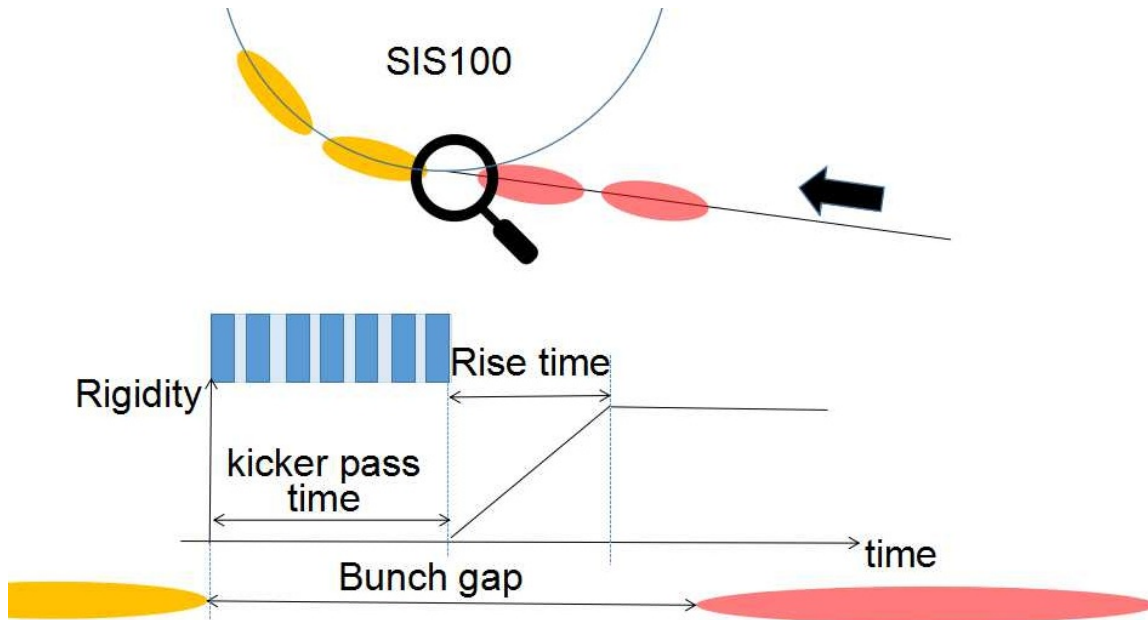


Figure 6.22: SIS100 injection kicker

Table 6.10: The delay for firing SIS00 injection kicker

Beam	$\beta$	kicker pass time $L/\beta c$	Rise time $1/20 \cdot T_{rev}^{SIS100}$	Preparation time $L/\beta c + 1/20 \cdot T_{rev}^{SIS100}$	bunch gap $2.25 \cdot T_{rev}^{SIS100}$
$H^+$	0.982	3ns	184ns	187ns	828ns
$U^{28+}$	0.568	22ns	318ns	333ns	1431ns
$U^{73+}$	0.872	15ns	207ns	222ns	932ns

## 6.4 Test setup for the data collection, merging and redistribution of the B2B transfer system

In this section, the test setup for the B2B transfer system is described, focusing only on the timing aspects.

### 6.4.1 Test functional requirement

The test setup achieves the following functional requirement.

- After receiving CMD\_B2B\_START, both the B2B source and target SCUs collect predicted phase equivalent data locally. The equivalence is a timestamp for the zero crossing point of the simulated Reference RF Signal of SIS18 and SIS100.
- The B2B target SCU transfers the frame containing the timestamp to the B2B source SCU.

## 6.4. Test setup for the data collection, merging and redistribution of the B2B transfer system

- After receiving the data, the B2B source SCU calculates the synchronization window.
- The B2B source SCU sends the frame containing the beginning of the synchronization window to the WR network.
- After receiving the frame, the trigger SCU produces TTL output indicating the start of the synchronization window.

### 6.4.2 Test setup

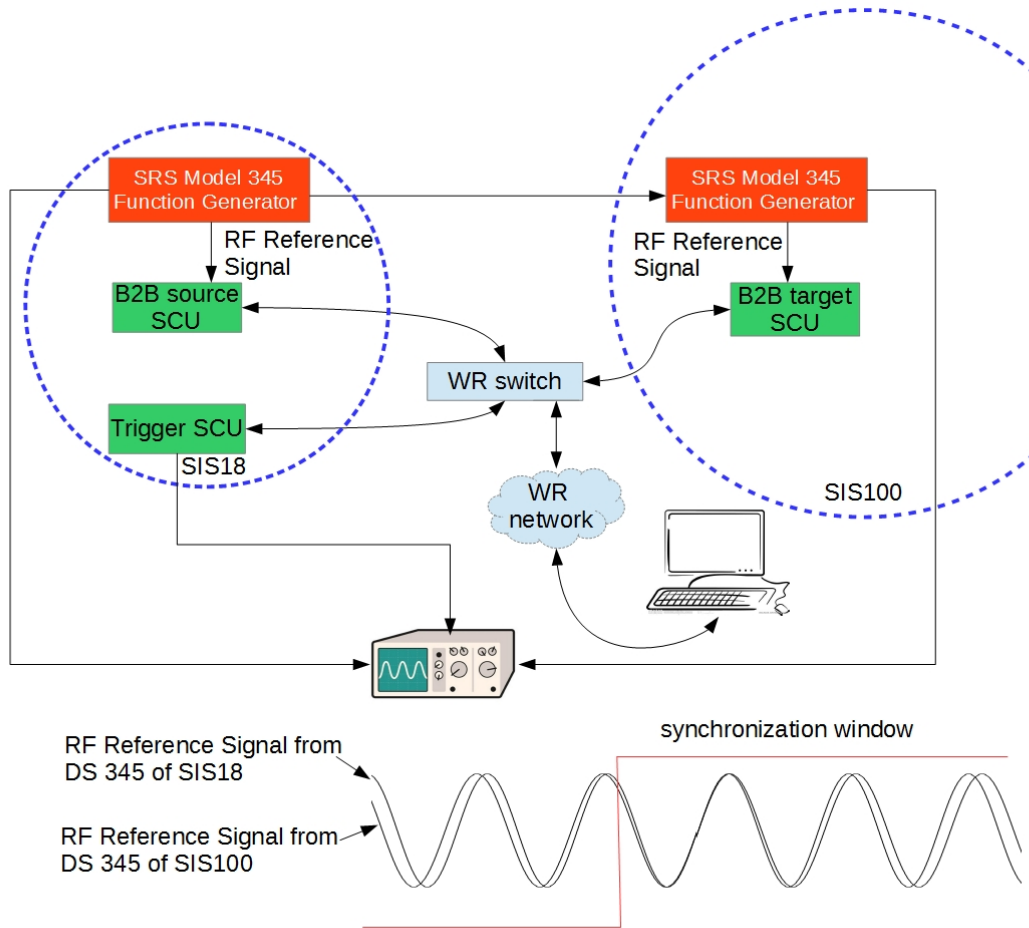


Figure 6.23: Schematic of the test setup

Fig. 6.23 shows the schematic of the test setup. In this test setup, two MODEL DS345 Synthesized Function Generators<sup>7</sup> are used, which are with the frequency accuracy of  $\pm 5$  ppm of the selected frequency to simulate Reference RF Signals of SIS18 and SIS100. DS345 of SIS18 uses an internal 10 MHz clock as an external reference clock for DS345 of SIS100. The B2B source SCU, B2B target SCU and trigger SCU are connected to the same WR switch, which connects to the timing

<sup>7</sup><http://www.thinksrs.com/downloads/PDFs/Manuals/DS345m.pdf>

## 6.4. Test setup for the data collection, merging and redistribution of the B2B transfer system

network. A PC<sup>8</sup> is used as a DM to produce the B2B start timing frame. Besides, it monitors the status of the B2B transfer programs in all SCUs. The oscilloscope is used to monitor the alignment of the two simulated Reference RF Signals within the synchronization window provided by the trigger SCU.

Fig. 6.24 shows the front and back view of the test setup. DS345 of SIS18 produces the sine wave of 1.572 200 MHz frequency for the oscilloscope and DS345 of SIS100 produces the sine wave of 1.572 000 MHz for the oscilloscope, which are achieved by the LEMO cables, see green line in Fig. 6.24. DS345 produces the TTL signal for the B2B source SCU, whose rising edge is synchronized to the positive zero crossing of the sine wave of 1.572 200 MHz frequency and DS345 of SIS100 produces the TTL signal for the B2B target SCU, whose rising edge is synchronized to the sine wave of 1.572 000 MHz, which are achieved by the LEMO cables, see red line in Fig. 6.24. So the beating frequency is 200 Hz and the synchronization period is 5 ms. The B2B source, target and trigger SCUs are connected to the WR switch, which are achieved by the optical fiber, see yellow line. The WR switch is connected to the PC and the WR network. The output of the synchronization window from the B2B trigger SCU is connected to the oscilloscope, which is achieved by the LEMO cable, see green line.

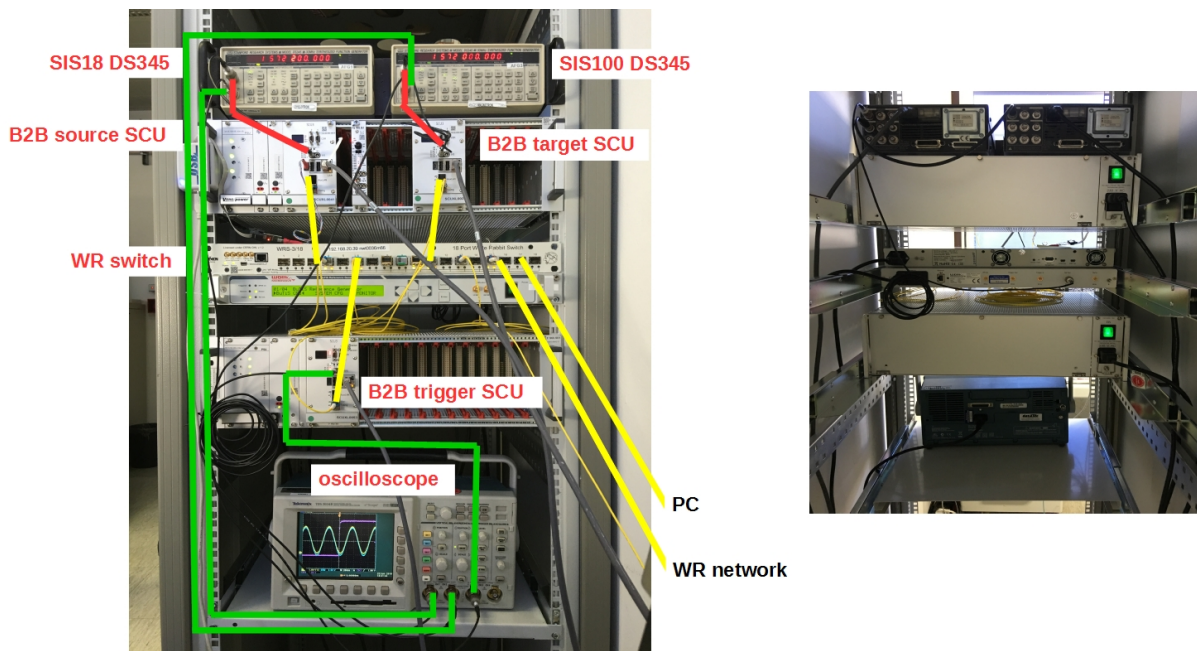


Figure 6.24: The front and back view of the test setup

Compared with the final scenario, there are some difference of the test setup.

- The SIS18 and SIS100 DS345 will be replaced by the PAP modules, which are installed in the B2B source and target SCUs as SCU slaves.
- All devices are installed in different racks. The SIS18 source SCU and B2B trigger SCU of the extraction kicker are installed in SIS18 and the SIS18 target SCU and B2B trigger SCU of the injection kicker are installed in SIS100. The connection is done via the WR network.

<sup>8</sup>A Linux personal computer is installed with the standard TR tools and library.  
<https://www-acc.gsi.de/wiki/Timing/TimingSystemNodesCurrentRelease>

## 6.4. Test setup for the data collection, merging and redistribution of the B2B transfer system

- The B2B source SCU has several other SCU slaves, e.g. Phase Shift Module (PSM) for the phase shift.
- The B2B trigger SCU considers not only the synchronization window, but also the kicker delay compensation from the SM. Besides, it has several SCU slaves, which coordinate the correct B2B extraction and injection kicker with other systems, e.g. MPS.

### 6.4.3 The firmware of the B2B transfer system

The B2B source, B2B target and trigger SCUs have different firmware running on their soft CPU, LM32<sup>9</sup>. The firmware are activated by the B2B start timing frame, *CMD\_START\_B2B*, which indicates the source and target synchrotrons of the B2B transfer.

- Firmware for the B2B source SCU

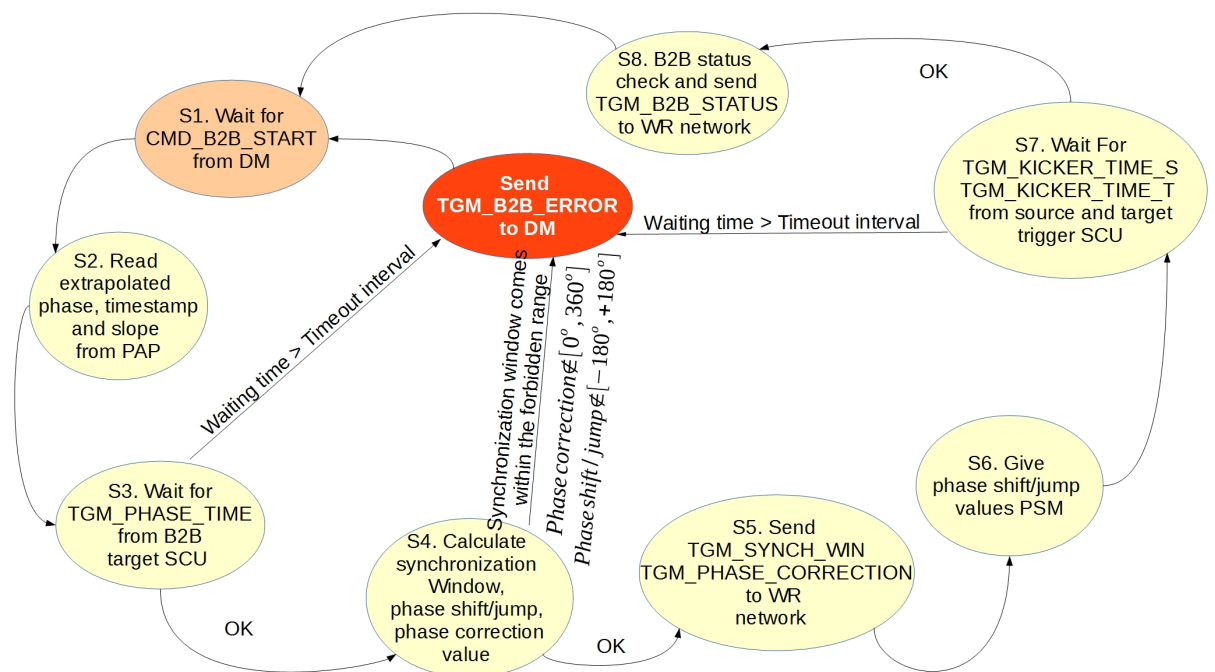


Figure 6.25: Flow chart of the firmware for B2B source SCU.  
Flow chart of the firmware for B2B source SCU. “Step“ is represented as “S“ in the figure.

The firmware for the B2B source SCU is the core program of the B2B transfer system. See Fig. 6.25.

- Step 1. The program waits for the *CMD\_START\_B2B* timing frame.
- Step 2. When it receives the timing frame *CMD\_START\_B2B*, it reads the extrapolated phase, the corresponding timestamp and the phase advance slope from the PAP module.

<sup>9</sup>LatticeMico32 is a 32-bit microprocessor soft core from Lattice Semiconductor optimized for field-programmable gate arrays (FPGAs).

## 6.4. Test setup for the data collection, merging and redistribution of the B2B transfer system

---

- Step 3. It waits for the TGM\_PHASE\_TIME timing frame from the B2B target SCU, which contains the extrapolated phase, the corresponding timestamp and the slope of the phase advance.
- Step 4. When it receives the timing frame TGM\_PHASE\_TIME within a specified timeout interval, it calculates the synchronization window, the phase shift/jump value and the phase correction value. Or it sends a timing frame TGM\_B2B\_ERROR to the WR network and goes back to the step 1, which indicates the timeout error of the frame. Besides, it checks whether the phase correction is in the range of  $0^\circ$  to  $360^\circ$ , the required phase shift in the range of  $-180^\circ$  to  $180^\circ$  and the start of the synchronization window not in the forbidden range. If at least one of them is not correct, it sends a timing frame TGM\_B2B\_ERROR to the WR network and goes back to the step 1, which indicates the calculation error.
- Step 5. It sends the timing frame TGM\_SYNCH\_WIN and TGM\_PHASE\_CORRECTION to the WR network. TGM\_SYNCH\_WIN indicates the start of the synchronization window and TGM\_PHASE\_CORRECTION is used for the trigger SCUs for the reproduction of the bucket label signal.
- Step 6. It gives the phase correction and phase shift/jump values to corresponding modules.
- Step 7. It waits for the timing frame TGM\_KICKER\_TIME\_S from the source trigger SCU and TGM\_KICKER\_TIME\_T from the target trigger SCU, which contains the extraction/injection kicker trigger and firing timestamp. When it does not receive the timing frames within a specified timeout interval, it sends a timing frame TGM\_B2B\_ERROR to the WR network and goes back to the step 1, which indicates the timeout error of the frame.
- Step 8. When it receives the timing frames mentioned in the step 7 within a specified timeout interval, it checks the B2B transfer status and sends TGM\_B2B\_STATUS to the WR network and goes to the step 1. The B2B transfer is successful, if all of the following checks are correct. Or the B2B transfer is failure.
  - \* Trigger time < firing time of the extraction kicker of the source synchrotron
  - \* Trigger time < firing time of the injection kicker of the target synchrotron
  - \* Firing time of the extraction kicker < firing time of the injection kicker

- Firmware for the B2B target SCU
-

## 6.4. Test setup for the data collection, merging and redistribution of the B2B transfer system

---

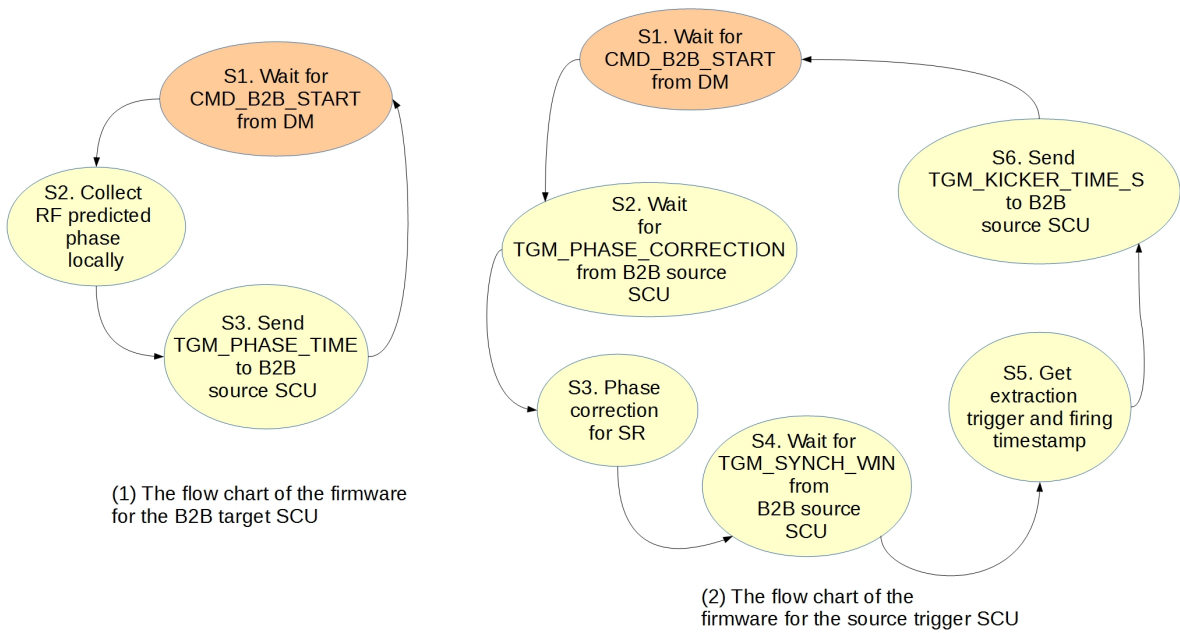


Figure 6.26: Flow chart of the firmware for B2B target SCU.  
Flow chart of the firmware for B2B target SCU. “Step“ is represented as “S“ in the figure.

Fig. 6.26 (a) shows the flow chart of the program of the B2B target SCU.

- Step 1. The program waits for the CMD\_START\_B2B timing frame.
- Step 2. When it receives the timing frame CMD\_START\_B2B, it collects the predicted phase.
- Step 3. It sends the TGM\_PHASE\_TIME timing frame to the B2B source SCU and goes back to the step 1.

- Firmware for the trigger SCU

Fig. 6.26 (b) shows the flow chart of the program of the source trigger SCU. For the target trigger SCU, the flow chat is same only with the different name of the timing frame TGM\_KICKER\_TIME\_T.

- Step 1. The program waits for the CMD\_START\_B2B timing frame.
- Step 2. The program waits for the TGM\_PHASE\_CORRECTION timing frame.
- Step 3. The program gives the phase correction value to the corresponding module for the bucket label signal reproduction.
- Step 4. When it receives the timing frame CMD\_START\_B2B, it waits for the timing frame TGM\_SYNCH\_WIN to indicate the synchronization window for the kicker trigger.
- Step 5. After the beam extraction, it collects the trigger and firing timestamp.
- Step 6. It sends the TGM\_KICKER\_TIME\_S timing frame to the B2B source SCU and goes back to the step 1.

## 6.4. Test setup for the data collection, merging and redistribution of the B2B transfer system

---

### 6.4.4 The time constraints of the B2B transfer system

For the B2B transfer system, the time constraints are very important and strict. Fig. 6.27 shows the time constraint of the system. The *CMD\_START\_B2B* is executed at  $t_{B2B}$ . The RF phase prediction needs 500  $\mu$ s, so the B2B source and target SCUs collect the phase data at  $t_{B2B} + 500 \mu\text{s}$  and need about 450 ns for the data collection. The B2B source SCU receives the timing frame TGM\_PHASE\_TIME at around  $t_{B2B} + 500 \mu\text{s} + 450 \text{ ns} + 500 \mu\text{s} \approx t_{B2B} + 1 \text{ ms}$ . The second 500  $\mu$ s is the upper bound latency of the WR network. After that, the B2B source SCU needs about 100  $\mu$ s for the calculation, the sending of the timing frame TGM\_SYNCH\_WIN and TGM\_PHASE\_CORRECTION and data transferring to the corresponding module. TGM\_SYNCH\_WIN is sent at around  $t_{B2B} + 1 \text{ ms} + 100 \mu\text{s} \approx t_{B2B} + 1.1 \text{ ms}$ . The trigger SCU receives TGM\_PHASE\_CORRECTION and TGM\_SYNCH\_WIN at around  $t_{B2B} + 1.1 \text{ ms} + 500 \mu\text{s} \approx t_{B2B} + 1.6 \text{ ms}$ . The 500  $\mu$ s is the latency of the WR network. The start of the synchronization window must be later than  $t_{B2B} + 1.1 \text{ ms} + 2.500 \mu\text{s} \approx t_{B2B} + 2.1 \text{ ms}$ , because the TGM\_SYNCH\_WIN must be transferred back to the DM and the DM transfers it further to the beam instrumentation devices via WR network. The upward to DM transfer needs maximum 500  $\mu$ s and the transfer from the DM to BI needs another 500  $\mu$ s. The upper bound B2B transfer time is 10 ms, which is decided by the duration of the stable beam. There is no hard real time for the collection of the trigger and firing timestamps and timing frame TGM\_KICKER\_TIME\_S sending, we give 1 ms for the source trigger SCU to do this task and the source trigger SCU sends TGM\_KICKER\_TIME\_S at around  $t_{B2B} + 10 \text{ ms} + 1 \text{ ms} \approx t_{B2B} + 11 \text{ ms}$ . The same time constraints is also for the target trigger SCU. The B2B source SCU receives TGM\_KICKER\_TIME\_S and TGM\_KICKER\_TIME\_T at around  $t_{B2B} + 11 \text{ ms} + 500 \mu\text{s} \approx t_{B2B} + 11.5 \text{ ms}$ . The 500  $\mu$ s is the latency of the WR network. The B2B source SCU sends TGM\_B2B\_STATUS at around  $t_{B2B} + 11.5 \text{ ms} + 100 \mu\text{s} \approx t_{B2B} + 11.6 \text{ ms}$ . The BI devices receives the timing frame TGM\_B2B\_STATUS at around  $t_{B2B} + 11.6 \text{ ms} + 2.500 \mu\text{s} \approx t_{B2B} + 12.6 \text{ ms}$ .

## 6.4. Test setup for the data collection, merging and redistribution of the B2B transfer system

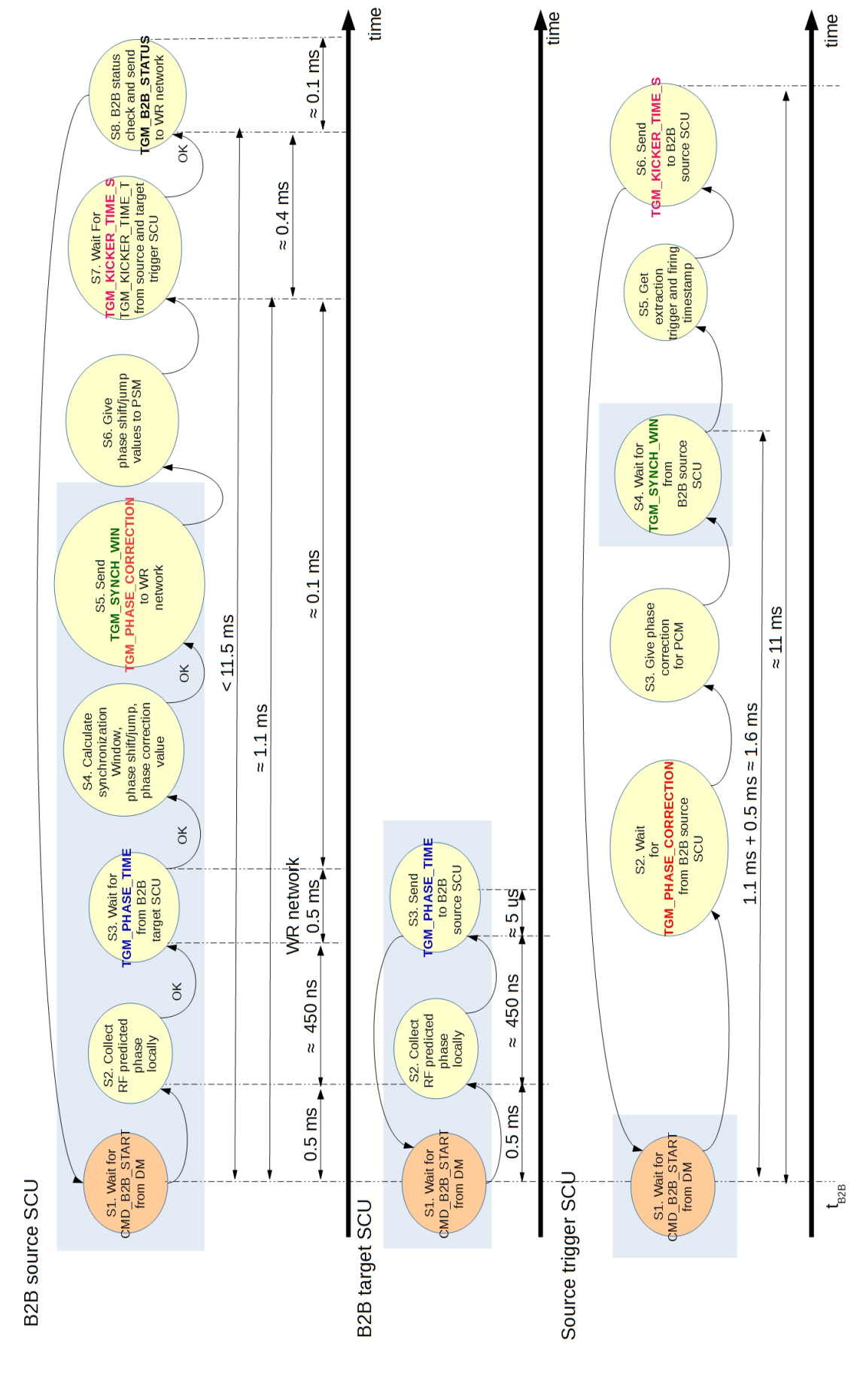


Figure 6.27: The time constraints of the B2B transfer system. The sent and received timing frame pairs have the same color. The test setup realizes the steps in the blue rectangle. (not drawn to accurate timescale)

#### **6.4. Test setup for the data collection, merging and redistribution of the B2B transfer system**

### 6.4.5 Test result

Because some modules of the B2B transfer system are still under the development, the test setup realizes parts of the whole function, mainly concentrated on the data collection from two simulated Reference RF signals, the calculation of the synchronization window and the distribution of the start of the synchronization window. The steps with the blue rectangle in Fig. 6.27 are realized in this test setup. The test result of the B2B programs on B2B source, B2B target and trigger SCUs are shown as follows.

```
1  
2 U28+ B2B transfer from SIS18 to SIS100 => Trigger SCU  
3 ======  
4 Waiting for timing frames ...
```

## 6.4. Test setup for the data collection, merging and redistribution of the B2B transfer system

---

5	>>>>>>>>>>>>>>>>>>>>>>>>> Receive TGM_SYNCH_WIN from WR network
6	Event execution timestamp: GMT 1970–01–08 21:07:27.450028674

After both B2B source and target programs receive the *CMD\_START\_B2B* frame, they trigger another unit connected to the System-on-Chip<sup>10</sup> (SoC) bus to get the timestamp of the next zero crossing point of the DS345 sine waves, which is simulated as an equivalent to the predicted phase. All timestamp are shown in the format of Greenwich Mean Time (GMT). The timestamp got by the B2B source SCU is Thu, Jan 8, 1970, 21:07:27 0.445405856 second and the timestamp got by the B2B target SCU is Thu, Jan 8, 1970, 21:07:27 0.445364560 second, see Line 10 and 14 of the test result of the B2B source SCU. The time difference between two timestamps is 41.296 µs. The frequency difference between SIS18 and SIS100 Reference RF Signals is 200Hz. It means that there are 200 more periods of the SIS18 Reference RF Signal within one second compared with the SIS100 Reference RF Signal. Every 5 ms (1/200 Hz) SIS18 Reference RF Signal has one period more than that of SIS100. The time is calculated by eq. 6.52, indicating the alignment of the zero crossing of two DS345 sine waves of SIS18 and SIS100. The time is named as “synchronization time”, denoted by  $\Delta t$ .

$$\frac{T_{h=2}^{SIS18}}{1/(f_{h=2}^{SIS18} - f_{h=10}^{SIS100})} = \frac{41.296\text{us}}{\Delta t} \mod T_{h=10}^{SIS100} \quad (6.52)$$

$$\Delta t = 4.622\,818\,\text{ms} \quad (6.53)$$

The number of the SIS18 Reference RF Signal periods for the synchronization is calculated as

$$\frac{\Delta t}{T_{h=2}^{SIS18}} = 7268 \quad (6.54)$$

we could get that the beating time  $\Delta t$  is 4.622 818 ms and the number of the SIS18 Reference RF Signal periods for the synchronization is 7268 for the test.

---

<sup>10</sup>A system-on-chip is an integrated circuit that integrates all components of a computer or other electronic system into a single chip.

# Chapter 7

## Conclusion and outlook

For many large scale accelerator facilities, it is inevitable to transfer bunched beam from one ring accelerator to another to gain higher energy or to accumulate beam for some research experiments. Without the proper transfer, the beam will be subject to various disturbances and even beam loss, e.g. dipole oscillation caused by the injection energy or phase error, quadrupole oscillation caused by the cavity voltage error. Hence, the proper bunch-to-bucket transfer between two accelerators is of great importance.

Facility for Antiproton and Ion Research (FAIR) aims at providing high-energy beam with high intensities. SIS100/300 of FAIR is under construction at GSI Helmholtz Centre for Heavy Ion Research GmbH at current stage. The B2B transfer has never been practiced between the existing machines, e.g. SIS18, ESR and CRYRING. The new developed Bunch-to-Bucket transfer system for FAIR in the dissertation is designed for all complex B2B transfer between FAIR accelerators. It is capable to transfer different species beam from one machine cycle to another. It is capable to parallel transfer beam through FAIR accelerators. It is also able to transfer the beam between two synchrotrons via FRS or Super FRS. It focuses first of all on the transfer from SIS18 to SIS100, but it will be firstly tested for the transfer from SIS18 to ESR and further to CRYRING.

The B2B transfer system for FAIR is introduced in the dissertation at hand from the functional point of view. The basic principles for B2B transfer are realized based on the existing FAIR technical basis (e.g. LLRF and FAIR control systems) and unique FAIR demands (e.g. Machine Protection System, MPS). The phase difference between two RF systems of two ring accelerators is obtained with the help of a shared reference signal at two ring accelerators. The source synchrotron works as the “B2B transfer master” for the rf phase collection, data (e.g. synchronization window, phase correction, phase shift and so on) calculation, synchronization window redistribution and B2B status check. In addition, the dissertation presents how FAIR accelerators apply the B2B transfer system and how precise the bunch-to-bucket transfer is achieved with the system. The rules for the application of the system is explained, which is determined by the relation between the circumference ratio/energy ratio and the cavity harmonic number of two synchrotron.

In addition, the beam dynamic of the  $U^{28+}$  B2B transfer from SIS18 to SIS100 is simulated for two synchronization methods, the phase shift and frequency beating method. The dissertation explains the timing constraints of the system, the calculation of the synchronization window and presents the usage of the WR network for

the B2B transfer system. Further, the SIS18 extraction and SIS100 injection kickers are analyzed for the different triggering possibilities.

The dissertation presents a test setup for the system, achieving the phase collection of two synchrotrons locally, phase transfer from the target to source synchrotron, synchronization window calculation at the source synchrotron, synchronization window redistribution to the WR network, synchronization window reproduced at the source/target synchrotron.

Although the B2B transfer system for FAIR is flexible and with high compatibility, there still exists several improvement.

In order to reduce the synchronization time, the synchronization process could be started during the acceleration. The phase difference between two Reference RF Signals of the source and target synchrotrons at the flattop could be predicted by comparison the phases of these two signals at any time during the acceleration. Once the phase difference at the flattop is predicted, the synchronization process can be carried out.

- Phase shift method

First, the radial loop must be turned off. At some time during the acceleration, the phases difference between the source and target synchrotrons are obtained with the help of the Synchronization Reference Signal, and the phase difference at the flattop is picked up from the look-up table. Then, a rf frequency modulation is superposed on the initial frequency pattern. The integration of the rf frequency modulation equals to the required phase difference. With this new frequency pattern, the phase difference at the flattop will be the required phase difference when the cavity rf frequency of the source and target synchrotrons reach the flattop.

- Frequency beating method

The radial loop keeps on. At some time during the acceleration, the phases difference between the source and target synchrotrons are obtained. Then, a frequency detune is superposed on the initial frequency pattern. With this new frequency pattern, the synchronization window will be calculated.

# **Appendix A**

## **B2B timing frames**

## APPENDIX A. B2B TIMING FRAMES

---

Table A.1: B2B timing frames

No	Fram Name	Event ID	Priority	Source	Destination
1	CMD_START_B2B		7	DM	Source and B2B target SCU
2	TGM_PHASE_TIME		6	B2B target SCU	B2B source SCU
3	TGM_SYNCH_WIN		6	B2B source SCU	DM, source and target Trigger SCUs
4	CMD_SYNCH_WIN		7	DM	Beam Instrumentation (BI)
5	TGM_PHASE_JUMP		6	B2B source SCU	B2B target SCU
6	TGM_PHASE_CORRECTION		6	B2B source SCU	Source Trigger SCU
7	TGM_KICKER_TRIGGER_TIME_S		6	Source Trigger SCU	B2B source SCU
8	TGM_KICKER_TRIGGER_TIME_T		6	Target Trigger SCU	B2B source SCU
9	TGM_B2B_STATUS		6	B2B source SCU	DM
10	CMD_B2B_STATUS		7	DM	BI
No	Content				Description
1	64 bits timestamp				Begin of the B2B transfer process
2	16 bits phase advance and 64 bits slop				Transfer of the phase advance and the slop
3	64 bits timestamp				Indication the start of the synchronization window
4	64 bits timestamp				Indication the start of the synchronization window
5	16 bits the expected jumped phase				Indication the jumped phase for the empty target machine
6	16 bits phase correction				Target revolution frequency reproduction
7	2 × 64 bits timestamp				Timestamps of trigger and firing of extraction kicker
8	2 × 64 bits timestamp				Timestamps of trigger and firing of injection kicker
9	64 bits timestamp + 1 bit				The actual beam extraction time and the status of the B2B system
10	64 bits timestamp + 1 bit				The actual beam extraction time and the status of the B2B system

## **Appendix B**

### **Timing frames transfer for the B2B transfer**

## APPENDIX B. TIMING FRAMES TRANSFER FOR THE B2B TRANSFER

---

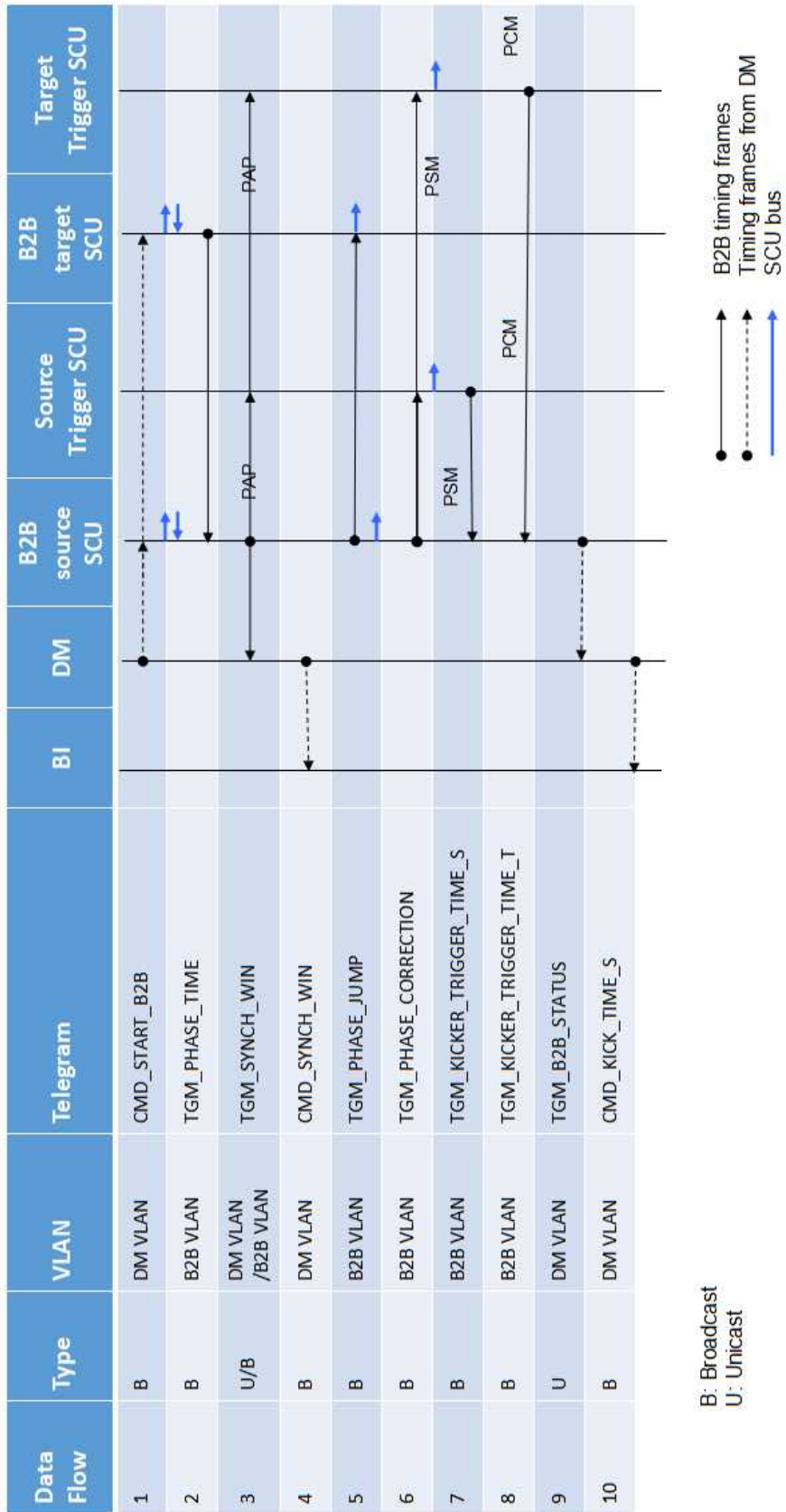


Figure B.1: Timing frames transfer for the B2B transfer

# Appendix C

## Parameters of B2B transfer for FAIR accelerator pairs

### C.1 Parameters for the B2B transfer from SIS18 to SIS100

		Proton		Heavy Ion	
	Unit	SIS18 Ext <sup>1</sup>	SIS100 Inj <sup>2</sup>	SIS18 Ext	SIS100 Inj
Design orbit	m	216.72	1083.6	216.72	1083.6
Inj orbit	m	216.72	1083.6	216.72	1083.6
$C_{SIS18} : C_{SIS100}$		5		5	
Ext kinetic energy	MeV/u	4000		200	
Inj kinetic energy	MeV/u		4000		200
Cavity h		1	10(1×4)	2	10(2×4)
$f_{rf}$	MHz	1.359	2.718	1.572	1.572
$T_{rf}$	μs	0.736	0.368	0.636	0.636
$f_{rev}$	MHz	1.359	0.272	0.786	0.157
$T_{rev}$	μs	0.736	3.678	1.272	6.359
Max $\Delta p/p$		±0.008	±0.01	±0.008	±0.01
$\Delta R/R$		$\pm 0.8 \times 10^{-4}$		$\pm 2.4 \times 10^{-4}$	
Slip factor <sup>3</sup>		-0.026		-0.647	
Transition Energy $\gamma_t$		10		5.8	
Compaction factor $\alpha_p$		0.010		0.030	
$\beta$		0.982	0.982	0.568	0.568
$\gamma$		5.294	5.294	1.215	1.215
		Injection four times		Injection four times	
		Frequency beating method			

### C.1. Parameters for the B2B transfer from SIS18 to SIS100

---

	MHz	$f_{rf} + \Delta f =$ 1.359 + 200Hz	$f_{rf} =$ 1.359	$f_{rf} + \Delta f =$ 1.572 +200Hz	$f_{rf} =$ 1.572
Beating frequency	Hz	200 Hz		200 Hz	
Synchronization period	ms	5		5	
Synchronization window	$\mu$ s	7.356		12.718	
Mismatch	degree	$\pm 0.31^\circ$		$\pm 0.50^\circ$	
Phase shift method					

Table C.1: Parameters for the B2B transfer from SIS18 to SIS100

## C.2 Parameters for the B2B transfer from SIS18 to ESR

		Proton/Heavy Ion		Heavy Ion	
	Unit	SIS18 Ext	ESR Inj	SIS18 Ext	ESR Inj
Design orbit	m	216.72	108.36	216.72	108.36
Inj orbit	m	216.72	108.36 +0.15	216.72	108.36 +0.15
$C_{SIS18} : C_{ESR}$		1.997		1.997	
Ext kinetic energy	MeV/u	550		30	
Inj kinetic energy	MeV/u		400		30
Cavity h		1	1	4	1
$f_{rf}$	MHz	0.989756	1.976777	1.373201	0.685651
$T_{rf}$	μs	1.010350	0.505874	0.728226	1.458468
$f_{rev}$	MHz	0.989756	1.976777	0.343300	0.685651
$T_{rev}$	μs	1.010350	0.505874	2.912903	1.458468
$\Delta p/p$ compared with design orbit			1%		1%
$\Delta R/R$			0.138%		0.138%
Slip factor		-0.480	-0.310	-0.909	-0.759
Transition Energy $\gamma_t$		10	2.357	5.8	2.357
Compaction factor $\alpha_p$		0.010	0.18	0.030	0.18
$\beta$		0.715	0.715	0.248	0.248
$\gamma$		1.429	1.429	1.032	1.032
		Accumulation beam in injection orbit		Accumulation beam in injection orbit	
Frequency beating method					
	kHz	$f_{rf}/1 =$ 988.388 + 1368Hz	$f_{rf}/2 =$ 988.388	$f_{rf}/2 =$ 685.652 + 948Hz	$f_{rf}/1 =$ 685.65250
Beating frequency	Hz	1368 Hz		948 Hz	
Synchronization period	ms	0.731		1.055	
Synchronization window	μs	2.034		2.917	
Mismatch	degree	$\pm 0.50^\circ$		$\pm 0.51^\circ$	
Phase shift method					
$\Delta R/R$ for RF frequency match		0.2%		0.1%	

## C.2. Parameters for the B2B transfer from SIS18 to ESR

---

For SIS18, it is impossible to change the orbit to match the RF frequency within the radius excursion range. So the phase shift method could not be implemented

Table C.2: Parameters for the B2B transfer from SIS18 to ESR

### C.3 Parameters for the B2B transfer from SIS18 to ESR via FRS

		Heavy Ion Beam	Rare Isotope Beam
	Unit	SIS18 Ext	ESR Inj
Design orbit	m	216.72	108.36
Inj orbit	m	216.72	108.36 +0.15
$C_{SIS18} : C_{ESR}$		1.997	
Ext kinetic energy	MeV/u	400	
Inj kinetic energy	MeV/u		400
Cavity h		1	1
$f_{rf}$	MHz	1.076965	1.976777
$T_{rf}$	μs	0.928535	0.505874
$f_{rev}$	MHz	1.076965	1.976777
$T_{rev}$	μs	0.928535	0.505874
$\Delta p/p$ compared with design orbit			1%
$\Delta R/R$			0.138%
Slip factor		-0.366	-0.310
Transition Energy $\gamma_t$		5.8	2.357
Compaction factor $\alpha_p$		0.030	0.18
$\beta$		0.778	0.715
$\gamma$		1.590	1.429
		Accumulation beam in injection orbit	
Frequency beating method			
	kHz	$f_{rf}/5 =$ 219.642 + 4249Hz	$f_{rf}/9 =$ 219.642
Beating frequency	Hz	4249 Hz	
Synchronization period	ms	0.235349	
Synchronization window	μs	9.106	
Mismatch	degree	$\pm 6.92^\circ$	
Phase shift method			
$\Delta R/R$ for RF frequency match		2%	

### C.3. Parameters for the B2B transfer from SIS18 to ESR via FRS

---

For SIS18, it is impossible to change the orbit to match the RF frequency within the radius excursion range. So the phase shift method could not be implemented

Table C.3: Parameters for the B2B transfer from SIS18 to ESR via FRS

## C.4 Parameters for the B2B transfer from ESR to CRYRING

		Proton/Antiproton		Heavy Ion					
	Unit	ESR Ext	CRYRING Inj	ESR Ext	CRYRING Inj				
Design orbit	m	108.36	54.17	108.36	54.17				
Ext orbit	m	108.36 +0.15		108.36 +0.15					
$C_{ESR} : C_{CRYRING}$		2		2					
Ext kinetic energy	MeV/u	30		4-10					
Inj kinetic energy	MeV/u		30		4-10				
Cavity h		1	1	1	1				
$f_{rf}$	MHz	0.686	1.372	0.254-0.401	0.508-0.802				
$T_{rf}$	μs	1.458	0.729	3.932-2.494	1.966-1.247				
$f_{rev}$	MHz	0.686	1.372	0.254-0.401	0.508-0.802				
$T_{rev}$	μs	1.458	0.729	3.932-2.494	1.966-1.247				
Slip factor		-0.759							
Transition Energy $\gamma_t$		2.357		2.357					
Compaction factor $\alpha_p$		0.18		0.18					
$\beta$		0.248	0.248	0.092-0.145	0.092-0.145				
$\gamma$		1.032	1.032	1.004-1.011	1.004-1.011				
		One time injection		One time injection					
Phase shift method									
There is no beam in CRYRING, so the phase jump of CRYRING is preferred.									

Table C.4: Parameters for the B2B transfer from ESR to CRYRING

## C.5 Parameters for the B2B transfer from CR to HESR

		Antiproton		Rare Isotope Beam	
	Unit	CR Ext	HESR Inj	CR Ext	HESR Inj
Design orbit	m	221.45	575	221.45	575
$C_{ESR} : C_{CRYRING}$		2.6		2.6	
Ext kinetic energy	GeV/u	3		0.74	
Inj kinetic energy	GeV/u		3		0.74
Cavity h		1	1	1	1
$f_{rf}$	MHz	1.317	0.507	1.125	0.433
$T_{rf}$	μs	0.759	1.972	0.889	2.309
$f_{rev}$	MHz	1.317	0.507	1.125	0.433
$T_{rev}$	μs	0.759	1.972	0.889	2.309
Max $\Delta p/p$		±3%		±1.5%	
Slip factor		-0.011		0.178	
Transition Energy $\gamma_t$		3.85		2.711	
Compaction factor $\alpha_p$		0.067			
$\beta$		0.972	0.972	0.830	0.830
$\gamma$		4.221	4.221	1.794	1.794
		100 times Injection per 10 seconds		100 times Injection per 10 seconds	
Frequency beating method					
	kHz	$f_{rf}/13 =$ 101.290 + 136Hz	$f_{rf}/5 =$ 101.426	$f_{rf}/13 =$ 86.493 + 113Hz	$f_{rf}/5 =$ 86.608
Beating frequency	Hz	136 Hz		113 Hz	
Synchronization period	ms	7.353		8.850	
Synchronization window	μs	19.719		23.090	
Mismatch	degree	±0.48°		±0.47°	
Phase shift method					
$\Delta R/R$ for RF frequency match		0.2%		0.1%	
The beam in CR is stochastic cooling and electrons exist during the B2B process. The phase shift method doesn't work. The remove of electrodes is about 100 ms.					

Table C.5: Parameters for the B2B transfer from CR to HESR

## C.6 Parameters for the B2B transfer from SIS100 to CR

		Proton→ Antiproton		Heavy Ion→ RIB					
	Unit	SIS100 Ext	CR Inj	SIS100 Ext	CR Inj				
Design orbit	m	1083.6	221.45	1083.6	221.45				
$C_{ESR} : C_{CRYRING}$		4.893		4.893					
Ext kinetic energy	GeV/u	28.8		1.5					
Inj kinetic energy	GeV/u		3		0.74				
Cavity h		5(1 bunch)	1	2(1 bunch)	1				
$f_{rf}$	MHz	1.345	1.318	0.512	1.124				
$T_{rf}$	μs	0.743	0.759	1.953	0.889				
$f_{rev}$	MHz	0.269	1.318	0.256	1.124				
$T_{rev}$	μs	3.716	0.759	3.906	0.889				
$\beta$		0.999	0.972	0.924	0.830				
$\gamma$		31.918	4.221	2.610	1.794				
		One time injection		One time injection					
Phase shift method									
There is no beam in CR, so the phase jump of CR is preferred.									

Table C.6: Parameters for the B2B transfer from SIS100 to CR

# Bibliography

- [1] Particle accelerator. URL [https://en.wikipedia.org/wiki/Particle\\_accelerator](https://en.wikipedia.org/wiki/Particle_accelerator).
- [2] P. Møller. Beam-residual gas interactions. Technical report, CERN, 1999. URL <http://cds.cern.ch/record/455561/files/p155.ps.gz>.
- [3] Thibault Ferrand, Harald Klingbeil, and Heiko Damerau. Synchronization of Synchrotrons for bunch-to-bucket Transfers. Technical report, 2015. URL <http://cds.cern.ch/record/2053285>.
- [4] J-PARC. URL <https://www.kek.jp/en/Facility/ACCL/J-PARC/>.
- [5] Brookhaven National Laboratory. URL [https://en.wikipedia.org/wiki/Particle\\_physics](https://en.wikipedia.org/wiki/Particle_physics).
- [6] Fermi National Accelerator Laboratory. URL <http://www.fnal.gov/pub/science/particle-accelerators/accelerator-complex.html>.
- [7] Institute of Modern Physics of the Chinese Academy of Sciences. URL [http://english.imp.cas.cn/au/bi/201312/t20131231\\_115141.html](http://english.imp.cas.cn/au/bi/201312/t20131231_115141.html).
- [8] Kaidi Man, Yizhen Guo, Guozhu Cai, Sengli Yang, and Shoujin Wang. Survey and Alignment of HIRFL-CSR at IMP. In Proc. IWAA2002, 2002. URL [http://www-group.slac.stanford.edu/met/IWAA/TOC\\_S/PAPERS/KMan02.pdf](http://www-group.slac.stanford.edu/met/IWAA/TOC_S/PAPERS/KMan02.pdf).
- [9] Jürgen Eschke. International Facility for Antiproton and Ion Research (FAIR) at GSI, Darmstadt. Journal of Physics G: Nuclear and Particle Physics, 31(6):S967, 2005. URL <http://iopscience.iop.org/article/10.1088/0954-3899/31/6/041/meta>.
- [10] FAIR - Facility for Antiproton and Ion Research, May 2011. URL <https://www.gsi.de//forschungbeschleuniger/fair.htm>.
- [11] P. Spiller and G. Franchetti. The FAIR accelerator project at GSI. Nuclear Instruments and Methods in Physics Research Section A, 561(2):305–309, 2006. URL <http://www.sciencedirect.com/science/article/pii/S0168900206000507>.
- [12] M. Steck, R. Bär, U. Blell, C. Dimopoulou, A. Dolinskii, P. Forck, B. Franzke, O. Gorda, V. Gostishchev, U. Jandewerth, and others. Advanced Design of the FAIR Storage Ring Complex. In In Proc. of EPAC, 2008. URL <https://accelconf.web.cern.ch/AccelConf/PAC2009/papers/fr1gri03.pdf>.

## BIBLIOGRAPHY

---

- [13] Fritz Nolden, K. Beckert, P. Beller, U. Blell, C. Dimopoulou, A. Dolinskii, U. Laier, G. Moritz, C. Muehle, I. Nesmiyan, and others. The Collector Ring CR of the FAIR project. *Proc. EPAC*, 3(1):5, 2006. URL <http://accelconf.web.cern.ch/AccelConf/e06/PAPERS/MOPCH077.PDF>.
- [14] T. Abe, I. Adachi, K. Adamczyk, S. Ahn, H. Aihara, K. Akai, M. Alois, L. Andricek, K. Aoki, Y. Arai, and others. Technical design report Collector Ring. *KEK Report*, 2010. URL <http://arxiv.org/abs/1011.0352>.
- [15] R. Toelle, K. Bongardt, J. Dietrich, F. Esser, O. Felden, R. Greven, G. Hansen, F. Klehr, A. Lehrach, B. Lorentz, and others. HESR at FAIR: Status of technical planning. 2007. URL <http://epaper.kek.jp/p07/PAPERS/TUPAN024.PDF>.
- [16] M. Lestinsky, A. Bräuning-Demian, H\aaakan Danared, M. Engström, W. Enders, S. Fedotova, B. Franzke, A. Heinz, F. Herfurth, A. Källberg, and others. CRYRING@ ESR: present status and future research. *Physica Scripta*, 2015 (T166):014075, 2015. URL <http://iopscience.iop.org/article/10.1088/0031-8949/2015/T166/014075/meta>.
- [17] M. Lestinsky and others. CRYRING@ ESR: A study group report. *GSI and FAIR Report*, 2012.
- [18] S Y Lee. *Accelerator Physics*. WORLD SCIENTIFIC, Singapore, 3 edition, November 2011. ISBN 978-981-4374-94-1 978-981-4374-95-8. URL <http://www.worldscientific.com/worldscibooks/10.1142/8335>.
- [19] Harms Barletta. Overview on Magnetic fields. URL [http://uspas.fnal.gov/materials/12MSU/xverse\\_dynamics.pdf](http://uspas.fnal.gov/materials/12MSU/xverse_dynamics.pdf).
- [20] R Garoby. Timing aspect of bunch transfer between circular machines. State of the art in the PS complex, PS/RF. Technical report, Note 84-6, 17 December 84, 1984.
- [21] Jochen Michael Grieser. *Beam phase feedback in a heavy-ion synchrotron with dual-harmonic cavity system*. PhD thesis, Technical University Darmstadt, 2015. URL <http://tuprints.ulb.tu-darmstadt.de/4634/>.
- [22] K. Gross, U. Hartel, U. Laier, D. Lens, K. P. Ningel, S. Schäfer, B. Zipfel, and H. Klingbeil. Bunch-by-Bunch Longitudinal RF Feedback for Beam Stabilization at FAIR. In *Proc. of IPAC*, 2015. URL <http://accelconf.web.cern.ch/AccelConf/IPAC2015/papers/mopha021.pdf>.
- [23] Eizi Ezura, Masahito YOSHII, Fumihiko TAMURA, and Alexander SCHNASE. Beam-Dynamics View of RF Phase Adjustment for Synchronizing J-PARC RCS with MR or MLF, 2008. URL <http://ccdb5fs.kek.jp/tiff/2008/0826/0826001.pdf>.
- [24] B. J. Holzer. Introduction to transverse beam dynamics. *CERN Yellow Report*, 2013. URL <http://arxiv.org/abs/1404.0923>.
- [25] Steve Werkema. Differential Relationships Between Momentum Magnetic Field, Orbit Length, and Revolution Frequency. Technical report, Fermi National

## BIBLIOGRAPHY

---

- Accelerator Laboratory (FNAL), Batavia, IL, 2001. URL <http://www.osti.gov/scitech/biblio/984579>.
- [26] Isfried Petzenhauser, Leif Baandrup, Henning Bach, Udo Blell, Guido Blokesch, Nils Hauge, Kim Laurberg, Michael Osemann, and Peter Spiller. Concept and Design of the Injection Kicker System for the FAIR SIS100 Synchrotron. In IPAC, pages 3582–3584, Busan, Korea,, 2016. JACOW, Geneva, Switzerland.
  - [27] Blell Udo. Injection and Extraction Components of SIS 100 / 300, 2014.
  - [28] T. Hoffmann. FESA—The front-End Software architecture at FAIR. PCaPAC08, 2008. URL <http://accelconf.web.cern.ch/AccelConf/pc08/papers/wep007.pdf>.
  - [29] Ralf Huhmann, Ralph C. Bär, Dietrich Hans Beck, Jutta Fitzek, Günther Fröhlich, Ludwig Hechler, Udo Krause, and Matthias Thieme. The FAIR control system—System architecture and first implementations. ICALEPCS, 2013. URL <http://epaper.kek.jp/ICALEPCS2013/papers/moppc097.pdf>.
  - [30] Dietrich Beck, R. Bar, Mathias Kreider, Cesar Prados, Stefan Rauch, Wesley Terpstra, and Marcus Zweig. The new White Rabbit based timing system for the FAIR facility. PCaPAC, 2012. URL <http://accelconf.web.cern.ch/Accelconf/pcapac2012/papers/fria01.pdf>.
  - [31] Peter Moritz. BuTiS—Development of a Bunchphase Timing System. GSI Scientific Report, 2006. URL <http://citeseerx.ist.psu.edu/viewdoc/download?doi=10.1.1.162.1765&rep=rep1&type=pdf>.
  - [32] B. Zipfel, P. Moritz, and others. Recent Progress on the Technical Realization of the Bunch Phase Timing System BuTiS. Proc. IPAC, pages 418–420, 2011. URL <http://accelconf.web.cern.ch/accelconf/ipac2011/papers/mopc145.pdf>.
  - [33] Dietrich Beck, Mathias Kreider, Cesar Prados, Wesley Terpstra, Stefan Rauch, and Marcus Zweig. The General Machine Timing System for FAIR and GSI. URL [https://www-acc.gsi.de/wiki/pub/Timing/TimingSystemDocuments/GMT\\_Description\\_v3-1.pdf](https://www-acc.gsi.de/wiki/pub/Timing/TimingSystemDocuments/GMT_Description_v3-1.pdf).
  - [34] Dietrich Beck. Timing Messages of GMT system for FAIR, 2015. URL <https://www-acc.gsi.de/wiki/Timing/TimingSystemEvent>.
  - [35] Harald Klingbeil, Ulrich Laier, Klaus-Peter Ningel, Stefan Schäfer, Christof Thielmann, and Bernhard Zipfel. New digital low-level rf system for heavy-ion synchrotrons. Physical Review Special Topics - Accelerators and Beams, 14(10), October 2011. ISSN 1098-4402. doi: 10.1103/PhysRevSTAB.14.102802. URL <http://link.aps.org/doi/10.1103/PhysRevSTAB.14.102802>.
  - [36] P. Baudrenghien. Low-level RF. 13(14):15, 2010. URL <https://cas.web.cern.ch/cas/Denmark-2010/Writeups/Baudrenghien.docx>.
  - [37] Marko Mandakovic. FAIR Fast Beam Abort System. URL [https://fair-wiki.gsi.de/foswiki/pub/FC2WG/FairC2WGMinutes/20151021\\_Fast\\_Beam\\_Abort\\_System\\_Mandakovic.pdf](https://fair-wiki.gsi.de/foswiki/pub/FC2WG/FairC2WGMinutes/20151021_Fast_Beam_Abort_System_Mandakovic.pdf).

## BIBLIOGRAPHY

---

- [38] P Kainberger. PZS - SIS/ESR-Pulszentrale, 2003. URL <https://www-acc.gsi.de/data/documentation/eq-models/pzs/gm-pzs.pdf>.
- [39] U. Krause and Volker Schaa. Re-engineering of the GSI control system. 2001. URL <http://arxiv.org/abs/physics/0111060>.
- [40] H. Liebermann and D. Ondreka. FAIR and GSI Reference Cycles for SIS18, 2013.
- [41] H. Liebermann and D. Ondreka. SIS100 Cycles, 2013.
- [42] J. Bai, T. Ferrand, D. Beck, R. Bär, O. Kester, D. Ondreka, C. Prados, and W. Terpstra. BUNCH TO BUCKET TRANSFER SYSTEM FOR FAIR. In ICALEPCS, 2015. URL <http://icalepcs.synchrotron.org.au/papers/wepgf119.pdf>.
- [43] T. Ferrand and J. Bai. System Simulation of Bunch-to-Bucket Transfer Between Synchrotrons. GSI Scientific Report, 2014. URL <http://repository.gsi.de/record/184160/files/FG-GENERAL-28.pdf>.
- [44] T. Ferrand and J. Bai. SYSTEM DESIGN FOR A DETERMINISTIC BUNCH-TO-BUCKET TRANSFER. In IPAC, 2015. URL <http://accelconf.web.cern.ch/AccelConf/IPAC2015/papers/wepma024.pdf>.
- [45] Thibault Ferrand. Development of the LLRF system for a deterministic Bunch-to-Bucket transfer for FAIR. PhD thesis, Technical University Darmstadt.
- [46] Matthias Thieme, Wolfgang Panschow, and Stefan Rauch. SCU system goes productive. GSI Scientific Report, 2013. URL <http://repository.gsi.de/record/68061/files/FG-CS-07.pdf>.
- [47] Jiaoni Bai and Thibault Ferrand. Concept of the FAIR Bunch To Bucket Transfer System, 2016.
- [48] F. Herfurth, A. Brauning-Demian, W. Enders, H. Danared, and others. The low energy storage ring CRYRING@ ESR. Proc. of COOL2013 (Murren, Switzerland), 2013. URL <https://accelconf.web.cern.ch/accelconf/COOL2013/papers/thpm1ha01.pdf>.
- [49] M. Steck, C. Dimopoulou, B. Franzke, O. Gorda, T. Katayama, F. Nolden, G. Schreiber, Germany D. Möhl, Switzerland R. Stassen, H. Stockhorst FZJ, and others. Demonstration of Longitudinal Stacking in the ESR with Barrier Buckets and Stochastic Cooling. page 140, Alushta, Ukraine, 2011. URL <http://accelconf.web.cern.ch/AccelConf/COOL2011/papers/proceed.pdf#page=150>.
- [50] A. V. Smirnov, D. A. Krestnikov, I. N. Meshkov, and others. Particle accumulation with a barrier bucket RF system. In COOL, 2009.
- [51] J. Bai12, R. Bär, D. Beck, T. Ferrand13, M. Kreider, D. Ondreka, C. Prados, S. Rauch, W. Terpstra, and M. Zweig. First Idea on Bunch to Bucket Transfer for FAIR. 2014. URL [http://epaper.kek.jp/PCaPAC2014/posters/fpo024\\_poster.pdf](http://epaper.kek.jp/PCaPAC2014/posters/fpo024_poster.pdf).

- [52] John R. Taylor. An introduction to error analysis: The study of uncertainty in physical measurements. Mill Valley, CA: Anonymous University Science Books, page 71ep, 1982.
- [53] U. Laier. Funktional-Spezifikation DDS, 2011.
- [54] Statistical and numerical tools in astrophysics I. Accuracy and precision. URL <http://www.astro.lu.se/Education/utb/ASTM11/lecture2.pdf>.
- [55] Cesar Prados and Jiaoni Bai. Testing the WR Network of the FAIR General Machine Timing System, 2016.
- [56] Calculating Optical Fiber Latency, 2012. URL <http://www.m2optics.com/blog/bid/70587/Calculating-Optical-Fiber-Latency>.

# Publications

- 2015 J. Bai, T. Ferrand, D. Beck, R. Br, O. Kester, D. Ondreka, C. Prados, and W. Terpstra. BUNCH TO BUCKET TRANSFER SYSTEM FOR FAIR. *In Proc. of ICAL EPICS*, 2015
- T. Ferrand and J. Bai. SYSTEM DESIGN FOR A DETERMINISTIC BUNCH-TO-BUCKET TRANSFER. *In Proc. of IPAC*, 2015
- 2014 J. Bai, D. Beck, R. Br, D. Ondreka, T. Ferrand, M. Kreider, C. Prados, S. Rauch, W. Terpstra, and M. Zweig. FIRST IDEA ON BUNCH TO BUCKET TRANSFER FOR FAIR. *In Proc. of PCaPAC*, 2014
- M. Kreider, J. Bai, R. Br, D. Beck, A. Hahn, C. Prados, S. Rauch, W. W. Terpstra, and M. Zweig. Launching the FAIR timing system with CRYRING. *In Proc. of PCaPAC*, 2014
- T. Ferrand and J. Bai. System Simulation of Bunch-to-Bucket Transfer Between Synchrotrons. *GSI Scientific Report*, 2014
- 2013 Bai Jiao-Ni, Zeng Lei, Wang Biao, Li Peng, Li Fang, Xu Tao-Guang, and Li Zi-Gao. Modified read-out system of the beam phase measurement system for CSNS. *Chinese physics C*, 37(10):107004, 2013
- D. Beck, J. Adamczewski-Musch, J. Bai, R. Br, J. Frhauf, J. Hoffmann, M. Kreider, N. Kurz, C. Prados, S. Rauch, and others. Paving the Way for the General Machine Timing System. *GSI Scientific Report*, 2013
- Mathias Kreider, Jiaoni Bai, Dietrich Beck, Cesar Prados, Wesley Terpstra, Stefan Rauch, and Marcus Zweig. Receiver Nodes of the General Machine Timing System for FAIR and GSI
- 2012 Jiaoni Bai, Shuai Xiao, Taoguang Xu, and Lei Zeng. The Development of Timing Control System for RFQ. *In Proc. of LINAC*, 2012

# Jiaoni Bai

---

## Curriculum Vitae

*"I am a slow walker, but I never stop walking." - Jiaoni Bai*

### Education

- 2013–Now **Doctoral Study**, *Goethe University, Frankfurt am Main, Germany*, .
- 2010–2013 **Master of Engineering Study in Computer Technology**, *Institute of High Energy Physics, Chinese Academy of Sciences, China, GPA – 8.0.*
- 2006–2010 **Bachelor of Engineering Study in Medical Informatics Engineering**, *Southern Medical University, China, GPA – 9.0.*

### PhD Thesis

- Title *Development of the timing system for the Bunch-to-Bucket transfer between the FAIR accelerators at GSI Helmholtz Centre for Heavy Ion Research GmbH*
- Professor Prof. Oliver Kester
- Supervisors Dr. Dietrich Beck and Dr. David Ondreka
- Description
  - Development of the Bunch-to-Bucket transfer system
  - Programming work on FPGA
  - Measurement of the White Rabbit network performance

### Master Thesis

- Title *The development of EPICS driver for customized VME hardwares*
- Supervisor Taoguang Xu
- Description
  - Development of the software interface between EPICS and VME hardware
  - Development of the operator controlling and monitoring interfaces by MEDM hardware
  - VxWorks program for Motorola VME board MVME5100

### Bachelor Thesis

- Title *The CCD performance test and analysis*
- Description
  - Investigation of the influence factors for CCD
  - Test how these factors influence CCD

## Awards

- 2012 Won "Scholarship of the head of the Institute of High Energy Physics, CAS" for master thesis
- 2007 Won second prize of "Mathematical Contest in Modeling in Southern Medical University"

## Key skills

- Intermediate Network engineering, Bash shell script and Visual Basic programming
- Advanced VHDL program for Altera FPGAs, C, Accelerator technology and beam dynamics, VxWorks programming and EPICS

## Computer literacy

- Basic Windows, Linux (Ubuntu/Debian), Microsoft Office and LaTeX applications
- Engineering Altera Quartus and Matlab applications
- Art design Photoshop and Corel VideoStudio application
- Web design Dreamweaver

## Languages

- Mandarin Mothertongue Chinese
- English Good written and spoken
- German Goethe-Zertifikat B2